Fakultät für Medizin
Institut für Virologie

Approaches to improve outcome of hepatitis B virus-specific chimeric antigen receptor T-cell therapy

Marvin Matthias Festag

Vollständiger Abdruck der von der Fakultät für Medizin der Technischen Universität München zur Erlangung des akademischen Grades eines

Doctor of Philosophy (Ph.D.)

genehmigten Dissertation.

Vorsitzender: Prof. Dr. Arthur Konnerth

Betreuerin: Prof. Dr. Ulrike Protzer

Prüfende der Dissertation:

1. Prof. Dr. Angela Krackhardt
2. Priv.-Doz. Dr. Sebastian Kobold

Die Dissertation wurde am 15.6.2018 bei der Fakultät für Medizin der Technischen Universität München eingereicht und durch die Fakultät für Medizin am 28.8.2018 angenommen.

Table of contents

Abstract

Despite the availability of a prophylactic vaccine, chronic hepatitis B virus (HBV) infection remains a major health concern with currently about 257 million people chronically infected. Chronic hepatitis B, which leads to 887,000 deaths per year, is the major cause of hepatocellular carcinoma (HCC) for which treatment options remain limited. HBV is rarely eliminated by available antivirals because they fail to target the viral template, the covalently closed circular DNA. $CD8^+$ T cell responses have been reported to greatly contribute to functional cure. Thus, adoptive T-cell therapy, in which HBV-specific T cells are transferred, appears as a promising approach not only for chronic hepatitis B but also for HBV-associated HCC. Previously, a chimeric antigen receptor recognizing the HBV envelope proteins on the surface of HBV-infected cells was generated (S-CAR), and T cells grafted with the receptor were successfully redirected towards HBV-infected hepatocytes *in vitro*. Using HBV-transgenic mice, which replicate HBV in hepatocytes, *in vivo* applicability of this approach was demonstrated. Transferred S-CAR-grafted $CD8^+$ T cells efficiently relocated to the liver causing a transient liver damage with no other obvious side effects, and very effectively controlled HBV replication. However, after an initial expansion, the pool of adoptively transferred T cells contracted, and remaining S-CAR-grafted T cells displayed diminished effector function over time leading to a rebound of viremia. Therefore, the central goal of this thesis was to investigate the underlying mechanisms of the limited antiviral effect and, based on preclinical models, to provide a better understanding of the therapeutic effect to be expected in clinical application.

In the first part, an immune response of the endogenous murine immune system against the human-derived domains of the S-CAR was analyzed. B- and T-cell responses were identified to target S-CAR and co-expressed truncated human epidermal growth factor receptor on transferred cells and contributed to the contraction of adoptively transferred T cells. If the immune system was ablated in genetically immunodeficient mice or by total body irradiation, transferred S-CAR T cells persisted in high numbers and exhibited a long-lasting antiviral effect. To study the therapeutic approach in the context of an intact endogenous immune system, immunocompetent mice were tolerized to the human alloantigens by a preceding transfer of non-functional CAR T cells after total body irradiation. In tolerized mice S-CAR T-cell therapy was comparably effective as in immunodeficient mice, although the therapy remained unable to eliminate the infection completely. Furthermore, in this mouse model, S-CAR T-cell therapy was safe and did not induce obvious therapy-limiting side effects.

S-CAR T-cell therapy remained unable to eliminate HBV in the *in vivo* model despite S-CAR T-cell persistence when graft rejection was prevented. Therefore, possibilities to enhance the therapeutic effect were investigated next. In the second part of the thesis, modified variants of

the S-CAR harboring alternative costimulatory domains were compared *in vitro* and *in vivo*. The results suggest that additional costimulation by an OX40 domain in a 3rd generation S-CAR do not enhance T-cell functionality in comparison to a 2nd generation S-CAR with CD3ζ and CD28 domains only *in vitro*. Furthermore, 4-1BB containing 2nd and 3rd generation S-CARs were also less efficient to target HBV-infected cells *in vitro* and *in vivo*.

In the third part of the thesis, the influence of inhibitory checkpoints on *in vivo* efficacy of S-CAR T cells was determined. Although transferred S-CAR T cells highly expressed programmed cell death protein-1 (PD-1) *in vivo* and secreted interleukin-10 (IL-10) upon *ex vivo* stimulation, genetic ablation of either molecule in the transferred cells did not enhance S-CAR T-cell efficacy *in vivo*. Intrahepatic immuno-stimulation with CpG was also not able to increase the antiviral effect of S-CAR T cells.

In the fourth part, the therapeutic approach using S-CAR T cells was transferred from the already established systems with human and murine cells to a non-human primate model with rhesus macaque cells. Macaque $CD8^+$ and $CD4^+$ T cells could be transduced to express the S-CAR and could be specifically activated by HBV-infected primary macaque hepatocytes. The results provide the basis for future investigations regarding *in vivo* efficacy and safety of S-CAR T-cell therapy in the rhesus macaque model.

Taken together, this thesis provides evidence that S-CAR T-cell therapy can exhibit a lasting antiviral effect in preclinical *in vivo* mouse models if cells are not rejected by the endogenous immune system. On the basis of these data, an S-CAR with CD3ζ and CD28 domains should be used without combinational therapy with PD-1 or IL-10 inhibitors as well as intrahepatic immuno-stimulation with CpG. Before advancing to the clinics, efficacy and safety of the therapeutic approach could be tested in the rhesus macaque model for HBV infection.

Zusammenfassung

Trotz der Verfügbarkeit eines prophylaktischen Impfstoffs ist chronische Hepatitis B Virus (HBV) Infektion weiterhin ein großes Gesundheitsproblem mit weltweit schätzungsweise 257 Millionen chronisch infizierten Menschen. Die chronische Hepatitis B führt jährlich zu ungefähr 887.000 Todesfällen und stellt den wichtigsten Auslöser des hepatozellulären Karzinoms (HCC) dar, für das es bisher nur unzulängliche Behandlungsmöglichkeiten gibt. Durch aktuelle antivirale Therapien wird das Virus nur selten eliminiert, da die virale kovalent geschlossene zirkuläre DNA in infizierten Zellen durch die Therapien nicht beseitigt wird. Es konnte gezeigt werden, dass Immunantworten durch $CD8^+$ T-Zellen in hohem Maße zu einer funktionellen Heilung beitragen. Daher scheint der adoptive Transfer von HBV-spezifischen T-Zellen ein vielversprechender Ansatz zu sein, die chronische Hepatitis B und HBV-assoziiertes HCC zu behandeln. Hierzu wurde bereits zuvor ein chimärer Antigenrezeptor gegen die HBV Hüllproteine generiert (S-CAR) und T-Zellen mit seiner Hilfe erfolgreich gegen HBV-infizierte Hepatozyten *in vitro* eingesetzt. In HBV-transgenen Mäusen, bei denen das Virus in Hepatozyten repliziert, konnte die *in vivo* Anwendbarkeit demonstriert werden. Die transferierten S-CAR T-Zellen migrierten in die Leber, lösten dort einen transienten Leberschaden aus ohne weitere offensichtliche Nebenwirkungen zu erzeugen und waren in der Lage die Replikation von HBV effektiv zu kontrollieren. Allerdings sank die Anzahl der transferierten Zellen nach einer initialen Expansion rapide und die verbliebenen Zellen zeigten eine reduzierte Funktionalität, sodass der therapeutische Effekt nur transient war. Deshalb war das Hauptziel dieser Dissertation die Mechanismen zu untersuchen, die zu dieser Limitation führten. Der therapeutische Nutzen, der bei klinischer Anwendung der Therapie zu erwarten ist, soll basierend auf präklinischen Modellen abgeschätzt werden.

Im ersten Teil der Arbeit wurde die Immunantwort des endogenen Immunsystems gegen die humanen Domänen des S-CARs analysiert. Es konnte gezeigt werden, dass sowohl B- als auch T-Zellantworten gegen den S-CAR und den zusätzlich exprimierten trunkierten humanen epidermalen Wachstumsfaktor-Rezeptor ausgebildet werden. Diese führten zur Abnahme der Anzahl transferierter S-CAR T-Zellen. Die Abstoßung der Zellen konnte in immundefizienten Mäusen und durch Ganzkörperbestrahlung verhindert werden, sodass die transferierten Zellen persistierten und einen anhaltenden antiviralen Effekt erzeugten. Damit die Therapie auch in einer immunkompetenten Maus getestet werden konnte, wurden Mäuse mit nicht funktionellen CAR T-Zellen gegen die humanen Alloantigene tolerisiert und anschließend therapiert. Die Therapie zeigte in diesen Mäusen eine vergleichbare Wirkung wie in immundefizienten Tieren, aber war auch hier nicht im Stande die Infektion komplett zu eliminieren. Außerdem konnte in diesem Mausmodell gezeigt werden, dass die S-CAR T-Zelltherapie sicher ist und keine starken Nebenwirkungen erzeugt.

Da HBV nicht komplett eliminiert wurde, selbst wenn S-CAR T-Zellen *in vivo* persistieren konnten, wurden Möglichkeiten untersucht, den therapeutischen Effekt zu erhöhen. Im zweiten Teil der Dissertation wurden S-CAR Varianten mit unterschiedlichen kostimulatorischen Signaldomänen *in vitro* und *in vivo* verglichen. Die Ergebnisse deuten darauf hin, dass eine zusätzliche OX40 Signaldomäne in einem S-CAR der dritten Generation die T-Zellfunktionalität im Vergleich zu einem S-CAR der zweiten Generation mit nur CD3ζ und CD28 Domänen *in vitro* nicht erhöht. Außerdem zeigen S-CARs mit einer 4-1BB Domäne eine niedrigere Funktionalität sowohl *in vitro* als auch *in vivo*.

Im dritten Teil der Arbeit wurde der Einfluss von inhibitorischen Molekülen auf die S-CAR T-Zellfunktionalität *in vivo* untersucht. Obwohl S-CAR T-Zellen *in vivo* PD-1 (englisch: programmed cell death protein-1) exprimierten und nach *ex vivo* Stimulation Interleukin-10 (IL-10) sekretierten, konnte der therapeutische Effekt durch genetische Manipulation des PD-1 bzw. IL-10 Locus in den transferierten Zellen nicht erhöht werden. Intrahepatische Immunstimulation mithilfe von CpG konnte den antiviralen Effekt von S-CAR T-Zellen ebenfalls nicht steigern.

Im vierten Teil der Arbeit wurde der Therapieansatz von den humanen und murinen Modellen auf ein Primatenmodel mit Zellen des Rhesus Makaken angewandt. $CD8^+$ und $CD4^+$ T-Zellen vom Rhesus Makaken konnten transduziert werden, exprimierten den S-CAR und konnten mit seiner Hilfe spezifisch von HBV-infizierten primären Hepatozyten des Rhesus Makaken aktiviert werden. Auf Basis dieser Daten können in Zukunft *in vivo* Untersuchungen der Effizienz und Sicherheit von S-CAR T-Zelltherapie in Rhesus Makaken *in vivo* durchgeführt werden.

Zusammenfassend demonstriert diese Dissertation, dass S-CAR T-Zellen in einem präklinischen *in vivo* Mausmodell einen anhaltenden therapeutischen Effekt haben, wenn die Zellen nicht vom endogenen Immunsystem abgestoßen werden. Die Daten zeigen, dass ein S-CAR mit CD3ζ und CD28 Signaldomänen ohne Kombinationstherapie mit PD-1 oder IL-10 Inhibitoren oder Immunstimulation mit CpG verwendet werden sollte. Vor der klinischen Anwendung können der Nutzen und die Sicherheit des Therapieansatzes in HBV-infizierten Rhesus Makaken untersucht werden.

Abbreviations

AAV	adeno-associated virus
Ad	adenovirus
AICD	activation-induced cell death
ALL	acute lymphocytic leukemia
ALT	alanine amino transferase
APC	antigen-presenting cell
BCR	B-cell receptor
bp	base pair
BSA	bovine serum albumin
CAR	chimeric antigen receptor
cccDNA	covalently closed circular DNA
CD	cluster of differentiation
CEA	carcinoembryonic antigen
CFSE	carboxyfluorescein succinimidyl ester
CHB	chronic hepatitis B
CLL	chronic lymphocytic leukemia
CMV	cytomegalovirus
CRS	cytokine release syndrome
CTLA-4	cytotoxic T-lymphocyte-associated protein-4
DC	dendritic cell
DMSO	dimethyl sulfoxide
DNA	deoxyribonucleic acid
E:T	effector to target ratio
EDTA	ethylenediaminetetraacetic acid
EGFRt	truncated epidermal growth factor receptor
ELISA	enzyme-linked immunosorbent assay
EMA	ethidium monoazide
ETV	entecavir
FACS	fluorescence-activated cell sorting
Fas	first apoptosis signal receptor
FasL	first apoptosis signal ligand
Fc	fragment, crystallizable

FCS	fetal calf serum
FDA	Food and Drug Administration
h	hours
HBc	HBV core protein
HBeAg	hepatitis B e antigen
HBsAg	hepatitis B surface antigen
HBV	hepatitis B virus
HBx	HBV X protein
HCC	hepatocellular carcinoma
HIV	human immunodeficiency virus
HLA	human leukocyte antigen
HRP	horseradish peroxidase
hNTCP	human NTCP
ICOS	inducible T-cell costimulator
ICS	intracellular cytokine staining
IFN-α	interferon-α
IFN-γ	interferon-γ
Ig	immunoglobulin
iIL-12	NFAT-regulated inducible single-chain IL-12 expression
IL	interleukin
iMATEs	intrahepatic myeloid-cell aggregates for T-cell population expansion
ip	infectious particles
ITAM	immunoreceptor tyrosine-based activation motif
JAK	janus kinase
kb	kilo base
LAL	liver-associated lymphocyte
MACS	magnetic-activated cell sorting
MFI	median fluorescence intensity
mg	milligram
MHC	major histocompatibility complex
min	minutes
ml	milliliter
mV	millivolt

MOI	multiplicity of infection
MVB	multivesicular body
NEAA	non-essential amino acids
NFAT	nuclear factor of activated T cells
ng	nanogram
NHL	non-Hodgkin lymphoma
NHP	non-human primate
NK cell	natural killer cell
nm	nanometer
nM	nanomolar
NOD	non-obese diabetic
ns	not significant
NSG	NOD-SCID-IL-2Rγnull
NTCP	sodium taurocholate cotransporting polypeptide
OD	optical density
PBMC	peripheral blood mononuclear cells
PBS	phosphate-buffered saline
PCR	polymerase chain reaction
PD-1	programmed cell death protein-1
PD-L1	programmed cell death ligand-1
PEG-IFN-α	pegylated IFN-α
Pen/Strep	penicillin / streptomycin
pgRNA	pregenomic RNA
PMH	primary macaque hepatocyte
PRNP	gene locus of prion protein
PSMA	prostate-specific membrane antigen
qPCR	quantitative PCR
rcDNA	relaxed circular DNA
RNA	ribonucleic acid
rpm	rounds per minute
RT	room temperature
RTCA	real-time cell analyzer
S-CAR	HBV S protein specific chimeric antigen receptor
scFv	single chain variable fragment

SCID	severe combined immunodeficiency
SEB	staphylococcal enterotoxin B
sec	seconds
SIN	self-inactivating
STAT	signal transducer and activator of transcription proteins
TCR	T-cell receptor
TDF	tenofovir disoproxil fumarate
Tim-3	T-cell immunoglobulin and mucin-domain containing-3
TM	transmembrane
TNF-α	tumor necrosis factor-α
Treg	regulatory T cell
wt	wildtype
µg	microgram
µl	microliter
µm	micrometer
µM	micromolar

1 Introduction

1.1 The hepatitis B virus

1.1.1 Virus structure and replication cycle

The hepatitis B virus (HBV) was first described by Dane et al. (1970) and is an enveloped double-stranded DNA virus from the hepadnavirus family. Until today, nine genotypes (A-I) and four major serotypes (adw, adr, ayw, ayr) have been described (Kramvis, 2014). The virus has a narrow host range infecting only humans and chimpanzees and a high tropism for hepatocytes and thus causes liver diseases (Wieland, 2015). The virion consists of the partially double-stranded relaxed circular DNA (rcDNA) with the HBV polymerase, a reverse transcriptase, attached. Both are located within the viral capsid, which consists of HBV core protein (HBc) forming the icosahedral capsid. The capsid is covered by the viral envelope made up of host lipids and three different variants of the HBV envelope protein (HBs) (Ganem, 1991). Those three envelope proteins share the same C-terminal domain but differ in the N-terminal domain due to different start codons for protein translation: the small (S) protein, consisting of the C-terminal S-domain, the medium (M) protein, which in addition carries the preS2-domain, and the large (L) protein, which in addition to S- and preS2-domains also contains a preS1-domain (Seeger and Mason, 2015).

Viral replication is depicted in Figure 1.1. HBV infects hepatocytes through unspecific and reversible binding to heparan sulfate proteoglycans followed by specific binding to its cellular receptor, the sodium taurocholate cotransporting polypeptide (NTCP) (Yan et al., 2012). The virus enters the cell via endocytosis and the viral envelope fuses with the endosomal membrane thus releasing the capsid into the cytosol. After transport of the capsid to the nucleus, the viral genome, the rcDNA, is released into the nucleus and repaired by the cellular machinery to form the covalently closed circular DNA (cccDNA). This episomal viral cccDNA serves as template for viral replication. Transcription of cccDNA produces viral RNAs from which viral proteins are translated (Seeger and Mason, 2015). Beside HBs and HBc, the non-structural HBV X protein (HBx), which among other functions enhances viral transcription (Bouchard and Schneider, 2004), and the secreted hepatitis B e antigen (HBeAg) with immunoregulatory functions are translated (Chen et al., 2004). Furthermore, a pregenomic RNA (pgRNA) is transcribed and after binding to HBV polymerase packaged into the viral capsid. Within the capsid, the HBV polymerase reverse transcribes the pgRNA into rcDNA and subsequently the matured capsid can take two different routes. On the one hand, it can be recycled and transported back to the nucleus like incoming capsids to release its rcDNA into the nucleus to increase the pool of cccDNA (Seeger and Mason, 2015). On the other hand, it

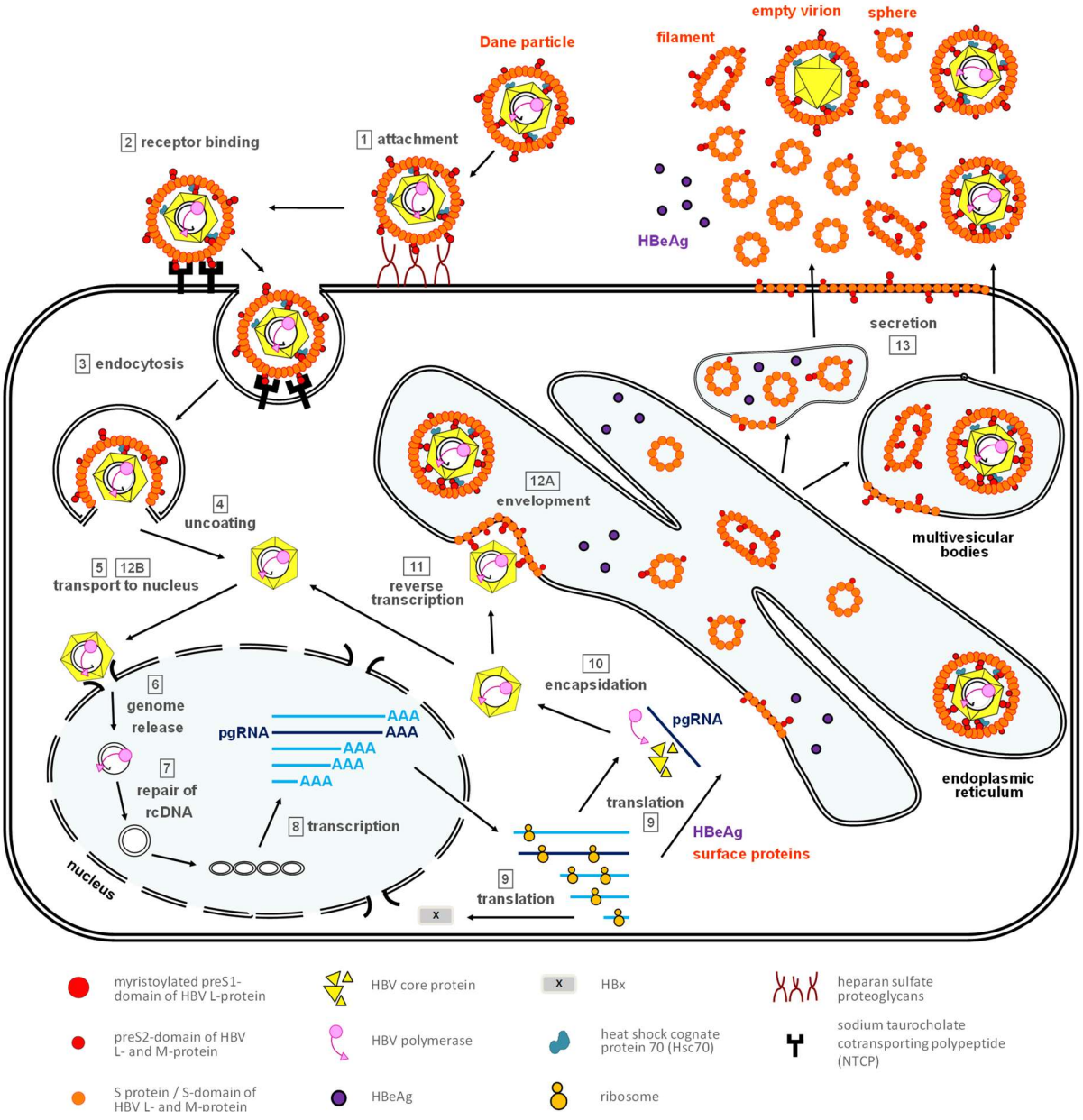

Figure 1.1 Hepatitis B virus life cycle.
(1) After unspecific binding to heparan sulfate proteoglycans, (2) the HBV virion binds to its cellular receptor sodium taurocholate cotransporting polypeptide (NTCP) and (3) is endocytosed. After (4) uncoating, and (5) transport to the nucleus (6) the viral genome is released into the nucleus. (7) Host proteins repair rcDNA to cccDNA and subsequently (8) transcription of viral RNAs takes place. (9) Viral proteins are translated and (10) the pgRNA encapsidated followed by (11) reverse transcription into rcDNA. The capsid (12A) is either enveloped by the envelope proteins S, M, and L or (12B) recycled and transported to the nucleus. The enveloped capsid is transported through the endoplasmic reticulum and multivesicular bodies and (13) secreted from the cell. Empty virions, filaments, spheres and HBeAg are also released from the cell. Beside in the viral envelope, proteins S, M and L also end up on the plasma membrane. Scheme was derived from Ko et al. (2017).

can be enveloped at multivesicular bodies (MVBs) and leave the cell as mature virion (Watanabe et al., 2007). Beside composing the viral envelope of mature virions, the HBV envelope proteins cover rcDNA-free capsids (empty virions) and furthermore leave the cell without capsid as non-infectious spherical or filamentous subviral particles, which can be determined as soluble hepatitis B surface antigen (HBsAg) in the blood of patients (Seeger and Mason, 2015). While spherical subviral particles are released via the constitutive secretory pathway, filamentous subviral particles like infectious viral particles bud into MVBs (Jiang et al., 2015). Fusion of MVBs with the plasma membrane results in cell surface expression of HBV envelope proteins that have not been included into viral envelopes or subviral particles and they can be detected on the plasma membrane of infected hepatocytes (Safaie et al., 2016).

1.1.2 HBV-associated liver diseases

Infection with HBV can have different outcomes that induce distinct kinds of liver diseases. The outcome strongly depends on age and immune status of the patient. While an infection of adults mostly induces a self-limiting acute infection, the virus frequently persists in infants and young children leading to a chronic infection.

1.1.2.1 Acute HBV infection

When adults get infected with HBV, about 95 % of them eliminate the virus. Symptoms range from an asymptomatic infection to a self-limited hepatitis and in rare cases a fulminant hepatitis. In regions with low HBV prevalence as in Europe and North America, the majority of HBV cases are acute infections obtained from unprotected sexual intercourse or injections mostly correlated with drug abuse. Importantly, HBV itself is non-cytopathic. The acute infection is characterized by a strong and polyclonal T-cell response, which induces the observed immune-mediated pathology in the liver due to lysis of HBV-infected hepatocytes. The mortality rate of an acute infection is 0.5 – 1 % due to fulminant hepatitis. (Peeridogaheh et al., 2018)

1.1.2.2 Chronic HBV infection

The serological marker of a chronic hepatitis B (CHB) is the detection of HBsAg in the blood for more than six months. High HBV prevalence is found in Africa and Asia, where infected mothers transmit the virus to the fetus during pregnancy or birth. For young children (ages 1 – 5 years), the risk of failure to eliminate the virus and develop CHB is 30 – 90 %. Beside young children, patients with a weak immune system are at high risk for developing CHB (Peeridogaheh et al., 2018). Chronic HBV infection is a major health concern with estimated 257 million people being chronically infected worldwide. In 2015, 887,000 patients died from HBV-associated liver diseases, namely liver cirrhosis and hepatocellular carcinoma (HCC)

(WHO, 2017) which represents the second leading cause for cancer-related death (Sartorius et al., 2015). Especially in the beginning, the infection is mostly asymptomatic without a high liver damage. In contrast to the acute infection, HBV-specific T cells are scarce and often dysfunctional (Bertoletti et al., 1994; Maini et al., 1999). However, a weak ongoing immune response in the liver is associated with liver fibrosis, cirrhosis and HCC. Within 5 years of infection, 8 – 20 % of patients develop liver cirrhosis, 20 % liver-failure and 1 – 5 % HCC, hence HBV being the leading cause to develop liver cirrhosis (30 % of all liver cirrhosis cases) and HCC (45 % of all HCC cases) (Peeridogaheh et al., 2018).

1.1.3 Hepatocellular carcinoma

Chronic HBV infection increases the risk to develop HCC. Several different promoting mechanisms of HBV infection have been proposed: The viral genome is integrated into the cellular genome in 85 – 90 % of HCC cases (Sung et al., 2012). Due to the integration, the expression of cellular genes can be altered, which potentially results in changes in proliferation if expression of proto-oncogenes is upregulated or downregulated in the case of tumor-suppressor genes. Enhanced proliferation increases the risk for mutations and eventually can lead to carcinogenesis. Furthermore, integration has been suggested to induce genomic instability (Ringehan et al., 2017). As a second mechanism, the viral envelope proteins have been claimed to promote tumorigenesis via the induction of endoplasmic reticulum stress when it accumulates in the cell. If envelope protein is overexpressed in a mouse model, mice show hepatocyte injury, which leads to compensatory proliferation and HCC development (Dunsford et al., 1990). Another HBV protein, namely the non-structural HBx, has also been proposed to promote HCC development. Amongst others, the upregulation of the cellular machinery that induces chromatin opening (Jung et al., 2007) and negative interference with DNA repair mechanisms (Arzumanyan et al., 2013) by HBx have been reported. Moreover, immune-mediated liver damage can drive HCC development. The low degree of immune-mediated liver damage and subsequent compensatory hepatocyte proliferation over years can lead to an increased mutation rate and ultimately HCC.

1.1.4 Prophylaxis and treatment options

An efficient possibility to prevent HBV infection is prophylactic vaccination with recombinant HBsAg, which induces anti-HBsAg antibodies. It has been approved since 1986 and induces protection in more than 95 % of vaccinated people (WHO, 2009). Thus, vaccination could prevent infection in adults if their immune system is not suppressed as upon radiation therapy or immunosuppressive regimens. For immunocompromised patients, as postexposure prophylaxis of unvaccinated individuals or to protect infants from transmission from an infected mother, hepatitis B immunoglobulin as passive vaccination is applied, which is derived from

plasma of vaccinated patients with high anti-HBsAg titers (Peeridogaheh et al., 2018). Active and passive vaccination in combination has shown protection of infants from vertical transmission from their infected mother in about 80 – 95 % of cases if both regimens are applied within a few hours after birth (Kumar et al., 2012).

While there are good options to prevent HBV infection, therapies for the high number of CHB patients are needed. Current approved therapies include two distinct approaches: On the one hand, modulation of the patient's immune system with interferon-α (IFN-α) or pegylated IFN-α (PEG-IFN-α) can help to induce an immune response against the virus. On the other hand, nucleos(t)ide analogs inhibit the HBV polymerase and prevent reverse transcription of pgRNA to rcDNA and thus maturation of capsids. Nucleos(t)ide analogs include lamivudine, telbivudine, entecavir (ETV), adefovir dipivoxil and tenofovir disoproxil fumarate (TDF). ETV and TDF are the most potent inhibitors of HBV polymerase and have a high genetic barrier for the virus to develop drug resistance (Lin et al., 2016; Terrault et al., 2016). Long-term treatment with ETV (Ono et al., 2012) or TDF (Buti et al., 2015) renders HBV undetectable in blood in 90 % of patients with only low incidence of treatment resistant virus strains (Buti et al., 2015; Tenney et al., 2009). Although ETV treatment decreases the risk to develop HCC by 60 %, a significant five to eight fold increased risk remains (Su et al., 2016).

Most guidelines recommend PEG-IFN-α, ETV and TDF as first-line treatment for CHB patients (Terrault et al., 2016). Although the combination therapy is very effective in suppressing viral replication, the cccDNA as template for viral replication is not targeted. As long as it remains in the nucleus of hepatocytes, discontinuation of therapy can lead to a rebound of viremia. The goal of current treatment is a "functional cure", which is defined as undetectable viral DNA and HBsAg in blood ideally followed by anti-HBsAg seroconversion persisting after therapy withdrawal. Functional cure is currently only achieved in one to three percent of patients (Gish et al., 2015). Even the absence of detectable HBsAg has been reported to be inconclusive for total virus elimination since immunosuppressive drugs or radiation therapy, e.g. due to treatment of a hematologic malignancy, can still allow viral reactivation (Perrillo et al., 2015). Taken together, additional treatment strategies are needed to target cccDNA in infected hepatocytes to prevent rebound of virus replication after cessation of antiviral therapy.

CHB patients that develop HCC have a poor prognosis. The only curative options are tumor resection and liver transplantation, but they are only an option for early stage HCC patients (Bruix et al., 2016). The standard of care for patients with more advanced HCC is the tyrosine kinase inhibitor sorafenib. However, sorafenib only provides a survival advantage of a few months and induces various adverse events (Cheng et al., 2009; Llovet et al., 2008). Other tyrosine kinase inhibitors are under clinical investigation but so far have not provided better efficacy and safety profiles. Recently, lenvatinib was approved as alternative first line

treatment, because it passed a non-inferiority trial but also did not enhance overall survival (Kudo et al., 2018).

1.2 The adaptive immune system

The adaptive immune system is the highly specific branch of the immune system and protects us from bacterial, viral and fungal infections as well as from malignantly transformed tumor cells. A vast amount of different specificities of immune effector cells is generated during development of the main cell types responsible for adaptive immunity, namely lymphocytes. B lymphocytes, or B cells, are responsible for humoral immunity against extracellular antigens while T lymphocytes, or T cells, target intracellular antigens via cell-mediated immunity. Both T and B cells originate from multipotent hematopoietic stem cells in the bone marrow. (Murphy and Weaver, 2016)

1.2.1 T cell-mediated immunity

The main populations of T cells are cytotoxic T cells, or $CD8^+$ T cells, and T helper cells, or $CD4^+$ T cells. The latter mostly have supportive function by secreting cytokines to initiate and enhance the function of $CD8^+$ T cells, B cells and the innate immune system. The main focus of this section is cytotoxic $CD8^+$ T cells, which execute the cell-mediated immunity of the adaptive immune system. They migrate through the body to find and eliminate cells that express foreign, intracellular antigens. Due to a distinct T-cell receptor (TCR) each $CD8^+$ T-cell clone has a certain specificity (as described in more details in section 1.3.1) (Murphy and Weaver, 2016).

Both $CD4^+$ and $CD8^+$ T cells need to discriminate between self and non-self-peptides. This is achieved by clonal deletion of T cells with a TCR with high affinity for a self-antigen. During development of the adaptive immune system, progenitors of T cells migrate from the bone marrow to the thymus where they are educated to differentiate between self and non-self-antigens. A vast number of different TCRs is generated by somatic V(D)J recombination of the α and β chain gene loci. Every T cell expressing its highly specific TCR is tested for its affinity towards major histocompatibility complex (MHC) molecules presenting endogenous peptides. Only T-cell progenitors that bind to peptide-MHC complexes with low affinity (= positive selection) but lack high affinity binding to any peptide-MHC complex (= negative selection) differentiate into mature T cells and leave the thymus. By this means most autoreactive T-cell clones are eliminated, and autoimmunity remains a rare event (Murphy and Weaver, 2016).

Upon activation $CD8^+$ T cells have different ways to mediate an immune response. On the one hand they secrete cytokines, e.g. tumor necrosis factor-α (TNF-α) and interferon-γ (IFN-γ), that can induce an upregulation of defense mechanisms in the target cell or make it more sensitive to apoptosis. Cytokines can also stimulate other immune cells to participate in the immune

response and additionally have an autocrine stimulatory effect on $CD8^+$ T cells. On the other hand, $CD8^+$ T cells are able to initiate apoptosis in target cells either by interaction of first apoptosis signal ligand (FasL) and first apoptosis signal receptor (Fas) on the target cell, or by the release of perforin and granzyme B. Both mechanisms activate the caspase cascade in target cells and subsequently lead to apoptosis. Moreover, the activation of $CD8^+$ T cells leads to clonal proliferation and therefore an enhanced immune response (Murphy and Weaver, 2016).

In addition to effector molecules, $CD8^+$ T cells also express molecules that can modulate their function inducing both positive and negative feedback upon activation. Upregulation of CD25, the high affinity interleukin-2 (IL-2) receptor chain allows more efficient binding of IL-2 and thus enhances proliferation. In contrast, expression of programmed cell death protein-1 (PD-1) by activated $CD8^+$ T cells makes them susceptible to inhibition via binding to programmed cell death ligand-1 (PD-L1), which can be expressed by other immune cells, infected target cells or tumor cells. The receptor T-cell immunoglobulin and mucin-domain containing-3 (Tim-3) functions in a similar way as T cells are inhibited upon binding to galectin-9. Another mode of action for T-cell inhibition is the expression of an antagonistic molecule to a costimulatory ligand. Cytotoxic T-lymphocyte-associated protein-4 (CTLA-4) binds to CD80/CD86 on antigen-presenting cells (APCs) with higher affinity than CD28 and therefore prevents costimulation via CD28. Furthermore, CTLA-4 transmits an inhibitory signal itself. $CD8^+$ T cells that express a combination of inhibitory molecules including PD-1, Tim-3 and CTLA-4 are considered to be exhausted (Murphy and Weaver, 2016).

Upon encounter of a foreign antigen, immunological memory is formed. Progeny of previously activated $CD8^+$ T cells differentiate into memory $CD8^+$ T cells, which have the potential to induce a faster immune response upon a second encounter with the same antigen (Murphy and Weaver, 2016). $CD8^+$ T cells are subdivided into four main states of differentiation, namely naïve, central-memory, effector-memory and effector cells, and can be distinguished by certain surface markers. Murine $CD8^+$ T cells are separated into states of differentiation for instance via the molecules CD62L and CD127 (Bachmann et al., 2005).

1.2.1.1 Adaptive immunity by $CD8^+$ T cells in HBV infection

A major difference between acute and chronic HBV infection is the functionality of the $CD8^+$ T-cell responses. While in an acute infection polyspecific and multifunctional HBV-specific T cells can be detected, $CD8^+$ T cells against HBV are scarce, have a narrow specificity and are dysfunctional in chronically infected patients (Bertoletti et al., 1994; Maini et al., 1999). During infection, HBV-specific T cells are enriched in the liver and reduce viral load by two distinct mechanisms: On the one hand, they lyse cells that are infected and thus induce a liver damage (Maini et al., 2000). On the other hand, cytokine-mediated antiviral effects also play a

role in HBV clearance (Guidotti et al., 1999) and studies in HBV-transgenic mice suggested that IFN-γ and TNF-α are mediators for non-cytolytic viral inhibition (Guidotti et al., 1996). Data from our lab provided evidence that IFN-γ and TNF-α execute their effect by inducing cccDNA degradation (Xia et al., 2016). Similar effects can be achieved by IFN-α and lymphotoxin-β (Lucifora et al., 2014).

The liver is an indispensable organ and regulatory mechanisms protect it from extended damage (Knolle and Thimme, 2014). In CHB $CD8^+$ T cells lose their effector functions sequentially, starting with a loss of cytotoxicity and IL-2 production, followed by an impairment to express IFN-γ and TNF-α, ultimately leading to a deletion of $CD8^+$ T cells (Wherry et al., 2007). The remaining cells express exhaustion markers like PD-1, CTLA-4 and Tim-3 (Bengsch et al., 2014; Schurich et al., 2011) and their genome wide expression profile suggests a metabolic impairment that leads to apoptosis (Lopes et al., 2008). Checkpoint inhibition of the PD-1/PD-L1 axis was able to partially restore T-cell function *in vitro* (Boni et al., 2007), enhance the effect of therapeutic vaccination in a woodchuck model (Liu et al., 2014) and increase proliferation and cytokine production of HBV-specific T cells in patients (Fisicaro et al., 2010). Additional stimulation of 4-1BB (CD137) with an agonistic antibody was able to enhance functionality of HBV-specific $CD8^+$ T cells from CHB patients *in vitro* (Fisicaro et al., 2012). Furthermore, regulatory T cells (Tregs) were shown to contribute to viral persistence as they can be detected in increased numbers (Stoop et al., 2005) and their depletion can enhance HBV-specific $CD8^+$ T-cell responses (Furuichi et al., 2005). In patients with HBV-associated HCC Tregs suppressed the anti-tumor response via the immunomodulatory cytokine interleukin-10 (IL-10) (Meng et al., 2017; Sharma et al., 2015; Shi et al., 2015). The influence of IL-10 was further emphasized by studies that suggested an association of IL-10 promoter polymorphisms with CHB (Moudi et al., 2016) and subsequent disease development upon CHB (Miyazoe et al., 2002). However, the effect of IL-10 is controversial and other data indicated that it supports immunopathology by inhibition of antigen-induced apoptosis of $CD8^+$ T cells (Fioravanti et al., 2017).

1.2.2 B cell-mediated immunity

In contrast to T cells, B cells target extracellular antigens. During maturation, each B cell develops a unique B-cell receptor (BCR) by somatic recombination similar to the process of TCR generation in T cells. The BCR consists of a heavy and a light chain both contributing to its specificity. Upon BCR binding to its cognate antigen and appropriate help from $CD4^+$ T cells, the B cell releases a soluble variant of the BCR, namely antibodies, also known as immunoglobulins. The released antibodies bind to the antigen which leads to elimination of the antigen. This can be achieved in several ways depending on the type of antigen. Firstly, antibody and antigen can form complexes that can activate the complement system. In the

case of bacteria or cells with bound antibodies complement activation leads to a disruption of the membrane and causes cell lysis. Small immune complexes are taken up by phagocytic cells via binding of complement to complement receptors or antibodies to Fc-receptors. Secondly, without complement activation, cell bound antibodies can activate natural killer (NK) cells through Fc-receptor binding and subsequently induce target cell lysis (Murphy and Weaver, 2016).

1.3 Adoptive T-cell therapy

T cell-mediated immunity has the potential to specifically target and eliminate cells that express a certain antigen. Targets can be cells that are infected with a virus and express proteins from the viral genome that are recognized as foreign. Furthermore, cancer cells can trigger an immune response due to mutations in endogenous proteins generating neoepitopes (Murphy and Weaver, 2016). However, the immune system sometimes fails to eliminate all infected or malignantly transformed cells because of inhibition or deletion of T cells that can recognize the foreign antigen. Moreover, not all tumor cells express and present neoepitopes and are therefore not susceptible to elimination by T cells. Many tumor cells exhibit an altered

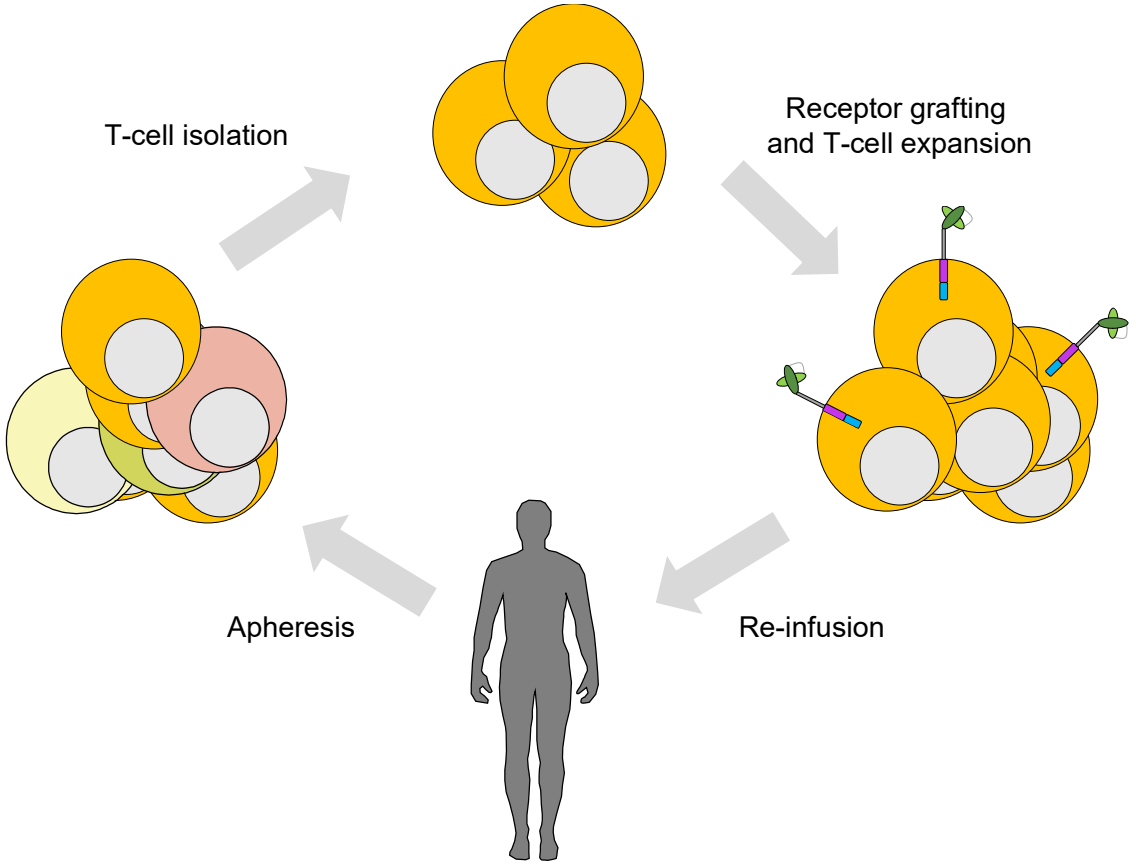

Figure 1.2 Principle of adoptive T-cell therapy.
PBMC are isolated from a patient by apheresis followed by potential isolation of T-cell subtypes. T-cells are then grafted with a receptor to confer a new specificity and expanded. Eventually, redirected T cells are re-infused into the patient to combat the corresponding disease.

expression level of endogenous proteins, so called tumor antigens. This can be proteins that are also expressed in healthy tissue but at a lower level, or proteins that are physiologically expressed exclusively during embryogenesis and early development (Bonini and Mondino, 2015). Tumor cells often cannot be recognized by T cells according to their tumor antigens because T-cell specificities against endogenous proteins are eliminated during T-cell development in the thymus (Linnemann et al., 2014).

Adoptive T-cell therapy tries to combat these issues by giving endogenous T cells a new specificity. The principle of this therapeutic approach is depicted in Figure 1.2. To treat a patient of a particular disease, peripheral blood mononuclear cells (PBMC) are extracted from the patient by apheresis. In the laboratory total PBMC can be used or a certain subtype of cells, e.g. $CD8^+$ or $CD4^+$ T cells can be isolated via magnetic-activated cell sorting (MACS) or fluorescence-activated cell sorting (FACS), and the cells are equipped with a new receptor. Different kinds of receptors can be delivered, either a natural TCR (section 1.3.1) that has been isolated elsewhere or an artificial receptor (section 1.3.2) (Levine et al., 2017). Various methods have been described to deliver the new receptor. Retroviral transduction is a common method which allows stable expression of the receptor because the retroviral genome is integrated into the host genome (Engels et al., 2003). This method relies on activation of T cells because only proliferating cells can be transduced by a retrovirus. Stable integration methods that can dispense T-cell activation include lentiviral vectors and *Sleeping Beauty* systems using minicircle vectors (Clauss et al., 2018; Monjezi et al., 2017). For transient expression messenger RNA transfection methods have been described (Birkholz et al., 2009). It is important to note that all the mentioned methods deliver the new receptor in addition to the already existing endogenous TCR. Due to safety concern methods have been established to prevent expression of the endogenous TCR thus only the new receptor is expressed (Bunse et al., 2014; Eyquem et al., 2017; Kamiya et al., 2018; MacLeod et al., 2017; Van Caeneghem et al., 2017). Once T cells express the new receptor, they can be expanded and eventually be re-infused into the patient. Due to their new specificity redirected T cells should be able to detect a particular antigen on target cells and reduce burden of an infection or a tumor.

1.3.1 TCR composition and signaling

The TCR is composed of an α and a β chain with a hypervariable domain in the extracellular part. TCRs recognize processed peptides presented on MHC class I molecules. In humans the MHC is termed human leukocyte antigen (HLA). All nucleated cells present peptides from intracellular proteins on MHC class I molecules and $CD8^+$ T cells can differentiate between self- and non-self-derived peptides and thus detect infected or malignant cells. The TCR of $CD4^+$ T cells in contrast recognizes processed extracellular peptides presented on MHC class II by APCs. The α and β chains lack intracellular signaling domains and associate with

the CD3 complex, which consists of one CD3γ chain, one CD3δ chain, and two CD3ε as well as two CD3ζ chains (Figure 1.3). Immunoreceptor tyrosine-based activation motifs (ITAMs) in the CD3 chains are responsible for signal transduction, with one ITAM in each CD3γ, CD3δ and CD3ε chain, and three ITAM in each CD3ζ chain. Upon binding its cognate peptide-MHC complex, the TCR is engaged and the T cell activated through the CD3 complex. This activation signal is considered as “signal 1”. Additional signals are necessary for a complete activation of the T cell. “Signal 2” can be delivered from APCs, namely dendritic cells (DCs), macrophages, and B cells, which express costimulatory molecules like CD80/CD86, 4-1BB ligand or OX40 ligand, which activate CD28, 4-1BB or OX40 (CD134) on the T cell, respectively. Furthermore, cytokines (e.g. IL-2, IL-12, IL-18, etc.) binding to their cognate receptor on the T cell transmit “signal 3”. If all signals are present, the T cell is fully activated and initiates its executive T-cell functions (Murphy and Weaver, 2016).

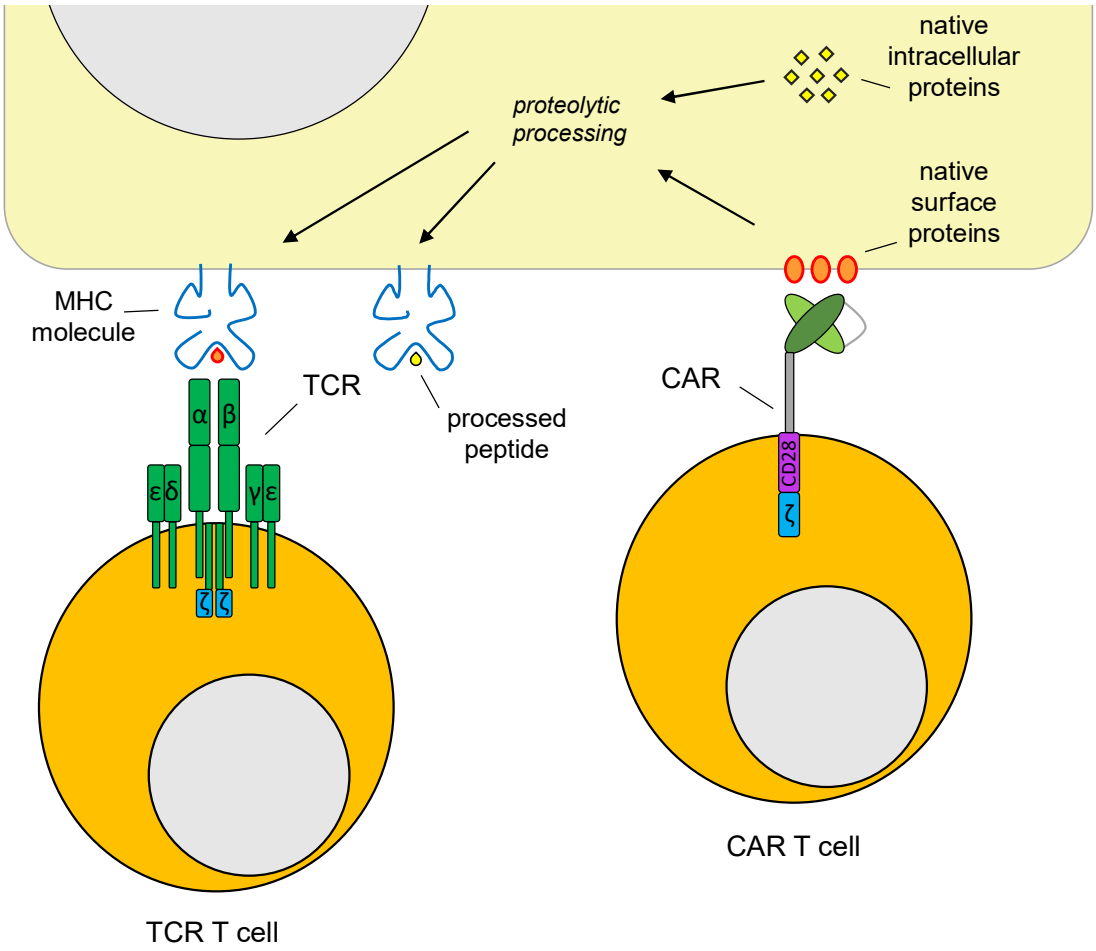

Figure 1.3 Antigen detection by TCR and CAR T cells.
Schematic representation depicting the difference in antigen recognition between TCR and CAR T cells. For the detection by a TCR T cell both surface and intracellular proteins can be proteolytically processed and presented as peptides on MHC molecules. Each TCR is restricted to a specific MHC molecule and can detect peptides in its context. CAR T cells in contrast bind to unprocessed native antigen on the target cell surface and cannot be directed against intracellular proteins.

1.3.2 Chimeric antigen receptor

Chimeric antigen receptors (CARs) are an artificial approach to give immune cells, e.g. $CD8^+$ T cells, a new specificity. The first CAR was described almost 30 years ago (Gross et al., 1989) and since then intensive studies have provided advances leading to the first clinically approved therapeutics against certain $CD19^+$ hematological malignancies in 2017 (Brower, 2017; Mullard, 2017). In contrast to natural TCRs, CARs detect native antigens without peptide presentation on MHC and can therefore be applied to all patients independent of their haplotype. Thus, CARs can only be directed towards cell surface proteins, while TCRs can also detect processed peptides from intracellular proteins when presented on MHC (Figure 1.3) (Harris and Kranz, 2016). Beside the CD19-specific CAR against hematological malignancies of the B-cell lineage (Kochenderfer et al., 2009; Milone et al., 2009), several other CARs have been described, including specificity for tumor antigens such as carcinoembryonic antigen (CEA) (Burga et al., 2015), GD2 (Richman et al., 2018), ErbB2 (Morgan et al., 2010), prostate-specific membrane antigen (PSMA) (Zhong et al., 2010) and glypican-3 (Chen et al., 2017; Gao et al., 2014) as well as for viral proteins of human immunodeficiency virus (HIV) (Hale et al., 2017; Leibman et al., 2017), HBV (Bohne et al., 2008) and hepatitis C virus (Sautto et al., 2016).

1.3.2.1 Design of CARs

A CAR is a chimeric protein that links the binding specificity of an antibody to domains that induce T-cell activation. A single chain variable fragment (scFv) is constructed from the variable domains of the heavy and light chain from an antibody of the desired specificity. Both domains are connected via a flexible linker, e.g. a glycine-serine linker (Figure 1.4 A) (Jensen and Riddell, 2014). The origin of the scFv plays an important role for clinical application. If the scFv was derived from a murine antibody, patients can develop an immune response against the alloantigen expressed on redirected T cells, which limits their engraftment and persistence (Lamers et al., 2011; Turtle et al., 2016). This can be overcome by the usage of a fully human scFv (Sommermeyer et al., 2017). The scFv is connected to the cell membrane of the T cell via an extracellular spacer that is often derived from an immunoglobulin. The length of the spacer can have an impact on the activity of the CAR because it influences the distance between effector and target cell (Hudecek et al., 2015). Furthermore, it was shown that CARs with a wildtype immunoglobulin G (IgG) spacer, that is able to bind to Fc-receptors, display a decreased survival *in vivo*. Prevention of Fc-receptor binding can enhance the effect of redirected T cells (Almasbak et al., 2015; Hudecek et al., 2015; Jonnalagadda et al., 2015).

Beside variations in specificity as well as length and origin of the extracellular spacer, reported CARs differ in their intracellular signaling domains. Depending on the kind and number of signaling domains, CARs have been grouped into different generations: The 1st generation of

CARs contain only the signaling domain of CD3ζ to activate T cells. The domain transmits a signal into the cell which is comparable to the signal upon TCR:CD3 complex engagement. *In vitro* these kinds of CARs display redirection potential, but the *in vivo* effect is very limited (Jensen and Riddell, 2014). This has been attributed to activation-induced cell death (AICD) and weak proliferation due to the lack of a costimulatory signal (Khalil et al., 2016). The issue has been solved by including a costimulatory domain, mostly from CD28 or 4-1BB in the 2nd generation of CARs. Due to the costimulatory domain, 2nd generation CARs display a more pronounced *in vivo* functionality. In CARs of the 3rd generation two costimulatory domains are included (Figure 1.4 B) (Jensen and Riddell, 2014).

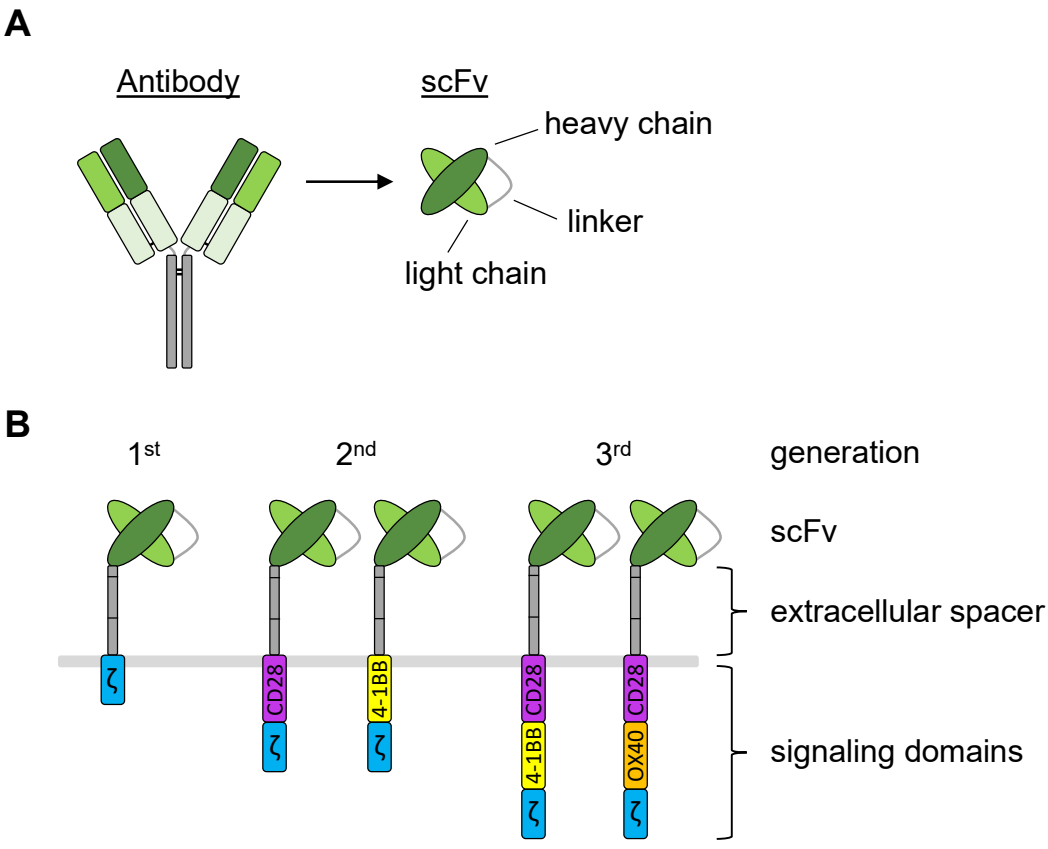

Figure 1.4 Design of chimeric antigen receptors.
A) A single chain variable fragment (scFv) is constructed from the variable domain of the heavy and light chains of an antibody that are connected via a linker. **B)** Schematic representation of different CAR generations. The scFv is connected via an extracellular spacer (e.g. IgG hinge-CH2-CH3, CD8) to signaling domains of CD3ζ (1st generation) or together with one (2nd generation) or two (3rd generation) costimulatory signaling domains (e.g. CD28, 4-1BB, OX40, etc.).

1.3.2.2 Costimulatory signaling domains

The incorporation of a costimulatory domain in the CAR was shown to provide a therapeutic advantage in comparison to 1st generation CARs (Imai et al., 2004; Kowolik et al., 2006). Different signal domains and their combinations will activate the T cell in a different manner leading to differences in T-cell functionality. The incorporation of CD3ζ is common in CAR design and a lot of different costimulatory signaling domains have been tested, most commonly CD28 and 4-1BB. Both CARs that are clinically approved at this time are from the 2nd generation, one of them with 4-1BB (Brower, 2017) and the other with CD28 costimulation (Mullard, 2017). Physiologically, CD28 is constitutively expressed on naïve T cells and provides costimulation upon binding to CD80/CD86 on APCs. In contrast, 4-1BB is only expressed upon T-cell activation and thus physiologically functions as a secondary costimulation upon binding its ligand 4-1BBL after T cells have already been activated (Pollok et al., 1993). Signaling through 4-1BB induces T-cell proliferation, enhances the production of IL-2 and inhibits apoptosis (Lee et al., 2002). The application of agonistic anti-4-1BB antibodies can enhance endogenous $CD4^+$ and $CD8^+$ T-cell responses against tumors (Melero et al., 1997). When 4-1BB is incorporated into anti-mesothelin or anti-folate receptor-α CARs, it provides an appropriate signal to allow expansion and persistence of redirected T cells, which in turn exhibit a more pronounced anti-tumor activity (Carpenito et al., 2009; Song et al., 2011).

Another costimulatory domain used in CARs is OX40. Comparable to the physiological expression pattern of 4-1BB, OX40 is also expressed upon activation of T cells and can provide secondary costimulation (Murphy and Weaver, 2016). Treatment with agonistic anti-OX40 antibodies provided evidence that OX40 activation can enable a dormant immune system to fight an infection and cancer (Humphreys et al., 2007; Weinberg et al., 2000). Anti-OX40 antibody treatment enhanced memory T-cell survival and the recall responses upon a second antigen encounter (Ruby et al., 2007). Incorporation of the OX40 signaling domain into an anti-CEA CAR induce an improved antitumor response (Hombach and Abken, 2011). Other costimulatory domains used in CARs are the inducible T-cell costimulator (ICOS) (Guedan et al., 2018; Shen et al., 2013) and CD27 (Song et al., 2012). Recently, the incorporation of a new type of costimulatory domain from IL-2 receptor-β was described for the first time. Induction of the JAK-STAT (janus kinase - signal transducer and activator of transcription proteins) signaling cascade downstream of the cytokine receptor domain provides better efficacy of CAR T cells in both liquid and solid tumor models (Kagoya et al., 2018).

In 3rd generation CARs two costimulatory signaling domains are incorporated. The idea is that they provide redirected T cells with the advantages of both signaling domains. A CAR containing costimulation from both CD28 and OX40 induced pronounced T-cell responses while it prevented their AICD as seen in a 2nd generation CD28 CAR (Hombach and Abken,

2011). This provided better tumor infiltration *in vivo* and prevented apoptosis of transferred cells (Hombach et al., 2013). In addition, OX40 costimulation prevented the expression of the inhibitory cytokine IL-10 upon CD28 signaling in $CD4^+$ T cells (Hombach et al., 2012). Costimulation of both CD28 and 4-1BB in one CAR was also reported to be beneficial because of increased cytokine release, *in vivo* T-cell survival and anti-tumor efficacy, which was in part contributed to lower induction of apoptosis (Zhong et al., 2010).

1.3.3 *In vivo* models to study CAR T-cell therapy

Preclinical *in vivo* studies investigating efficacy and safety of CAR T-cell approaches are mostly performed in mouse models. They differ largely in the species origin of CAR T cells and tumor cells as well as in the composition of endogenous immune cells. Murine models may e.g. be syngenic, transgenic, xenograft and humanized models.

In syngenic models CAR T cells and tumor cells are of murine origin. Furthermore, the studies are performed in the context of an endogenous immune system, which can influence both efficacy and safety of the approach. Here, the study of on-target off-tumor toxicity is possible if the target antigen is also expressed in healthy tissue. If both CAR T cells and healthy target cells are from the same species, T-cell effector functions through Fas/FasL interaction and perforin/granzyme B secretion can induce target cell lysis to the full extent (Siegler and Wang, 2018). A study could demonstrate that NKG2D-CAR T cells display lethal toxicity in a syngenic mouse model, while there were no side effects observed in a xenograft model (VanSeggelen et al., 2015). Moreover, the behavior of endogenous immune cells upon CAR T-cell therapy can be investigated in a syngenic mouse model. Thus, another investigation with NKG2D-CAR T cells revealed that cytokines of CAR T cells activate myeloid cells that subsequently promote tumor rejection (Spear et al., 2012). However, many differences between the murine and human immune system have been described and therefore the transfer of results from syngenic or transgenic mouse models to the human setting needs to be done with caution (Mestas and Hughes, 2004).

Like syngenic ones, transgenic mouse models also contain murine CAR T cells, tumor cells, and endogenous immune cells, but the tumor antigen is of human origin. Usually mice exhibit a knockout of the murine genes while the human one is knocked-in. Under these conditions a CAR specific for a human tumor antigen can be studied in an immunocompetent host. However, up to now, most transgenic mouse models for instance for human CEA and ErbB2 have underestimated on-target off-tumor effects, and only one of three and one of four, respectively, recapitulated the clinically observed severity of side effects (Siegler and Wang, 2018).

The most common preclinical models to study CAR T-cell therapies are xenograft models, which use immunodeficient mice injected with human tumor and CAR T cells for proof-of-concept studies. Currently, many studies utilize NOD-SCID-IL-2Rγnull (NSG) mice in which the interaction of transplanted human effector and target cells can be studied. However, the effect is studied under non-physiological conditions since the model lacks any interaction with other immune cells or healthy human tissue. This virtual vacuum can influence CAR T-cell engraftment, the therapeutic effect as well as safety, and therefore results cannot be easily transferred to the clinical situation (Siegler and Wang, 2018). Nevertheless, a xenograft model is meaningful to study for instance CAR T cells that constitutively express human cytokines (Markley and Sadelain, 2010). Furthermore, immunodeficient mouse models allow the usage of patient-derived tumor xenografts as personalized target (Zhao et al., 2010).

A more sophisticated mouse model to study the interaction of human tumor and CAR T cells are humanized mice, which harbor, depending on the model, a functional endogenous human immune system to a greater of lesser extent. In one model, NSG mice are transplanted with human hematopoietic stem cells. Because these mice do not contain a thymus, T-cell development is not complete (Wege, 2018). Another more complicated possibility is the BLT (bone marrow, liver, thymus) model. Here, human fetal bone marrow, liver and thymus tissue are transplanted and allow the generation of a better developed T-cell compartment (Holzapfel et al., 2015). BLT mice have been utilized to study a CAR T-cell approach for the treatment of HIV infection (Zhen et al., 2015).

Since the immune system of humans and non-human primates (NHPs) are closely related, NHP models are suitable to study especially cytokine release syndrome (CRS) and neurotoxicity of CAR T-cell approaches, which are only poorly recapitulated by mouse models. After investigating efficacy of an approach in mouse models, the study in NHPs can yield a better understanding of the safety profile. The shortcoming of NHP models is the low number of animals that can be used in the investigation (Siegler and Wang, 2018). In a recent study a model for CRS and neurotoxicity with CD20-specific CAR T cells was established hopefully providing a better understanding of the nature of these serious adverse events (Taraseviciute et al., 2018). Other studies have investigated the functionality of CARs specific for ROR1 (Berger et al., 2015), HIV (Zhen et al., 2017), CD127 (Kunkele et al., 2017) and ErbB2 (Nellan et al., 2018).

1.3.4 Clinical application of CAR T cells

CAR T-cell therapy has reached clinical application in numerous trials. As of 2016, 220 CAR T-cell trials were documented, 188 of them were still ongoing (Hartmann et al., 2017). It has shown substantial results in treatment resistant B-cell leukemia and lymphoma. Interestingly, results of the first two trials, almost 20 years ago, were not very promising. Treatment of

ovarian cancer or metastatic renal cell carcinoma with CAR T cells did not result in any anti-tumor response (Kershaw et al., 2006; Lamers et al., 2006). The breakthrough was achieved with a very effective CAR directed against CD19, which can target different hematological malignancies of the B-cell lineage, including acute lymphocytic leukemia (ALL), chronic lymphocytic leukemia (CLL), and non-Hodgkin lymphoma (NHL). The results of anti-CD19 CAR T-cell treatment have been impressive. Of 243 anti-CD19 CAR T cell-treated patients, 60 % had an objective response. In some trials, even 85 % of patients reached complete response. The patient population usually consists of highly pretreated patients that have not responded to previous standard treatment regimens or had suffered from disease progression after an initial response (Hartmann et al., 2017). The conducted trials are almost exclusively single-armed and do not compare the therapy outcome with the standard treatment. However, comparison to the retrospective SCHOLAR-1 trial, which summarized the prognosis of NHL patients under standard treatment indicates the substantial benefit of anti-CD19 CAR T-cell therapy (Crump et al., 2017). A recent study directly compared anti-CD19 CAR T-cell therapy with chemotherapy in ALL patients indicating a tremendously increased 12-month survival rate (60.9 % vs. 10.1 %) (Wei et al., 2018). Comparing the therapeutic effects towards different $CD19^+$ hematological malignancies, the strongest effect is observed in ALL, followed by NHL, and the least effect in CLL patients (Hartmann et al., 2017).

While showing promising therapeutic success, CAR T-cell therapy may be also dangerous and a high portion of patients suffer from serious side effects (Neelapu et al., 2017). The most severe ones are CRS and neurotoxicity, which have led to the death of several patients. Both of them seem to be induced by IL-6 and IL-1 of macrophage origin upon CAR T-cell therapy as reported recently by two groups (Giavridis et al., 2018; Norelli et al., 2018). The origin of neurotoxicity, manifesting as e.g. encephalopathy, aphasia, somnolence and tremor, has not been fully understood. A disruption of the blood–brain barrier upon cytokine-induced endothelial cell activation in the central nervous system seems to play a role (Gust et al., 2017; Mackall and Miklos, 2017). As treatment of severe CRS and neurotoxicity administration of the antagonistic anti-IL-6 receptor antibody tocilizumab has been approved (Le et al., 2018) and is able to reduce the symptoms while not influencing CAR T-cell persistence or the response rate (Davila et al., 2014; Maude et al., 2014; Neelapu et al., 2017).

In 2017, two anti-CD19 CAR T-cell therapies received clinical approval by the U.S. Food and Drug Administration (FDA), namely CTL019 by Novartis (Brower, 2017) and KTE-C19 by Kite Pharma, a Gilead company (Mullard, 2017). The multicenter ZUMA-1 trial with 22 institutions, which investigated KTE-C19, revealed that the production in a centralized facility and safe administration is feasible and could obtain response rates comparable to previous reports from single institution trials (Neelapu et al., 2017). Similar results were seen in a smaller trial investigating CTL019 (Schuster et al., 2017). The third main competitor in the field is Juno

Therapeutics, which was recently acquired by Celgene. Their anti-CD19 CAR T-cell product JCAR-017 is still in clinical trials and has not yet received FDA approval.

While anti-CD19 CAR T cells perform consistently well in the clinics, very little encouraging data has been published about CAR T cells directed against solid tumors. Remissions have only been observed in single patients (Hartmann et al., 2017). One exception is a GD2-specific CAR: In a phase I clinical trial the authors observed a complete response of more than 50 % in neuroblastoma patients (Louis et al., 2011). The lower therapeutic effect of CAR T cells in solid tumors in comparison to $CD19^+$ hematological malignancies has been mostly attributed to the necessity of T cells to penetrate the tumor tissue and the hostile microenvironment in solid tumors. Several approaches aim at solving these issues and will likely lead to more effective CAR T-cell therapies in the future.

1.3.5 CAR T-cell therapy of CHB and HBV-associated HCC

Clinical observations provide evidence that CHB patients and patients with HBV-associated HCC could benefit from HBV-specific T-cell therapy. A recent report suggested that discontinuation of therapy with nucleos(t)ide analogs is safe if functional T cells can be detected and they will subsequently control the virus (Rivino et al., 2018). Furthermore, case reports indicated that CHB patients with leukemia were able to eliminate the virus upon bone marrow transplant form a donor with HBV-specific T-cell responses (Ilan et al., 1993; Lau et al., 1997). HBV-specific TCRs have been identified and if they were expressed in T cells, they exhibited an antiviral effect both *in vitro* (Gehring et al., 2011; Wisskirchen et al., 2017) and in humanized mice *in vivo* (Kah et al., 2017). The feasibility of this approach was shown in an HCC patient who upon T-cell therapy showed a substantial response in serum HBsAg levels before the disease eventually progressed (Qasim et al., 2015).

As previously reported, CHB patients under potent antiviral therapy still retain a large number of S protein expressing hepatocytes (5 – 30 %) (Wursthorn et al., 2006). Since S protein is also expressed on the plasma membrane of HBV-infected cells and HBV-associated HCC (Safaie et al., 2016) it is a suitable target protein for a CAR T-cell therapy. In previous work a scFv specific for the S-domain of all three HBV envelope proteins was isolated from a scFv library derived from HBsAg-vaccinated individuals (Kürschner, 2000). The scFv, termed C8, was incorporated into a 2^{nd} generation CAR (S-CAR) harboring an IgG1 spacer and signal domains of CD3ζ and CD28. *In vitro* experiments revealed that the S-CAR can redirect human T cells towards HBV-replicating hepatoma cells and HBV-infected primary human hepatocytes. Expression of cytokines and target cell lysis was induced and infected cells cultures were cured from HBV (Bohne et al., 2008). Further *in vivo* studies revealed that S-CAR-redirected murine $CD8^+$ T cells specifically home to the liver of HBV-transgenic mice and induce a transient mild to moderate liver damage. HBV DNA and cytoplasmic HBc in the

liver as well as viral parameters in the serum decreased upon CAR T-cell therapy but rose again after S-CAR T cells vanished from treated mice (Krebs et al., 2013). In contrast to adoptive T-cell therapy utilizing HBV-specific TCRs, the S-CAR functions independent of HLA. Thus, while TCR-redirected T cells can only be applied to patients who express the correct HLA molecule, S-CAR T-cell therapy could benefit all patients with CHB or HBV-associated HCC who express sufficient amounts of surface S protein on hepatocytes.

1.4 Aims of this thesis

Chronic HBV infection and HBV-associated HCC are a remaining major health concern with limited treatment options and rarely can be cured. Adoptive T-cell therapy utilizing a CAR to redirect T cells towards infected cells is a promising approach that could enhance therapeutic outcome. A CAR specific for the S-domain of HBV envelope proteins has been developed and studied both *in vitro* and *in vivo* in an HBV-transgenic mouse model. Studies indicated that the *in vivo* therapeutic effect was only transient, and viremia recurred after contraction of S-CAR T cells.

The first question addressed in this thesis was which underlying mechanisms caused the observed limited antiviral effect *in vivo*. To this end, sequential transfers of S-CAR T cells should be performed, and the influence of the endogenous adaptive immune system investigated. Utilizing the newly obtained knowledge, modifications of the mouse model should be employed that would allow a better understanding of efficacy and safety of S-CAR T-cell therapy *in vivo*.

Since the antiviral effect was still limited after modifications of the mouse model in the first part of this thesis, I investigated possibilities to improve the therapeutic outcome. In the second part, I asked which 2nd and 3rd generation S-CARs harboring alternative costimulatory domains exhibited the strongest antiviral effect. Different variants of the S-CAR should be generated and compared regarding their potential to redirect human and murine T cells *in vitro* and in mice *in vivo*. This investigation should permit selection of a construct, which should be used in future studies.

In the third part, I examined if checkpoint inhibition of the immune-regulatory molecules PD-1 an IL-10 as well as intrahepatic immune stimulation by CpG could enhance the functionality of transferred S-CAR T cells. The results should highlight if the tested approaches could be beneficial as combinatory treatment with S-CAR T cells in clinical application.

In the fourth part of this thesis, I aimed at establishing transduction and co-culture settings to investigate rhesus macaque S-CAR T cells *in vitro*. Expression of the S-CAR in macaque T cells and its functionality in the latter should be explored. This work should prepare future studies of S-CAR T-cell functionality and safety of this approach in HBV-infected rhesus macaques *in vivo*.

2 Results

2.1 Improvement of mouse model to study S-CAR T-cell therapy

Previous results from our laboratory indicated that the S-CAR could redirect T cells towards and cure HBV-infected hepatocytes (Bohne et al., 2008). Furthermore, *in vivo* application of S-CAR-redirected T cells into HBV-transgenic mice induced a significant, but transient antiviral effect (Krebs et al., 2013). HBV-transgenic mice are a suitable model to investigate therapeutic approaches targeting HBV infection *in vivo* because they replicate HBV constantly in the liver without induction of an immune response. This mimics a chronic HBV infection in humans although the infection due to the transgenic nature of the model cannot be cured. T-cell transfer experiments in this model have shown that after initial T-cell expansion and an efficient antiviral effect, S-CAR T cells vanish, and viral parameters rise again. The following experiments aim at explaining this phenomenon and describe a solution for more sustained T-cell transfer studies.

2.1.1 Serial transfer of S-CAR T cells into immunocompetent mice does not induce a sustained antiviral effect

The observed vanishing of S-CAR T cells approximately two weeks after transfer (Krebs et al., 2013) could be due to T-cell exhaustion or AICD. To this end, I investigated whether a second transfer of S-CAR T cells could lead to a more sustained antiviral effect. Therefore, I engineered murine $CD8^+$ T cells to express the S-CAR and transferred them sequentially on day 0 and day 20 into HBV-transgenic mice. A second group of mice received the T-cell product only on day 20 (Figure 2.1 A). The rate of $CD8^+$ T cells expressing the S-CAR after retroviral transduction was about 60 % at both transfer time points (Figure 2.1 B). Donor cells carried the congenic marker CD45.1 to differentiate transferred cells from the endogenous $CD45.2^+$ cells. I detected total transferred cells on day 25 in peripheral blood in comparable concentrations in both groups (Figure 2.1 C). However, liver damage indicated by a rise of serum alanine amino transferase (ALT) levels five to seven days later was exclusively detected after the first but not after the second transfer of S-CAR T cells (Figure 2.1 D). Notably, S-CAR-expressing T cells could only be detected after the first but not after the second transfer (Figure 2.1 E). Upon isolation of lymphocytes from spleen and liver on day 33, cells were rested overnight (phosphate-buffered saline = PBS), cultured on plate-bound HBsAg or anti-CD3/anti-CD28 antibodies (Figure 2.1 F). HBsAg-specific activation of transferred cells from neither liver nor spleen could be detected by intracellular cytokine staining (ICS). In contrast, via quantitative polymerase chain reaction (qPCR) analysis I detected low numbers of S-CAR integrates in both liver and spleen tissue on day 33 in both groups (Figure 2.1 G). The qPCR result indicated that a low number of S-CAR T cells persisted *in vivo* although they were below

the limit of detection for flow cytometry-based assays (Figure 2.1 E and F). The absence of transduced cells as well as the absence of a liver damage upon a second adoptive transfer of S-CAR T cells suggested alternative mechanism for treatment failure than T-cell exhaustion and AICD.

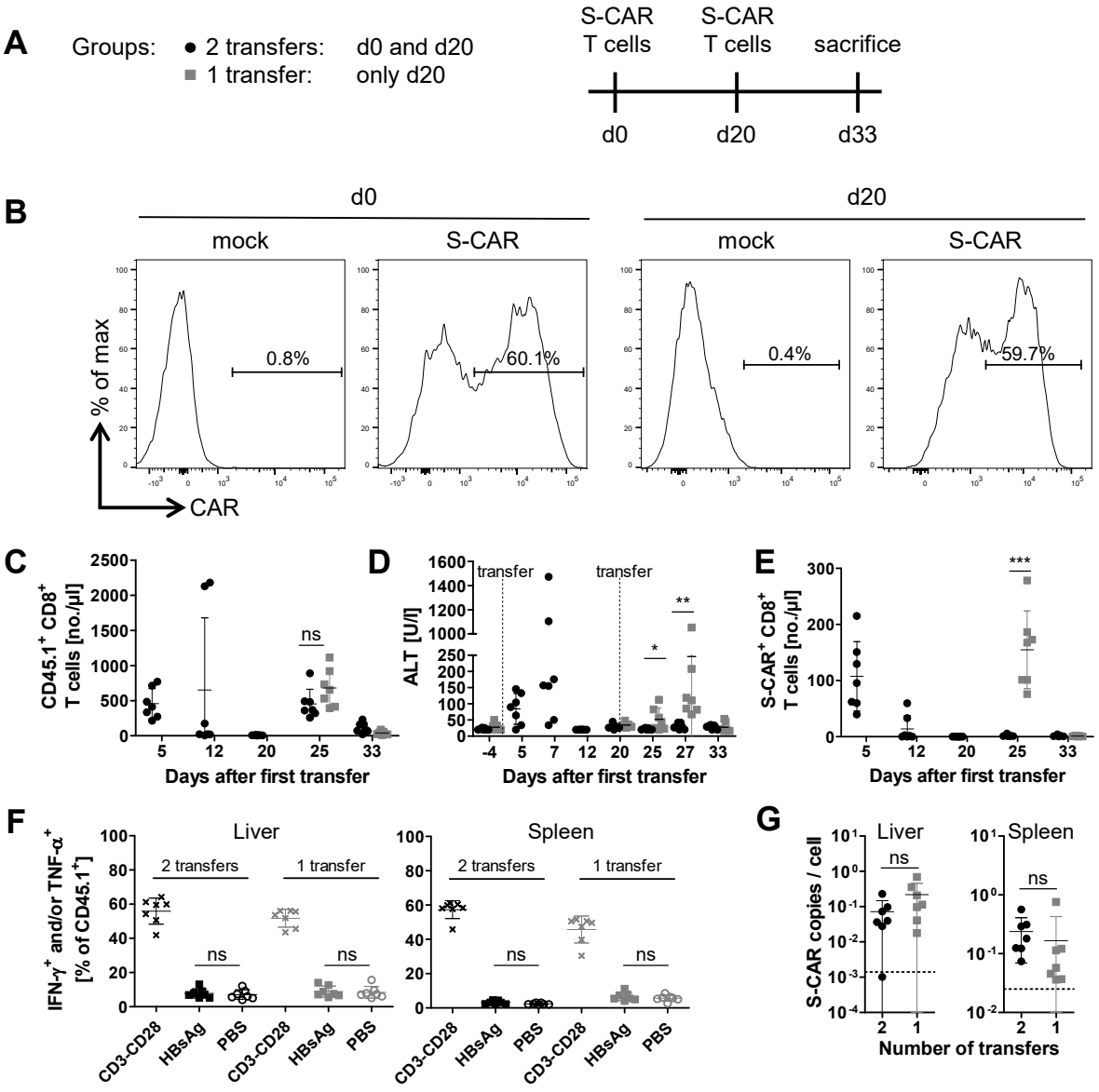

Figure 2.1 Two sequential transfers of S-CAR T cells into HBV-transgenic mice.
A) 4 x 10^6 CD45.1$^+$ S-CAR T cells were transferred twice (d0 and d20) or only once (d20) into CD45.2$^+$HBV-transgenic mice. CD45.1$^+$ cells in peripheral blood and serum parameters were monitored over time. **B)** Flow cytometry plot of CD8$^+$ T cells before each transfer. **C)** Concentration of CD45.1$^+$ CD8$^+$ T cells in peripheral blood. **D)** Serum ALT levels monitored over time. **E)** Concentration of S-CAR$^+$ CD8$^+$ T cells in peripheral blood. **F)** Lymphocytes were isolated from liver and spleen on day 33 and cultured on anti-CD3/anti-CD28 antibody-coated, HBsAg-coated or PBS control plates overnight. Transferred cells were identified by CD45.1 and expression of intracellular cytokines was analyzed via flow cytometry the following day. **G)** qPCR analysis of genomic S-CAR copies in liver and spleen on day 33 normalized to the single copy gene *PRNP*. All data are presented as values of single mice and mean values ± SD. (n=7; Mann Whitney test, ns = not significant, * = p<0.05, ** = p<0.01, *** = p<0.001)

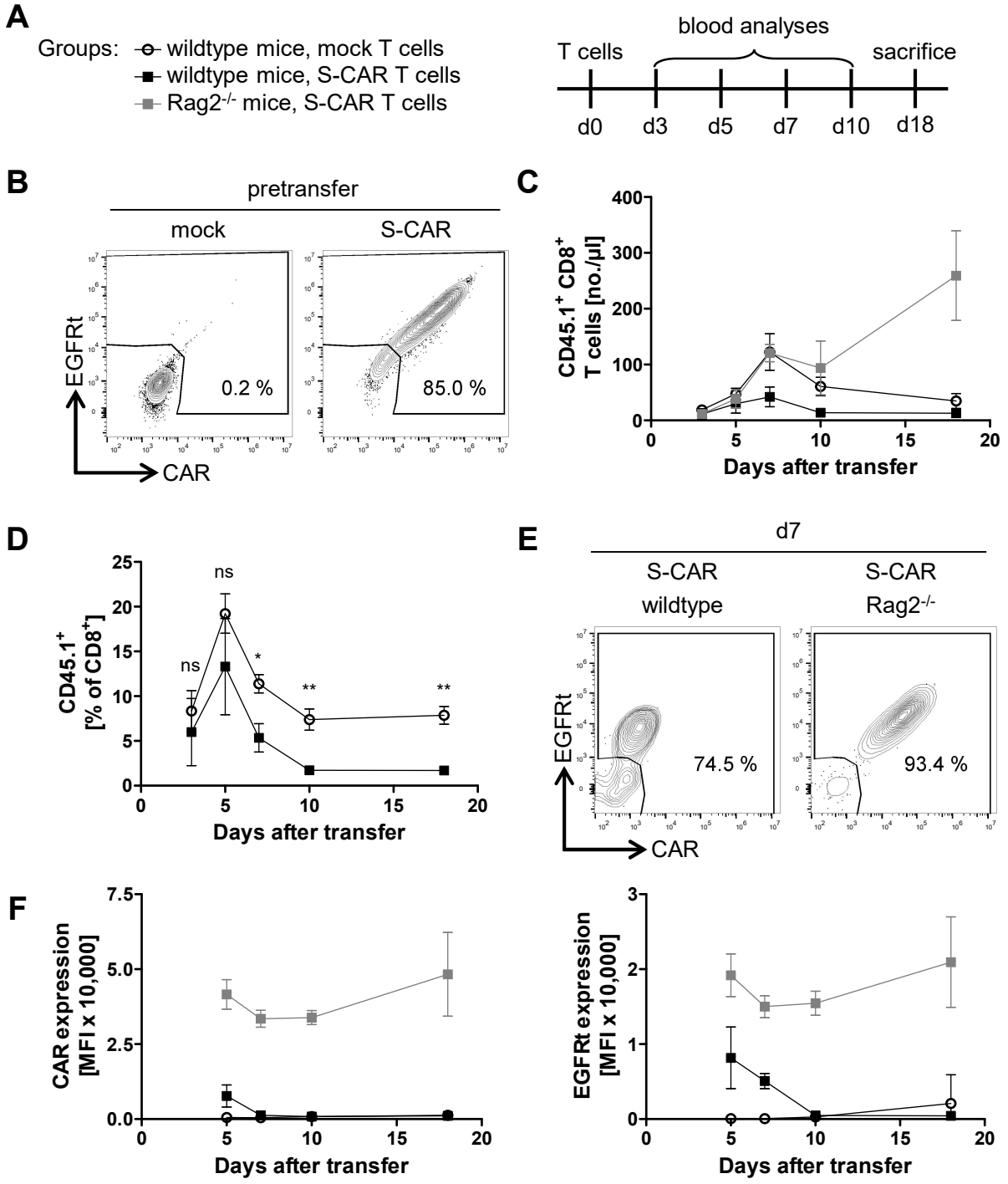

Figure 2.2 Influence of the adaptive immune system on S-CAR T-cell persistence.
A) 2.7 x 10^6 CD45.1$^+$ S-CAR$^+$ and EGFR$^+$ T cells or mock cells were transferred into CD45.2$^+$ wildtype C57BL/6 (n=5 per group) or Rag2$^{-/-}$ (n=3) mice. CD45.1$^+$ cells in peripheral blood were monitored over time by flow cytometry. **B)** Flow cytometry plot of CD8$^+$ T cells on day of transfer. **C)** Concentration of CD45.1$^+$ cells. **D)** Proportion of CD45.1$^+$ cells of all CD8$^+$ T cells over time in wildtype mice. **E)** Example plot depicting surface S-CAR and EGFRt expression on CD45.1$^+$ cells on day 7. **F)** Median fluorescent intensity (MFI) of surface S-CAR and EGFRt expression on CD45.1$^+$ cells. All data are presented as mean values ± SD. (Mann Whitney test, ns = not significant, * = p<0.05, ** = p<0.01)

2.1.2 The adaptive immune system limits S-CAR T-cell persistence

Poor survival of S-CAR T cells compared to untransduced transferred T cells from the T-cell product suggested an immune response of the endogenous immune system to the human-derived domains of the S-CAR construct. To address this theory, I transferred T cells that co-expressed the S-CAR and the transduction marker truncated human epidermal growth factor receptor (EGFRt) into HBV-naïve wildtype mice (Figure 2.2 A). The T-cell product had a transduction rate of 85 % as determined by flow cytometry analysis (Figure 2.2 B). In wildtype mice S-CAR T-cell persistence was limited in comparison to transferred mock T cells without transgene expression although both cell types could be detected at comparable numbers on day 3 (Figure 2.2 C and D). In contrast, if I transferred S-CAR T cells into Rag2$^{-/-}$ mice, they persisted in at least as high numbers as mock T cells until day 18 (Figure 2.2 C). S-CAR expression on transferred cells could only be detected until day 5, EGFRt expression until day 7 (Figure 2.2 E and F). This phenomenon could be explained by S-CAR internalization due to activation or anti-S-CAR antibodies. Taken together, the adaptive immune system, which is present in wildtype but not Rag$^{-/-}$ mice, seemed to influence S-CAR T-cell persistence.

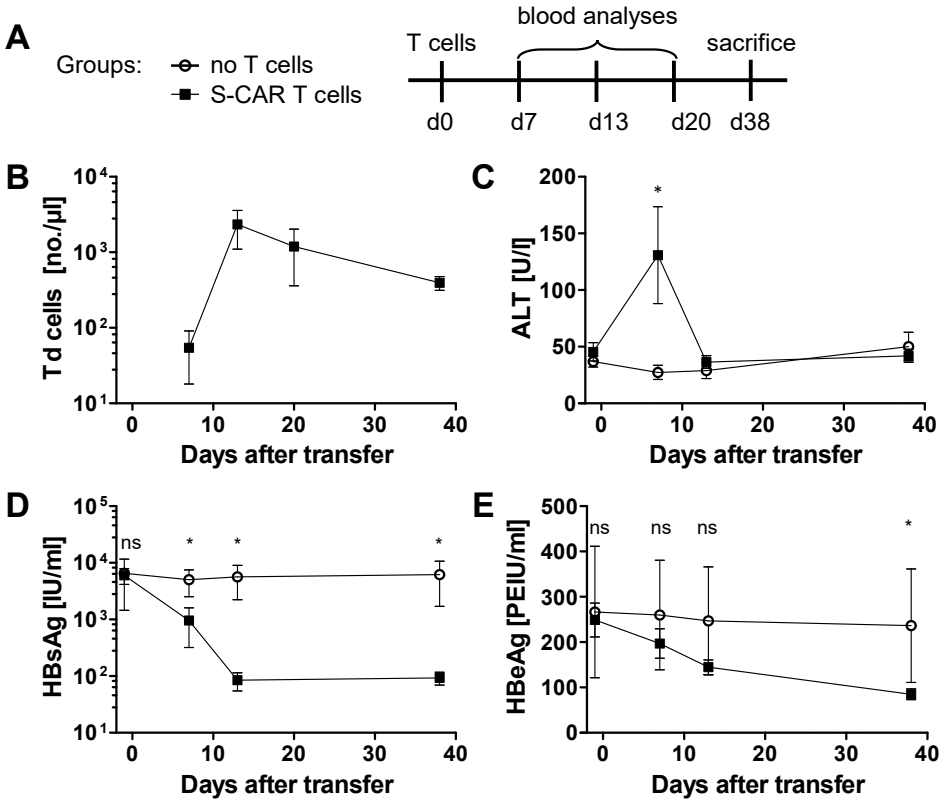

Figure 2.3 Antiviral effect of S-CAR T cells in immunodeficient mice.
A) AAV-HBV-infected CD45.2^{+} Rag2$^{-/-}$/IL-2R$\gamma^{-/-}$ mice were injected with 1 x 10^{6} CD45.1^{+} S-CAR^{+} and EGFR^{+} T cells (n=5) or remained untreated (n=3). CD45.1^{+} cells in peripheral blood and serum parameters were monitored over time. **B)** Concentration of transduced (Td = S-CAR^{+} and/or EGFRt^{+}) cells. **C)** Serum ALT levels. **D)** HBsAg levels in serum. **E)** HBeAg levels in serum. All data are presented as mean values ± SD. (Mann Whitney test, ns = not significant, * = $p<0.05$)

The mouse model using adeno-associated virus vector for HBV genome delivery (AAV-HBV) (Dion et al., 2013) has been established in our laboratory to study persistent HBV infection. In this model for chronic HBV infection curative treatment would be feasible since not all hepatocytes are transduced and in contrast to HBV-transgenic mice may be replaced by HBV-naïve cells. To investigate the potential to induce an antiviral effect without influences of the adaptive immune system, I adoptively transferred S-CAR T cells into AAV-HBV-infected Rag2$^{-/-}$/IL-2R$\gamma^{-/-}$ mice (Figure 2.3 A). Rag2$^{-/-}$ mice lack B and T cells, IL-2Rγ-deficiency in addition prevents the development and maturation of NK cells. In this setting, S-CAR T cells could still be detected until day 38 after transfer (Figure 2.3 B). T-cell therapy induced a transient mild to moderate liver damage (Figure 2.3 C). Furthermore, HBsAg (Figure 2.3 D) and HBeAg (Figure 2.3 E) as viral parameters in serum both decreased. HBsAg decreased by about 99 % until day 13 and remained at that level. HBeAg continuously decreased until day 38 when it reached about 40 % of pretreatment values. The results indicate that S-CAR T cells exhibit a continuous antiviral effect if they are not targeted by an adaptive immune response in immunodeficient Rag2$^{-/-}$/IL-2R$\gamma^{-/-}$ mice.

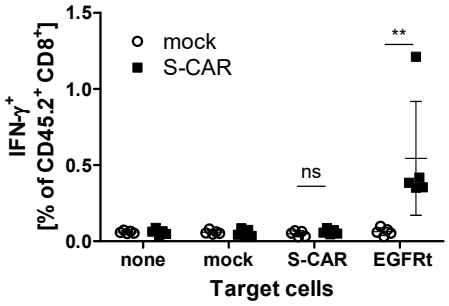

Figure 2.4 Endogenous CD8$^+$ T-cell response against the S-CAR and EGFRt.
Splenocytes from mice that had received mock or S-CAR$^+$/EGFRt$^+$ T cells (Figure 2.2) were isolated on day 18. 1 x 10^6 splenocytes were cultured alone or co-cultured overnight with 1 x 10^5 CD45.1$^+$ CD8$^+$ T cells expressing no transgene, only the S-CAR or only EGFRt. Endogenous CD45.2$^+$ CD8$^+$ T cells were stained intracellularly for IFN-γ and analyzed the next day via flow cytometry. Data are presented as values of single mice and mean values ± SD. (n=5, Mann Whitney test, ns = not significant, ** = p<0.01)

As shown in Figure 2.2 C, S-CAR T cells persisted in Rag2$^{-/-}$ mice that harbor functional NK cells, but not B and T cells. Hence, both B and T cells could be responsible for reduced survival of S-CAR T cells. To determine which kind of immune response resulted in S-CAR T-cell rejection in immunocompetent mice, I co-cultured splenocytes from recipient mice from Figure 2.2 overnight with transgene expressing CD8$^+$ T cells (Figure 2.4). An ICS on the next day revealed that endogenous CD8$^+$ T cells expressed IFN-γ if co-cultured with EGFRt-expressing target cells. This indicated a CD8$^+$ T-cell immune response against this human-derived protein. In contrast, I did not detect a CD8$^+$ T-cell response against the S-CAR although it also contains human-derived domains, namely the extracellular C8 scFv and a human IgG1 spacer, a human CD28 transmembrane domain, and intracellular signaling domains of human CD28 and CD3ζ. Furthermore, CD4$^+$ T-cell responses were neither detected against the S-CAR nor against EGFRt (data not shown).

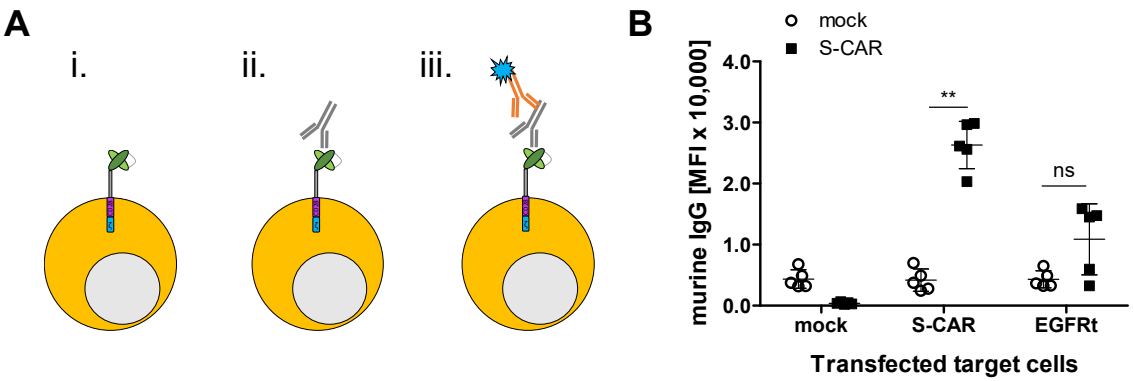

Figure 2.5 Anti-S-CAR and anti-EGFRt antibody detection via flow cytometry assay.
A) S-CAR and EGFRt expressing PlatE cells (i.) were stained with 1:200 diluted serum of mice that had received mock or S-CAR$^+$/EGFRt$^+$ T cells (Figure 2.2) (ii.). Bound antibodies were detected with a fluorochrome-labelled anti-mouse-IgG antibody (iii.) and analyzed by flow cytometry. **B)** MFI of stained anti-S-CAR and anti-EGFRt antibodies. Data are presented as values of single mice and mean values ± SD. (n=5, Mann Whitney test, ns = not significant, ** = $p<0.01$)

S-CAR expression decreased faster than EGFRt expression *in vivo* (Figure 2.2 F), this suggested that anti-S-CAR antibodies were present in serum of recipient mice, since S-CAR-reactive T cells could not be detected (Figure 2.4). To test serum for anti-S-CAR and anti-EGFRt antibodies, I incubated transgene expressing target cells with serum and stained bound antibodies with a fluorochrome-labelled anti-mouse-IgG antibody (Figure 2.5 A). Flow cytometry analysis revealed antibody production against both the S-CAR and EGFRt molecules (Figure 2.5 B).

To confirm this result and to investigate which domains of the S-CAR are targeted by the antibodies, an enzyme-linked immunosorbent assay (ELISA) was established (Figure 2.6 A). Only the extracellular domains of the S-CAR – the human IgG1 spacer and the C8 scFv – are potential targets for antibodies. The ELISA could confirm the presence of anti-S-CAR antibodies and demonstrated that they were directed against both the human IgG1 spacer (Figure 2.6 B) and the C8 scFv (Figure 2.6 C).

Taken together, the results suggested that immunocompetent mice mount an immune response against the human alloantigens expressed on S-CAR T cells. Human derived EGFRt induced both B- and T-cell responses, while the S-CAR was only a target of B-cell responses. The observed immune responses probably limited the survival of S-CAR T cells *in vivo* and prevented long-term viral control. Lack of endogenous B and T cells could prevent S-CAR T-cell rejection and allowed a persistent antiviral effect. This effect impeded a meaningful investigation of S-CAR T-cell therapy in immunocompetent mice.

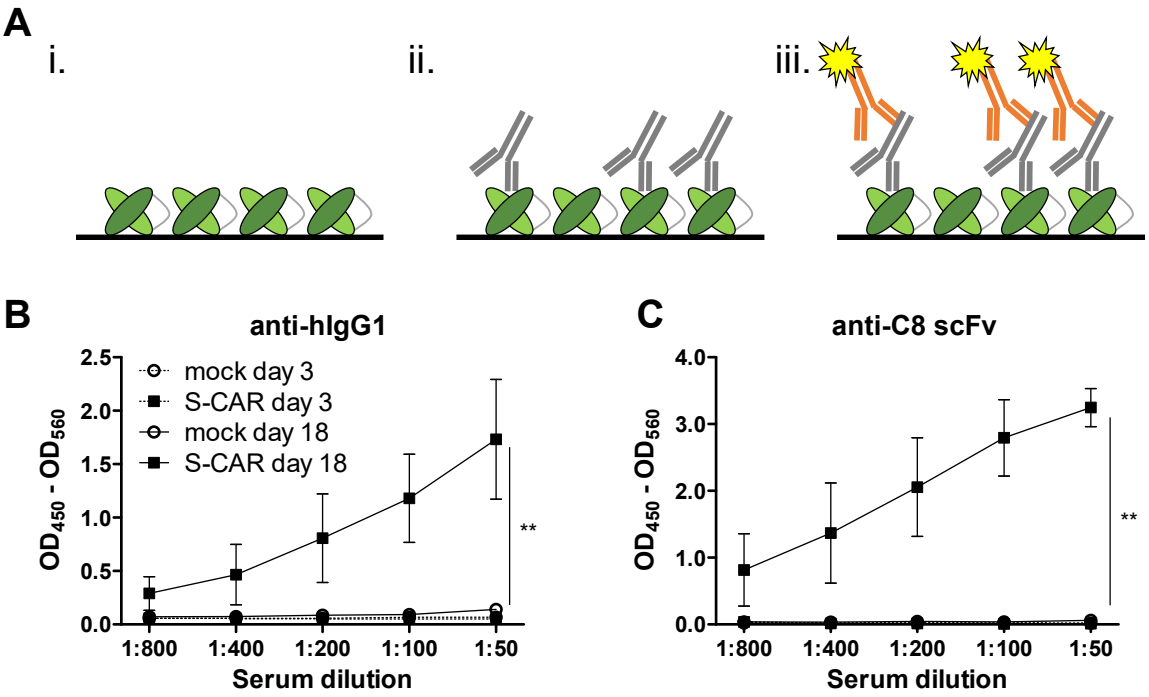

Figure 2.6 Anti-S-CAR antibody detection via ELISA assay.
A) C8 scFv or human IgG1 antibody were coated on plates (i.) followed by incubation of diluted serum of mice that had received mock or S-CAR^{+}/EGFRt^{+} T cells (Figure 2.2) (ii.). Bound antibodies were detected with a horseradish peroxidase-(HRP)-labelled anti-mouse-IgG antibody (iii.). **B)** ELISA result for anti-human-IgG1 antibodies. **C)** ELISA result for anti-C8 scFv antibodies. Background value of diluted serum on uncoated plates was subtracted in each ELISA. All data are presented as mean values ± SD. (n=5 mice, no technical replicates, Mann Whitney test, ** = $p<0.01$)

2.1.3 A murine IgG1 spacer does not prevent the immune response against the C8 scFv

Next, I investigated possibilities to prevent the host-versus-graft response, allowing us to study S-CAR T-cell therapy in immunocompetent mice. To this end, the number of immunogenic epitopes was reduced by exchanging the spacer to a murine IgG1 domain and removing EGFRt. The intracellular signaling domains remained unaltered as they seemed to be non-immunogenic (Figure 2.4). Thus, in this S-CAR only the human-derived C8 scFv remained as a potentially immunogenic epitope (Figure 2.7 A). I investigated these modified S-CAR T cells by transferring them into HBV-transgenic mice monitoring them for 26 days (Figure 2.7 B). Transduction rate of T cells with human and murine spacer before the transfer was 62 % and 32 %, respectively (Figure 2.7 C). S-CAR T cells with a murine IgG1 spacer could be activated by plate-bound HBsAg *in vitro.* For low concentrations of HBsAg they secreted comparable amounts of IFN-γ. In contrast, at the highest concentration tested (2.5 μg/ml) S-CAR T cells with the human IgG1 spacer exhibited enhanced IFN-γ secretion in comparison to the murine IgG1 spacer variant (Figure 2.7 D). Upon transfer into HBV-transgenic mice, only human IgG1

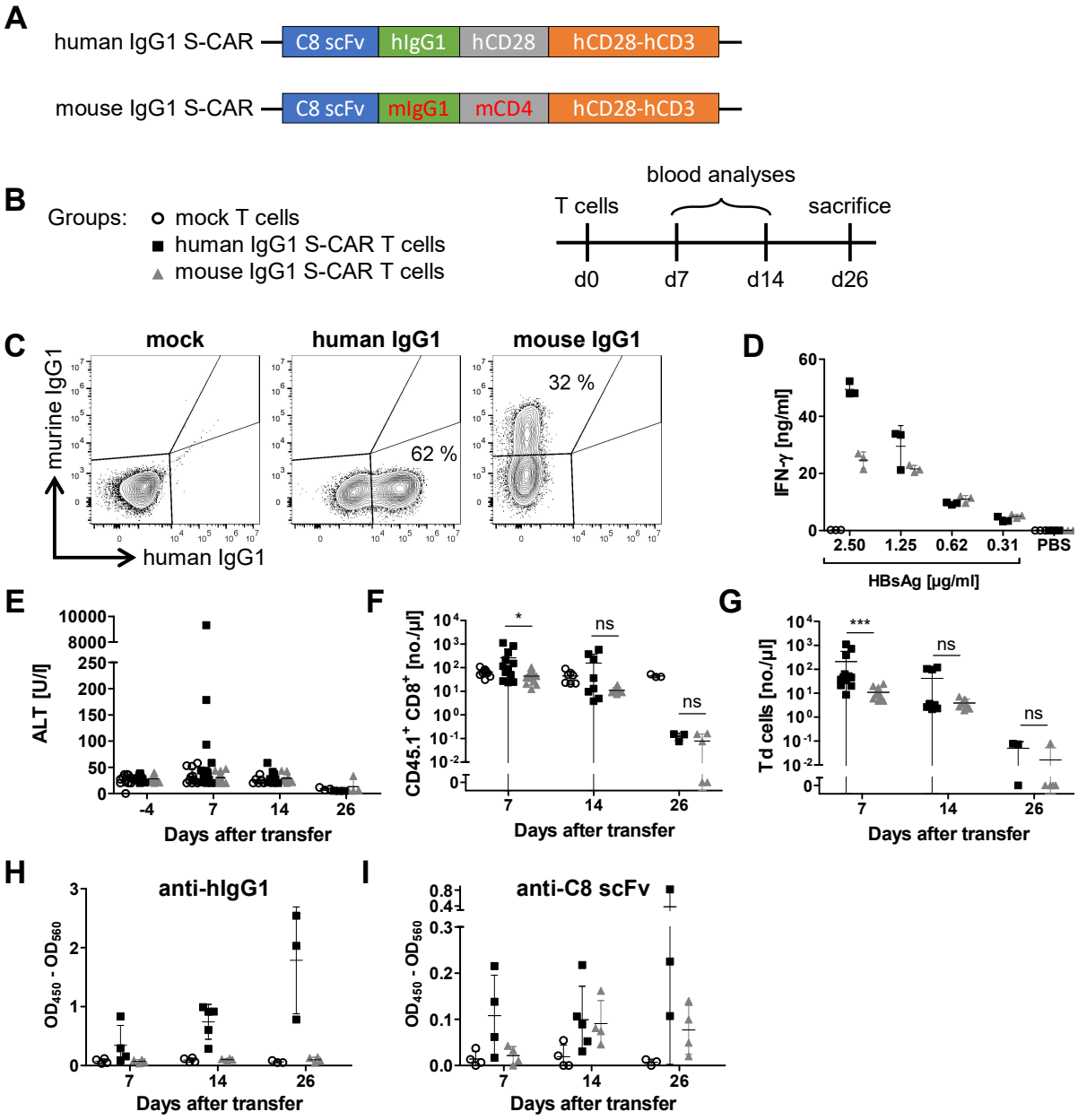

Figure 2.7 Immune response against the C8 scFv in the S-CAR with a murine spacer. CD45.2⁺ HBV-transgenic mice were injected with 2 x 10^6 CD45.1⁺ T cells expressing S-CARs with either human or murine IgG1 spacer. CD45.1⁺ cells in peripheral blood and serum parameters were monitored over time. **A)** Scheme of S-CAR constructs containing either human or murine IgG1 spacers. Red letters mark exchanged domains. Blue box: C8 scFv, green box: extracellular spacer, grey box: transmembrane domain, orange box: intracellular signaling domains **B)** Scheme of experimental design and summary of experimental groups. **C)** Flow cytometry plot of CD8⁺ T cells on day of transfer. **D)** 5 x 10^4 S-CAR⁺ T cells from day 0 were cultured on HBsAg-coated plates. Secreted IFN-γ in 16-hour supernatant was detected by ELISA. **E)** Serum ALT levels monitored over time. **F)** Concentration of CD45.1⁺ CD8⁺ T cells over time. **G)** Concentration of transduced (Td = S-CAR⁺) CD8⁺ T cells over time. **H)** ELISA result for anti-human-IgG1 antibodies. **I)** ELISA result for anti-C8 scFv antibodies. Serum was diluted 1:50. Background value of diluted serum on uncoated plates was subtracted in each ELISA. All data are presented as values of single mice and mean values ± SD. (mock n=11, human and murine IgG1 n=12 per group, n=4 animals per group were sacrificed on day 7 and day 14 each, Mann Whitney test, ns = not significant, *** = p<0.001)

S-CAR T cells induced a transient liver damage (Figure 2.7 E) and a higher concentration of transferred cells in comparison to mock T cells circulated in peripheral blood (Figure 2.7 F). The species origin of the IgG1 spacer did not influence the rapid decline of transduced cells (Figure 2.7 G). Most importantly, while anti-hIgG1 antibodies were only induced in human IgG1 S-CAR-treated mice (Figure 2.7 H), both treatment groups developed an antibody response against the C8 scFv (Figure 2.7 I). Thus, the maximal reduction of immunogenic epitopes in the S-CAR without changing the scFv did not prevent the rejection by the endogenous immune system. Immune responses remained an issue for the study of S-CAR T cells in immunocompetent mice.

2.1.4 Irradiation allows long-term persistence and a lasting antiviral effect

Beside genetic elimination of the adaptive immune system, sublethal total body irradiation is another possibility to prevent rapid rejection of cells expressing alloantigens. To allow short-term tolerance of S-CAR T cells in AAV-HBV-infected wildtype mice, they were irradiated one day before transfer (Figure 2.8 A). The concentrations of endogenous B cells (Figure 2.8 B), $CD8^+$ T cells (Figure 2.8 C), $CD4^+$ T cells (Figure 2.8 D) and NK cells (Figure 2.8 E) were heavily decreased upon irradiation (B cells: ~3 $\log_{10}$, $CD8^+$ T cells: ~2.4 $\log_{10}$, $CD4^+$ T cells: ~1.7 $\log_{10}$, NK cells: ~1.3 $\log_{10}$). Endogenous cells regained physiological concentrations two to three months after irradiation (Figure 2.8 B-E). I observed an expansion and persistence of transferred S-CAR T cells in peripheral blood until day 140 only if mice were irradiated in advance (Figure 2.8 F and G). Strikingly, they persisted in high numbers even after the endogenous immune system had been re-established. On day 140 after transfer, I detected S-CAR T cells also in liver (mean = 67 million) and spleen (mean = 34 million) (Figure 2.8 H).

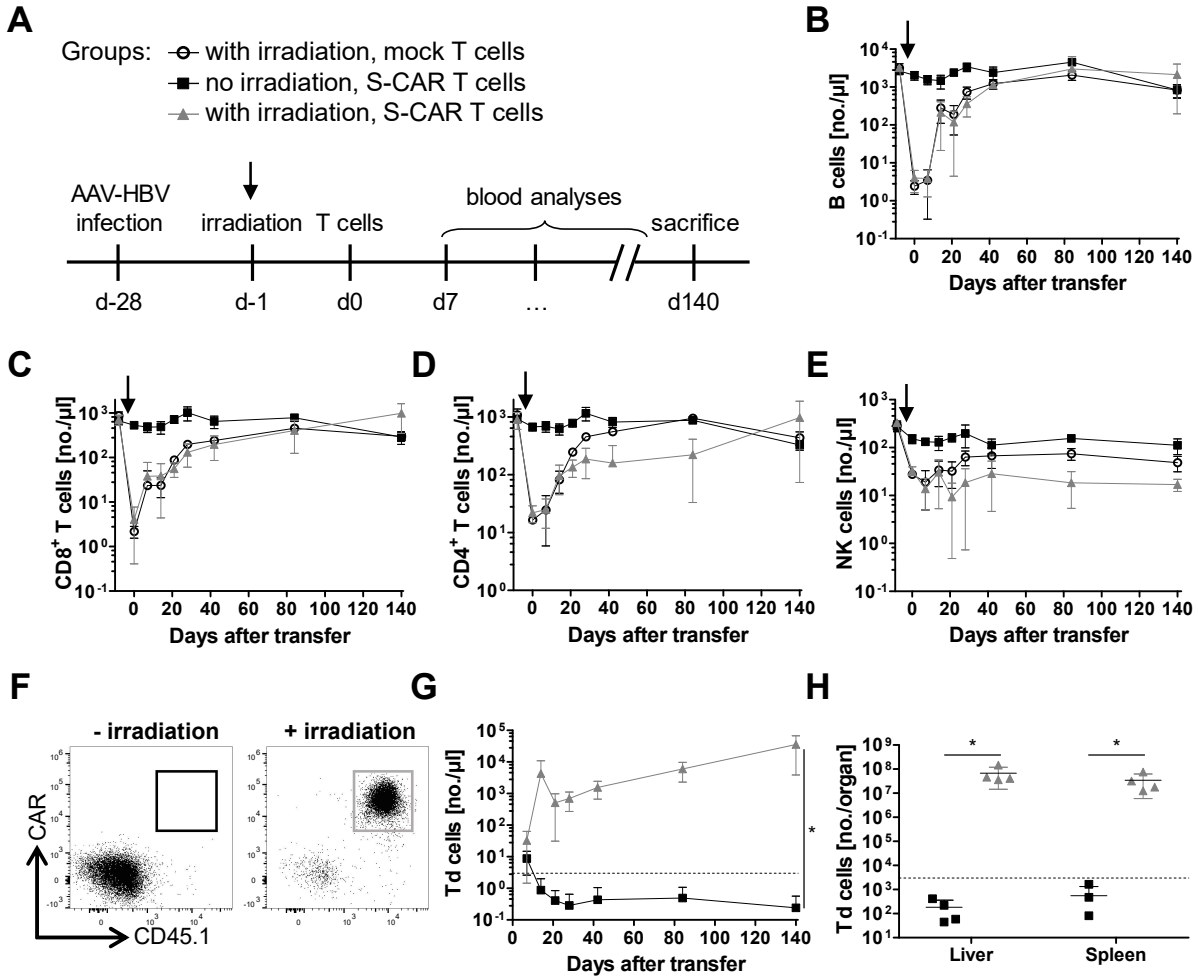

Figure 2.8 Engraftment of S-CAR T cells in irradiated mice.
A) AAV-HBV-infected CD45.2$^+$ mice were injected with 1 x 10^6 CD45.1$^+$ S-CAR$^+$/EGFR$^+$ or mock T cells one day after sublethal total body irradiation (indicated by black arrow). Endogenous CD45.1$^-$ and transferred CD45.2$^+$ cells in peripheral blood were monitored by flow cytometry analysis on days 0, 7, 14, 21, 28, 42, 84 and 140 after transfer. **B)** Concentration of CD45.1$^-$ CD19$^+$ B cells. **C)** Concentration of CD45.1$^-$ CD8$^+$ T cells. **D)** Concentration of CD45.1$^-$ CD4$^+$ T cells. **E)** Concentration of CD45.1$^-$ NK1.1$^+$ NK cells. **F)** Example flow cytometry plot of CD8$^+$ cells on day 28 in S-CAR$^+$/EGFRt$^+$ T cell-treated mice with or without prior irradiation. **G)** Concentration of transduced (Td = S-CAR$^+$ and/or EGFRt$^+$) cells. **H)** Count of transduced (Td = S-CAR$^+$ and/or EGFRt$^+$) cells in liver and spleen 140 days after transfer. Dashed line indicates limit of detection for transduced cells. B-E, G: Data are presented as mean values ± SD. H: Data are presented as values of single mice and mean values ± SD. (n=4, Mann Whitney test, * = $p<0.05$)

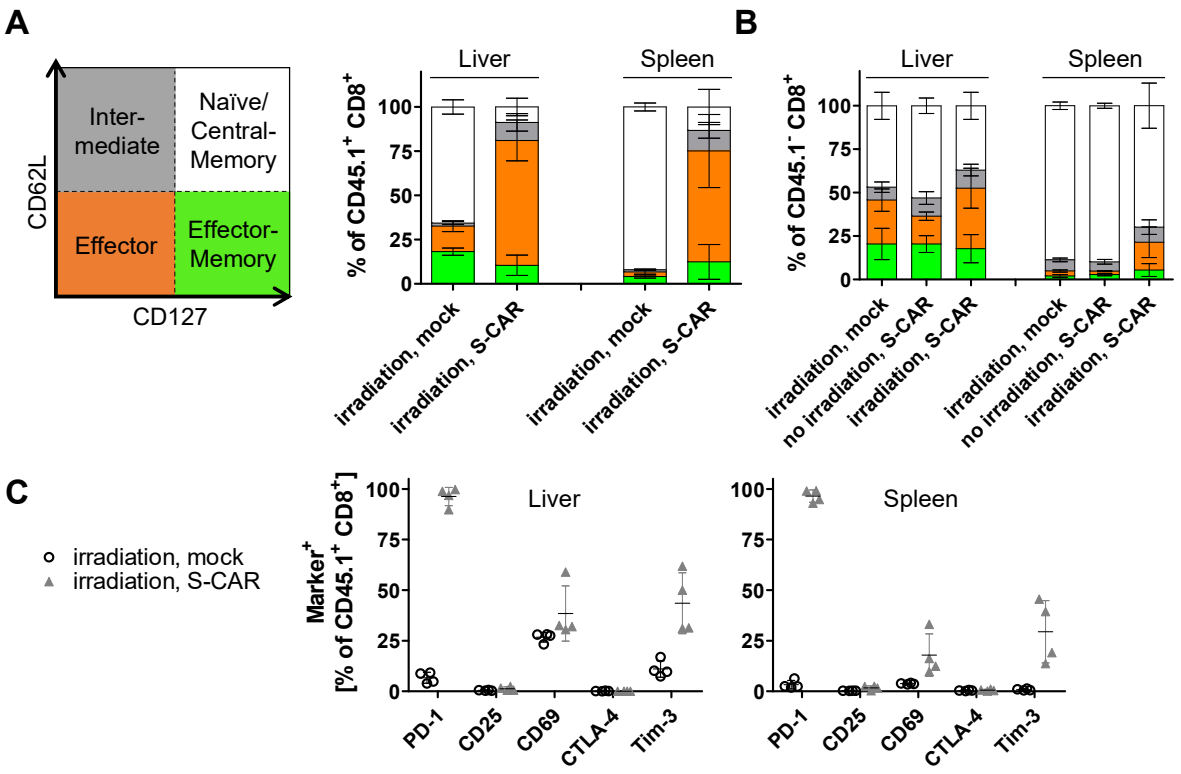

Figure 2.9 Influence of irradiation on the phenotype of transferred and endogenous CD8⁺ T cells.
LALs and splenocytes were isolated on day 140 from mock or S-CAR⁺/EGFRt⁺ T cell-injected CD45.2⁺ mice (Figure 2.8) and analyzed by flow cytometry. **A)** Memory marker expression (CD62L and CD127) of CD45.1⁺ and **B)** CD45.1⁻ CD8⁺ T cells. **C)** Expression of activation (PD-1, CD25, CD69) and exhaustion (CTLA-4, Tim-3) markers of CD45.1⁺ T cells. A-B: Data are presented as mean values ± SD. C: Data are presented as values of single mice and mean values ± SD. (n=4)

After isolation of transduced cells on day 140, I determined their expression of memory, activation and exhaustion markers in spleen and liver. S-CAR T cells from both organs mostly exhibited an effector phenotype (CD62L⁻ CD127⁻, 60 – 70 %). Mock-transduced CD8⁺ T cells in contrast, had a phenotype of naïve/central-memory CD8⁺ T cells (CD62L⁺ CD127⁺, 60 - 70 % in liver, 89 - 94 % in spleen) (Figure 2.9 A). Further analysis revealed that the composition of endogenous CD8⁺ T cells in spleen and liver was comparable in irradiated and non-irradiated mice. Only if mice were treated with S-CAR T cells after irradiation, the composition changed and a lower proportion of endogenous CD8⁺ T cells was of a naïve/central memory phenotype (Figure 2.9 B). In comparison to mock T cells, S-CAR T cells were highly positive for PD-1 and partially expressed Tim-3 and CD69 but were negative for CD25 and CTLA-4 (Figure 2.9 C). It is worth noting that S-CAR T cells from liver and spleen showed a comparable profile (Figure 2.9 A and C) suggesting an extrahepatic activation of S-CAR T cells as discussed later.

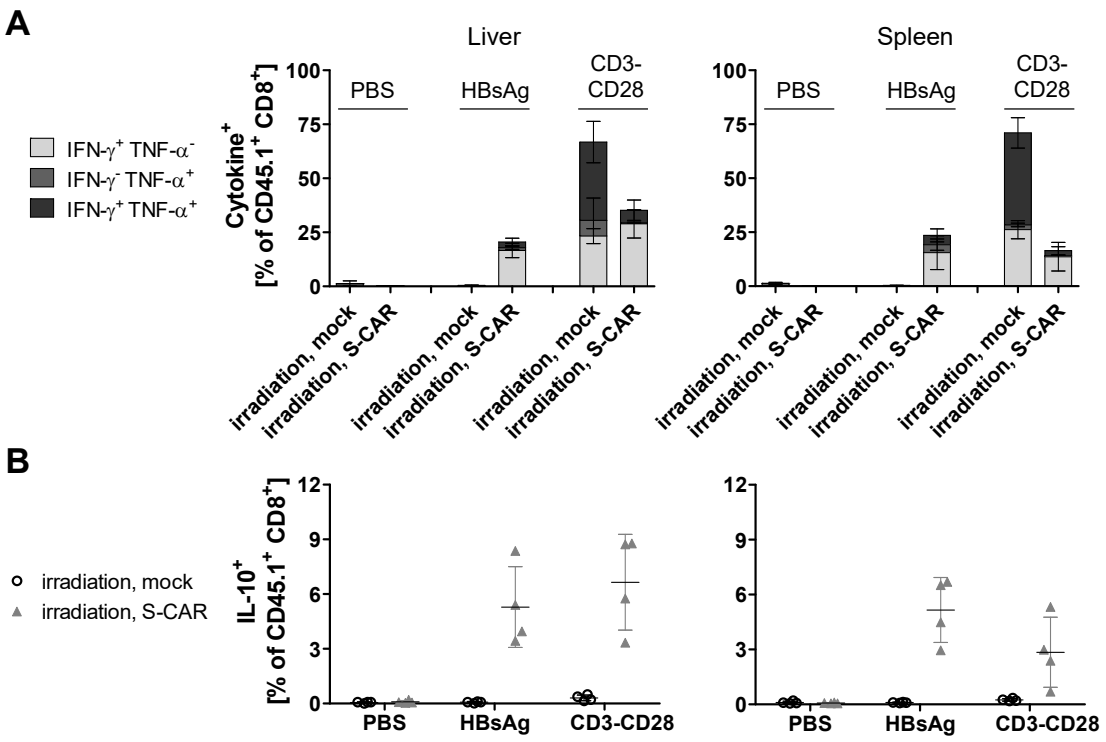

Figure 2.10 Functionality of S-CAR T cells after long-term *in vivo* survival in irradiated, immunocompetent mice.
LALs and splenocytes were isolated on day 140 from mock or S-CAR$^+$/EGFRt$^+$ T cell-injected CD45.2$^+$ mice (Figure 2.8) and cultured overnight on PBS-treated, HBsAg-coated, or anti-CD3/anti-CD28 antibody-coated plates. On the following day expression of cytokines by CD45.1$^+$ cells was detected via an ICS. **A)** IFN-γ and TNF-α expression upon specific and unspecific stimulation. **B)** IL-10 expression upon specific and unspecific stimulation. A: Data are presented as mean values ± SD. B: Data are presented as values of single mice and mean values ± SD. (n=4)

Next, the *ex vivo* functionality of S-CAR T cells after long-term *in vivo* circulation was investigated. Therefore, freshly isolated cells from liver and spleen were rested overnight or cultured on HBsAg- or anti-CD3/anti-CD28 antibody-coated plates. Staining of intracellular cytokines revealed that transduced S-CAR T cells extracted from livers and spleens could still be activated and expressed the proinflammatory cytokines IFN-γ and to a lower extent TNF-α upon specific and unspecific activation (Figure 2.10 A). Interestingly, a larger proportion of mock T cells (~66 %) than S-CAR T cells (~35 %) from the liver expressed cytokines upon unspecific stimulation. In transferred cells isolated from the spleen the difference was even more pronounced (~71 % versus ~16 %). This suggests that S-CAR T cells are partially exhausted at this timepoint. Furthermore, only S-CAR T cells expressed IL-10 upon stimulation (Figure 2.10 B) In summary, upon irradiation of recipient mice and after long-term *in vivo* circulation, S-CAR T cells retained a limited functionality and displayed a partially exhausted phenotype.

In mice receiving S-CAR T cells after irradiation, I determined the antiviral effect. Both groups that received S-CAR T cells with or without prior irradiation displayed elevated serum ALT levels on day 7. On day 40 only irradiated mice treated with S-CAR T cells showed again moderate ALT elevation. No liver damage could be detected thereafter (Figure 2.11 A). HBsAg in serum decreased by 1 log_{10} in both S-CAR T cell-treated groups independent of prior irradiation. Subsequently, HBsAg rebounded at day 80 in mice without prior irradiation (Figure 2.11 B). Only one mouse developed anti-HBsAg antibodies with low HBsAg detectable on day 140 (Figure 2.11 C). In irradiated mice HBsAg continued to decrease to approximately 1 % of pretreatment values until day 140 (Figure 2.11 B). HBeAg decreased gradually only in irradiated and S-CAR T cell-treated mice. On day 140, HBeAg had dropped about 75 % in comparison to mock T cell-treated and to non-irradiated mice (Figure 2.11 D). The antiviral effect was confirmed by qPCR analysis. AAV and HBV DNA copies in the liver were significantly lower in irradiated and S-CAR T cell-treated mice (Figure 2.11 E).

Summarizing these results, if mice were irradiated one day before S-CAR T-cell transfer, S-CAR T cells persisted even after the endogenous immune system had recovered regarding both cell numbers and cell type composition. Isolated transferred cells expressed markers of exhaustion but retained part of their functionality *ex vivo*. The expression of proinflammatory

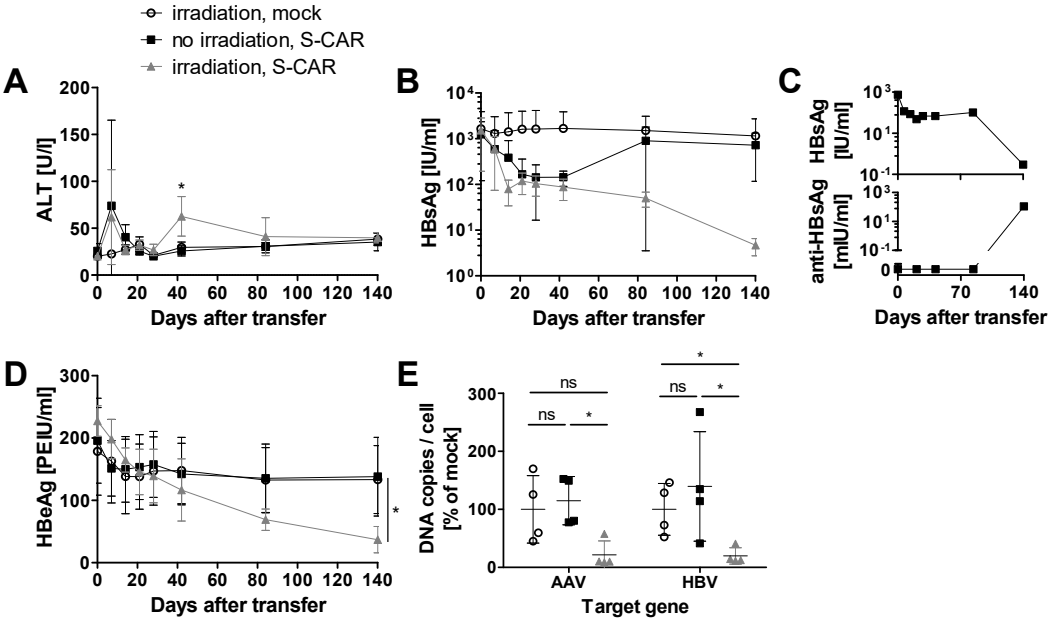

Figure 2.11 Antiviral effect of S-CAR T cells in irradiated mice.
Viral parameters in serum and liver were analyzed in mice irradiated one day before S-CAR$^+$/EGFRt$^+$ T-cell transfer (Figure 2.8). **A)** Serum ALT levels monitored over time. **B)** HBsAg levels in serum. **C)** HBsAg and anti-HBsAg antibody levels in one mouse with spontaneous seroconversion. **D)** HBeAg levels in serum. **E)** Intrahepatic AAV and HBV DNA copies per cell (single copy gene *PRNP* as reference) on day 140 determined via qPCR. Values were normalized to mock T cell-injected mice. A, B, D: Data are presented as mean values ± SD. C: Data are presented as values of a single mouse. E: Data are presented as values of single mice and mean values ± SD. (n=4, Mann Whitney test, ns = not significant, * = $p<0.05$)

cytokines by S-CAR T cells was decreased in comparison to mock T cells, and S-CAR T cells additionally expressed IL-10 upon *ex vivo* re-stimulation. If S-CAR T cells persisted *in vivo*, they induced a continuous antiviral effect over time.

2.1.5 Tolerization of mice allows long-term S-CAR T-cell persistence

Next, I aimed at inducing tolerance to the human alloantigens before S-CAR T-cell transfer. To this end, non-functional S-decoy-(Δ)-CAR T cells that co-expressed EGFRt were transferred into AAV-HBV-infected mice one day after irradiation (Figure 2.12 A). The SΔ-CAR construct contains the same extracellular domains, but the intracellular T-cell signaling domains are exchanged to a cytoplasmic domain of the nerve growth factor receptor rendering the SΔ-CAR uncapable of activating T cells. Thus, SΔ-CAR T cells should neither proliferate nor induce an antiviral effect in AAV-HBV-infected mice. I hypothesized that the presence of the human alloantigen in the SΔ-CAR and of EGFRt during recovery of the endogenous immune system might be sufficient for the induction of tolerance. As observed before, irradiation of mice induced a depletion of endogenous B- and T-cell populations (Figure 2.12 B-D). Their physiological concentrations were regained two to three months after irradiation. Upon transfer, SΔ-CAR T cells persisted in low concentration for more than three months (Figure 2.12 E) when functional S-CAR T cells were eventually transferred. If mice had been tolerized by previous irradiation and SΔ-CAR T cells transfer, they did not mount an antibody response against the human IgG1 or C8 scFv domains (Figure 2.12 F). Neither did these mice develop a $CD8^+$ T-cell response against the EGFRt alloantigen (Figure 2.12 G). Functional S-CAR T cells displayed proliferative potential and survived until the end of the experiment (d110) in tolerized mice (Figure 2.12 H-I). In contrast, if mice were only irradiated but not tolerized, they mounted B- and T-cell responses against the human alloantigens and S-CAR T cells vanished rapidly from the peripheral blood. This indicates that functionality of the endogenous immune system had been re-established after irradiation at the time of functional S-CAR T-cell transfer. Tolerance and persistence of S-CAR T cells was induced by the preceding SΔ-CAR T-cell transfer.

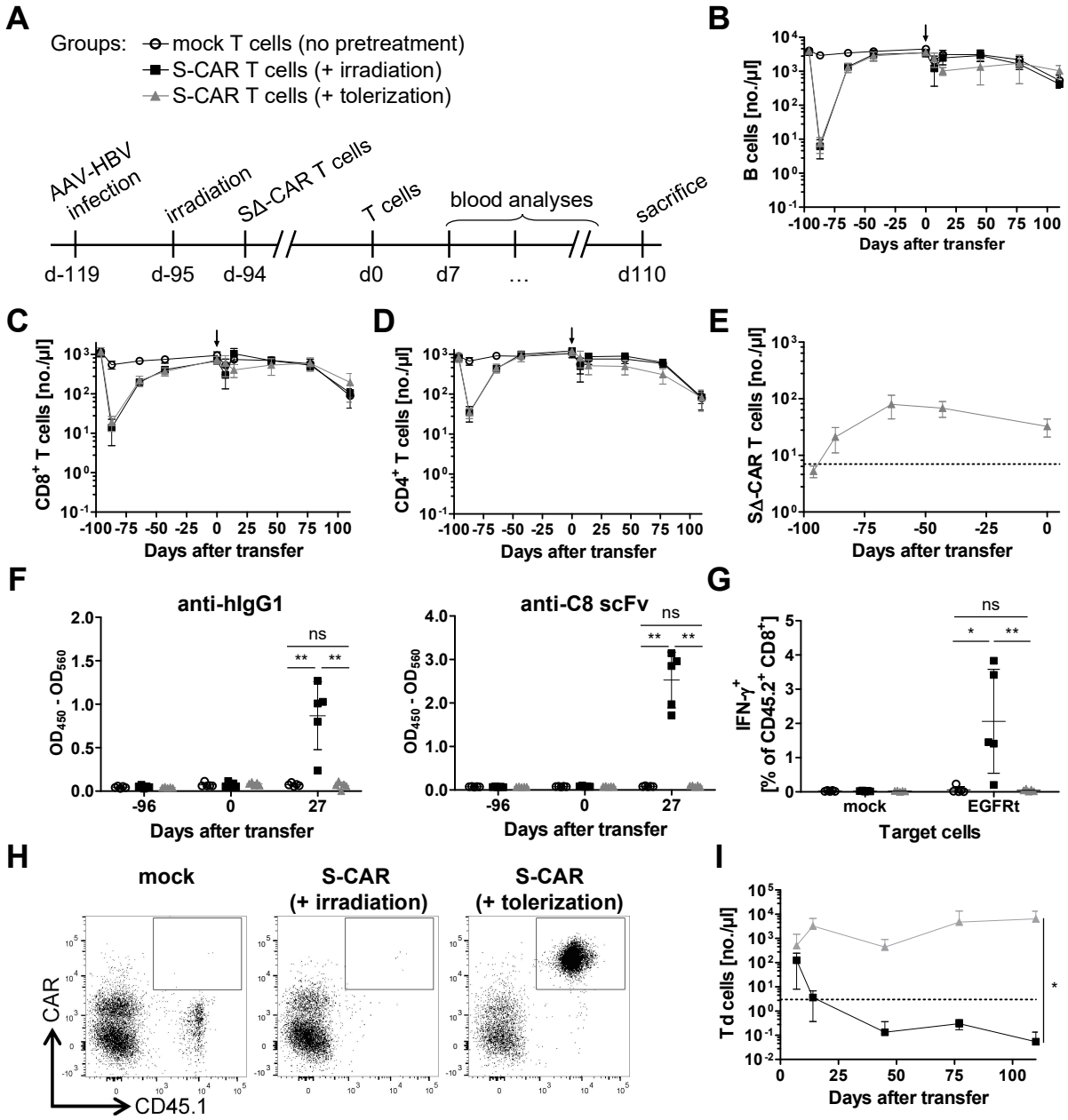

Figure 2.12 Engraftment of S-CAR T cells in tolerized mice.
A) AAV-HBV-infected CD45.2⁺ mice were injected with 5 x 10^6 CD45.1⁺ SΔ-CAR⁺/EGFRt⁺ T cells one day after sublethal total body irradiation. 94 days later 3 x 10^6 CD45.1⁺/CD45.2⁺ S-CAR⁺/EGFRt⁺ T cells were transferred. Mice that received S-CAR⁺/EGFRt⁺ T cells were either only irradiated (= irradiation) or were irradiated and received SΔ-CAR⁺/EGFRt⁺ T cells (= tolerization). Mice that received mock T cells were not pretreated. Endogenous CD45.1⁻ and transferred CD45.1⁺ and CD45.1⁺/CD45.2⁺ cells in peripheral blood were monitored by flow cytometry analysis on days -96, -87, -64, -43, 0 before, as well as on days 7, 14, 45, 77 and 110 after S-CAR⁺/EGFRt⁺ T-cell transfer. **B)** Concentration of CD45.1⁻ CD19⁺ B cells. **C)** Concentration of CD45.1⁻ CD8⁺ T cells. **D)** Concentration of CD45.1⁻ CD4⁺ T cells. **E)** Concentration of CD45.1⁺ SΔ-CAR T cells. **F)** ELISA result for anti-human-IgG1 and anti-C8 scFv antibodies. Serum was diluted 1:200. Background value of diluted serum on uncoated plates was subtracted in each ELISA. **G)** ICS of splenocytes from recipient mice after overnight co-culture with EGFRt expressing CD8⁺ T cells. Pregated on CD45.1⁻ CD8⁺ T cells. **H)** Example flow cytometry plot of CD45.1⁺/CD45.2⁺ cells in peripheral blood on day 77. **I)** Concentration of transduced (Td = S-CAR⁺ and/or EGFRt⁺) T cells. B, C, D, E, I: Data are presented as mean values ± SD. F, G: Data are presented as values of single mice and mean values ± SD. (n=5, Mann Whitney test, ns = not significant, * = p<0.05, ** = p<0.01)

After 110 days, I isolated liver-associated lymphocytes (LALs) and splenocytes and analyzed the expression of memory, activation and exhaustion markers. Mock and S-CAR T cells were compared. As previously observed (Figure 2.9), the largest proportion of S-CAR T cells exhibited an effector phenotype ($CD62L^-$ $CD127^-$) in liver and spleen. Mock T cells, in contrast, mostly expressed markers of naïve/central-memory $CD8^+$ T cells ($CD62L^+$ $CD127^+$) in both organs (Figure 2.13 A). The composition of endogenous $CD8^+$ T-cell subtypes was comparable between all three treatment groups (Figure 2.13 B). Almost all S-CAR T cells in liver and spleen expressed PD-1 and a large proportion in addition CD69 (Figure 2.13 C). In contrast to previous results (Figure 2.9 C), no expression of Tim-3 or CTLA-4 was observed.

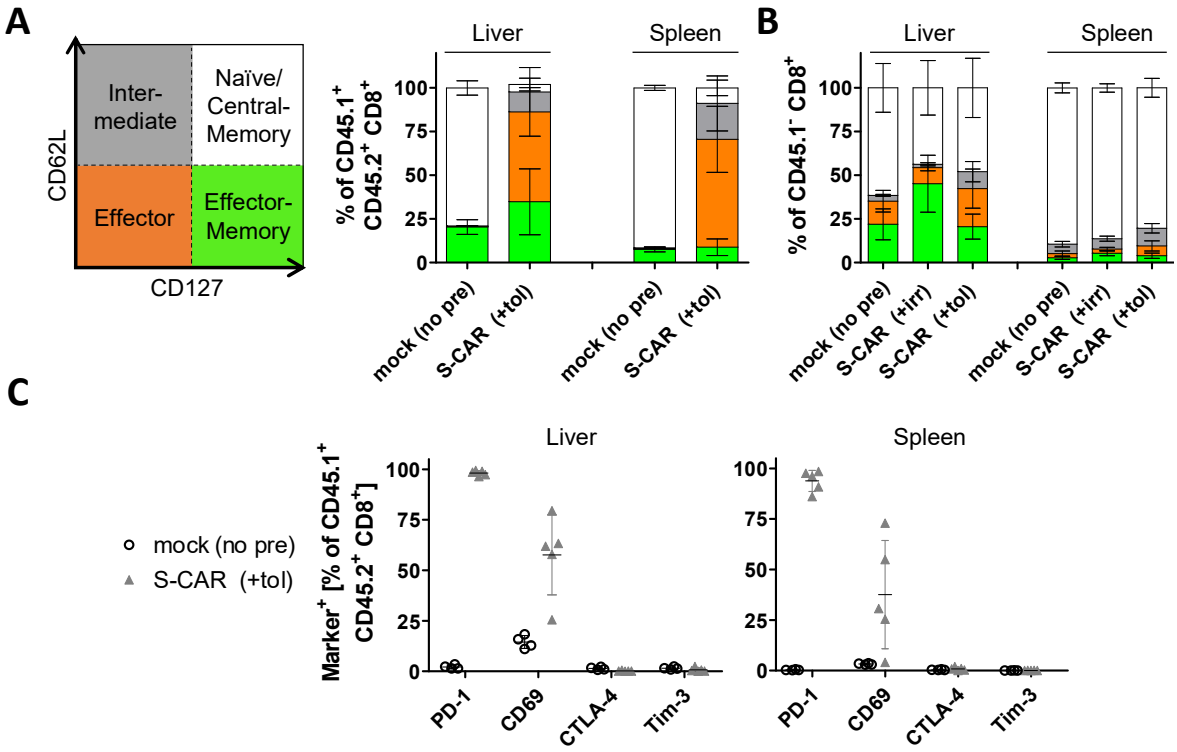

Figure 2.13 Expression of memory, activation and exhaustion markers on S-CAR T cells after long-term *in vivo* survival in tolerized, immunocompetent mice.
LALs and splenocytes were isolated on day 110 from mock or $S\text{-}CAR^+/EGFR^+$ T cell-injected mice (Figure 2.12) and analyzed by flow cytometry. **A)** Memory marker expression (CD62L and CD127) of $CD45.1^+/CD45.2^+$ and **B)** $CD45.1^-$ $CD8^+$ T cells. **B)** Activation and exhaustion marker expression (PD-1, CD69, CTLA-4, Tim-3) of $CD45.1^+/CD45.2^+$ $CD8^+$ T cells. A-B: Data are presented as mean values ± SD. C: Data are presented as values of single mice and mean values ± SD. (n=5)

The *ex vivo* functionality of S-CAR T cells after long-term *in vivo* survival was also determined. S-CAR T cells from liver and spleen expressed IFN-γ upon specific and unspecific stimulation (Figure 2.14 A and B). Thus, they retained their functionality even after long-term *in vivo* survival.

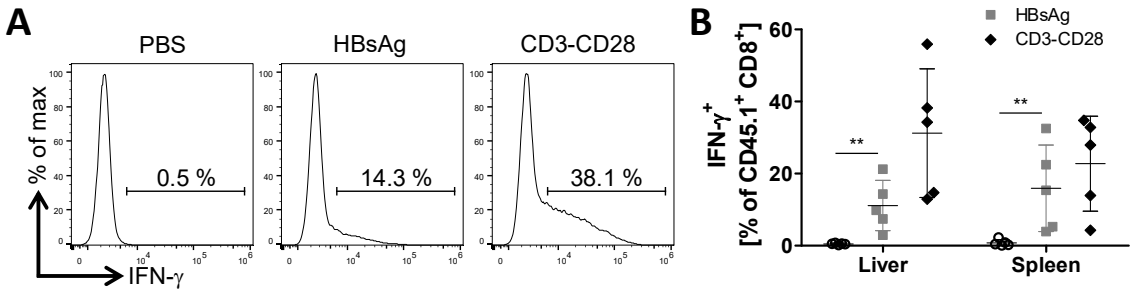

Figure 2.14 Functionality of S-CAR T cells after long-term *in vivo* survival in tolerized, immunocompetent mice.
LALs and splenocytes were isolated on day 110 from tolerized and S-CAR$^+$/EGFRt$^+$ T cell-injected mice (Figure 2.12) and cultured overnight on PBS-treated, HBsAg-coated or anti-CD3/anti-CD28 antibody-coated plates. On the following day expression of IFN-γ by CD45.1$^+$/CD45.2$^+$ T cells was detected via an ICS. **A)** Example plot of ICS result of LALs. **B)** IFN-γ expression upon specific and unspecific stimulation. Data are presented as values of single mice and mean values ± SD. (n=5)

2.1.6 S-CAR T-cell persistence in tolerized mice permits the induction of a lasting antiviral effect

In animals, in which S-CAR T cells could expand and survive due to tolerization before transfer, I determined the antiviral effect. Serum ALT levels were slightly elevated over the course of treatment, although statistically significant only on day 110 (Figure 2.15 A) The viral parameter HBsAg decreased to about 1 % of pretreatment values (Figure 2.15 B). Both serum HBeAg (Figure 2.15 C) as well as AAV and HBV DNA copies in the liver (Figure 2.15 D) decreased about 60 % in comparison to control groups. However, the therapy did not cure mice from HBV infection since not all HBV-positive hepatocytes were eliminated.

Taken together, this modified mouse model for HBV infection allows persistence of alloantigen expressing T cells and hence long-term studies of their therapeutic effect. The transfer of SΔ-CAR T cells induced tolerance to the alloantigen expressed on T cells, namely the S-CAR and EGFRt. When functional S-CAR T cells were transferred after the immune system had recovered from irradiation both regarding cell numbers and functionality, they persisted in tolerized mice. S-CAR T-cell therapy was able to reduce viral parameters substantially, but failed to cure the infection.

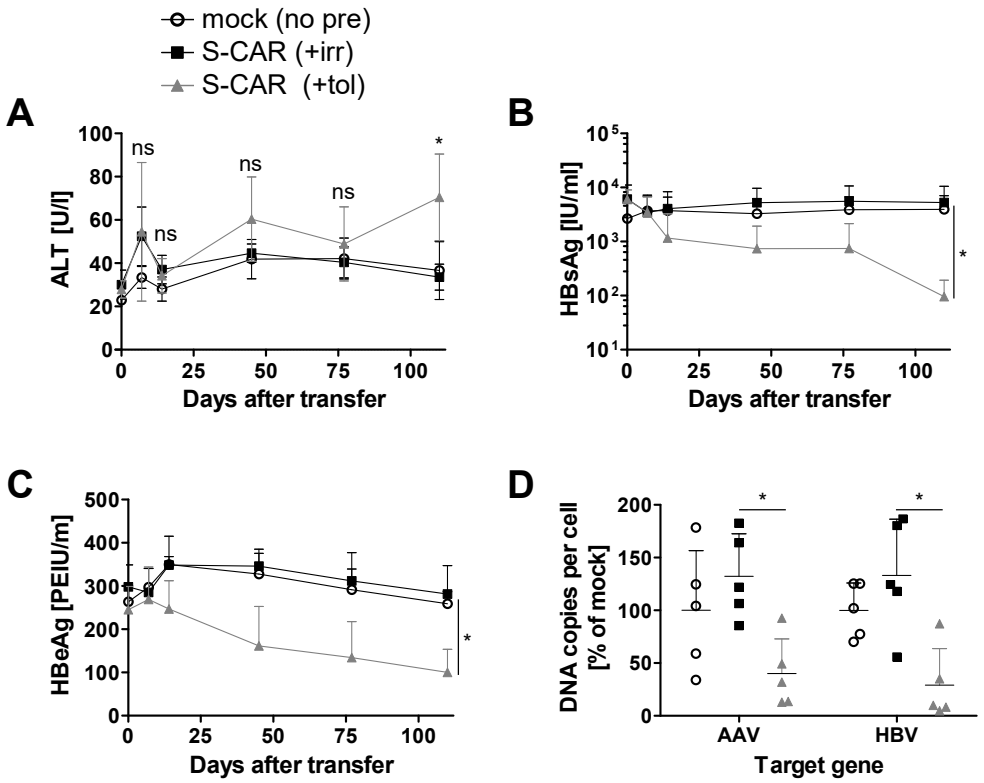

Figure 2.15 Antiviral effect of S-CAR T cells in tolerized mice.
Viral parameters in serum and liver tissue were analyzed in tolerized mice upon S-CAR$^+$/EGFRt$^+$ T-cell transfer (Figure 2.12) **A)** Serum ALT levels monitored over time. **B)** HBsAg levels in serum. **C)** HBeAg levels in serum. **D)** Intrahepatic AAV and HBV DNA copies per cell (single copy gene *PRNP* as reference) determined via qPCR. Values were normalized to mock T cell-treated mice. A, B, C: Data are presented as mean values ± SD. D: Data are presented as values of single mice and mean values ± SD. (n=5, Mann Whitney test, ns = not significant, * = $p<0.05$)

2.2 Generation and comparison of different 2nd and 3rd generation S-CARs

The results of the previous section indicate that the therapeutic effect of S-CAR T cells both *in vitro* and *in vivo* is limited and treated mice are not cured. Since the first description of CARs in 1989 (Gross et al., 1989) this technology had made several advances. The exchange and addition of intracellular signaling domains has been shown to provide advantages under certain conditions. In the following segment I will compare S-CARs that harbor different signaling domains. Both *in vitro* and *in vivo* studies will provide a better understanding whether the constructs differ in their potency to induce an antiviral effect.

2.2.1 3rd generation S-CAR constructs can activate human T cells *in vitro*

To investigate the influence of different signaling domains in the S-CAR, new constructs with additional signaling domains were generated by molecular cloning. The S-CAR used in previous studies harbored signaling domains of CD28 and CD3ζ (in this chapter termed 28z). This 2nd generation S-CAR was modified by adding domains of OX40 or 4-1BB C-terminally of CD3ζ. These 3rd generation S-CARs were termed 28zOX and 28zBB, respectively (Figure 2.16 A). All constructs contained EGFRt as a transduction marker. Human PBMC were retrovirally transduced and analyzed by flow cytometry for their transduction rate and surface expression of the different S-CAR constructs (Figure 2.16 B). The transduction rate (determined as EGFRt$^+$ cells) was comparable between all S-CAR constructs (transduction rate: 81 – 90 %). Nevertheless, S-CAR expression was not comparable. The 2nd generation S-CAR (28z) was expressed at the highest level. Both 3rd generation S-CARs could be detected in lower density on the surface of transduced cells. Especially the addition of the OX40 domain (28zOX) reduced surface expression of the S-CAR (Figure 2.16 B). To determine the functionality of the 3rd generation S-CARs in comparison to the 28z S-CAR, transduced PBMC were cultured on plate-bound HBsAg. All S-CAR versions induced HBsAg-specific release of IFN-γ by the PBMC as determined by ELISA. In comparison to the 2nd generation S-CAR both addition of OX40 and 4-1BB as signaling domains reduced IFN-γ release by about 50 % (Figure 2.16 C). Since equal numbers of EGFRt$^+$ T cells were employed, a possible explanation is the decreased surface expression of 3rd generation S-CARs.

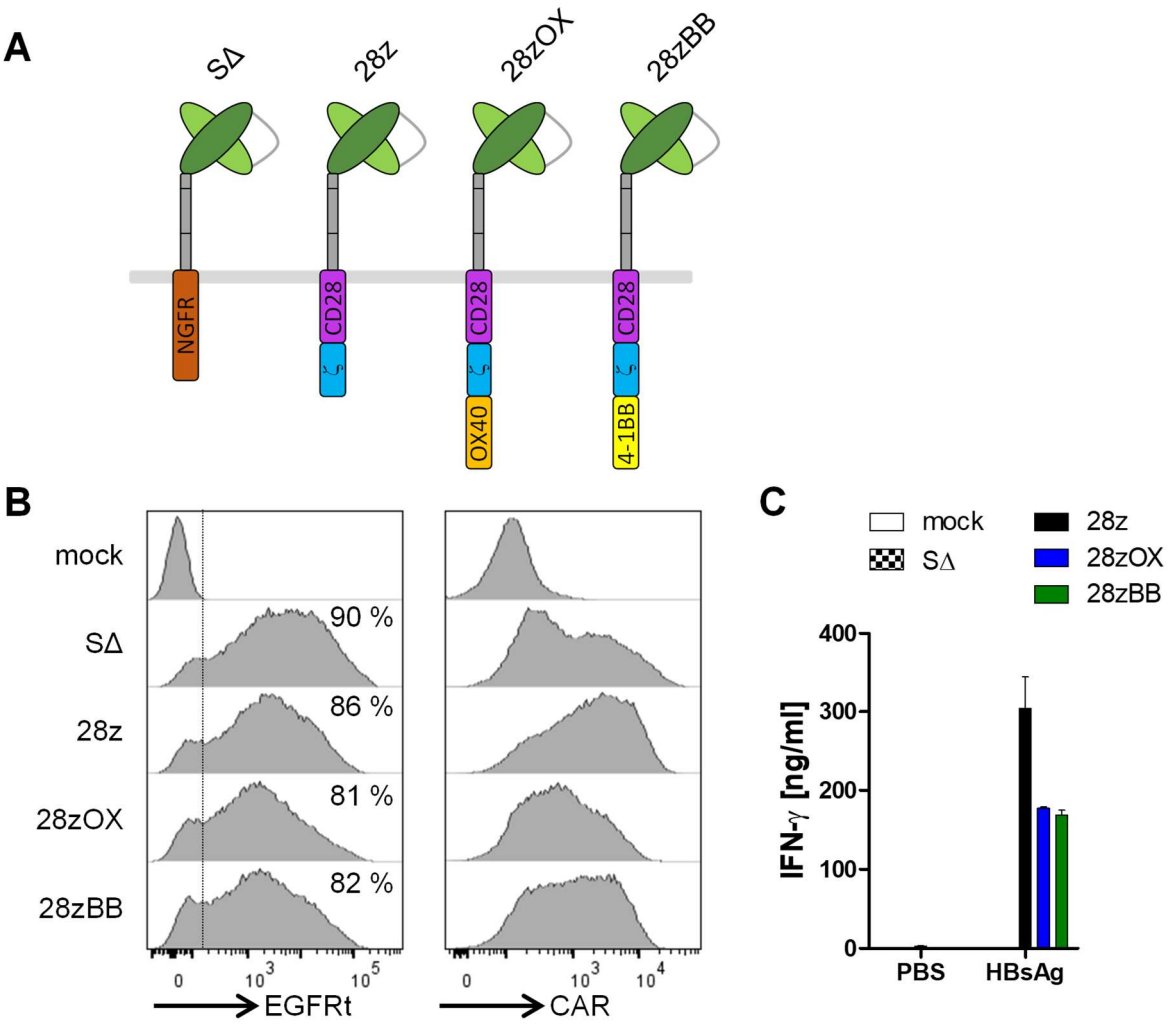

Figure 2.16 Expression and *in vitro* functionality of 3rd generation S-CARs.
Human PBMC were retrovirally transduced to express different 2nd and 3rd generation S-CAR constructs. **A)** Scheme of different S-CAR constructs. All versions carry the C8 scFv (light and dark green). S-CARs contain a wildtype IgG1 spacer consisting of hinge-CH2-CH3 domains (grey). Utilized intracellular domains were derived from nerve growth factor receptor (NGFR, brown), CD28 (purple), OX40 (orange), 4-1BB (yellow) and CD3ζ (blue) **B)** Histogram view of flow cytometry analysis that determines transduction rate via EGFRt surface expression (left panel) and S-CAR surface expression (right panel). **C)** Retrovirally transduced PBMC that mostly consisted of $CD4^+$ and $CD8^+$ T cells, were cultured on HBsAg-coated plates (2.5 μg/ml) or PBS control wells. Secreted IFN-γ in supernatant of 1 x 10^5 transduced T cells was detected by ELISA after 20 hours. Data are presented as mean values ± SD. (n=3)

2.2.2 Addition of OX40 or 4-1BB domains to the S-CAR does not enhance specific target cell killing of human S-CAR T cells *in vitro*

S-CAR T cells can induce an antiviral effect by specific killing of cells that express the S protein (Bohne et al., 2008). I assessed this cytotoxic effect comparing 2nd and 3rd generation S-CARs. Huh-S cells, which express the S protein from a transgene under the control of a cytomegalovirus (CMV) promoter, served as target cells. Progenitor Huh7 cells without transgene expression served as a negative control. Both adherent target cell types were co-

cultured with S-CAR T cells and target cell viability was assessed via the xCELLigence real-time cell analyzer (RTCA). Figure 2.17 A indicates that 28z S-CAR T cells specifically reduced target cell viability of Huh7-S cells in a dose-dependent manner while control target cell remained viable. Investigation of T cells expressing different S-CARs under these conditions revealed that addition of OX40 or 4-1BB did not induce an enhanced target cell killing. S-CAR T cells with the OX40 domain (28zOX) were comparably efficient in target cell killing as the 2nd generation S-CAR T cells (28z) (duration until half-maximal effect: 28z = 14.5 h, 28zOX = 13.0 h). Addition of 4-1BB (28zBB) even reduced the cytotoxic effect of S-CAR T cells. Target cell viability decreased with slower kinetics (duration until half-maximal effect: 28zBB = 21 h). Nevertheless, after 36 hours of co-culture all three functional S-CAR versions had induced a reduction of target cell viability by almost 100 % (Figure 2.17 B). Taken together, under these conditions a second costimulatory domain of OX40 or 4-1BB did not provide an advantage for the cytotoxic effect of S-CAR T cells. The addition of 4-1BB even decreased T-cell effector functions.

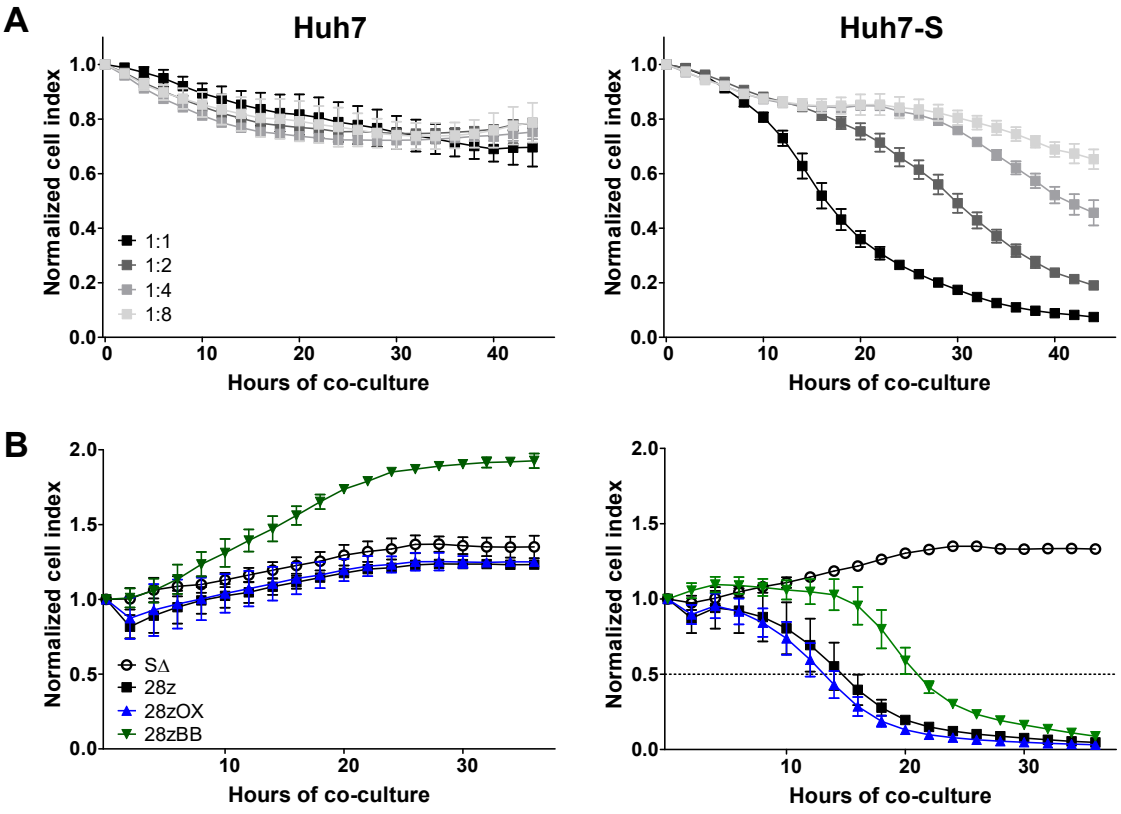

Figure 2.17 *In vitro* cytotoxic effect of transduced human PBMC expressing different 2nd and 3rd generation S-CAR constructs.
Retrovirally transduced PBMC (Figure 2.16) were cultured with Huh7 or S protein-expressing Huh7-S cells as target cells. Cell viability of target cells was determined with the xCELLigence RTCA displayed as normalized cell index (normalized to start of co-culture). **A)** Normalized cell index of target cells in co-culture with 28z S-CAR T cells in different effector to target ratios (E:T). **B)** Normalized cell index of target cells in co-culture with transduced PBMC comparing different S-CAR constructs (E:T=1:1). Dotted line marked normalized cell index of 0.5. All data are presented as mean values ± SD. (n=3)

2.2.3 Additional costimulation fails to enhance proliferation of S-CAR T cells

An effective immune response *in vivo* is not only characterized by effector functions like cytokine release and target cell killing. Proliferation of activated T cells is essential to increase the amount of effector cells that can contribute to the antiviral effect. I compared the proliferation induced by S-CAR stimulation between different S-CAR variants in a carboxyfluorescein succinimidyl ester (CFSE) dilution assay. Flow cytometry analysis revealed that $CD4^+$ and $CD8^+$ S-CAR T cells specifically proliferated upon HBsAg contact in comparison to control cells (mock-treated or EGFRt-negative). Additional OX40 signaling in a 3rd generation S-CAR also induced proliferation of both T-cell subsets but to a lower extent. 4-1BB signaling only led to slight proliferation of $CD8^+$ S-CAR T cells while I did not detect any proliferating $CD4^+$ S-CAR T cells (Figure 2.18).

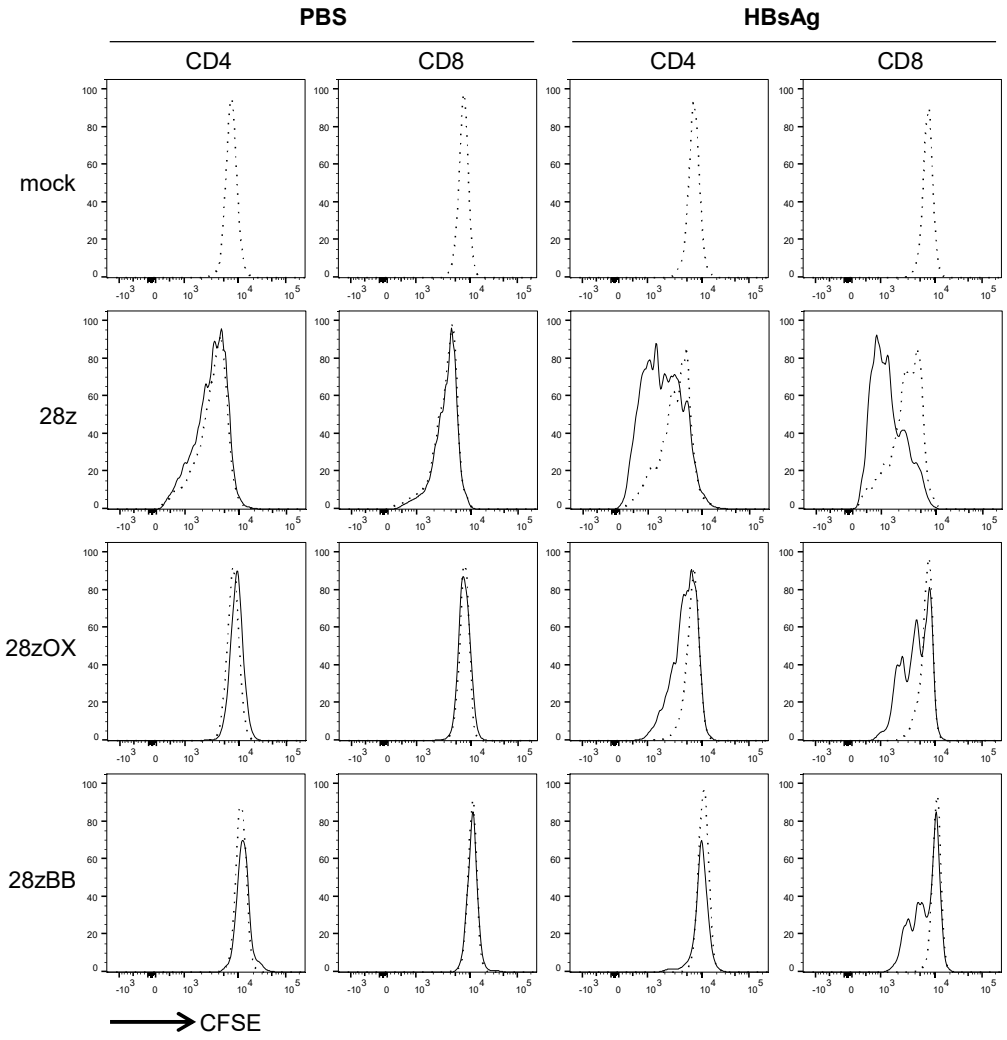

Figure 2.18 Proliferative potential of S-CAR T cells *in vitro.*
Retrovirally transduced PBMC (Figure 2.16) were stained with CFSE and cultured on HBsAg-coated wells (5 μg/ml) or PBS control wells. Dilution of CFSE was determined by flow cytometry after 96 hours. Cells were pregated on $CD4^+$ and $CD8^+$ T cell, and on transduced ($EGFRt^+$, solid lines) and non-transduced ($EGFRt^-$, dotted lines).

2.2.4 An additional costimulatory domain in the S-CAR fails to enhance killing of HBV-infected HepG2-NTCP cells

In 3rd generation CARs the additional costimulatory domain can be added at different positions of the construct. As described in chapter 2.2.1 one possibility is at the C-terminus of the CD3ζ domain. Another site for the domain is between the CD28 and CD3ζ signaling domains. Altered distances from the plasma membrane of each domain and the three-dimensional orientation towards each other could change functionality of the S-CAR. Therefore, I constructed additional versions of the S-CAR (Figure 2.19 A). In addition to two more 3rd generation S-CARs (28OXz and 28BBz), a 2nd generation S-CAR that harbors a 4-1BB domain instead of the CD28 domain (BBz) was used. I expressed all constructs in human PBMC and analyzed

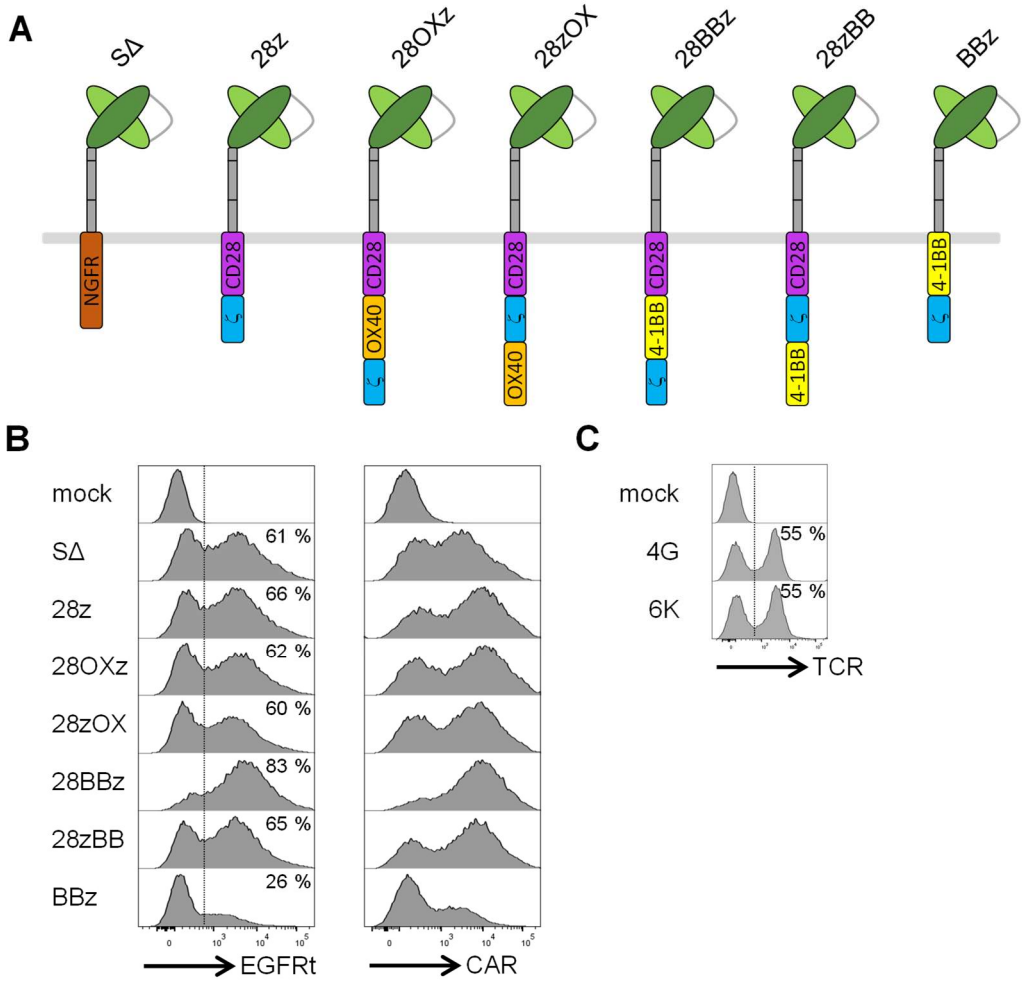

Figure 2.19 Expression of different 2nd and 3rd generation S-CAR constructs.
Human PBMC were retrovirally transduced to express different 2nd and 3rd generation S-CAR constructs. **A)** Scheme of different S-CAR constructs. All versions carry the C8 scFv (light and dark green). S-CARs contain a wildtype IgG1 spacer consisting of hinge-CH2-CH3 domains (grey). Utilized intracellular domains were derived from nerve growth factor receptor (NGFR, brown), CD28 (purple), OX40 (orange), 4-1BB (yellow) and CD3ζ (blue). **B)** Histogram view of flow cytometry analysis that determines transduction rate via EGFRt surface expression (left panel) and S-CAR surface expression (right panel). **C)** Histogram view of flow cytometry analysis staining transgenic control TCRs 4G and 6K. PBMC consisted mostly of $CD4^+$ and $CD8^+$ T cells.

the transduced PBMC by flow cytometry. The transduction rate was determined by EGFRt expression and was between 60 and 66 % (right panel). Only the 28BBz S-CAR displayed higher (83 %) and the 2nd generation BBz S-CAR lower expression levels (26 %) (Figure 2.19 B). As controls, I also transduced PBMC with two HBV-specific TCRs, namely 4G and 6K (Wisskirchen et al., 2017), with a transduction rate of 55 % (Figure 2.19 C). 4G and 6K are specific for peptides from the S and core protein, respectively.

Huh7-S target cells used previously for *in vitro* studies of S-CAR T-cell cytotoxicity expressed the S protein from a transgene. The density of S protein on HBV-infected cells is presumably lower. To achieve physiological levels of S protein, I infected HepG2-NTCP cells, a hepatoma cell line, with HBV. Furthermore, this model allows monitoring of viral parameters such as HBeAg in the supernatant.

The potency of different S-CAR variants to induce killing of HBV-infected HepG2-NTCP cells and to reduce viral parameters was compared. If PBMC expressed S-CARs with only CD28 or with an additional costimulatory domain of OX40, cell viability of target cells decreased comparably. In contrast, all S-CARs, 2nd and 3rd generation, that harbored a 4-1BB domain exhibited lower potential to induce cytotoxicity (Figure 2.20 A). A similar pattern was observed when the supernatants were analyzed for secreted IFN-γ as a marker for T-cell activation (Figure 2.20 B) and HBeAg as viral parameter (Figure 2.20 C). Only S-CAR T cells that did not contain the 4-1BB signaling domain secreted IFN-γ and reduced HBeAg in the supernatant. The 2nd generation S-CAR 28z was at least as potent as S-CARs with additional OX40

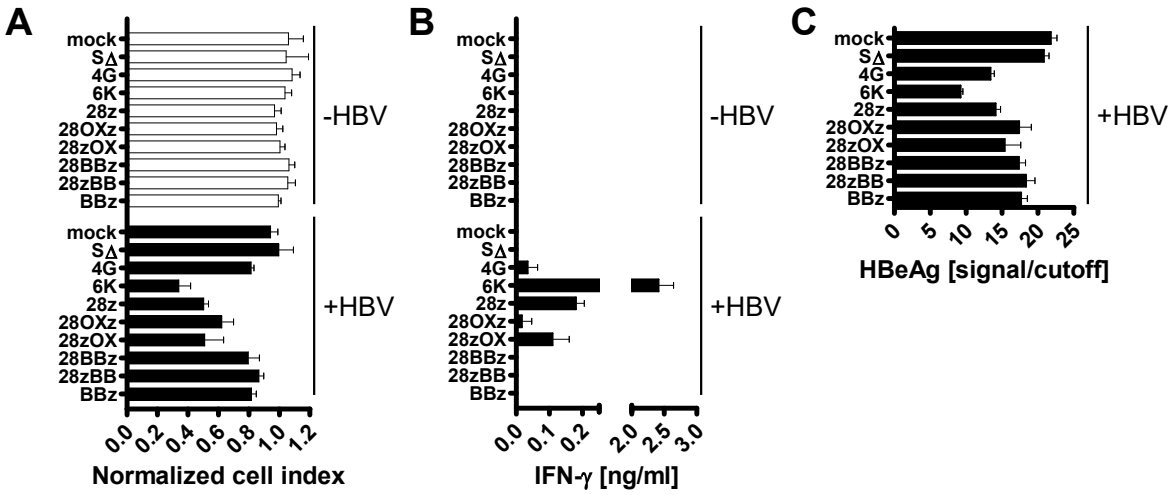

Figure 2.20 Antiviral effect of different S-CAR constructs towards HBV-infected HepG2-NTCP cells *in vitro.*
Retrovirally transduced human PBMC (Figure 2.19) were cultured with HBV-infected (multiplicity of infection (MOI) =100) HepG2-NTCP cells. Cytotoxicity, activation and antiviral effect induced by different S-CAR construct was compared (5 x 10^4 EGFRt$^+$ T cells, E:T=1:1) **A)** Cytotoxicity depicted as normalized cell index of xCELLigence RTCA (normalized to start of co-culture) at 80 hours of co-culture. **B)** Secreted IFN-γ in supernatant after 72 hours. **C)** Secreted HBeAg in supernatant after 72 hours. All data are presented as mean values ± SD. (n=3)

signaling. However, the results do not provide any evidence for an advantage of OX40 or 4-1BB signaling domains in the S-CAR, they even indicate a negative effect of an additional 4-1BB domain. Importantly, the S-CAR was able to redirect T cells towards HBV-infected HepG2-NTCP cells with physiological S protein surface expression. The antiviral effect was comparable to the effect induced by the S protein-specific TCR 4G, but less pronounced than the effect by the core protein-specific TCR 6K.

Taken together, the *in vitro* investigation of transduced human PBMC expressing different variants of the S-CAR revealed the following: Overall, S-CARs with OX40 signaling (28OXz, 28zOX) or without it (28z) performed comparably in all addressed aspects of T-cell functionality. Notably, if I added a 4-1BB signaling domain (28BBz, 28zBB) or exchanged the CD28 to a 4-1BB domain (BBz), S-CAR T cells functioned less efficient. Although these *in vitro* results strongly suggest that the 2nd generation 28z S-CAR outperforms especially S-CARs containing a 4-1BB signaling domain, further *in vivo* studies were needed to confirm this result.

2.2.5 S-CARs with murine 4-1BB signaling domains demonstrate lower *in vivo* functionality

The results suggest a reduction of the T-cell functionality and antiviral activity by a 4-1BB signaling domain in the S-CAR. This conclusion is in contrast to several published studies with other 4-1BB-containing CAR constructs. Hence, I decided to investigate this in an *in vivo* setting where the 4-1BB domain could confer a survival advantage. *In vivo* mouse models are the most complex experimental setting to compare functionality of CAR T cells in the preclinical setting. In contrast to *in vitro* experiments, the interaction with other cell types, cell migration and T-cell survival have a more pronounced effect on the outcome.

In our mouse model for S-CAR T-cell therapy we transfer murine S-CAR T cells into HBV-positive mice. To compare different combinations of signaling domains in this model, I first designed additional S-CAR constructs. These new variants contained murine costimulatory domains of CD28 and 4-1BB in addition to the murine signaling domain of CD3ζ. S-CARs contained either only one or both costimulatory domains. Transduction rates of murine CD8$^+$ T cells varied in the presented experiment (SΔ: 84.6 %, m28z: 75.6 %, mBBz: 59.1 %, m28zBB: 41.0 %) (Figure 2.21 A). When transduced murine S-CAR T cells were cultured on plate-bound HBsAg, all S-CAR variants induced release of IFN-γ. Consistent with previous results comparing human costimulatory domains, T cells that expressed the S-CAR with only CD28 costimulation released approximately twice as much IFN-γ (Figure 2.21 B). Since functionality for all S-CARs with murine signaling domains was demonstrated, I proceeded and compared them *in vivo*.

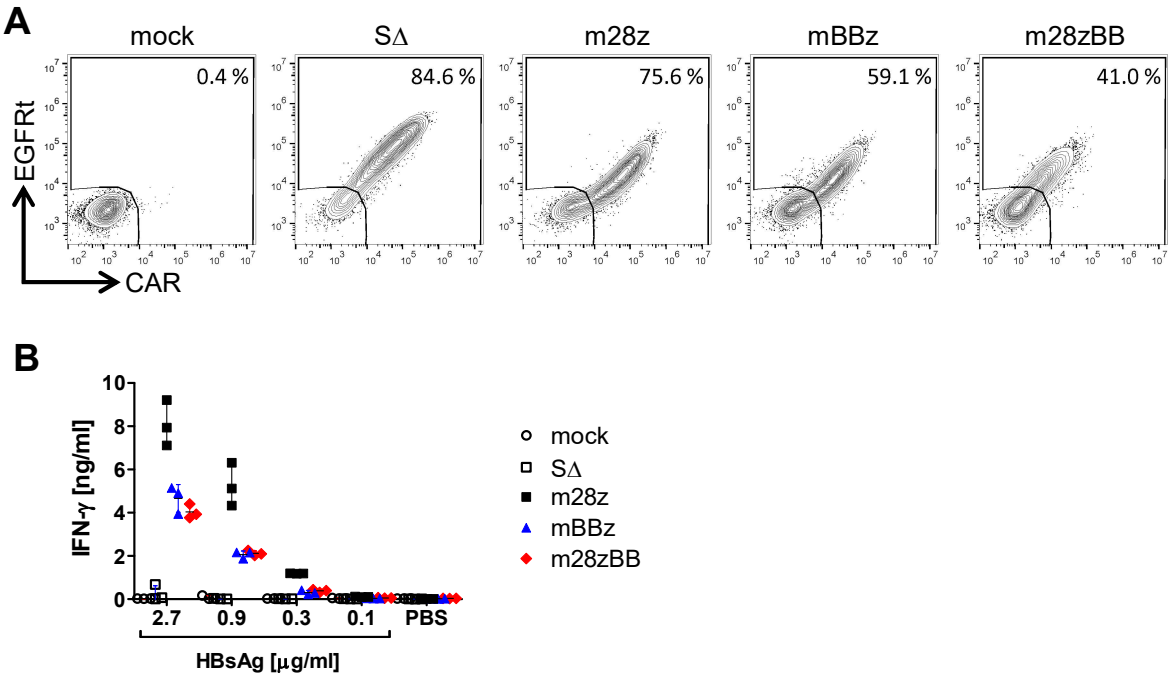

Figure 2.21 *In vitro* stimulation of transduced murine CD8⁺ T cells expressing different murine 2nd and 3rd generation S-CAR constructs.
Murine CD8⁺ T cells were retrovirally transduced to express different S-CAR constructs with murine signaling domains and EGFRt. Extracellular and transmembrane (TM) domain remained as in the S-CARs previously described (human FcΔ IgG1 spacer, human CD28 TM). **A)** Flow cytometry analysis of CD8⁺ T cells depicting S-CAR and EGFRt expression. **B)** Secreted IFN-γ in 16-hour supernatant of 5 x 10^4 transduced T cells cultured on HBsAg-coated or PBS control wells determined by ELISA. All data are presented as single and mean values ± SD. (n=3)

For *in vivo* comparison I transferred transduced murine CD8⁺ T cells into AAV-HBV-infected Rag2$^{-/-}$/IL-2Rγ$^{-/-}$ mice (Figure 2.22 A). Transduction rates before transfer were determined by flow cytometry analysis and varied between 45.9 % (SΔ, m28zBB) and 78.6 % (m28z) (Figure 2.22 B). Upon transfer, CD8⁺ T cells that expressed the m28z S-CAR demonstrated higher concentration in peripheral blood in comparison to SΔ-CAR T cells and 4-1BB-containing S-CAR T cells (mBBz, m28zBB) over the course of treatment. Both S-CAR variants with a costimulatory 4-1BB domain failed to provide signaling for enhanced proliferation or survival (Figure 2.22 C). At the time of sacrifice (d40), transduced T cells in liver and spleen displayed a comparable result (Figure 2.22 D). Furthermore, the proportion of transduced cells in the transferred cells was determined in liver and spleen. While the proportion was approximately 90 % in liver and 60 – 85 % in spleen for m28z S-CAR treated mice, it was substantially lower in the other treatment groups (liver: 50 – 65 %, spleen: 10 – 25 %) (Figure 2.22 E).

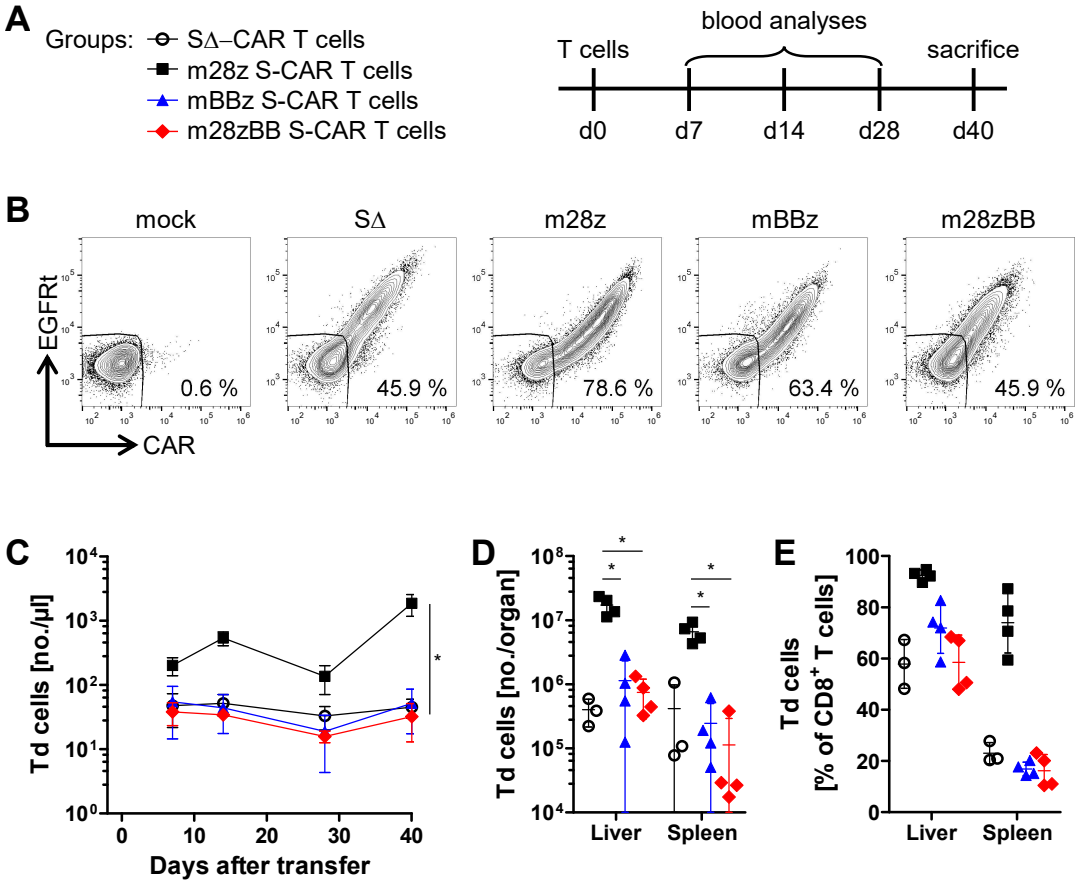

Figure 2.22 *In vivo* persistence of S-CAR T cells with different CD28 and 4-1BB containing S-CAR constructs.
A) AAV-HBV-infected Rag2$^{-/-}$/IL-2R$\gamma^{-/-}$ mice were injected with 5 x 10^5 S-CAR$^+$/EGFRt$^+$ T cells. S-CARs contained different murine signaling domains. Transduced (Td = S-CAR$^+$ and /or EGFRt$^+$) CD8$^+$ T cells in peripheral blood were monitored by flow cytometry analysis on days 7, 14, 28, and 40. **B)** Flow cytometry analysis of CD8$^+$ T cells before transfer. **C)** Concentration of transduced (Td = S-CAR$^+$ and/or EGFRt$^+$) T cells in peripheral blood. **D, E)** Transduced T cells in liver and spleen 38 days after transfer. **D)** Total count. **E)** Proportion of CD8$^+$ T cells. C: Data are presented as mean values ± SD. D, E: Data are presented as values of single mice and mean values ± SD. (n=3 mice for SΔ, n=4 mice for m28z, mBBz and m28zBB per group, Mann Whitney test, ns = not significant, * = p<0.05)

Forty days after transfer I isolated LALs as well as splenocytes and analyzed the expression of memory, activation and exhaustion markers by flow cytometry. Transferred cells expressing SΔ-CAR and S-CARs with 4-1BB costimulatory domain (mBBz, m28zBB) exhibited a comparable phenotype both in liver and spleen. In the liver most transferred cells expressed markers of effector-memory CD8$^+$ T cells while in the spleen they were mostly of a naïve/central-memory phenotype (Figure 2.23 A). In contrast, transferred cells in the m28z S-CAR T cells treatment group were mostly effector – and not effector-memory or naïve/central-memory – CD8$^+$ T cells in both liver and spleen. Regarding activation and exhaustion markers, expression of PD-1 and CD69 was upregulated in m28z S-CAR T cells in comparison to SΔ-CAR T cells in liver and spleen (Figure 2.23 B). 4-1BB containing S-CAR T cells displayed a slight upregulation of both markers only in the liver. I did not detect any

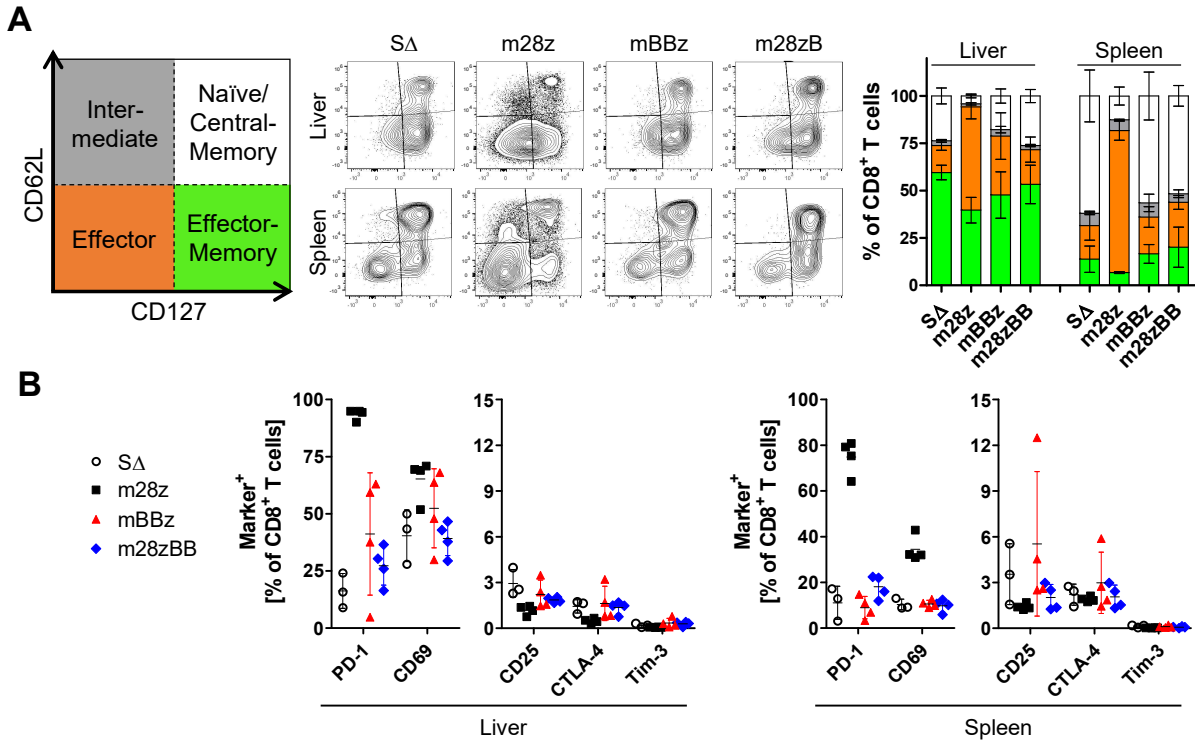

Figure 2.23 Expression of memory, activation and exhaustion markers on S-CAR T cells with different murine CD28 and 4-1BB S-CAR constructs after *in vivo* survival.
LALs and splenocytes were isolated on day 40 from S-CAR T cell-injected Rag2$^{-/-}$/IL-2Rγ$^{-/-}$ mice (Figure 2.22) and analyzed by flow cytometry. **A)** Memory marker expression (CD62L and CD127) of transferred CD8$^+$ T cells. **B)** Activation and exhaustion marker expression (PD-1, CD69, CD25, CTLA-4, Tim-3) of transferred CD8$^+$ T cells. A: Data are presented as mean values ± SD. B: Data are presented as values of single mice and mean values ± SD. (n=3 mice for SΔ; n=4 mice for m28z, mBBz and m28zBB per group)

specific upregulation of either CD25, CTLA-4, or Tim-3 in any treatment group that had received functional S-CAR T cells.

To test T-cell functionality after *in vivo* survival, freshly isolated LALs and splenocytes were rested overnight or stimulated on plate-bound HBsAg or plate-bound anti-CD3/anti-CD28 antibodies (Figure 2.24). Only m28z S-CAR T cells exhibited HBsAg-specific expression of IFN-γ and low amounts of TNF-α. In contrast, transferred cells from all treatment groups expressed IFN-γ upon unspecific stimulation. Here, I detected more TNF-α expression by SΔ-CAR, mBBz and m28zBB S-CAR T cells than by m28z S-CAR T cells. Taken together, transferred cells from treatment groups with a 4-1BB costimulatory domain displayed a phenotype and functionality comparable to control SΔ-CAR T cells. This could be due to low activation of T cells or a loss of activated T cells.

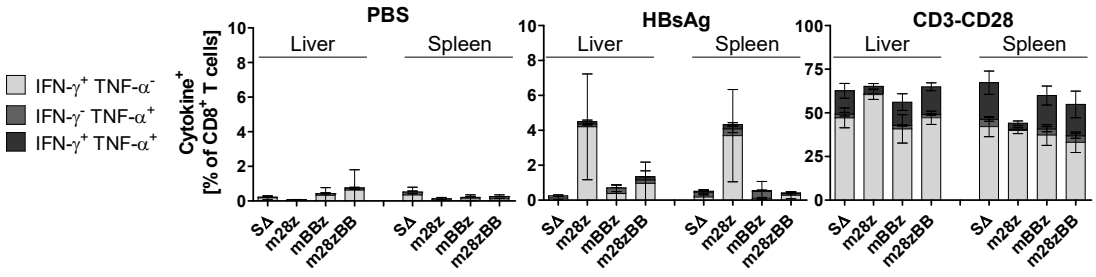

Figure 2.24 *Ex vivo* functionality of S-CAR T cells with different murine CD28 and 4-1BB containing S-CAR constructs after *in vivo* survival.
LALs and splenocytes were isolated on day 40 from S-CAR T cell-injected Rag2$^{-/-}$/IL-2Rγ$^{-/-}$ mice (Figure 2.22) and cultured overnight on PBS-treated, HBsAg-coated or anti-CD3/anti-CD28 antibody-coated plates. On the next day expression of IFN-γ and TNF-α by transferred CD8^{+} T cells was detected via an ICS. Data are presented as mean values ± SD. (n=3 mice for SΔ; n=4 mice for m28z, mBBz and m28zBB per group)

When AAV-HBV-infected Rag2$^{-/-}$/IL-2Rγ$^{-/-}$ mice were treated with S-CAR T cells harboring murine signaling domains, transferred T cells did not induce liver toxicity as determined by stable serum ALT levels (Figure 2.25 A). The body weight also remained stable suggesting no strong side-effects (Figure 2.25 B). Only m28z S-CAR T cells induced an antiviral effect indicated by a decrease of HBsAg (Figure 2.25 C) and HBeAg (Figure 2.25 D) in serum. Viral parameters in treatment groups with a costimulatory domain of 4-1BB in the S-CAR remained unaltered over the course of treatment.

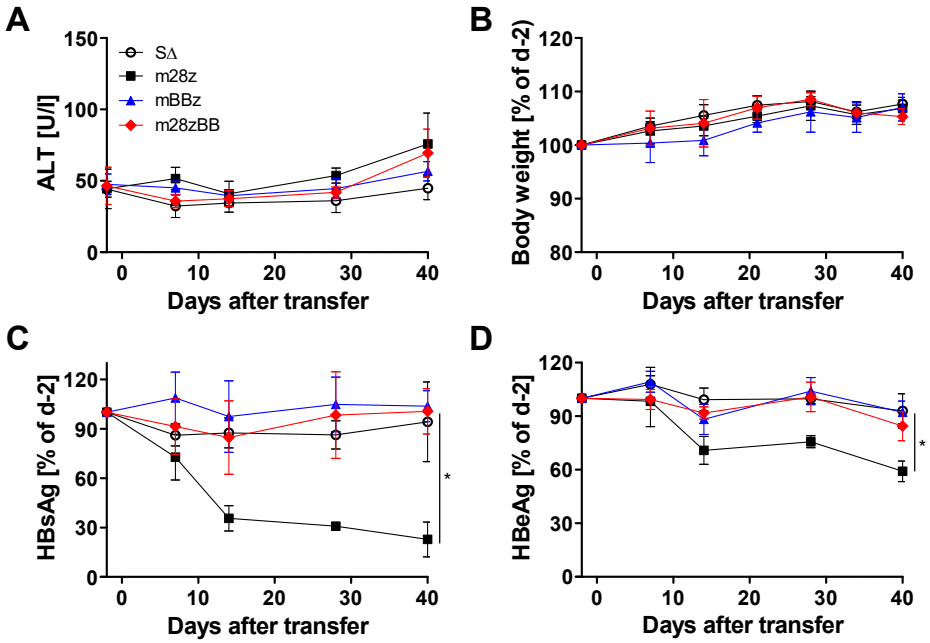

Figure 2.25 Antiviral effect of S-CAR T cells with different murine CD28 and 4-1BB containing S-CAR constructs.
Viral parameters in serum were analyzed in mice injected with S-CAR T cells that expressed different S-CAR constructs (Figure 2.22). **A)** Serum ALT levels monitored over time. **B)** Change in body weight in comparison to day -2. **C)** HBsAg levels in serum in comparison to day -2. **D)** HBeAg levels in serum in comparison to day -2. All data are presented as mean values ± SD. (n=3 mice for SΔ; n=4 mice for m28z, mBBz and m28zBB per group, Mann Whitney test, * = $p<0.05$)

To summarize this section, I compared different S-CAR variants that differed in their costimulatory signaling domains both *in vitro* and *in vivo*. Human signaling domains were compared in human T cells, and murine signaling domains in the mouse counterparts. Consistent through all experiments, the data suggest that presence of a 4-1BB costimulatory domain induces less T-cell activation, expansion and persistence and a lower antiviral effect. OX40 signaling was only tested *in vitro*, but it also failed to enhance S-CAR T-cell functionality under the tested conditions. The results do not provide any evidence that additional signaling by OX40 or 4-1BB would give any advantage for the therapeutic outcome.

2.3 Immune-regulatory mechanisms

As indicated by the experiments described in section 2.1.4, a transfer of S-CAR T cells was not curative within 140 days of treatment since HBV-positive hepatocytes remained even after long-term *in vivo* persistence of S-CAR T cells. Immune-regulatory mechanisms can be part of the failure of the immune system to eliminate an infection. Two well-described checkpoints are PD-1 and IL-10. Previous data indicated that both proteins were expressed by isolated S-CAR T cells. In the following section I addressed the relevance of these molecules for the therapeutic outcome of S-CAR T-cell therapy. Furthermore, intrahepatic immuno-stimulation by CpG was applied to enhance T-cell proliferation and functionality.

2.3.1 PD-1-deficiency fails to enhance the antiviral effect of S-CAR T cells *in vivo*

PD-1 is expressed on activated T cells and makes them susceptible to inhibition by binding to PD-L1 or PD-L2. To investigate the influence of PD-1 I could use checkpoint inhibition antibodies or genetic deletion of PD-1 (Nishimura et al., 1998). As a first step I chose the latter because it promised to be the more efficient approach. PD-1$^{-/-}$ CD8^{+} T cells can be used as

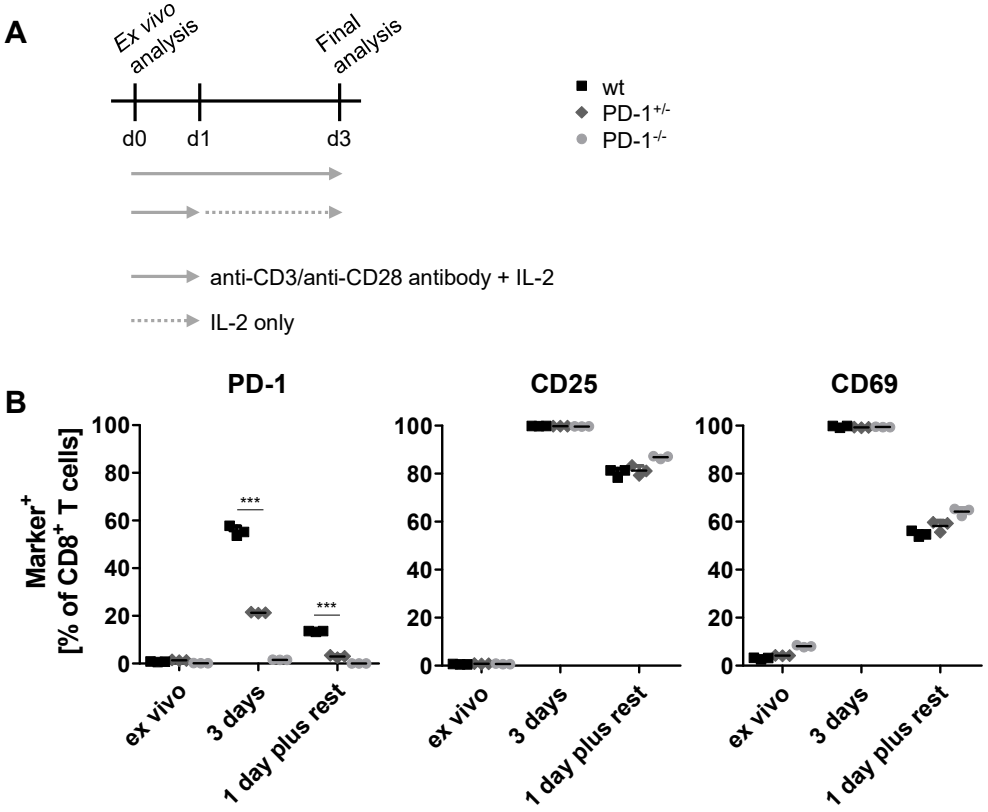

Figure 2.26 Expression of activation markers by CD8^{+} T cells upon *in vitro* stimulation. **A)** Splenocytes of wildtype (wt), PD-1$^{+/-}$, and PD-1$^{-/-}$ mice were isolated and 7 x 10^5 cells/well stimulated on anti-CD3/anti-CD28 antibody-coated 24-plates and with 300 IU/ml IL-2. Antibody stimulation was withdrawn in one group after one day (1 day plus rest). Expression of activation markers was determined *ex vivo* and on day 3. **B)** Flow cytometry analysis of activation marker expression (PD-1, CD25, CD69). All data are presented as mean values ± SD. (n=3, biological replicates, one donor mouse per genotype group, unpaired T-test, *** = p<0.001)

donor cells for S-CAR T-cell production. They can be transferred in comparison to wildtype S-CAR T cells or cells that carry only one intact PD-1 allele. Heterozygous donor cells would be the choice if they expressed PD-1 upon activation in the same manner as wildtype cells. When I stimulated murine splenocytes for three days with anti-CD3/anti-CD28 antibodies or for one day plus two days of resting (Figure 2.26 A), I could show that more wildtype $CD8^+$ T cells expressed PD-1 (wildtype: 57 %, heterozygous: 21 %). Other activation markers (CD25 and CD69) were expressed comparably (Figure 2.26 B). The discrepancy of PD-1 expression between wildtype and PD-1 heterozygous $CD8^+$ T cells provided the base for usage of wildtype donor mice as control in the following *in vivo* investigation.

To investigate the relevance of PD-1 expression on S-CAR T cells, I transferred transduced murine PD-$1^{-/-}$ or wildtype cells into AAV-HBV-infected Rag$2^{-/-}$/IL-2R$\gamma^{-/-}$ mice (Figure 2.27 A). Initially, PD-$1^{-/-}$ S-CAR T cells could be detected in higher concentrations in peripheral blood (day 7 – day 21) (Figure 2.27 B). During the second half of the treatment period, this difference disappeared. At day 42 comparable numbers of transduced T cells were detected in liver and spleen in both groups (Figure 2.27 C). Transferred cells from both treatment groups were composed of comparable T-cell subsets regarding memory marker expression (Figure 2.27 D) and a similar proportion of cells expressed CD69 and Tim-3 in liver and spleen (Figure 2.27 E). Only in the spleen a slightly larger proportion of transduced PD-$1^{-/-}$ $CD8^+$ T cells expressed CD69 than wildtype cells. When transferred cells were stimulated after isolation, cells from both treatment groups expressed IFN-γ, TNF-α, and IL-10 in comparable amounts (Figure 2.27 F). Regarding the antiviral effect, both S-CAR T-cell products provided a similar therapeutic outcome. They both induced a slight transient elevation of serum ALT levels (Figure 2.27 G). Although HBsAg decreased faster in the PD-$1^{-/-}$ treatment group, eventually, in both treatment groups a comparable reduction of approximately 96 % was reached (Figure 2.27 H). HBeAg levels of both groups decreased to about 55 % of untreated mice (Figure 2.27 I). Taken together, T-cell proliferation, functionality and the antiviral effect were not altered by PD-1-deficiency of transferred cells. The results suggest that PD-1-expression on S-CAR T cells does not limit S-CAR T-cell functionality *in vivo*.

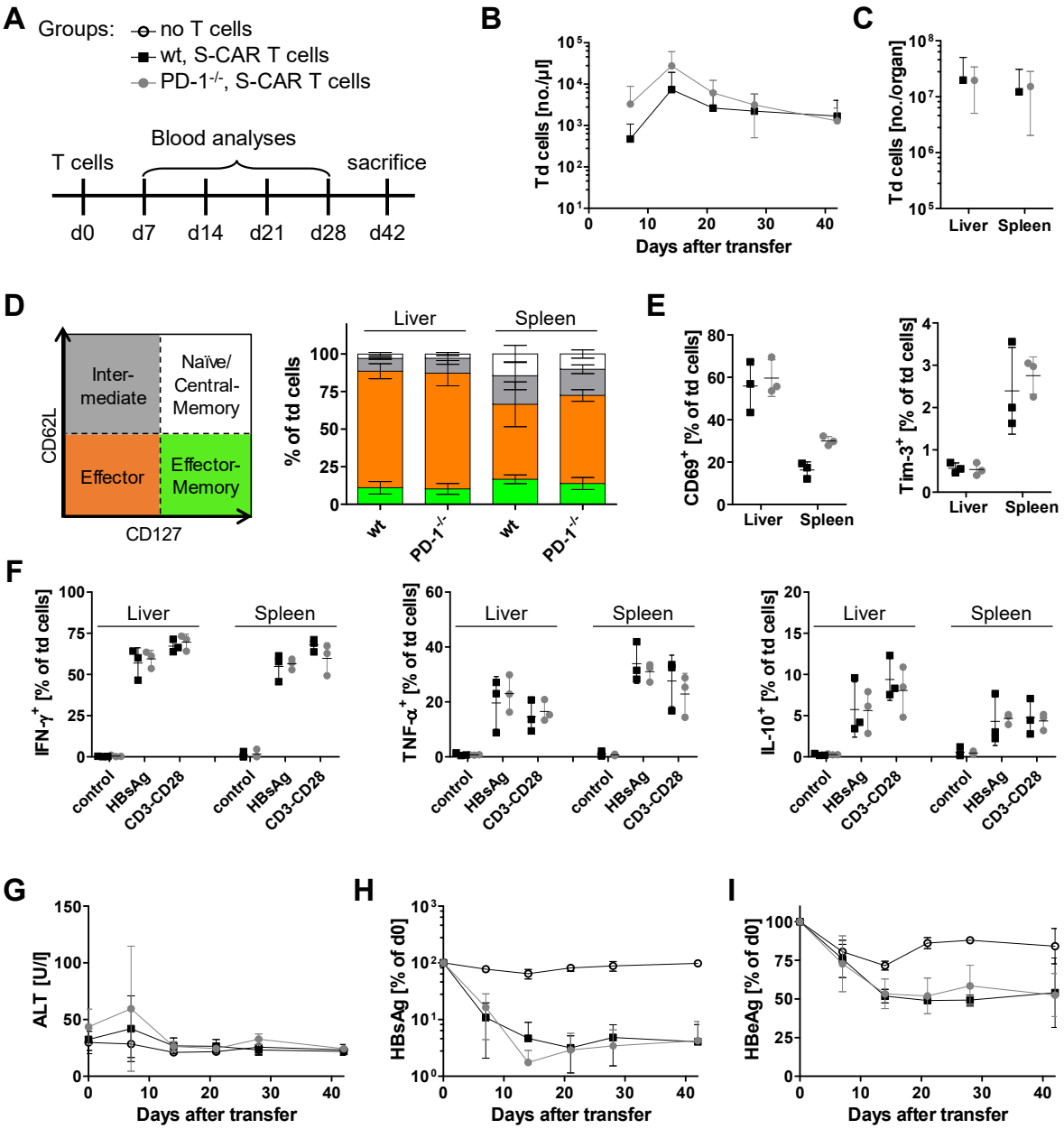

Figure 2.27 Influence of PD-1-deficiency on *in vivo* T-cell expansion, phenotype and antiviral effect of S-CAR T cells.
A) AAV-HBV-infected Rag2$^{-/-}$/IL-2Rγ$^{-/-}$ mice were injected with 1 x 10^6 S-CAR$^+$/EGFR$^+$ T cells. Donor CD8$^+$ T cells were derived from wildtype or PD-1$^{-/-}$ mice. Transduced (Td = S-CAR$^+$ and/or EGFRt$^+$) CD8$^+$ T cells in peripheral blood and viral parameters were monitored on days 7, 14, 21, 28, and 42. **B)** Concentration of transduced (Td = S-CAR$^+$ and/or EGFRt$^+$) T cells in peripheral blood. **C)** Number of transduced T cells in liver and spleen on day 42. **D)** Memory marker expression (CD62L and CD127) of transduced CD8$^+$ T cells on day 42. **E)** Activation (CD69) and exhaustion (Tim-3) marker expression of transduced CD8$^+$ T cells on day 42. **F)** Expression of IFN-γ, TNF-α and IL-10 upon specific (HBsAg) and unspecific (anti-CD3/anti-CD28) stimulation of transduced CD8$^+$ T cells on day 42. **G)** Serum ALT levels. **H)** HBsAg levels in serum. **I)** HBeAg levels in serum. B, C, D, G, H, I: Data are presented as mean values ± SD. E, F: Data are presented as values of single mice and mean values ± SD. (n=2, untreated mice; n=3, injected mice)

2.3.2 Human S-CAR T cells release IL-10 upon *in vitro* stimulation

As described above, murine S-CAR T cells expressed IL-10 upon *ex vivo* stimulation. To determine the relevance of this finding for the clinical application, I asked whether human T cells would behave similarly. Therefore, I cultured transduced human PBMC on HBsAg-positive target cells (Huh7-S) or control cells and analyzed the release of cytokines by ELISA (Figure 2.28 A). S-CAR T cells released IFN-γ (left panel) and IL-10 (right panel) upon HBsAg contact. Next, the same effector cells were cultured on plate-bound HBsAg and the cytokine expression analyzed via an ICS. Both $CD4^+$ and $CD8^+$ T cells released TNF-α and IL-10 upon HBsAg contact. The majority of IL-10 was expressed by $CD4^+$ T cells (Figure 2.28 B and C). Therefore, I conclude that human $CD4^+$ and $CD8^+$ S-CAR T cells can express and release IL-10 upon HBsAg-specific activation, as seen previously in murine $CD8^+$ S-CAR T cells (Figure 2.10 B).

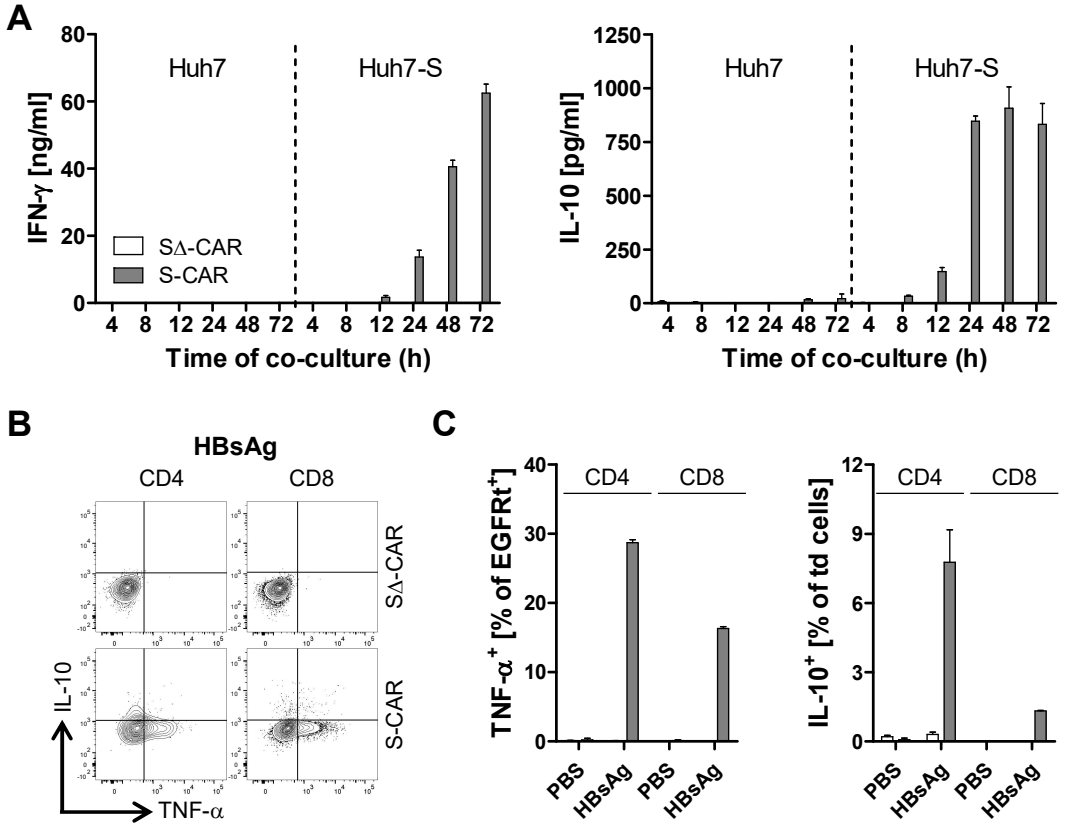

Figure 2.28 IL-10 expression and release by human S-CAR T cells upon *in vitro* stimulation.
A) Retrovirally transduced S-CAR expressing human PBMC were co-cultured with Huh7 or S protein-expressing Huh7-S cells. Secreted IFN-γ and IL-10 in supernatant were determined by ELISA. **B)** Retrovirally transduced S-CAR expressing human PBMC were cultured on HBsAg-coated or PBS control wells overnight. Expression of TNF-α and IL-10 were determined via an ICS the following day. Exemplary flow cytometry plot of ICS. **C)** Summary of TNF-α and IL-10 expression by $EGFRt^+$ $CD4^+$ or $CD8^+$ T cells. All data are presented as mean values ± SD. (n=3)

2.3.3 IL-10-deficiency of transferred cells or intrahepatic immuno-stimulation does not influence S-CAR T-cell functionality *in vivo*

Since IL-10 is expressed by both human and murine S-CAR T cells it could be part of the limited antiviral effect. To investigate the influence of IL-10 on the therapeutic outcome of S-CAR T-cell therapy, I used IL-10$^{-/-}$ mice as donors for CD8^{+} T cells. Wildtype donor mice served as control. In parallel, I also tested if the application of CpG has an influence on S-CAR T cells. CpG is a ligand for Toll-like receptor 9 and is known to induce iMATEs (intrahepatic myeloid-cell aggregates for T-cell population expansion), which serve as a hub for T-cell proliferation (Huang et al., 2013b). The induction of iMATEs has been shown to enhance functionality of T cells that have been induced by therapeutic vaccination (Anna Kosinska, Nina Kallin, unpublished data). In this setting I applied CpG (or a control oligonucleotide) intravenously on the day of S-CAR T-cell transfer (Figure 2.29 A).

The transduction rate of murine CD8^{+} T cells was approximately 70 % (Figure 2.29 B). S-CAR T cells could be detected in comparably high concentrations (~10,000 transduced cells/μl) in the peripheral blood in all three treatment groups (Figure 2.29 C). On the day of final analysis (day 74), I detected comparable total numbers of transduced cells in liver and spleen independent of IL-10-deficiency and CpG application (Figure 2.29 D).

Further analysis revealed that transduced S-CAR T cells from all treatment groups exhibited a similar composition of memory/effector CD8^{+} T-cell subsets regarding their expression of CD62L and CD127 (Figure 2.29 E). Upon *ex vivo* stimulation, a comparably low amount of functional S-CAR T cells expressed TNF-α. Furthermore, cells from treatment groups with or without CpG expressed IL-10, except for a lack of IL-10 expression by IL-10$^{-/-}$ cells, as expected. Only SΔ-CAR T cells expressed higher amounts of TNF-α (30 – 60 %) upon unspecific stimulation and no IL-10 (Figure 2.29 F).

Over the course of treatment liver enzyme levels and viral parameters were monitored. None of the treatments induced a rise of serum ALT levels (Figure 2.29 G). Viral parameters in all three S-CAR treatment groups decreased comparably: HBsAg to approximately 1 % (Figure 2.29 H) and HBeAg to about 30 % of pretreatment values (Figure 2.29 I). To sum up, IL-10-deficiency or CpG application failed to enhance T-cell proliferation and functionality during S-CAR T-cell therapy. As seen above regarding PD-1-deficiency, the limitations of S-CAR T-cell therapy in our mouse model appears to be of a different cause and will be discussed below.

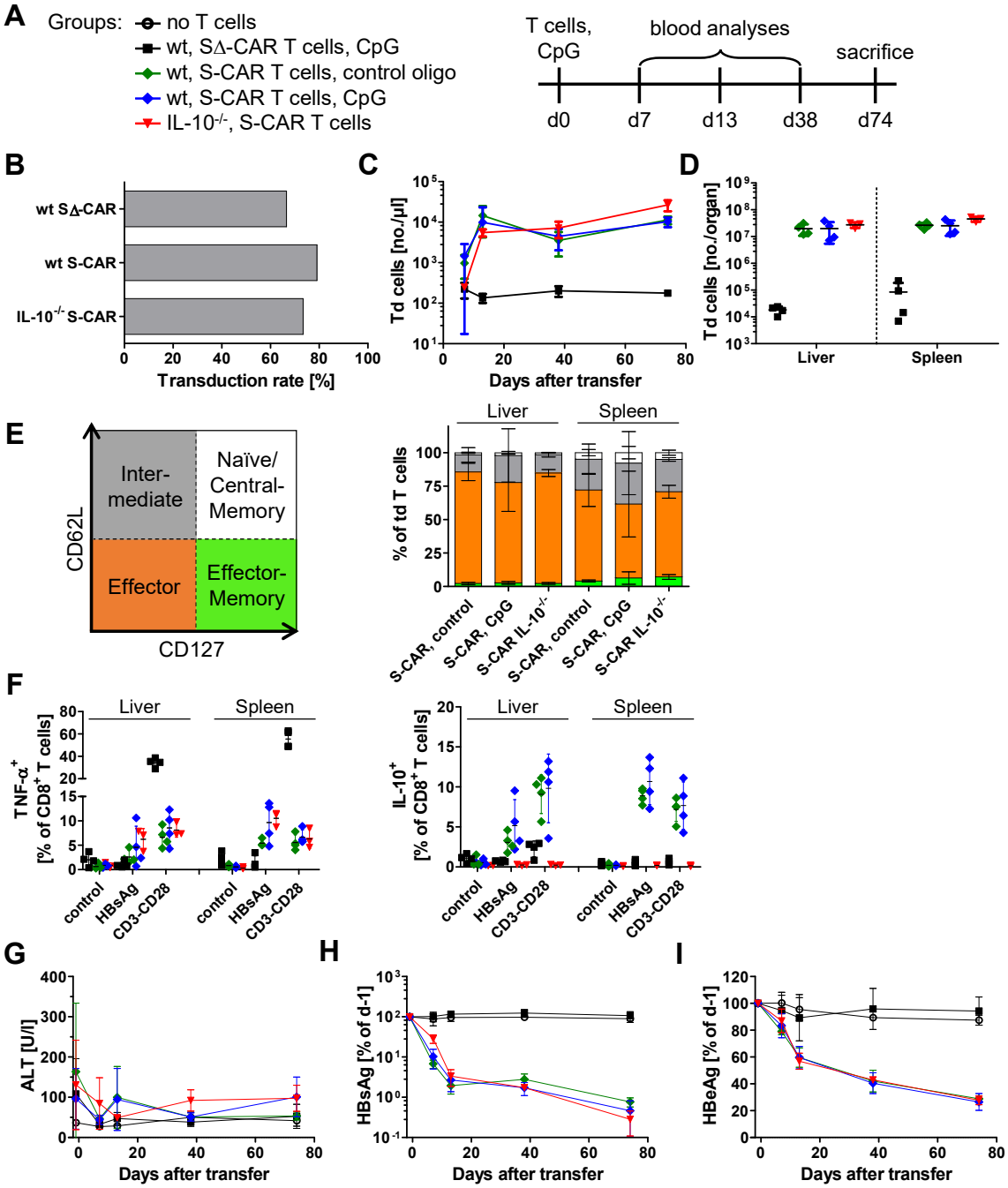

Figure 2.29 Influence of IL-10-deficiency and iMATE induction on *in vivo* T-cell expansion, phenotype and antiviral effect of S-CAR T cells.
A) AAV-HBV-infected Rag2$^{-/-}$/IL-2Rγ$^{-/-}$ mice were injected with 2 x 10^6 S-CAR$^+$/EGFRt$^+$ CD8$^+$ T cells. Donor CD8$^+$ T cells were derived from wildtype or IL-10$^{-/-}$ mice. On the day of transfer, CpG was applied intravenously. Transduced (Td = S-CAR$^+$ and/or EGFRt$^+$) CD8$^+$ T cells in peripheral blood and viral parameters were monitored on days -1, 7, 13, 38, and 74. **B)** Transduction rate of CD8$^+$ T cells on day of transfer (d0). **C)** Concentration of transduced (Td = S-CAR$^+$ and/or EGFRt$^+$) T cells in peripheral blood. **D)** Count of transduced T cells in liver and spleen on day 74. **E)** Memory marker expression (CD62L and CD127) of transduced CD8$^+$ T cells on day 74. **F)** Expression of TNF-α and IL-10 upon specific (HBsAg) and unspecific (anti-CD3/anti-CD28) stimulation of transferred CD8$^+$ S-CAR T cells on day 74. **G)** Serum ALT levels. **H)** HBsAg levels in serum. **I)** HBeAg levels in serum. C, E, G, H, I: Data are presented as mean values ± SD. D, F: Data are presented as values of single mice and mean values ± SD. (n=3 mice for untreated and IL-10$^{-/-}$ S-CAR T cell-treated mice per group; n=4 mice for CpG and control oligo groups per group)

2.4 Investigation of S-CAR T cells in macaque model for HBV infection

Sophisticated *in vivo* models are essential to obtain a deep understanding of functionality and safety of T-cell therapy approaches. As described above, the *in vivo* mouse model for HBV infection suggests that S-CAR T-cell therapy is safe and shows an antiviral effect but fails to cure the infection. Prior to a clinical application, additional *in vivo* studies in non-human primates would be desirable to address particularly safety aspects of the therapeutic approach. Recently, a model for HBV infection in rhesus macaques (*Macaca mulatta*) was described (Burwitz et al., 2017). In the following the technology to generate and assess S-CAR T cells was transferred to macaque effector and target cells.

2.4.1 Macaque T cells can express the S-CAR and can be activated by HBsAg

As a first step of transferring S-CAR technology to the rhesus macaque model, transduction of rhesus macaque T cells needed to be established. To this end, three different stimulation protocols were compared (Staphylococcal enterotoxin B = SEB, IL-2, interleukin-15 = IL-15) and the expression of EGFRt and the S-CAR was determined via flow cytometry (Figure 2.30 A). All three stimulation protocols allowed for transduction of around 80 % of macaque $CD4^+$ and $CD8^+$ T cells. During transduction, only macaque cells that were stimulated with IL-15 proliferated comparable (33-fold) to human PBMC (Figure 2.30 B).

The S-CAR that was expressed in macaque T cells contained human signaling domains for CD28 and CD3ζ. To investigate if these domains were functional in macaque T cells, I cultured transduced macaque T cells on plate-bound HBsAg or anti-CD3/anti-CD28 antibodies for unspecific stimulation. An ICS the next day revealed that macaque $CD8^+$ T cells expressed IFN-γ and TNF-α upon HBsAg contact comparable to transduced human $CD8^+$ T cells (IFN-γ: 40 – 70 %; TNF-α: 20 – 40 %). A larger proportion of macaque S-CAR $CD8^+$ T cells that had been activated with the SEB protocol expressed TNF-α than cells from the other activation protocols. Interestingly, the result differed for $CD4^+$ T cells. Both upon HBsAg-specific and unspecific activation only a small proportion of macaque $CD4^+$ T cells expressed IFN-γ or TNF-α. In contrast, human $CD4^+$ T cells were nearly as potent to express cytokines as human $CD8^+$ T cells (Figure 2.30 C). Although T-cell expansion was more pronounced with the IL-15 stimulation protocol, the SEB protocol was chosen for subsequent experiments since under these conditions the highest expression level of proinflammatory cytokines was induced upon specific stimulation.

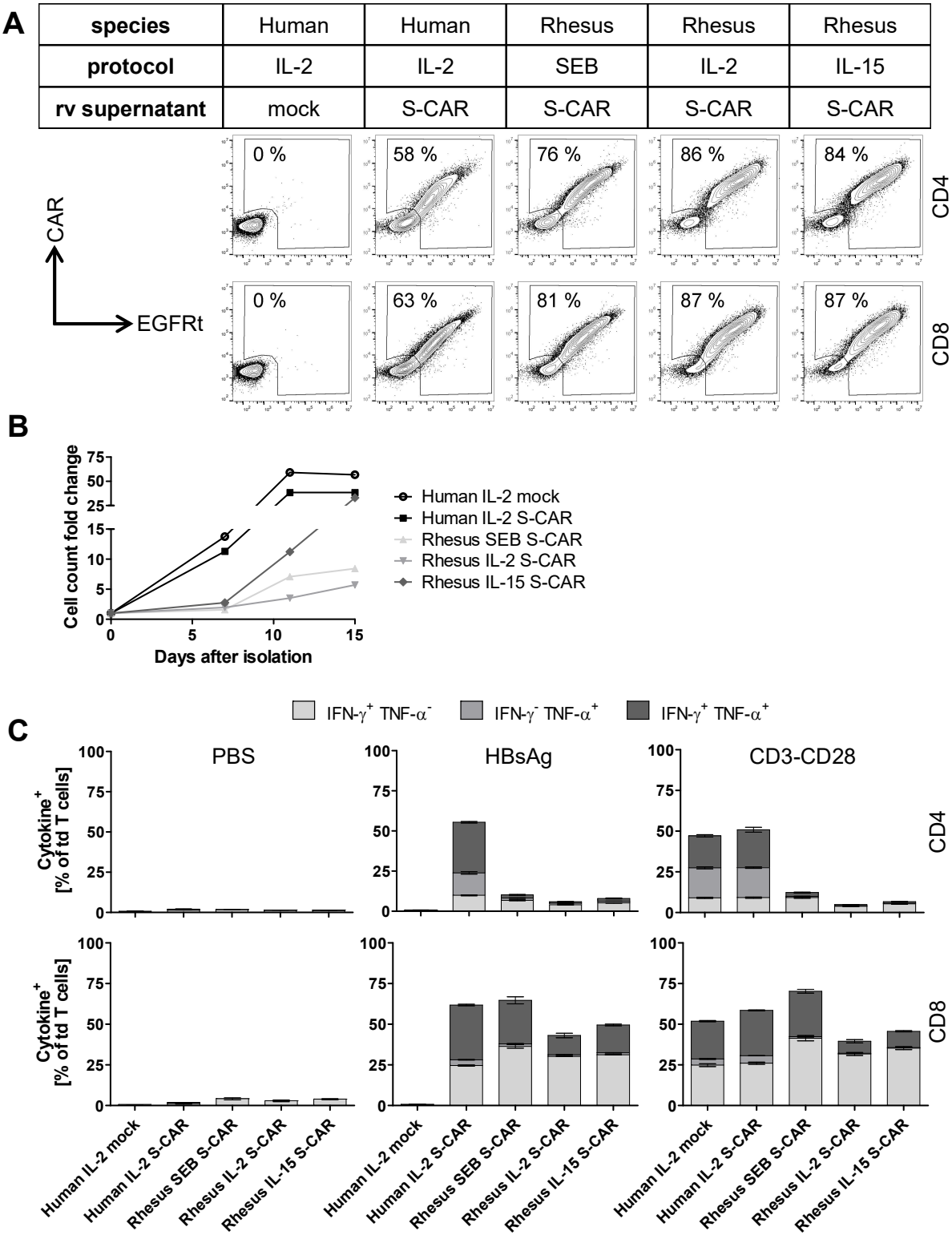

Figure 2.30 Transduction of rhesus macaque PBMC to express the S-CAR.
Macaque PBMC were activated and retrovirally (rv) transduced using three different activation protocols (SEB, IL-2, IL-15). Transduction of human PBMC served as control. **A)** Flow cytometry analysis of macaque PBMC. Expression of S-CAR and EGFRt in $CD4^+$ and $CD8^+$ T cells. **B)** *In vitro* expansion during and after transduction. **C)** Transduced macaque PBMC (1×10^5 total PBMC/well) were cultured overnight on PBS-treated, HBsAg- or anti-CD3/anti-CD28-coated wells. Cytokine expression of transduced (td = $S\text{-}CAR^+$ and/or $EGFR^+$) $CD4^+$or $CD8^+$ T cells upon specific and unspecific stimulation was determined via an ICS the following day. C: Data are presented as mean values ± SD. (n=3)

2.4.2 S-CAR T cells can be activated by S protein-expressing macaque primary hepatocytes

Since activation of macaque T cells via the S-CAR was possible, I proceeded and investigated S-CAR T-cell functionality against macaque target cells. The following experiments were performed in cooperation with Julia Hasreiter in the laboratory of Benjamin Burwitz at the Vaccine and Gene Therapy Institute (OR, USA). To this end, primary macaque hepatocytes (PMHs) were isolated and transduced with an adenoviral vector to transfer the HBV genome (Ad-HBV) (Figure 2.31 A). When macaque S-CAR T cells were co-cultured with these target

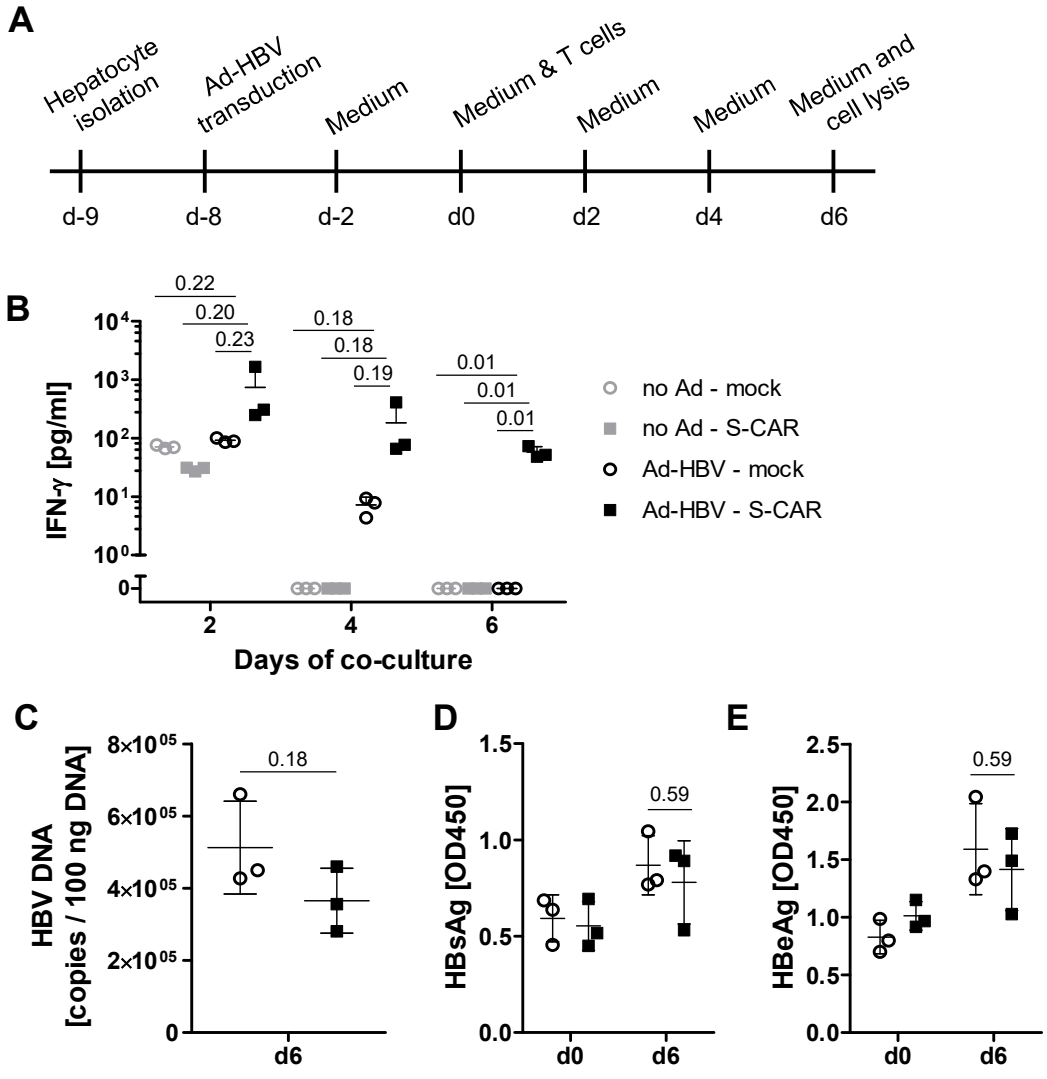

Figure 2.31 Antiviral effect of redirected macaque PBMC against Ad-HBV-transduced PMHs *in vitro*.
A) PMHs were isolated on day -9 and transduced with Ad-HBV on day -8. The co-culture with macaque S-CAR T cells was started on day 0. Media was exchanged on days -2, 0, 2, and 4. On day 6, target cells were harvested. **B)** Secreted IFN-γ in 48-hour supernatant was determined on day 2, day 4 and day 6 by ELISA. **C)** Intracellular HBV DNA on day 6. **D)** HBsAg in 48-hour supernatant on day 6. **E)** HBeAg in 48-hour supernatant on day 6. All data are presented as single and mean values ± SD. (n=3, unpaired T-test, p-values depicted above line)

cells, they specifically released IFN-γ (Figure 2.31 B). To investigate the antiviral effect, viral parameters in the target cells as well as in the supernatant were monitored. Analysis of HBV DNA in the target cells at the end of co-culture (day 6) revealed that there was only a tendency for a reduction in the S-CAR T-cell treatment group in comparison to mock T cells (Figure 2.31 C). HBsAg (Figure 2.31 D) and HBeAg (Figure 2.31 E) in the supernatant on day 6 were not reduced in comparison to day 0 and treatment with mock T cell.

As a next step, the antiviral effect of macaque S-CAR T cells was determined in a newly established HBV infection model in PMHs. Expression of human NTCP (hNTCP) has been determined as the limiting factor for a proper HBV infection of PMHs (Burwitz et al., 2017).

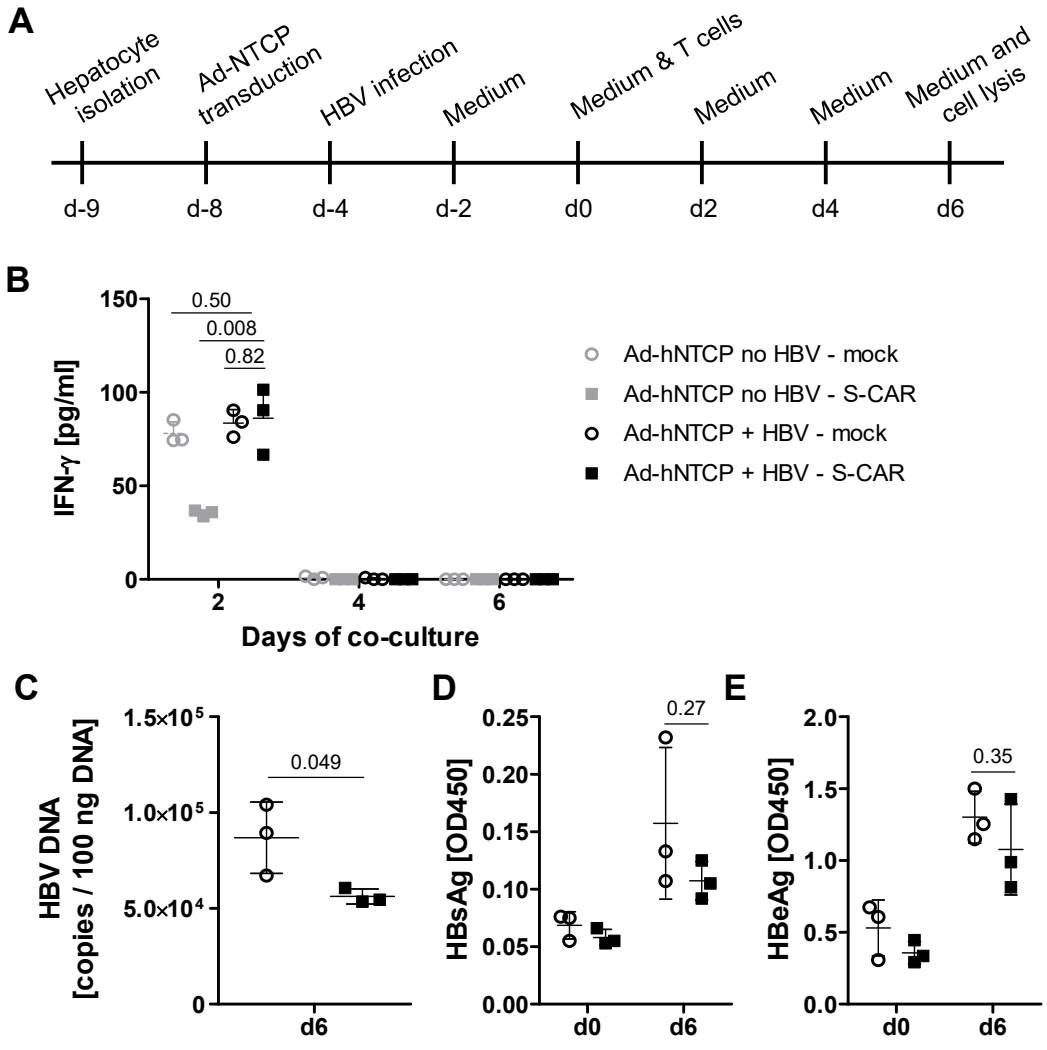

Figure 2.32 Antiviral effect of redirected macaque PBMC against HBV-infected PMHs *in vitro*.
A) PMHs were isolated on day -9 and transduced with Ad-hNTCP on day -8 and infected with HBV on day -4. The co-culture with macaque S-CAR T cells was started on day 0. Media was collected completely on days -2, 0, 2, 4 and 6. On day 6, target cells were harvested. **B)** Secreted IFN-γ in 48-hour supernatant was determined on day 2, day 4 and day 6 by ELISA. **C)** Intracellular HBV DNA on day 6. **D)** HBsAg in 48-hour supernatant on day 0 and day 6. **E)** HBeAg in 48-hour supernatant on day 0 day 6. All data are presented as single and mean values ± SD. (n=3, unpaired T-test, p-values depicted above line)

Therefore, PMHs were isolated and transduced with Ad-hNTCP followed by an infection with HBV (Figure 2.32 A). Upon co-culture of macaque S-CAR T cells with HBV-infected PMHs, we detected a low but specific secretion of IFN-γ on day 2. While mock T cell released the same amount of IFN-γ on HBV-infected and HBV-naïve target cells, the amount was increased for S-CAR T cells (Figure 2.32 B). Analysis of viral DNA in the target cells at the end of co-culture (day 6) revealed that there was a reduction in the S-CAR T-cell treatment group in comparison to mock T cells (Figure 2.32 C). HBsAg (Figure 2.32 D) and HBeAg (Figure 2.32 E) were not affected by S-CAR T-cell treatment.

Overall, the data indicate that macaque S-CAR T cells could be activated by S protein on PMHs and released IFN-γ both in the Ad-HBV model and with proper HBV infection. However, IFN-γ levels were low and T-cell activation did not lead to a pronounced antiviral effect.

3 Discussion

3.1 Immune responses against the S-CAR and EGFRt

Previous data from our laboratory indicated that a transfer of S-CAR T cells into immunocompetent HBV-transgenic mice induces a significant, but transient antiviral effect. After an initial expansion, S-CAR T-cell numbers declined approximate two weeks after transfer (Krebs et al., 2013). In the first section of this dissertation, I investigated the reason for the observed limitations which could be due to T-cell exhaustion, AICD or an immune response against the S-CAR. To this end, S-CAR T cells were transferred sequentially into HBV-transgenic mice. This showed that a second transfer of S-CAR T cells did not induce any liver toxicity and only low numbers of transduced cells could be detected in peripheral blood (Figure 2.1). Thus, a strong influence of T-cell exhaustion and AICD could be excluded since the activity of freshly transferred S-CAR T cells should not be affected by previously activated S-CAR T cells that had gone into a state of exhaustion or had undergone AICD. Theoretically, expansion of S-CAR T cells can be influenced by a prior antiviral effect that decreased HBsAg levels and could therefore also explain differences in engraftment as well as expansion between S-CAR T cell-pretreated and treatment-naïve mice. However, differences in engraftment were only observed regarding S-CAR$^+$ T cells and not in S-CAR$^-$ T cells which indicates a preferential prevention of S-CAR$^+$ T-cell engraftment. Thus, I proposed that the endogenous immune system of the recipient mice mounted an immune response against the human-derived domains of the S-CAR or the co-expressed transduction marker EGFRt. Indeed, the results strongly indicated that the adaptive immune system recognizes the proteins as foreign and rejects T cells that express the alloantigens since S-CAR T cells persisted in Rag2$^{-/-}$ mice but not in wildtype mice (Figure 2.2). S-CAR T cells engrafted better in immunodeficient Rag2$^{-/-}$ mice than mock cells in wildtype mice. This could be due to the immunological vacuum in immunodeficient Rag2$^{-/-}$ mice and no competition for cytokines that are essential for T-cell survival (Berger et al., 2009). Another explanation could be low tonic signaling of the S-CAR without binding to S protein inducing low proliferation of S-CAR T cells, as observed by others with a GD2-specific CAR (Long et al., 2015).

Next, I investigated the immune response in more detail and found that EGFRt was targeted by both CD8$^+$ T- and B-cell responses while I could only detect B-cell responses against the S-CAR (Figure 2.4, Figure 2.5, Figure 2.6). CD4$^+$ T-cell responses were not detected. This was surprising since it should correlate with the observed B-cell responses. It may be that the assay to detect T-cell responses was not suitable to detect CD4$^+$ T-cell responses. S-CAR- and EGFRt-derived peptides need to be presented by APCs on MHC class II molecules to stimulate

cognate $CD4^+$ T cells specifically. Pools of overlapping peptides for the S-CAR and EGFRt would thus be a more appropriate approach to test for $CD4^+$ T-cell responses.

The observed immune responses most probably induced vanishing of S-CAR T cells in immunocompetent mice. However, a low number of cells seemed to escape depletion and S-CAR integrates could still be detected in liver and spleen tissue (7 – 23 integrates per 100 total cells) (Figure 2.1 G). The proportion of transduced cells is likely far lower because transduced cells will have about ten S-CAR integrates at a transduction rate of about 60 % (Antje Malo, personal communication). In earlier data from our laboratory, after *in vivo* survival for 64 days, S-CAR expression on transferred cells was absent in direct *ex vivo* staining but could be rescued by an overnight rest. Furthermore, the detected $S\text{-}CAR^+$ cells still expressed IFN-γ in an HBsAg-specific fashion (Böttinger, 2014). In retrospective, this result could be explained by the presence of antibodies that are directed against the S-CAR. These antibodies could either mask S-CAR molecules on the cell surface or induce S-CAR internalization. If anti-S-CAR antibodies were internalized together with the S-CAR, this could also explain the escape of a low number of S-CAR T cells from depletion by the immune system. In any case, staining of the S-CAR for flow cytometry analysis would be hampered but possibly rescued by an overnight rest after bound antibodies have detached. In contrast to the data by Nina Böttinger, I detected neither S-CAR expression on transferred cells after overnight rest nor HBsAg-specific expression of IFN-γ (data not shown and Figure 2.1 F). In both the old report and the data presented here, S-CAR T cells did not co-express EGFRt. Since I could not detect a $CD8^+$ T-cell response against the CAR, the decline of S-CAR T cells is supposedly only mediated by antibodies. The discrepancy between both results could be due to technical issues of the assay or intensity differences of the immune response against S-CAR T cells. A difference in intensity could be induced by varying expression levels of the S-CAR.

In an attempt to prevent the immune response against the S-CAR, the construct was partially murinized. Unexpectedly, S-CAR T cells with a human IgG1 spacer initially engrafted better and induced higher liver toxicity than cells with a murine IgG1 spacer (Figure 2.7). A mayor difference between both constructs was the transmembrane domain that was from human CD28 in the human IgG1 S-CAR and from murine CD4 in the case of the murine IgG1 S-CAR. The transmembrane domain can influence the activity of CAR molecules (Bridgeman et al., 2010) and could be the reason for differences in the induction of T-cell proliferation and liver toxicity. Most importantly, when only the C8 scFv remained as an immunogenic human target in the S-CAR, T cells still vanished from immunocompetent mice and antibodies against the C8 scFv could be detected (Figure 2.7G and I). To study an S-CAR variant in an immunocompetent mouse, the C8 scFv could also be modified. For murinization the framework of the scFv would need to be exchanged which is feasible but would implicate disadvantages: Changing the framework of a scFv can change its affinity to the cognate antigen but also to

other antigens and therefore might alter its specificity. Ideally the same scFv should be studied in preclinical models as the one used in future clinical applications to have a sophisticated knowledge about its potential but also about its hazard. Therefore, other ways to circumvent the immune response of the murine immune system against the human-derived domains were investigated.

3.2 Tolerization of immunocompetent mice to the S-CAR and EGFRt

In clinical application, ideally, a fully-human CAR should be used to prevent rejection of CAR T cells by the patient's immune system. Rejection of CAR T cells carrying a murine scFv in patients has previously been reported and lead to decreased response rates (Turtle et al., 2015). In contrast to the treatment of $CD19^+$ hematological malignancies with CAR T cells, patients will not receive chemotherapeutic preconditioning due to the risk of enhanced viral replication upon lymphodepletion in the case of CHB or HCC treatment by S-CAR T-cell therapy. Therefore, the preclinical investigation of S-CAR T-cell therapy in an immunocompetent rather than immunocompromised mouse model is preferred. It is expected to provide an efficacy and safety profile that has more relevance for clinical application. Since I decided to study our fully-human S-CAR in an immunocompetent mouse, I depended on tolerance to the alloantigens in the mouse model.

In contrast to my observation that T cells that express EGFRt were targeted by a $CD8^+$ T-cell response, Paszkiewicz et al. (2016) previously described that EGFRt-expressing T cells can persist in their mouse model for 150 days. A major difference compared to my settings was total body irradiation of recipient mice one day prior to T-cell transfer. When I included irradiation in my experimental setup, I also induced long-term tolerance to the S-CAR and EGFRt alloantigens. S-CAR T cells could be detected at high numbers 140 days after transfer in peripheral blood, spleen and liver (Figure 2.8). In this experiment, S-CAR T cells were transferred one day after irradiation, thus at the start of therapy, when the immune system was strongly depressed, and mice could not be considered immunocompetent. Therefore, I investigated if I could also induce tolerance to the alloantigens by a transfer of non-functional SΔ-CAR T cells. Due to a lack of activation signal, they persisted only at low numbers in peripheral blood (20 – 40 cells/μl). Nevertheless, the low numbers of SΔ-CAR T cells were sufficient to induce tolerance and cells persisted. When functional S-CAR T cells were transferred three months later the endogenous immune cells had regained physiological concentrations. Furthermore, functionality of the immune system had also been reestablished as indicated by a rejection of S-CAR T cells if mice had only been irradiated but did not receive SΔ-CAR T cells. These results suggest that the transfer of functional S-CAR T cells was at a timepoint at which the recipient mice can be considered immunocompetent. When SΔ-CAR-tolerized mice were treated with S-CAR T cells, transduced cells were not rejected and

persisted for more than three months (Figure 2.12). Thus, the presented methodology of irradiation and transfer of non-functional SΔ-CAR T cells induces long-lasting tolerance to the alloantigens.

Immune tolerance can be achieved by two distinct means, namely central and peripheral tolerance. Central tolerance of T cells is induced in the thymus. During T-cell development and after TCR gene rearrangement, T cells are assessed for their specificity. Only T cells with a non-self TCR-specificity can leave the thymus and become part of the pool of mature peripheral T cells. Since auto-reactive T cells are excluded, the T-cell pool does not target self-tissue and auto-immune diseases remain a rare event. If autoreactive T cells escape negative selection in the thymus, peripheral tolerance comes into play (Mueller, 2010). Tissue damage is prevented by conversion of T cells to Tregs, suppression or induction of anergy. B cells experience similar selection mechanisms (Nemazee, 2017). In their case, central tolerance is achieved during maturation in the bone marrow. If autoreactive B cells escape negative selection, absent $CD4^+$ T-cell help in the periphery prevents B-cell activation and antibody production.

In my setting, the alloantigens expressed on transferred T cells are present during replenishment of the immune cell pool after irradiation (Figure 2.12). It was previously reported that in rats intrathymic antigen inoculation after total body irradiation can induce selective non-responsiveness to an alloantigen, e.g. bovine gamma globulin (Staples et al., 1966). Similarly, intrathymic transplantation of pancreatic islet allografts after lymphodepletion regimen led to acceptance of islets grafts both in and outside the thymus (Posselt et al., 1990). Clonal deletion induced by recognition of alloantigens was reported as mode-of-action for selective non-responsiveness (Turvey et al., 1999). In the case of the SΔ- or S-CAR T-cell transfer, the adoptively transferred T cells will be distributed throughout the body and probably also migrate to the thymus. Here, cross-presentation of peptides by thymic dendritic cells (DCs) (Proietto et al., 2008) could induce negative selection for both $CD4^+$ and $CD8^+$ T cells with specificities for S-CAR or EGFRt epitopes. This would directly prevent $CD8^+$ T-cell responses and indirectly B-cell responses because of the absent $CD4^+$ T-cell help. Induced central tolerance is likely the mode-of-action of tolerance induction to transferred S-CAR T cells. The data suggests that the presence of the alloantigens during recovery from total body irradiation deluded the immune system in a way that the human-derived domains are self-antigens and must not be targeted.

3.3 Transferability of the tolerization model to other CAR T-cell approaches

The described model is possibly transferable to other CAR T-cell approaches that depend on tolerization against the respective CAR but also against the human derived target protein. In comparison to models utilizing immunodeficient mice, the tolerized model offers the advantage

that mice have a complete immune system at the time of transfer. Depending on the tumor entity or infection that is targeted by CAR T-cell therapy, patients will also have a complete immune system at the time of treatment. While chemotherapeutic lymphodepleting preconditioning before anti-CD19 CAR T-cell transfer for hematological malignancies is applied in virtually all treatment protocols, this will not be the case for all other CAR T-cell approaches. For example, in the case of HBV infection and HBV-associated HCC, lymphodepleting regimes are contraindicated. Several studies have reported that chemotherapy in chronic HBV carriers leads to virus reactivation (Cheng et al., 2004; Lok et al., 1991; Nakamura et al., 1996). Even depletion of B cells only using anti-CD20 antibodies results in life-threatening HBV reactivation (Perceau et al., 2006). Similar observations were obtained regarding Hepatitis C virus carriers (Torres et al., 2018). Furthermore, a functional endogenous immune system might also be of advantage during CAR T-cell therapy. Once tumor cells are targeted by the transferred CAR T cells, a supporting endogenous immune response against neoepitopes of tumor cells could develop. An additive or even synergistic effect on the therapeutic outcome is conceivable.

In the tolerized mouse model reported here, the transfer of CAR T cells into patients without chemotherapeutic pretreatment can be imitated. The expansion and migration of CAR T cells in patients without a lymphodepleting regimen differ from conditions that offer more space in the lymphoid compartment as found in pretreated patients or immunodeficient mice (Berger et al., 2009). The tolerization model will allow the investigation regarding interactions with the endogenous immune system and how they will influence efficacy and safety of the therapy. The influence of checkpoint inhibition that targets other immune cells than the co-administered CAR T cells could be determined. Beside humanized mouse models that harbor human immune cells, to my knowledge this is the only model that allows the study of a CAR with human-derived domains in the context of an intact endogenous immune system of the recipient. In contrast to humanized mouse models, I transferred murine T cells in this syngenic model which is of special importance for long-term studies. If human immune cells are transferred into mice, graft-versus-host disease can develop (Shultz et al., 2012), which can induce T-cell proliferation and side-effects that are independent of the CAR.

The usage of murine T cells in preclinical mouse models also goes along with disadvantages: For once, if the CAR, as in the presented study the S-CAR, contains human signaling domains it cannot be excluded, that their function differs in murine cells in comparison to their human equivalent. Therefore, both results about expansion and efficacy as well as about safety need to be interpreted with caution. Along the same line, the murine and human immune system differ in many regards, 60 of them being described by Mestas and Hughes (2004). A well-known example when murine immunotherapy models terribly failed to predict clinical outcome is TGN1412, an agonistic antibody targeting CD28 (Attarwala, 2010). Although preclinical data

in wildtype mice and rhesus macaques suggested a good safety profile, in a phase I clinical trial all six patients suffered from severe inflammatory reactions and multiorgan failure. When the drug was tested in humanized mice with transplanted PBMC later on, they displayed similar severity of side effects as observed in the clinics (Weissmuller et al., 2016). The usage of a humanized mouse model in addition to the already conducted studies before clinical application could have prevented the terrible outcome of the clinical trial. Another important aspect regarding the difference between the murine and human immune system is the higher resistance of mice to cytokine storms (Seok et al., 2013). Side-effects like CRS and neurotoxicity of CAR T-cell therapy as seen in clinical examination (Badieyan and Hoseini, 2018) would therefore be underestimated in a syngenic mouse model like ours.

In the case of the S-CAR, the humanized mouse model would also need human hepatocytes in addition to a human immune system. Mouse models have been developed that allow induction of apoptosis of murine hepatocytes that are subsequently replaced by transferred human hepatocytes. The human immune system is established in these otherwise immunocompromised mice by transferring $CD34^+$ hematopoietic stem cells (Bility et al., 2014; Strick-Marchand et al., 2015). These models permit an HBV infection of engrafted human hepatocytes and investigating immunotherapeutic approaches like the transfer of S-CAR T cells. However, they are very laborious and only a portion of mice gets engrafted with human hepatocytes and immune system successfully explaining the high price for successfully engrafted mice (~3,000 $ / mouse). For studies that dispense with an endogenous immune system, mice that only harbor human hepatocytes could be used which are less expensive (~300 $ / mouse).

Taken together, although the presented tolerized mouse model also has disadvantages as described above, I believe that its usage will contribute to a more comprehensive understanding of T-cell therapy approaches. It will allow for the study of interactions with the endogenous immune system and how intervention using checkpoint inhibition could be beneficial. In combination with other models, especially humanized mouse models, preclinical evaluation of T-cell therapies will lead to more efficient and safer products to treat patients.

3.4 Comparison of costimulatory signaling domains

The *in vitro* and *in vivo* functionality of S-CAR expressing T cells has been described previously (Bohne et al., 2008; Krebs et al., 2013) and could be verified in this thesis in immunodeficient (Figure 2.3) and tolerized mice (Figure 2.15). However, S-CAR T cells did not cure the mice and HBV-positive hepatocytes survived the therapy. The S-CAR used in these studies contained the CD3ζ and the CD28 signaling domains. In recent years, other groups have performed comprehensive studies comparing CARs with different signaling domains in their therapeutic setting (Hombach and Abken, 2011; Karlsson et al., 2015; Milone et al., 2009).

Comparison of different signaling domains is of relevance for every scFv and antigen combination. Differences in affinity of scFvs and in the expression level of their antigen on the respective target cell can influence the extent of T-cell activation. While strong signaling domains and a high affinity scFv might be necessary for a CAR targeting cells with a weakly expressed antigen, the same signaling domains and scFv might induce AICD if the CAR targets a highly expressed antigen. Along this line, Kunkele et al. (2015) reported that CAR signaling has a threshold above which *in vivo* efficacy decreases. Another aspect to consider for scFv affinity is that some tumor antigens are not exclusively expressed on tumor cells. Thus, a CAR with weak signaling domains, or a low affinity scFv is needed to limit T-cell functions towards tumor cells that express the antigen in high amounts while keeping the T cell in a quiescent state upon encounter of a healthy cell with low antigen expression. Furthermore, *in vivo* studies can determine if a certain signaling domain combination is beneficial for the respective tissue or tumor microenvironment.

Since 4-1BB signaling and OX40 signaling have been suggested to be beneficial for CAR T-cell functionality, I adapted these results and tested different domain combinations in our therapeutic setting. The data suggested that a 4-1BB signaling domain in the S-CAR reduces activation of T cells and a subsequent antiviral effect. This was the case both if the 4-1BB domain was present exclusively or in addition to CD28 and applied both *in vitro* and *in vivo*. While transduced T cells released IFN-γ in a short-term experiment when cultured on plate-bound HBsAg (Figure 2.16), *in vitro* killing of S protein expressing target cells (Figure 2.17) or HBV-infected target cells (Figure 2.20) by human 4-1BB domain containing S-CAR T cells was largely reduced. Comparable results were obtained when investigating transduced murine $CD8^+$ T cells expressing an S-CAR with a murine 4-1BB domain. $CD8^+$ T cells could be activated to release IFN-γ in an HBsAg-dependent manner although 4-1BB CAR T cells expressed lower amounts of IFN-γ than CD28 CAR T cells (Figure 2.21). However, 4-1BB CAR T cells could not be detected in higher numbers than non-functional SΔ-CAR T cells *in vivo* (Figure 2.22) nor did they induce an antiviral effect (Figure 2.25). S-CAR variants with a 4-1BB domain were also comparable in other regards to SΔ-CAR T cells *in vivo:* They had a similar phenotype regarding memory, activation and exhaustion markers (Figure 2.23). Moreover, upon isolation after *in vivo* survival, they failed to express cytokines upon HBsAg-specific stimulation. Like SΔ-CAR T cells, they expressed higher amounts of TNF-α than S-CAR T cells without a 4-1BB signaling domain upon unspecific activation (Figure 2.24). All these data indicated that 4-1BB S-CAR T cells have low or absent functionality *in vivo*. One possible explanation could be a lower sensitivity for its cognate antigen, the S protein. *In vitro* data indicated that 4-1BB containing S-CAR constructs had a lower sensitivity (Figure 2.21) which could have a major impact in the *in vivo* setting. If they prevent cells from reaching an activation threshold, T-cell expansion and antiviral activity would be abolished.

In the functional comparison for CAR constructs, difference in surface expression could have an impact. For the *in vitro* investigation of the cytotoxic effect, 3rd generation S-CAR constructs containing a 4-1BB domain (28zBB, 28BBz) were at least as highly expressed as the 2nd generation S-CAR with CD28 and CD3ζ domains only (28z). In contrast, T cells transduced with the 2nd generation 4-1BB S-CAR (BBz) expressed lower amounts of the S-CAR on the cell surface (Figure 2.19), which could in part explain the decreased sensitivity and functionality (Figure 2.20). If fewer S-CAR molecules are on the cell surface, the probability of binding to all accessible S proteins on the target cell is decreased and T-cell activation diminished. The same is true for the *in vivo study*. The low expression of the 3rd generation S-CAR (m28zBB) (Figure 2.22 B) could play a role in abrogating *in vivo* expansion (Figure 2.22 C) and T-cell functionality (Figure 2.25).

Over-activation of S-CAR T cells could drive 4-1BB signaling domain containing S-CAR T cells into exhaustion and apoptosis. However, some aspects argue against overactivation as the cause for the reduced antiviral effect: In short-term *in vitro* experiments 4-1BB containing S-CAR T cells expressed less cytokines than their counterparts without a 4-1BB domain in the S-CAR (Figure 2.16, Figure 2.21). Furthermore, if activated 4-1BB S-CAR T cells were lost due to AICD, a selective loss in comparison to untransduced T cells from the T-cell product would be expected. The proportion of transduced cells of total transferred cells would have been changed which was not the case (Figure 2.22). In contrast, Gomes-Silva et al. (2017) recently described that high expression of a 2nd generation CD19-specific CAR with 4-1BB costimulation induced ligand-independent tonic signaling in T cells and reduced their survival. The effect was observed if the CAR was expressed from a retroviral vector, which allowed a positive feedback loop and increased CAR expression. Impeded T-cell survival *in vivo* also lead to a lowered therapeutic effect. The authors showed that this effect was true for several CARs with different scFv and target proteins. They were able to prevent toxicity and enhanced anti-tumor functionality by a reduction of CAR expression and switching to a self-inactivating (SIN) lentiviral vector system. The reported data are the only to my knowledge that at first glance indicate a benefit of CD28 costimulation in comparison to 4-1BB which I have also observed. However, this effect was only true in a non-SIN retroviral vector system due to tonic signaling.

Other published data comparing CD28 and 4-1BB containing 2nd generation CARs describe mostly advantages of the 4-1BB domain. One study reported that different CARs induced a distinct metabolic state of the redirected T cell. While the 4-1BB domain in an anti-CD19 CAR enhanced respiratory capacity and increased fatty acid oxidation in $CD8^+$ T cells, signaling through a CD28 CAR enhanced glycolysis. Moreover, the T-cell phenotype was different, giving yield to either $CD8^+$ central memory or effector memory T cells with a 4-1BB or CD28 CAR, respectively (Kawalekar et al., 2016). These differences could explain the *in vivo*

advantage of a 4-1BB CAR in a xenograft mouse model for primary human pre-B-cell ALL (Milone et al., 2009). Furthermore, an anti-GD2 4-1BB CAR prevented T-cell exhaustion upon tonic CAR signaling as observed with CD28 CARs which enhanced their long-term persistence *in vivo* (Long et al., 2015). Another study compared the therapeutic effect of CD28 and 4-1BB CAR T cells and demonstrated that CD28 induced more active T cells exhibiting a quick therapeutic effect. The therapeutic effect of 4-1BB CAR T cells in contrast was slower but since they persisted longer, eventually the same effect was achieved (Zhao et al., 2015). This difference in kinetics could be clinically confirmed. A recent clinical comparison of CD28 and 4-1BB CAR T cells in a small cohort of ALL patients revealed that while response rates were similar with both therapies, 4-1BB CAR T cells displayed longer persistence *in vivo* (Li et al., 2018).

The data regarding the costimulatory domain comparison in the S-CAR reported here contrast with the above mentioned published results. This indicated that results obtained from a CAR directed against a specific antigen cannot be directly transferred to a different CAR. The activation of the T cell by a CAR and subsequent functionality depends on more than the signaling domains in the CAR. The affinity of the scFv to its cognate antigen, the density of both the CAR and its antigen on the respective cell surface and possibly also the type of target cell influence T-cell functionality. The data regarding the S-CAR is inconclusive and additional studies are necessary to understand how the difference in functionality between the different S-CAR variants with and without a 4-1BB signal domain is triggered.

As a second additional costimulatory domain OX40 was tested in 3rd generation S-CAR constructs. The comparison of T cells with comparable transduction rates and surface expression of different S-CAR variants *in vitro* did not reveal any advantage of an additional OX40 signaling domain (Figure 2.19, Figure 2.20). Two 3rd generation S-CARs with the OX40 domain between the domains of CD28 and CD3ζ or C-terminally of CD3ζ were functionally comparable and induced similar T-cell activation and antiviral activity. This result is coherent with a report suggesting that additional OX40 signaling does not enhance target cell killing or cytokine release *in vitro*. The positive effect only becomes apparent in an *in vivo* comparison: Due to decreased apoptosis of CAR T cells harboring both CD28 and OX40 costimulation, they induced an improved antitumor response (Hombach and Abken, 2011). Moreover, costimulation of CD8^{+} T cells with an anti-OX40 antibody enhanced memory T-cell survival (Ruby et al., 2007). *In vitro* I did not determine the influence of an OX40 signaling domain in the S-CAR on the induction of apoptosis or memory T-cell survival upon T-cell activation. Moreover, an *in vivo* comparison still needs to be performed to determine if the positive effects described above also apply in our therapeutic setting.

3.5 Limitations for a curative S-CAR T-cell therapy

In contrast to published *in vitro* data (Bohne et al., 2008), in this thesis the investigation of S-CAR T-cell therapy in various models for HBV infection did not provide any evidence that it will be curative in clinical application. *In vitro* studies with HBV-infected target cells in the human (Figure 2.20) and macaque (Figure 2.31, Figure 2.32) setting showed S-CAR T-cell activation but no pronounced antiviral effect. Only when Huh7-S cells that expressed the S protein from a transgene were used as target cells, S-CAR T cells efficiently killed 100 % of target cells (Figure 2.17). However, these target cells fail to recapitulate the clinical situation because HBV-transgenic cells have a higher density of S protein on the cell surface than HBV-infected cells (Lila Zhao, unpublished data). *In vivo* studies in immunodeficient or tolerized mice indicated that S-CAR T cells could decrease HBeAg and intrahepatic viral DNA by approximately 70 % within 140 days of treatment but HBV-positive hepatocytes remained (Figure 2.11). This was the case although S-CAR T cells were detected in high numbers systemically (Figure 2.8). Somehow S-CAR T cells strongly proliferated and persisted but failed to eliminate all HBV-positive hepatocytes.

3.5.1 Impact of immune-regulatory mechanisms

Transferred cells expressed PD-1 (Figure 2.9 C) and were therefore susceptible to inhibition via this inhibitory checkpoint. Furthermore, they expressed IL-10 upon HBsAg-specific and unspecific stimulation (Figure 2.10 B) which could lead to autoinhibition. However, when I used either PD-1- (Figure 2.27 I) or IL-10-deficient (Figure 2.29 I) mice as donors for S-CAR T-cell therapy, the antiviral effect remained unchanged in comparison to wildtype S-CAR T cells. Both molecules did not influence the therapeutic outcome. One possible explanation could be a compensatory upregulation of other inhibitory mechanisms. Lamichhane et al. (2017) reported that DCs express higher amounts of IL-10 upon PD-1 blockade and only combinational therapy of both PD-1 and IL-10 checkpoint inhibitors augmented antitumor responses. However, PD-1-deficiency in my hands did not lead to enhanced IL-10 expression (Figure 2.27 F), neither was Tim-3, another inhibitory checkpoint, more upregulated than on wildtype S-CAR T cells (Figure 2.27 E). These results are in contrast to previous studies that reported an enhanced CAR T-cell efficacy upon PD-1 blockade in xenograft models using a PSMA-specific CAR (Serganova et al., 2017) and a mesothelin-specific CAR (Cherkassky et al., 2016). An explanation could be that murine $CD8^+$ T cells as in our syngenic mouse model are less susceptible to be inhibited via the PD-1/PD-L1 axis than human $CD8^+$ T cells in a xenograft model. Furthermore, in contrast to both studies, I used genetic ablation of PD-1 in our model which was reported to induce terminally differentiated exhausted $CD8^+$ T cells (Odorizzi et al., 2015). Another approach investigating immuno-stimulation by iMATE induction (Huang et al., 2013b) also failed to influence S-CAR T cells. With and without iMATE induction

S-CAR T cells were comparable regarding their phenotype, the potential to express cytokines and the induction of an antiviral effect.

Taken together, the results indicate that neither PD-1 on S-CAR T cells nor IL-10 expressed by the latter as well as intrahepatic immuno-stimulation alter the antiviral effect. The cause for the limited therapeutic effect still needs to be determined. The influence of IL-10 expressed by endogenous cells would be another possibility. To this end, the treatment of SΔ-CAR-tolerized IL-10-deficient and wildtype mice could be compared.

3.5.2 Sensitivity of S-CAR T cells as limiting factor

Another T-cell therapy approach from our laboratory utilizes HBV-specific TCRs instead of the S-CAR to redirect T cells towards HBV-infected cells. It was previously shown that S-CAR T cells are less sensitive to become activated by HBV-infected target cells than T cells that express an HBV-specific TCR, specifically the TCR 6K, which is specific for a peptide of HBc (Karin Wisskirchen, personal communication). Human T cells equipped with 6K were activated by target cells infected with a lower multiplicity of infection (MOI) of HBV and the antiviral effect was stronger. For higher MOIs and a lower avidity TCR the antiviral effect was more comparable between S-CAR and TCR-redirected T cells. In the macaque model for HBV infection 6K-expressing T cells were also assessed in parallel to S-CAR T cells and induced a stronger antiviral effect (Hasreiter, 2018). Similar observations, but less pronounced, were obtained with the S protein-specific TCR 4G in human (Karin Wisskirchen, personal communication) and macaque T cells (Hasreiter, 2018). Moreover, TCR-transduced murine T cells were investigated in the mouse model for HBV infection. To do this, mice need expression of human HLA-A2 on hepatocytes, thus mice were co-infected with AAV-HBV and AAV-HLA-A2. When murine $CD4^+$ and $CD8^+$ T cells were transduced with three different HBV-specific TCRs separately – 4G, 6K and WL31, which is specific for a peptide of the S protein – and a mix of them transferred into AAV-HBV/AAV-HLA-A2-co-infected $Rag2^{-/-}$/IL-$2R\gamma^{-/-}$ mice, they induced a pronounced antiviral effect. HBsAg and HBeAg in serum as well as intrahepatic AAV and HBV DNA copies decreased by two to three logs (Hasreiter, 2018). Although mice treated with TCR-engrafted T cells were not cured, the remaining HBV^+ hepatocytes likely lacked HLA-A2 expression if they were only transduced with AAV-HBV. Hence, the transferred TCR-redirected T cells failed to recognize them. In future experiments viral vectors containing both the HBV genome and HLA-A2 in one construct will exclude the possibility of single-positive hepatocytes.

The difference in T-cell functionality and antiviral effect between S-CAR- and TCR-redirected T cells could be due to sensitivity issues. While S-CAR T cells only efficiently targeted Huh7-S cells (Figure 2.17) and failed to exhibit a pronounced antiviral effect against HBV-infected HepG2-NTCP (Figure 2.20) or PMHs (Figure 2.31,Figure 2.32) as well as in AAV-HBV-infected

mice (Figure 2.3, Figure 2.11, Figure 2.15) in my hands, TCR-redirected T cells work efficiently in all investigated models. A major difference between TCRs and CARs is their affinity to their cognate ligand, the peptide-MHC complex and an unprocessed cell surface protein respectively. While physiological TCR affinity range is 10^4 – 10^6 M^{-1}, most scFv on CARs have an affinity range of 10^6 – 10^9 M^{-1}. The lower affinity of TCRs seems to correlate with a higher sensitivity. It has been reported that only one MHC molecule presenting the correct peptide on the target cell is sufficient for T-cell activation (Huang et al., 2013a; Sykulev et al., 1996). Along this line, it has been suggested that the fast off-rate of a low-affinity TCR/peptide-MHC complex interaction allows serial triggering of different TCR molecules and thus T-cell activation with low sensitivity (Huang et al., 2013a; Valitutti et al., 1995). In contrast, high affinity scFv of CARs have a slow off-rate which mostly abrogates serial CAR activation by the same ligand. Consequently, CARs need higher surface expression of their ligand to induce T-cell activation. It has been reported that anti-CD20 CAR T cells need as many as 200 molecules/cell to induce target cell lysis. For cytokine release a higher number of target proteins, approximately 200 – 5000 molecules/cell, was necessary (Watanabe et al., 2015). Stone et al. (2012) reported comparable results regarding a carbohydrate-specific CAR. In another study, T-cell activation by TCRs was compared to CARs that contain a scFv constructed of the variable domains of the α and β chain of the respective TCR. Although these CARs bind the same peptide-MHC complex, they displayed a 90 – 99 % lower sensitivity (Harris et al., 2018).

Data from our laboratory indicate that the target of the S-CAR, the HBV S protein, is only expressed in low molecule numbers on the surface of target cells. Immunofluorescence staining revealed low surface expression on infected cells only if they were infected with a high MOI of 200 – 1000 while surface expression could not be detected with lower MOI (Lila Zhao, unpublished data). Although the exact number of molecules on HBV-infected cells still needs to be determined, the data suggests that it is low, consequently leading to insufficient S-CAR T-cell activation and the limited antiviral effect.

Sensitivity does not only depend on the number of S protein molecules on the surface of target cells but also on the affinity of the S-CAR to the S protein. The S-CAR binds to different HBV genotypes and serotypes of S protein in different affinities. Data from our laboratory indicate that the difference in binding capacity of C8 scFv to plate-bound HBsAg from different genotypes and serotypes differ about 10-fold between HBsAg variants with the lowest and highest binding (Antje Malo, personal communication). Genotype D with serotype ayw displays lower binding to C8 scFv than other variants, still, this genotype is used in the *in vitro* infection model of HepG2-NTCP cells and *in vivo* in the AAV-HBV model. In contrast, Huh7-S cells, which could be targeted more efficiently, express S protein of genotype A. The cure of HBV-infected hepatocytes as observed by Bohne et al. (2008) upon S-CAR T-cell therapy *in vitro* could be due to a similar reason, namely the usage of an HBV genotype that can be more

efficiently targeted by S-CAR T cells. Unfortunately, I was unable to obtain detailed information about the HBV variant used in that study. If sensitivity issues limit the efficacy of S-CAR T cells as described in this thesis, a higher binding ability to the low number of S protein molecules on the target cell surface could enhance their effect. Thus, it would be worthwhile to investigate other HBV variants in the HepG2-NTCP infection model *in vitro* and the AAV-HBV model *in vivo*.

3.5.3 Influence of soluble HBsAg

Another difference between TCR- and S-CAR-redirected T cells that could have an influence on the therapeutic effect is the kind of ligand they bind. While TCR-redirected T cells detect processed peptides presented on MHC, S-CAR T cells bind to the unprocessed S protein. Since the S protein, in form of HBsAg, is released from infected cells and can be found in the supernatant of cell cultures *in vitro* as well as in blood of HBV^+ animals *in vivo*, S-CAR T cells can bind to the soluble variant. If S-CAR molecules bind HBsAg, the number of S-CAR molecules capable to bind S protein on infected cells will decrease. This would lead to a decreased sensitivity in comparison to TCR-redirected T cells, which are not able to bind any soluble antigen via their TCR. Several results suggested HBsAg binding by S-CAR T cells: If the decrease of HBsAg was only due to a decreased release from HBV^+ hepatocytes, all viral parameters should decrease comparably. However, upon S-CAR T-cell therapy serum levels of HBsAg decreased faster and more pronounced (96 – 99 %) than HBeAg levels and hepatic HBV DNA levels (~70 %) (Figure 2.11, Figure 2.15). This was also the case in immunodeficient mice (Figure 2.3), hence HBsAg decrease due to anti-HBsAg antibody development can be excluded. Other data from our laboratory indicated that there is no major difference in half-life between HBsAg and HBeAg in the blood (Thomas Michler, personal communication). Furthermore, in my data the drop of HBsAg inversely correlated with the S-CAR T-cell concentration in peripheral blood over time (Figure 2.8 G and Figure 2.11 B, Figure 2.12 I and Figure 2.15 B). *In vitro* data indicated that soluble HBsAg can induce IFN-γ release by S-CAR T cells although only to a lower extent than plate-bound HBsAg (Meyer-Berg, 2016). S-CAR T-cell activation by soluble HBsAg in peripheral blood would also explain the higher systemic S-CAR T-cell concentration in blood and in spleen in comparison to other results with TCR-redirected T cells. In the AAV-HBV/AAV-HLA-A2 co-infection mouse model, T-cell numbers in the periphery remained low in comparison (20 cells/μl vs. 10^3 – 10^4 cells/μl) and still induced a more pronounced antiviral effect (Hasreiter, 2018). Along the same line, S-CAR T cells in liver and spleen displayed a comparable phenotype and re-stimulation potential which also indicated extrahepatic S-CAR T-cell stimulation *in vivo* (Figure 2.9, Figure 2.13). To test if S-CAR T cells are activated extrahepatically, BLITC (bioluminescence imaging of T cells) mice could be used as donors for S-CAR T-cell production. They express luciferase upon T-cell

activation, therefore, it can be monitored over time and organ-specifically *in vivo* (Szyska et al., 2018). Furthermore, transduction of mice with an AAV-HBV mutant expressing S protein that is not secreted will indicate the influence of soluble HBsAg on S-CAR T-cell therapy.

3.6 Strategies to enhance efficacy and safety of S-CAR T-cell therapy

Strong advances have been achieved by adding further signaling domains into CARs. However, as described above, as one attempt to enhance S-CAR T-cell functionality, the inclusion of an additional 4-1BB or OX40 signaling domain, did not increase the antiviral effect (Figure 2.20, Figure 2.25). As a next step, a different kind of signaling domain, namely a cytokine receptor signaling domain that would activate the downstream JAK-STAT pathway could be tested. In addition to CD3ζ (signal 1) and CD28 (signal 2) it could deliver cytokine engagement (signal 3) to the T cell. This has been reported to enhance proliferation and anti-tumor effect *in vivo* (Kagoya et al., 2018) and might also increase sensitivity.

Additional ways to further increase T-cell effector functions, tumor penetration, and therapeutic efficacy as well as safety are under investigation in other T-cell approaches. Especially the treatment of solid tumors remains a challenging task which is attributed, among other reasons, to the tumor's inhibitory microenvironment. Furthermore, tumor cells can downregulate the expression of the tumor antigen to escape the elimination by CAR T cells. One approach for further increase of activity is the usage of an armored CAR. Here, CAR T cells are equipped with an additional transgene that allows secretion of a molecule to enhance the therapeutic effect. In a syngenic mouse model the activation-induced expression of IL-12 (iIL-12) by CAR T cells could attract macrophages into the tumor. The expression was under the control of the nuclear factor of activated T cells (NFAT) promotor. Consequently, the elimination of tumor cells that had shut down the expression of the tumor antigen to escape CAR T-cell therapy was enhanced (Chmielewski et al., 2011). Along this line, the inducible expression of IL-18 by CAR T cells enhanced their efficacy against solid tumors (Chmielewski and Abken, 2017; Hu et al., 2017). I adapted this approach to our setting and under my supervision Helena Meyer-Berg constructed a combinatory construct containing both the S-CAR and NFAT-regulated inducible IL-12 expression (Meyer-Berg, 2016). She could show that murine S-CAR-iIL-12 T cells were more sensitive to low plate-bound HBsAg concentrations and released increased amounts of IFN-γ as compared to S-CAR T cells without IL-12 expression. As a next step, this approach will be transferred to the mouse model to investigate if inducible IL-12 expression can enhance the antiviral effect without inducing strong side-effects.

The usage of other molecules than proinflammatory cytokines have also been reported. Expression of heparanase from a transgene permitted better tumor infiltration of CAR T cells by degrading heparan sulfate proteoglycans and extended the survival of mice in a xenograft $GD2^+$ tumor model (Caruana et al., 2015). Moreover, even when CAR T cells manage to

migrate into the tumor, the microenvironment can lower their activity through the expression of inhibitory molecules like PD-1 or IL-10. Secretion of a checkpoint inhibitor targeting the PD-1/PD-L1 axis by CAR T cells (Li et al., 2017) or the simultaneous administration of CAR T cells and anti-PD-1 antibodies (John et al., 2013a; John et al., 2013b) enhanced CAR T-cell activity against solid tumors.

Other groups have reported the expression of two CARs with distinct specificities in one T cell. This approach can bring two advantages: On the one hand, dual-specific CAR T cells decrease the probability for emergence of antigen-negative tumor cells if triggering of one CAR is sufficient for T-cell activation. To escape, tumor cells would need to lose expression of both antigens (Chen et al., 2018; Martyniszyn et al., 2017). On the other hand, safety of CAR T-cell therapy can be addressed by the expression of two CARs. Many tumor antigens are not exclusively expressed on tumor cells but also on healthy tissue, even though to a lower extent. This is the case for e.g. ErbB2, CEA and glypican-3 as well as CD19. CAR T cells directed against these antigens can exhibit an on-target off-tumor effect and induce side effects, which can even be lethal as in the case of an ErbB2-specific CAR (Morgan et al., 2010). The depletion of healthy B cells by CD19-specific CAR T cells is another example of the on-target off-tumor effect while this side-effect is manageable by the administration of immunoglobins. To prevent dangerous side effects, CAR T cells can be constructed in a way that the activation of the T cell is dependent on both CARs. Thus specificity is increased because T cells are only activated by target cells that express both antigens (Roybal et al., 2016). In our setting, the S-CAR could be combined with a CAR that is specific for the tumor antigen glypican-3 expressed on HCC (Chen et al., 2017; Gao et al., 2014). Targeting two antigens at once could increase total sensitivity of CAR T cells.

Beside efficacy, the safety of CAR T-cell approaches is also an important issue to consider. As shown by the here presented results, S-CAR T cells highly proliferated *in vivo* and persisted in high numbers systemically (Figure 2.12). If side-effects were induced by the transferred cells, their depletion could prevent further tissue damage or even lethal complications. A way to increase safety of CAR T-cell therapy requires the co-expression of a molecule that allows the selective depletion of CAR T cells upon development of severe side effects. Expression of caspase 9 that can be activated upon administration of a dimerizer permits efficient CAR T-cell depletion (Budde et al., 2013). Other safety mechanisms depend on the application of an antibody to deplete CAR cells, such as the expression of EGFRt (Wang et al., 2011). The truncated molecule lacks the extracellular ligand binding domains 1 and 2 as well as the intracellular signaling domains. The extracellular domains 3 and 4 remain and allow targeting of EGFRt expressing cells with the clinically approved anti-EGFR antibody cetuximab. Antibody administration allows efficient depletion of $EGFRt^+$ CAR T cells *in vivo* (Paszkiewicz

et al., 2016; Wang et al., 2011). Furthermore, EGFRt can serve as a surrogate marker of transduced T cells as in the here presented studies.

3.7 Macaque HBV infection model for S-CAR T-cell therapy

As a last step before clinical application, the assessment of S-CAR T-cell therapy in a non-human primate (NHP) model would be desirable. Due to its similarities with the human immune system the investigation of toxicities in the context of a NHP would be more meaningful than in mouse models (Siegler and Wang, 2018). Other CAR T-cell approaches with an anti-ROR1 CAR (Berger et al., 2015) and an anti-CD127 CAR (Kunkele et al., 2017) indicated the safety profile of the therapy before the first in-human trial. Hence, I adapted the well-established technology to redirect murine and human T cells to equivalent cells from the rhesus macaque, *Macaca mulatta*. Retroviral transduction of macaque T cells proved feasible using different stimulation protocols. During transduction T cells proliferated with different stimulation protocols because the administered human cytokines (IL-2 and IL-15) were cross-reactive with the macaque cytokine receptors. The S-CAR was able to activate $CD8^+$ T cells HBsAg-specifically and induced expression of IFN-γ and TNF-α (Figure 2.30).

Strikingly, the result was different in case of $CD4^+$ T cells: Directly after the transduction procedure they were almost unresponsive to both HBsAg-specific and unspecific stimulation as they expressed only low amounts of IFN-γ and TNF-α while human $CD4^+$ T cells expressed cytokines at levels comparable to $CD8^+$ T cells (Figure 2.30). Other activation markers than cytokine expression were not determined. The prior treatment included stimulation by anti-CD3 and anti-CD28 antibodies. This stimulus can induce internalization of both engaged and non-engaged TCRs including their CD3 subunits (San Jose et al., 2000). For subsequent stimulation by the anti-CD3 antibody, surface expression of TCRs including their CD3 subunits is essential. The observed difference could be explained by diverging kinetics of internalization and re-trafficking to the cell surface between macaque $CD4^+$ and $CD8^+$ cells as well as between macaque and human $CD4^+$ T cells. To determine if this was the case, flow cytometry analysis of CD3 surface expression should be investigated. Whether association of CARs with CD3 subunits effects signaling through the CAR, is still discussed in the field. Conflicting data have been published. On the one hand, it was reported that expression of a CAR that can associate with the TCR complex increased signaling through the TCR. As soon as association was prevented by mutations in the CD3ζ domain of the CAR, signaling through the CAR was diminished (Bridgeman et al., 2010). On the other hand, Kamiya et al. (2018) reported that surface expression of CD3 was neglectable for CAR signaling. Beside TCR internalization, other negative feedback loops upon CD3/CD28 engagement during transduction could explain the effect observed. If they target signaling components downstream of both the TCR and the CAR, they would prevent T-cell activation in either case.

Our results indicated that macaque S-CAR T cells can be activated by S protein-expressing primary macaque hepatocytes and can induce a slight antiviral effect only detectable on the level of intracellular HBV DNA (Figure 2.31, Figure 2.32). However, it is unclear if the human signaling domains used in the S-CAR can activate macaque $CD8^+$ T cells as well as their human counterparts. Investigation of T-cell activation in a titration of HBsAg could give an idea if functionality is comparable. Due to a lack of macaque PBMC I could not complete these analyses. As observed in the human setting *in vitro* as well as in the murine setting *in vivo*, the therapy was not curative within the investigated time frame. One possible limitation for all investigated models is the low surface expression of S protein on target cells which could be below the sensitivity of S-CAR T cells as discussed above (section 3.5.2).

Even without previously shown curative effect, S-CAR T cells should be tested *in vivo* in the macaque model for HBV infection. For this investigation one will need to consider a possible immune response against the human-derived domains for the S-CAR as described in this thesis if S-CAR T cells were administered into immunocompetent mice. Furthermore, results from a cooperation partner suggest that chimpanzees can also develop a B-cell response against the S-CAR (data not shown). For the application in rhesus macaques S-CAR T-cell rejection would need to be prevented by transient immunosuppression regimen or tolerization to the antigen as described in this thesis. In summary, the presented data indicated that the investigation of S-CAR T cells in the macaque model for HBV infection is feasible allowing further studies, especially *in vivo* investigations, to determine safety of the T-cell therapy.

3.8 Final evaluation and outlook

Since present treatment strategies fail to eliminate HBV in most cases, new strategies are needed to target the virus. In addition, novel therapies for HBV-associated HCC are urgently needed as it represents the second leading cause of cancer-related death. Adoptive T-cell therapy could play an important role in future treatment strategies because it has the potential to eliminate the viral template cccDNA from all infected hepatocytes. The here presented data focused on studying the therapeutic potential of S-CAR T cells *in vivo.* Furthermore, limitations were investigated, and approaches tested to increase the antiviral efficacy of S-CAR-redirected T cells.

In order to study S-CAR T-cell functionality *in vivo*, a suitable mouse model is essential. Evidence was provided that the S-CAR cannot be studied in regular immunocompetent mice since they developed an immune response against the human-derived S-CAR domains in the construct. I was able to circumvent this issue by finding a way to induce tolerance to the human alloantigens in immunocompetent mice. This permitted the study of S-CAR T cells in the context of a functional endogenous immune system. The transferred cells persisted in high numbers and provided a substantial antiviral effect *in vivo*. It still needs to be explored, if the

induction of tolerance can also be applied to other CAR T-cell approaches that utilize constructs with human-derived domains and are therefore also susceptible to immune-mediated rejection in immunocompetent mice.

Subsequently, experiments were conducted that compared S-CAR constructs containing different costimulatory domains. The data do not provide any evidence that OX40 or 4-1BB costimulatory domains in the S-CAR enhance the antiviral effect in comparison to the previously used S-CAR with only CD3ζ and CD28 signaling domains. The cause of the decreased functionality by S-CARs containing a 4-1BB domain still needs to be explored. Furthermore, experiments could determine if an S-CAR construct containing the OX40 domain permits enhanced *in vivo* functionality although it remained unaltered *in vitro*.

In the third section of this thesis, I explored the cause of the limited antiviral effect of S-CAR T cells and could show that the effect of PD-1 on transferred cells and IL-10 expressed by the latter are negligible. Intrahepatic immuno-stimulation did not enhance the therapeutic effect. Since T-cells that are engrafted with HBV-specific TCRs provide a more pronounced antiviral effect, I would like to propose that immune-regulatory mechanisms in the liver are not the leading cause of the limited effect. Sensitivity issues of the S-CAR in comparison to HBV-specific TCRs are more likely to be the challenge. Future experiments should focus on exploring whether the functionality of S-CAR T cells in enhanced if target cells express S protein of genotypes A and B, which have a higher affinity to the C8 scFv. Moreover, the potential of other signaling domains to increase T-cell activation could be investigated. Furthermore, an armored S-CAR that induces IL-12 or IL-18 expression upon T-cell activation could be tested. The positive feedback loop provided by the secreted cytokine could increase sensitivity to the low surface expression of S protein on target cells.

To prepare further studies of the S-CAR in an NHP model for HBV infection, I showed feasibility of S-CAR expression in NHP T cells and T-cell functionality upon signaling through the S-CAR. Before clinical application, the approach could be tested in NHP *in vivo* to address efficacy and especially safety.

Taken together, S-CAR T-cell therapy is a promising approach to cure CHB and HBV-associated HCC. The presented data indicate that the S-CAR as it was used here is not able to eradicate HBV, but improvements can possibly be achieved by different means as described above. Furthermore, other HBV genotypes than the one used in this thesis can possibly be targeted more efficiently without further modifications of the S-CAR. Since the S-CAR is independent of HLA molecules, especially patients who cannot be treated with available HBV-specific TCRs due to an inappropriate HLA haplotype could benefit from S-CAR T-cell therapy.

4 Materials and Methods

4.1 Materials

4.1.1 Devices and technical equipment

Product	Supplier
Açu-jet pro	Brand
Architect™	Abbott
BEP III (HBeAg measurement)	Siemens
Big centrifuge 5920R	Eppendorf
CytoFLEX S	Beckman Coulter
ELISA-Reader infinite F200	Tecan
Flow cytometer FACS Canto II™	BD Biosciences
Freezing device	Nalgene / biocision Coolcell
Fusion Fx7	Peqlab
Incubator Heracell 150	Heraeus Holding GmbH
LightCycler® 480 II	Roche Diagnostics
MACS separator MultiStand	Miltenyi
NanoDrop One	Thermo Scientific
Nanophotometer OD600	IMPLEN GmbH
Neubauer improved hemocytometer	Brand
NucleoCounter NC-250	Chemometec
Pipettes	Eppendorf
Radiation Source	Buchler
Reflotron® Reflovet Plus	Roche Diagnostics
Shaker and incubator for bacteria	INFORS AG; Heraeus Holding GmbH
Sterile hood HERA safe	Thermo Scientific
T professional Trio Thermocycler	Analytik jena
Table-top centrifuge 5417R	Eppendorf
Thermo Mixer F1.5	Eppendorf
xCELLigence RTCA Single Plate	ACEA Biosciences

4.1.2 Consumables

Product	Supplier
96-well plates for qPCR, FrameStar 480/96	4titude
Cell culture flasks, dishes, plates	TPP
Cell strainer 100 μm	Falcon
Cryo vials	Greiner Bio One
Cuvettes	Implen
ELISA 96-well plates Nunc MaxiSorb	Thermo Scientific
E-Plate VIEW 96	ACEA Biosciences
FACS 96-well V-bottom plates	Roth
Falcon tubes 15 ml / 50 ml	Greiner Bio One
Filcons, sterile, 30 μm	SLG
Filter tips	Greiner Bio One
Filters 0.45 μm and 0.2 μm	Sarstedt
MACS separation columns (MS, LS)	Miltenyi Biotech
Microvette 500 LH-Gel	Sarstedt
Needles	Braun
Non-tissue culture treated plates (24-well)	Falcon
PCR tubes	Thermo Scientific
Pipette tips 10 μl – 1 ml	Biozym / Greiner Bio One / Gilson
Pipettes (disposable) 2, 5, 10, 25, 50 ml	Greiner Bio One
Reaction tubes 1.5 ml, 2 ml	Greiner Bio One, Eppendorf
Reagent reservoirs, sterile	Corning
Reflotron ALT stripes	Roche Diagnostics
Surgical Disposable Scalpels	Braun
Syringes	Braun

4.1.3 Chemicals and reagents (additives)

Product	Supplier
2-Phenoxyethanol	Roth
Acetic acid	Roth
Agarose	PeqLab
Ammonium chloride (NH_4Cl)	Roth
Ampicillin	Roth

Antibiotics/Antimycotics, 100x	Fisher Scientific
Biocoll separating solution (density 1.077 g/ml)	Biochrom
Blasticidin	Gibco
Bovine serum albumin (BSA)	Roth
Brefeldin A	Sigma
Carboxyfluorescein succinimidyl ester (CFSE)	Thermo Fisher Scientific
CD8a (Ly2) MicroBeads (130-049-401)	MACS Miltenyi Biotec
Collagen R	Serva
CountBright Absolute Counting Beads	Thermo Fisher Scientific
CpG (ODN 1668)	InvivoGen
CpG control (ODN 1668 control)	InvivoGen
Cytofix/Cytoperm	BD Biosciences
D (+) Glucose monohydrate	Roth
Dimethyl sulfoxide (DMSO)	Sigma
DMEM	Gibco
DMEM/F12	Gibco
DNA ladder 1kb / 100bp	Eurogentec
EDTA	Roth
EDTA di-sodium salt (Na_2EDTA)	Roth
Ethanol	Roth
Ethidium monoazide (EMA)	Sigma
Fetal calf serum (FCS)	Gibco
Fixable Viability Dye eF780	eBioscience
Geneticin Selective Antibiotic (G418 Sulfate)	Gibco
Gentamicin, 40 mg/ml	Ratiopharm
Glycerol	Roth
HBSS	Gibco
Heparin-Natrium 25000	Ratiopharm
Hepes 1 M	Gibco
Human serum	Own production (AG Protzer)
IL-12 (murine)	Provided by Edgar Schmitt, Mainz
IL-15 (recombinant human)	Peprotech
IL-2 Proleukin	Novartis
Isopropanol	Roth
L-Glutamine, 200 mM	Gibco
LightCycler 480 SYBR green master mix	Roche
Lipofectamine 2000	Invitrogen

Non-essential amino acids (NEAA), 100x	Gibco
OptiMEM	Gibco
Paraformaldehyde (PFA), 4 %	ChemCruz
PEG 6000	Merck
Penicillin Streptomycin, 10,000 U/ml (100x)	Gibco
Percoll density gradient media	GE Healthcare
Perm/Wash	BD Biosciences
Phosphate-buffered saline (PBS) 10x	Gibco
Polybrene	Millipore
Poly-L-lysine	Sigma-Aldrich
Potassium bicarbonate ($KHCO_3$)	Roth
Propidium iodide	Roth
Protamine sulfate	LEO Pharma
Puromycin	InvivoGen
RetroNectin 1μg/μl	Takara
Roti gel stain	Roth
RPMI 1640	Gibco
RPMI 1640 Dutch modified	Gibco
SOC medium	Sigma-Aldrich
Sodium chloride	Roth
Sodium pyruvate, 100mM	Gibco
Solution 18	Chemometec
Staphylococcal enterotoxin B (S4881)	Sigma-Aldrich
Sulfuric acid (2N)	Roth
Tissue-Tek O.C.T.	Sakura
TMB solution	Thermo Fisher Scientific
Tris	Roth
Trypan blue	Gibco
Trypsin-EDTA	Gibco
Tryptone	Roth
Tween 20	Roth
Versene	Gibco
Yeast extract	Roth
β-Mercaptoethanol, 50 mM	Gibco

4.1.4 Buffers

Buffer	Ingredients
ACK lysis buffer	150 mM NH_4Cl 10 mM $KHCO_3$ 0.1 mM Na_2EDTA pH 7.2 – 7.4 in H_2O
ELISA assay diluent	1 % BSA in PBS
FACS buffer	0.1 %BSA in PBS
MACS buffer	0.5 % BSA 2 mM EDTA pH 7.2 in PBS
PBS-T	0.05 % Tween 20 in PBS
Tris-acetate-EDTA buffer (50x)	2 M Tris 2 M Acetic acid 50 mM EDTA pH 8.0 in H_2O

4.1.5 Enzymes

Product	Supplier
Collagenase IV	Sigma-Aldrich
FastAP	Thermo Fisher Scientific
FastDigest restriction enzymes	Thermo Fisher Scientific
Phusion Hot Start Flex 2x Master Mix	New England Biolabs
T4 DNA Ligase	Thermo Fisher Scientific

4.1.6 Proteins

Protein	Source
C8 scFv	Sophia Schreiber, AG Protzer
HBsAg, serotype ayw, CHO	Roche

4.1.7 Kits

Product	Supplier
ARCHITECT anti-HBsAg Reagent Kit	Abbott
ARCHITECT HBeAg Reagent Kit	Abbott
ARCHITECT HBsAg Reagent Kit	Abbott
Enzygnost HBe	Siemens
GeneJET Plasmid Miniprep Kit	Thermo Fisher Scientific
HBeAg BioAssay ELISA Kit	US Biological lifeSci
HBsAg BioAssay ELISA Kit	US Biological lifeSci
Human IFN-γ uncoated ELISA	Invitrogen
Human IL-10 ELISA Max Standard Set	Biolegend
Monkey IFN-γ ELISA development kit (HRP)	Mabtech
Mouse IFN-γ uncoated ELISA	Invitrogen
NucleoSpin Tissue	Macherey-Nagel
Plasmid *Plus*Midi Kit	Qiagen
QIAquick Gel Extraction Kit	Qiagen

4.1.8 Cell lines and bacteria

Cell Line (antibiotic selection)	Description	Source
GALV (Miller et al., 1991)	Retroviral packaging cell line to transduce human and murine cells	AG Protzer
HepG2-NTCP K7 (10 μg/ml Blasticidin)	Clonal HepG2 cell line with transgenic expression of human NTCP	Daniela Stadler, AG Protzer
HT1080	Fibrosarcoma cell line	AG Protzer
Huh7 (Nakabayashi et al., 1982)	Human hepatoma cell line	AG Protzer
Huh7-S (10 μg/ml Blasticidin)	Human hepatoma cell line with transgenic CMV-driven expression of S protein	Oliver Quitt, AG Protzer
PlatE (Morita et al., 2000) (10 μg/ml Blasticidin; 1 μg/ml Puromycin)	Retroviral packaging cell line to transduce murine cells	AG Protzer
RD114 (Ward et al., 2003) (0.2 μg/ml Puromycin; 400 μg/ml Zeocin)	Retroviral packaging cell line to transduce human cells	AG Protzer

Bacteria	Description	Source
Stbl3	Escherichia coli, chemical competent	Invitrogen

4.1.9 Antibodies

Antibody	Dilution	Article number	Supplier
Cetuximab-Biotin	1:100	7862371012	Merck Serono
Granzyme B-PE	1:100	GRB04	Invitrogen
hCD28 (for stimulation)		16-0289-85	eBioscience
hCD3 (for stimulation)		16-0037-85	eBioscience
hCD3 (for stimulation)		560770	BD Biosciences
hCD3 (for stimulation)		3610-1-50	Mabtech
hCD49d (for stimulation)		16-0499-85	eBioscience
hCD4-APC	1:200	17-0048-42	eBioscience
hCD4-PE-Cy7	1:100	317414	Biolegend
hCD8-APC-Cy7	1:100	47-0088-42	eBioscience
hCD8-Pb	1:50	PB984	Dako
hIFN-γ-FITC	1:50	554700	BD Biosciences
hIgG-DyLight650	1:200	ab97006	Abcam
hIgG-FITC	1:200	SLBG4031	Sigma
hIgG-PE	1:200	12-4998-82	eBioscience
hIL-10-PE	1:50	554498	BD Biosciences
hTNF-α-Pb	1:50	48-7349-42	eBioscience
mCD127-APC	1:100	17-1271-82	eBioscience
mCD19-PE-CF549	1:200	562291	BD Biosciences
mCD19-PerCp-Cy5.5	1:200	561113	BD Biosciences
mCD25-PE	1:200	553866	BD Biosciences
mCD28 (for stimulation)			AG Feederle
mCD3 (for stimulation)			AG Feederle
mCD3-PerCP-Cy5.5	1:100	45-0031-80	eBioscience
mCD45.1-APC-eF780	1:200	47-0453-82	eBioscience
mCD45.1-BV660	1:200	563754	BD Biosciences
mCD45.1-FITC	1:200	11-0453-85	eBioscience
mCD45.2-PE	1:200	12-0454-83	eBioscience
mCD4-APC	1:100	17-0041-83	eBioscience
mCD4-PE-Cy7	1:200	25-0042-82	eBioscience

mCD4-PO	1:100	MCD0430	Caltag
mCD4-V500	1:200	560782	BD Biosciences
mCD62L-PE-Cy7	1:100	25-0621-82	eBioscience
mCD69-PE-Cy7	1:200	25-0691-82	eBioscience
mCD8a-Pb	1:100	558106	BD Biosciences
mCD8-PE	1:200	553033	BD Biosciences
mCD8-PE-Cy7	1:200	100721	Biolegend
mCD8-PerCP-Cy5	1:200	45-0081-82	eBioscience
mCD8-V500	1:100	560776	BD Biosciences
mCTLA-4-PerCP-Cy5.5	1:200	106316	Biolegend
mIFN-γ-APC	1:200	554413	BD Biosciences
mIFN-γ-FITC	1:300	554411	BD Biosciences
mIgG1-PE	1:200	550083	BD Biosciences
mIgG-HRP	1:1000	A4416-1ML	Sigma-Aldrich
mIgG-PE	1:200	12-4010-82	eBioscience
mIL-10-PE	1:100	12-7101-82	eBioscience
mNK1.1-PE-Cy7	1:100	25-5941-82	eBioscience
mPD-1-FITC	1:100	11-9981-85	eBioscience
mPD-1-PacBlue	1:100	48-9981-80	eBioscience
mTim-3-APC	1:100	134006	Biolegend
mTNF-α-PE-Cy7	1:200	557644	BD Biosciences
Streptavidin-Pb	1:250	48-4317-82	eBioscience
Streptavidin-PE	1:250	12-4317-87	eBioscience

4.1.10 Primers

Primers were purchased from Microsynth AG, Balgach, Switzerland.

Primer name	Sequence	Application
AAV ITR fw	AACCCGCCATGCTACTTATCTACGT	qPCR, AAV DNA
HBV X rev	CACACAGTCTTTGAAGTAGGCC	qPCR, AAV DNA
ScFvC8 1 fw	CCCTGGTCACCGTCTCCTCA	qPCR, CAR integrates
ScFvC8 2 rev	TTGGTCCCTCCGCCGAATA	qPCR, CAR integrates
HBV S fw	GCCTCATCTTCTTGTTGGTTC	qPCR, HBV DNA
HBV S rev	GAAAGCCCTACGAACCACTGAAC	qPCR, HBV DNA
PrP fw	TGCTGGGAAGTGCCATGAG	qPCR, normalization
PrP rev	CGGTGCATGTTTTCACGATAGTA	qPCR, normalization

4.1.11 Plasmids

All plasmids had a pMP71 backbone and could be used to produce retroviral vector containing the respective transgene or to express the transgene product in transfected cells.

pMP71 plasmid (laboratory number)	Transgene product(s)	Application	Source
S-CAR(hC8) (#511)	S-CAR (human wt IgG1 - human CD28 - CD3)	Figure 2.1 Figure 2.4 Figure 2.5 Figure 2.7	Karin Wisskirchen, AG Protzer
S-CAR(FcΔ)+ EGFRt (#571)	S-CAR (human FcΔ IgG1 - human CD28 - CD3) - T2A - EGFRt	Figure 2.2 Figure 2.3 Figure 2.8 Figure 2.12 Figure 2.27 Figure 2.29 Figure 2.30 Figure 2.31 Figure 2.32	own construction
Decoy(FcΔ)+ EGFRt (#538)	SΔ-CAR (human FcΔ IgG1 - NGFR) - T2A - EGFRt	Figure 2.12 Figure 2.21 Figure 2.22 Figure 2.29	own construction
EGFRt (#273)	EGFRt	Figure 2.4 Figure 2.5	own construction
mhS-CAR+EGFRt (#372)	S-CAR (mouse wt IgG1 – human CD28 - CD3) - T2A - EGFRt	Figure 2.7	own construction
Decoy+EGFRt (#576)	SΔ-CAR (human wt IgG1 - NGFR) - T2A - EGFRt	Figure 2.16 Figure 2.19 Figure 2.28	own construction
S-CAR(28z)+ EGFRt (#515)	S-CAR (human wt IgG1 - human CD28 - CD3) - T2A - EGFRt	Figure 2.16 Figure 2.19 Figure 2.28	Nina Kallin, AG Protzer
S-CAR(28OXz)+ EGFRt (#274)	S-CAR (human wt IgG1 - human CD28 - OX40 - CD3) - T2A - EGFRt	Figure 2.19	own construction
S-CAR(28zOX)+ EGFRt (#573)	S-CAR (human wt IgG1 - human CD28 - CD3 - OX40) - T2A - EGFRt	Figure 2.16 Figure 2.19	own construction
S-CAR(28BBz)+ EGFRt (#275)	S-CAR (human wt IgG1 - human CD28 - 4-1BB - CD3) - T2A - EGFRt	Figure 2.19	own construction
S-CAR(28zBB)+ EGFRt (#572)	S-CAR (human wt IgG1 - human CD28 - CD3 - 4-1BB) - T2A - EGFRt	Figure 2.16 Figure 2.19	own construction

S-CAR(BBz)+ EGFRt (#561)	S-CAR (human wt IgG1 - human CD28[TM only] - 4-1BB - CD3) - T2A - EGFRt	Figure 2.19	Sophia Schreiber, AG Protzer
S-CAR(mCD28z)+ EGFRt (#470)	S-CAR (human FcΔ IgG1 - human CD28[TM only] – murine CD28 - CD3) - T2A - EGFRt	Figure 2.21 Figure 2.22	own construction
S-CAR(mCD28zBB)+ EGFRt (#472)	S-CAR (human FcΔ IgG1 - human CD28[TM only] – murine CD28 - CD3 - 4-1BB) - T2A - EGFRt	Figure 2.21 Figure 2.22	own construction
S-CAR(mBBz)+ EGFRt (#471)	S-CAR (human FcΔ IgG1 - human CD28[TM only] – murine 4-1BB - CD3) - T2A - EGFRt	Figure 2.21 Figure 2.22	own construction
S-CAR(28z)+EGFRt +PrP (#652)	S-CAR (human wt IgG1 - human CD28 - CD3) - T2A – EGFRt + PrP	Figure 2.1	Antje Malo, AG Protzer

4.1.12 Media

Medium	Ingredients	
Collagenase medium	DMEM/F12	500 ml
	Gentamicin, 50 mg/ml	0.5 ml
	Collagenase IV	25 mg
DMEM full medium	DMEM	500 ml
	FCS	50 ml
	Pen/Strep, 10,000 U/ml	5.5 ml
	L-Glutamine, 200 mM	5.5 ml
	NEAA, 100x	5.5 ml
	Sodium pyruvate, 100 mM	5.5 ml
Freezing medium	FCS	90 %
	DMSO	10 %
HepG2 Diff medium	DMEM	500 ml
	FSC	5 ml
	Pen/Strep, 10,000 U/ml	5.5 ml
	L-Glutamine, 200 mM	5.5 ml
	NEAA, 100x	5.5 ml
	Sodium pyruvate, 100mM	5.5 ml
	DMSO	10.5 ml

Human T-cell medium (hTCM)	RPMI 1640	500 ml
	FSC	50 ml
	Pen/Strep, 10,000 U/ml	5.5 ml
	L-Glutamine, 200 mM	5.5 ml
	NEAA, 100x	5.5 ml
	Sodium pyruvate, 100 mM	5.5 ml
	HEPES	5.5 ml
	Gentamicin	208 µl
LB medium pH 7.0	Tryptone	10 g
	Yeast extract	5 g
	NaCl	10 g
	in 1 liter H_2O	
Murine T-cell medium (mTCM)	RPMI Dutch modified	500 ml
	FCS	50 ml
	Pen/Strep, 10,000 U/ml	5.5 ml
	L-Glutamine, 200 mM	5.5 ml
	NEAA, 100x	5.5 ml
	Sodium pyruvate, 100 mM	5.5 ml
	β-Mercaptoethanol	550 µl
PH medium	DMEM/F12	500 ml
	bovine growth serum	55 ml
	HEPES buffer, 1 M	11.5 ml
	Glucose, 50 mg/ml	6 ml
	L-glutamine, 200 mM	5.5 ml
	antibiotic/antimycotic, 100x	5.5 ml
	Gentamicin, 50mg/ml	1 ml
R15 medium	RPMI 1640	500 ml
	FCS	75 ml
	Pen/Strep	5.5 ml
	L-Glutamine, 200mM	5.5 ml
RPMI full medium	RPMI 1640	500 ml
	FCS	50 ml
	Pen/Strep, 10,000 U/ml	5.5 ml
	L-Glutamine, 200 mM	5.5 ml
	NEAA, 100x	5.5 ml
	Sodium pyruvate, 100 mM	5.5 ml

Transfection medium	DMEM	500 ml
	FCS	50 ml
	L-Glutamine, 200 mM	5.5 ml
	NEAA, 100x	5.5 ml
	Sodium pyruvate, 100 mM	5.5 ml
Wash medium	RPMI 1640	500 ml
	Pen/Strep, 10,000 U/ml	5.5 ml

4.1.13 Viral vectors

Viral vector	Description	Source
AAV-HBV	AAV genome serotype 2 containing the 1.2 overlength genome of HBV genotype D packed into AAV capsid serotype 8 (Dion et al., 2013)	Plateforme de Thérapie Génique (Nantes, France)
Ad-HBV	2nd generation serotype 5, containing the 1.3 overlength genome of HBV genotype D	Antje Malo, AG Protzer
Ad-hNTCP	2nd generation serotype 5, containing the open reading from of human NTCP	Jochen Wettengel, AG Protzer

4.1.14 Mouse strains

Mouse line	Description	Source
CD45.1	C57BL/6, expressing congenic marker CD45.1	AG Busch, Microbiology
CD45.1/CD45.2	C57BL/6, cross-bred of wildtype and CD45.1 mice	Own breeding
HBVxfs	C57BL/6, HBV-transgenic, 1.3 overlength genome, frame-shift mutation in X protein	AG Protzer
IL-10$^{-/-}$	C57BL/6, homozygous deficiency in IL-10 locus	AG Haller, Chair of Nutrition and Immunology
PD-1$^{-/-}$	C57BL/6, homozygous deficiency in PD-1 locus	AG Oxenius, ETH Zürich
Rag2$^{-/-}$	C57BL/6, homozygous deficiency in Rag2 locus; no B- and T-cell development	AG Knolle, Molecular Immunology and Experimental Oncology
Rag2$^{-/-}$/IL-2R$\gamma^{-/-}$	C57BL/6, homozygous deficiency in Rag2 and IL-2Rγ locus; no B-, T- and NK-cell development	AG Busch, Microbiology
Wildtype	C57BL/6J wildtype	Janvier

4.1.15 Software

Software	Application	Supplier
FlowJo, version 10.4	Flow cytometry analysis	BD Biosciences
LightCycler 480 SW 1.5.1	qPCR analysis	Roche
Prism 5.01	Graph design, ELISA calculations, statistical analyzes	GraphPad Software Inc.
RTCA Software 2.0	xCELLigence viability analysis	ACEA Biosciences
Serial Cloner	DNA and protein sequence analysis	SerialBasics

4.2 Methods

4.2.1 Molecular biological methods

4.2.1.1 Polymerase chain reaction (PCR)

PCRs for cloning were performed using the Phusion Hot Start Flex 2x master mix following manufacturer's instructions. In short, 2.5 µl of each 10 µM primer and 1 – 5 ng plasmid DNA were added to 25 µl 2x master mix and H_2O added to a total reaction volume of 50 µl. The PCR program was performed the following:

	Temperature [°C]	**Time [sec]**	**Cycles**
Denaturation	98	30	1
Denaturation	98	10	30
Annealing	55-65 (depending on primers)	20	
Elongation	72	30 per 1kb	
Elongation	72	600	1
Cooling	4		1

To fuse two DNA fragments by PCR, equimolar fragments (total of 300 ng) with 18 base pair (bp) overlap were run without primers with a PCR program (see above) for 15 cycles. Following, flanking primers were added, and additional 15 cycles run. Annealing temperature could differ between the two PCR runs.

4.2.1.2 Restriction digest

Restriction digests of plasmids and PCR products were performed to analyze plasmids and to obtain fragments for molecular cloning. Plasmid DNA or PCR product were mixed with 2 µl FastDigest Green Buffer (10x) an up to 1 µl of each needed FastDigest restriction enzyme not exceeding 10 % (volume/volume) of total volume. H_2O was added to a total reaction volume of 20 µl followed by a 30 – 60 min incubation at 37°C. In restriction digests to obtain a plasmid backbone for subsequent ligation 1 µl FastAP, which dephosphorylates 5' and 3' ends, was added to prevent self-ligation without an insert.

4.2.1.3 Agarose gel to analyze DNA fragments

Digested or undigested plasmids or PCR products were analyzed on a 1 % agarose gel prepared with Tris-acetate-EDTA buffer freshly supplemented with 6 µl Roti gel stain per 100 ml total volume. Samples were run together with a DNA ladder at 80 – 150 mV until desired separation of fragments had been achieved.

4.2.1.4 DNA extraction from agarose gel

Fragments for subsequent ligation were cut out from the agarose gel using a scalpel avoiding excessive ultraviolet light exposure. DNA was extracted using the QIAquick Gel Extraction Kit according to manufacturer's instructions.

4.2.1.5 DNA ligation and bacteria transformation

A total of 100 ng of DNA fragments were ligated in a molar ratio of 3:1 (insert:backbone) in a total volume of 20 µl with 2 µl T4 DNA ligase buffer and 1 µl T4 DNA ligase filled up with H_2O. The reaction was incubated 30 min at RT, followed by 60 min on ice. Stbl3 bacteria were thawed on ice, up to 5 µl ligation reaction added to 50 µl bacteria broth and incubated on ice for 20 min. Next, the heat shock was performed for 45 sec in a water bath at 42°C. Bacteria were chilled on ice for 2 – 3 min before 500 µl SOC medium was added and bacteria shook for one hour at 225 rpm. In the end, 200 µl of bacteria were spread on antibiotic-resistance plates and incubated overnight at 37°C.

4.2.1.6 Amplification and isolation of plasmid DNA

Bacteria containing respective plasmids were amplified in overnight cultures in LB medium supplemented with 100 µg/ml ampicillin (37°C, 185 rpm). Bacteria cultures were grown until a maximal optical density (OD_{600}) of 1.5 and subsequently harvested by centrifugation (3400g, 10 min, 4°C). Plasmid DNA of small cultures (1 – 3 ml) and of large cultures (20 – 50 ml) were isolated using the GeneJET Plasmid Miniprep Kit and the Plasmid *Plus*Midi Kit, respectively, following manufacturer's instructions.

4.2.1.7 Determination of DNA concentrations

Plasmid and genomic DNA concentrations were determined on a NanoDrop One using the appropriate buffer solution as blank.

4.2.1.8 Sequencing

For sequencing of plasmid DNA, 20 µl sample (20 – 50 ng/µl) and 20 µl primer (10 µM) were sent to the external provider GATC Biotech. Sequencing results could be downloaded from their webpage for subsequent analysis with Serial Cloner software.

4.2.1.9 DNA isolation from liver tissue

Approximately 20 mg of fresh liver tissue was transferred to 180 µl T1 buffer of the NucleoSpin Tissue Kit and stored at -20°C or -80°C until further processing. At time of isolation, samples were thawed, and DNA extracted following manufacturer's instructions.

4.2.1.10 Quantitative PCR

Quantitative PCR was performed in a reaction including 5 µl LightCycler 480 SYBR green master mix, 0.5 µl of each primer (stock concentration = 20 µM) and 4 µl sample (≤50 ng total DNA). To determine AAV (primers: AAV ITR fw and HBV x rev) and HBV (primers: HBV S fw and HBV S rev) DNA copies per cell, the values were normalized to the single copy gene *PRNP* (primers: PrP fw and PrP rev). As standard a 2-fold step serial dilution of pooled samples from mice with the highest serum HBeAg level at the final timepoint was used. Retroviral integrates (primers: ScFvC8 1 fw and ScFvC8 2 rev) per cell were normalized to the single copy gene *PRNP*. As standard served a 10-fold step serial dilution of plasmid DNA (#652). The measurement was performed on a LightCycler® 480 II system and analyzed by advanced relative quantification using the LightCycler 480 software.

The qPCR program for AAV and HBV DNA copies normalized to PRNP was the following:

	Temperature [°C]	**Time [sec]**	**Ramp [°C/sec]**	**Acquisition mode**	**Cycles**
Denaturation	95	300	4.4		1
Amplification	95 60 72	15 10 25	4.4 2.2 4.4	single	45
Melting	95 65 95	10 60	4.4 2.2 0.11	continuous, 5/°C	1
Cooling	40	30	2.2		1

S-CAR integrates normalized to *PRNP* was measured with following qPCR program:

	Temperature [°C]	**Time [sec]**	**Ramp [°C/sec]**	**Acquisition mode**	**Cycles**
Denaturation	95	300	4.4		1
Amplification	95 60 72	25 10 30	4.4 2.2 4.4	single	40
Melting	95 65 95	10 60	4.4 2.2 0.11	continuous, 5/°C	1
Cooling	40	30	2.2		1

4.2.2 General cell culture methods

4.2.2.1 Culture of adherent cell lines

All cells were incubated at 37°C, 5 % CO_2 and 95 % humidity. The maintenance cultures of adherent cells were cultured in DMEM full medium and cells passaged 1:5 to 1:10 when they reached 90 % confluency. PlatE, RD114 and GALV cells could be harvested by vigorous resuspension, HT1080, HepG2-NTCP, Huh7 and Huh7-S cells were treated with trypsin (HepG2-NTCP in addition with versene) (5 – 10 min, 37°C) to obtain a single-cell suspension. Culture flasks or plates for HepG2-NTCP cells were treated with collagen (1:10 in H_2O, 1 h, 37°C) and washed twice with PBS before seeding cells.

4.2.2.2 Counting of cells

For counting, cells were harvested and resuspended thoroughly to obtain a single-cell suspension. Counting was performed by diluting 10 µl of the cell suspension with 10 µl trypan blue and counting by eye under the microscope using a Neubauer improved hemocytometer. Alternatively, cells were counted by adding 1 µl of Solution 18 to 20 µl of cell suspension and performing an automated measurement on NucleoCounter NC-250.

4.2.2.3 Freezing/Thawing of cells

Freezing of cells was performed by resuspending pelleted cells in 1 ml of prechilled freezing medium per cryo vial. Vials were transferred to a prechilled freezing device and stored immediately at -80°C for slow temperature decline. On the next day cryo vials were transferred from the freezing device to a box at -80°C or in liquid nitrogen. To thaw cells, prewarmed wash medium from a 15 ml falcon tube was added to frozen cryo vials and slowly transferred forth and back until it was thawed. Cells were centrifuged (450g, 5 min, RT) and seeded in the appropriate flask with the respective culture medium.

4.2.2.4 Transfection of cells

Cell were seeded in poly-L-lysine-treated (1:20 in PBS, 1 h, 37°C) 6-well plates to obtain a confluency of 50 – 70 % at day of transfection. 5 µg plasmid DNA was sterilized on a heat block (10 min, 70°C) and subsequently diluted in OptiMEM (RT) to a total volume of 125 µl. In a separate tube, 5 µl Lipofectamine 2000 was added to 120 µl OptiMEM (RT). After a separate incubation for 5 min at RT, diluted DNA was added to diluted Lipofectamine 2000, carefully mixed and incubated 20 min at RT. After exchanging the cell culture medium to 2 ml transfection medium, the DNA/Lipofectamine 2000 mix was added to the cells and incubated four to six hours or overnight at 37°C. Subsequently medium was exchanged to the appropriate culture medium.

4.2.3 Isolation of primary cells

4.2.3.1 Murine and macaque splenocyte isolation

For the isolation of splenocytes, spleens were mashed through a 100 μm cell strainer into a 50 ml falcon tube using a plunger of a 2 ml syringe. The cell strainer was cleaned from cells with cold wash medium followed by additional mashing repeatedly. After pelleting (450g, 5 min, 4°C), the cells were resuspended in 2 ml ACK lysis buffer and incubated 2 min at RT. 30 ml wash medium was added, splenocytes pelleted (450g, 5 min, 4°C) and resuspended in the appropriate volume and medium or buffer for subsequent procedures.

4.2.3.2 Murine liver-associated lymphocyte isolation

Liver tissue was mashed through a 100 μm cell strainer into a 50 ml falcon tube using a plunger of a 2 ml syringe. The cell strainer was cleaned from cells with cold wash medium followed by additional mashing repeatedly. After pelleting (450g, 5 min, 4°C), cells were resuspended in 12.5 ml collagenase medium (12.5 ml wash medium containing 10 mg collagenase) and incubated for 20 min at 37°C with repeated shaking. Cells were pelleted and resuspended in 4 ml PBS-buffered 40 % Percoll solution and carefully layered on top of 4 ml PBS-buffered 80 % Percoll solution in a 15 ml falcon tube. After centrifugation (1400g, 20 min, RT, no brake) the LAL fraction as white ring between the two Percoll solution layers was transferred to a new 15 ml falcon tube. LALs were washed twice with wash medium and resuspended in the appropriate volume and medium or buffer for subsequent procedures.

4.2.3.3 Murine PBMC isolation

15 μl heparinized peripheral blood from Microvette 500 LH-Gel tubes was added to 230 μl PBS in a 96-well V-bottom plate and pelleted (450g, 2 min, 4°C). Cells were resuspended in 230 μl ACK lysis buffer and incubated for 2 min at RT. Subsequently, cells were pelleted (450g, 2 min, 4°C) and washed twice with 200 μl FACS buffer.

4.2.3.4 Human PBMC isolation

Peripheral blood was collected into a syringe containing heparin and diluted 1:1 with wash medium. Up to 30 ml of diluted blood was layered on top of 15 ml isotone Biocoll separating solution (density 1.077 g/ml) in a 50 ml falcon tube and centrifuged (1200g, 20 min, RT, no brake). The lymphocyte fraction as white ring was transferred into a new 50 ml falcon tube and washed twice with wash medium (300g, 10 min, RT) followed by resuspension in the appropriate volume and medium or buffer for subsequent procedures.

4.2.3.5 Macaque PBMC isolation

Macaque peripheral citrate blood was obtained from the “Deutsches Primatenzentrum” in Göttingen, Germany. PBMC were isolated following the protocol to isolate human PBMC (section 4.2.3.4).

4.2.3.6 Primary macaque hepatocyte isolation

An intact liver lobe was first perfused with 250 ml HBSS followed by perfusion with 100 ml collagenase medium. Additional 150 ml collagenase medium was re-circulated through the liver lobe at 42°C for 1 hour. After digest, the liver lobe was physically broken up using scalpels and a plunger of a 3 ml syringe. The cell suspension was serially filtered using a tea filter and a 100 μm cell strainer to remove cell clumps and obtain a single-cell suspension. Next, cells were washed with PH medium three times with distinct centrifugation steps in between (1.: 100g; 2.: 70g; 3.: 50g; all at 4°C for 3 min). Isolated PMHs were then seeded on collagen-coated 12-well plates at 2.5 x 10^5 cells/well in PH medium. After four hours, cells were washed three times with HBSS and cultured with PH medium overnight. The following day medium was exchanged to PH medium supplemented with 1.8 % DMSO.

4.2.4 Retroviral transduction

4.2.4.1 Production of retroviral supernatants

Retroviral supernatants were obtained from transiently transfected or stably transduced HEK293 cell-based retroviral packaging cell lines PlatE, RD114 and GALV. PlatE were used for transduction of murine T cells, RD114 for transduction of human T cells as well as of PlatE, and GALV for transduction of RD114. In the case of transient transfection, packaging cell lines were transfected with pMP71 plasmids coding for the transgenes. For details about transfection see section 4.2.2.4. Supernatant containing retroviral vector was collected two and three days after transfection and 0.45 μm filtered. On day two fresh medium was added to cells. Stable retroviral packaging cells were created by transduction of PlatE and RD114 with retroviral supernatant from transiently transfected RD114 and GALV, respectively. Transduction efficacy ranged from 1 – 20 % and transduced cells were enriched by surface staining of the transgene product and subsequent isolation by FACS. An additional enrichment for highly expressing packaging cells could further enhance viral vector production. Cell culture medium was enriched with retroviral vector for 24 hours when cells reached about 70 % confluency and 0.45 μm filtered. Supernatant was used immediately for subsequent procedure or stored at -80°C.

4.2.4.2 Titration of retroviral supernatants

RD114 supernatants for the transduction of human T cells was titrated before transduction to achieve comparable transduction rates. On day one, 5 x 10^5 HT1080 per well were seeded in DMEM full medium on a 6-well plate and incubated for four to six hours until cells adhered to well. The medium was exchanged to medium containing retroviral supernatant in serial dilution supplemented with 8 μg/ml polybrene and incubated for 24 hours. On day two, the medium was exchanged to DMEM full medium and cells incubated for additional 24 hours. Cells were harvested the following day and the surface expression of the transgene product stained with an antibody and transduction rate of HT1080 determined by flow cytometry. The concentration of infectious particles (ip) were calculated with following formula:

$$\frac{\mathrm{ip}}{ml} = \frac{\%\ positive\ cells}{100} \times dilution\ factor\ of\ supernatant \times 20 \times cell\ number\ at\ seeding\ time$$

4.2.4.3 Human PBMC transduction

For stimulation of human PBMC, non-tissue culture-treated 24-well plates were coated with anti-CD3 (5 μg/ml, 16-0037-85, eBioscience) and anti-CD28 (0.05 μg/ml, 16-0289-85, eBioscience) antibodies diluted in PBS (250 μl/well, 2 h, 37°C). Next wells were blocked with 2 % BSA in PBS (30 min, 37°C) and subsequently washed twice with PBS. Freshly isolated or thawed human PMBC were resuspended in 1.5 ml hTCM supplemented with IL-2 (300 U/ml) per 1 x 10^6 PBMC and well. After incubation for 48 hours at 37°C, PBMC were transduced two days in a row. Therefore, non-tissue culture-treated 24-well plates were coated with diluted RetroNectin (250 μl/well, 20 μg/ml in PBS, 2 h, RT). Diluted RetroNectin was collected and stored at 4°C for re-use the following day and wells blocked with 2 % BSA in PBS (30 min, 37°C). After wells were washed twice with PBS, 1 ml diluted or undiluted viral supernatant was applied per well and centrifuged (2000g, 2 h, 32°C). Following, the viral supernatant was discarded and 5 x 10^5 – 8 x 10^5 activated PBMC were transferred per well in 1.5 ml hTCM supplemented with IL-2 (180 U/ml). Cells were centrifuged (1000g, 10 min, 32°C) and subsequently incubated at 37°C. The following day, PBMC were transduced again in the same manner. PBMC were transferred to RetroNectin- and retrovirus-coated plates well-by-well without adjusting the concentration or addition of IL-2. The following day, cells were harvested and adjusted to 1.25 x 10^5 – 2.5 x 10^5 cells/ml hTCM supplemented with IL-2 (180 U/ml) for expansion. Cell were readjusted to latter condition every 3 – 4 days until functional assessment or freezing around ten days after initial activation.

4.2.4.4 Murine CD8$^+$ T cells transduction

For stimulation of murine CD8$^+$ T cells, tissue culture-treated 12-well plates were coated with anti-CD3 (AG Feederle) and anti-CD28 (AG Feederle) antibodies (10 μg/ml in PBS, 460 μl/well, 2 h, 37°C) and washed twice with PBS. Freshly isolated murine splenocytes (section 4.2.3.1) were enriched for CD8$^+$ T cells by MACS. Therefore, splenocytes were washed once with MACS buffer (450g, 5 min, 10°C) and resuspended in 90 μl MACS buffer and 10 μl CD8a MicroBeads per 2 x 10^7 cells. After incubation (15 min, 4°C, in dark) splenocytes were washed once with MACS buffer, cell-clumps removed (30 μm filcons) and CD8$^+$ T cells enriched on a MACS separation column following manufacturer's instructions. After elution and one washing step, enriched CD8$^+$ T cells were adjusted to 5 x 10^5 cells/ml mTCM supplemented with IL-12 (5 ng/ml). Cells were seeded in antibody-coated wells (3 ml/well) and cells incubated overnight at 37°C. The following day 2 ml supernatant was removed and stored at 37°C. The remaining 1 ml cell suspension was transferred to a fresh 12-well plate and 1 ml retroviral supernatant supplemented with protamine sulfate (4 μg/ml) added (final concentration protamine sulfate = 2 μg/ml). CD8$^+$ T-cell/retrovirus suspension was spinoculated (850g, 2 h, 32°C). Next, 1 ml supernatant was removed and 2 ml of the stored supernatant supplemented with protamine sulfate (2 μg/ml) added. Cells were resuspended and incubated overnight at 37°C. The following day, similar procedure was performed with a few modifications: After removing 2 ml of the supernatant, the remaining cell suspension stayed in the well and retroviral supernatant was directly applied. After spinoculation, the whole cell suspension remained in the well and the stored supernatant was added without addition of fresh protamine sulfate (total volume per well = 4 ml). Subsequently, cells were incubated overnight at 37°C, harvested the following day and the transduction rate analyzed by flow cytometry. Cells were washed and resuspended in appropriate medium or buffer for subsequent procedures.

4.2.4.5 Macaque PBMC and splenocyte transduction

Macaque PBMC or splenocytes were stimulated with different protocols for transduction.

<u>Plate-bound antibodies and human IL-2 or IL-15</u>

Non-tissue culture-treated 24-well plates were coated with anti-CD3 (BD, #560770, 1 μg/ml) and anti-CD28 (eBioscience, 16-0289-85; 0.5 μg/ml) antibodies in PBS (250 μl/well, 2 h, 37°C) followed by blocking with 2 % BSA in PBS (30 min, 37°C) and two washes with PBS. 1 x 10^6 PBMC in 1.5 ml hTCM supplemented with either IL-2 (300 U/ml) or IL-15 (10 ng/ml) were seeded per well and incubated at 37°C for 48 hours. On the day of transduction, cells were harvested, centrifuged (450g, 5 min, RT) and resuspended in 1.5 ml hTCM supplemented with either IL-2 (180 U/ml) or IL-15 (10 ng/ml). For expansion after transduction, cells were

harvested and adjusted to 2.5 x 10^5 cells/ml hTCM supplemented with either IL-2 (180 U/ml) or IL-15 (10 ng/ml).

Soluble antibodies and staphylococcal enterotoxin B

Up to 5 x 10^6 PBMC or splenocytes were stimulated in 1 ml R15 medium supplemented with IL-2 (100 U/ml), SEB (2 μg/ml), anti-CD3 (0.3 μg/ml, Mabtech), anti-CD28 (1.5 μg/ml, eBioscience) and anti-CD49d (1.5 μg/ml, eBioscience) antibodies at 37°C. After 24 hours, cells were harvested and washed three times with 5 ml RPMI full medium. After the last wash, cells were resuspended in 1 ml R15 supplemented with IL-2 (100 U/ml) and incubated at 37°C until transduction on the following day. On the day of transduction cell concentration was adjusted to 1 x 10^6 cells/1.5 ml supplemented with IL-2 (180 U/ml). For expansion after transduction, cells were harvested and adjusted to 2.5 x 10^5 cells/ml hTCM supplemented with IL-2 (180 U/ml).

Transduction for all stimulation protocols was performed 48 hours after initial stimulation following plate-preparation protocol with RetroNectin for the transduction of human PBMC (section 4.2.4.3). 1.5 ml cell suspension were seeded per well. Macaque PBMC and splenocytes were only transduced once and expanded the next day as described for each stimulation protocol. T-cell functionality was assessed seven days after initial stimulation.

4.2.5 *In vitro* HBV infection experiments

For HBV-infection, HepG2-NTCP were cultured in 6-well plates and when 90 % confluent differentiated by changing to HepG2 Diff medium. After differentiation for three days, virus was added in 3 ml HepG2 Diff medium supplemented with 4 % PEG 6000. After 24 hours, cells were washed three times with PBS and incubated with HepG2 Diff medium until further processing. Ad-hNTCP-transduced PMHs were infected with HBV in a comparable manner. They were transduced in 12-well plates and 1 ml of PH medium supplemented with 1.8 % DMSO and 4 % PEG 6000 was used as infection media.

4.2.6 T-cell stimulation and co-culture experiments

4.2.6.1 T-cell culture on plate-bound HBsAg or anti-CD3/anti-CD28 antibodies

Flat-bottom tissue culture-treated 96-well plates were coated with 100 μl HBsAg of the indicated concentration diluted in PBS overnight at 4°C or for two hours at 37°C. For unspecific stimulation of murine T cells, 100 μl anti-CD3 and anti-CD28 antibodies (10 μg/ml in PBS, AG Feederle) were coated on the latter plates overnight at 4°C or for two hours at 37°C. In the 24-well format 250 μl of each diluted stimulant was added. Before the addition of cells, the wells were washed twice with PBS. Freshly transduced T cells (5 x 10^4 – 2 x 10^5 cell/well) or

freshly isolated splenocytes as well as LALs (2.5 x 10^5 – 5 x 10^5 cells/well) were transferred in 200 µl of the appropriate medium (hTCM for human cells; mTCM for murine cells) to the precoated plate. Cells were centrifuged onto the plate (450g, 30 sec) and incubated for the indicated time at 37°C. For the analysis of intracellular cytokine expression by ICS (section 4.2.9.2), Brefeldin A (human and macaque cells = 0.2 µg/ml; murine cells 1 µg/ml) was added one hour after start of stimulation and cells subsequently cultured for additional 4 – 16 hours at 37°C.

4.2.6.2 Cell viability assay with xCELLigence RTCA

To determine the cell viability in co-culture experiments, 100 µl/well of the appropriate culture medium depending on the target cell type was added to an xCELLigence 96-well plate and the blank impedance value determined. Next, target cells were seeded one day before start of co-culture. In the case of Huh7 and Huh7-S, 3 x 10^5 cells were seeded in 100 µl/well DMEM full medium. HepG2-NTCP had been infected with HBV in 6-wells, harvested 7 days later and 4 x 10^5 cells seeded in 100 µl/well HepG2 Diff medium. Impedance measurement was performed overnight. On the same day, transduced T cells from an expansion culture or freshly thawed cells were cultured at 1 x 10^6 cells/ml hTCM without IL-2 overnight. In the morning of the following day, medium of the xCELLigence plate was exchanged to 100 µl of the appropriate co-culture medium (Huh7/Huh7-S: hTCM; HepG2-NTCP: 50 % hTCM + 50 % HepG2 Diff medium and the measurement continued. Four to six hours later, T cells were added in 100 µl of the appropriate co-culture medium and in different effector to target ratios assuming 6 x 10^5 cells/well Huh7/Huh7-S cells and 4 x 10^5 cells/well HepG2-NTCP cells. Impedance measurement was continued for the indicated time frame. Cell viability was determined as cell index normalized to the start of co-culture.

4.2.6.3 Determination of T-cell immune response in immunocompetent mice

To determine a T-cell immune response, 1 x 10^6 splenocytes from mice that had received S-CAR$^+$/EGFRt$^+$ or mock T cells previously were co-cultured with 1 x 10^5 transduced CD8$^+$ T cells in 200 µl mTCM in round-bottom 96-well plates at 37°C. One hour after start of stimulation, Brefeldin A (1 µg/ml) was added and the co-culture continued for 16 hours at 37°C until an ICS (section 4.2.9.2) on the following day.

4.2.6.4 Primary macaque hepatocytes and T-cell co-culture

PMHs were transduced with Ad-hNTCP or Ad-HBV one day after isolation follow by a medium change after 16 – 24 hours (PH diff supplemented with 1.8 % DMSO). Four days later, Ad-hNTCP-transduced PMHs were infected with HBV (section 4.2.5). During co-culture with transduced macaque T cells, the medium was changed to a 1:1 mix of PH medium and R15 medium supplemented with 0.9 % DMSO.

4.2.7 Mouse experiments

4.2.7.1 Injections

For AAV-HBV infection, virus stock was diluted and per mouse 2 x 10^{10} viral genomes in 200 µl PBS injected intravenously into the tail vein. For T-cell transfer, the desired number of transduced $CD8^+$ T cells (0.5 – 5 x 10^6 per mouse) was resuspended in 200 µl cold PBS per mouse. Cell suspension was kept on ice until shortly before intraperitoneal injection. If indicated, mice received total body irradiation (5 Gray) one day prior to T-cell transfer. For the induction of iMATEs, CpG or the control oligonucleotide (10 µg / 200 µl PBS / mouse) were injected intravenously into the tail vein.

4.2.7.2 Bleeding

To obtain peripheral blood, living mice were bled from the cheek and approximately 100 µl blood collected into a Microvette 500 LH-Gel tube and mixed by inverting.

4.2.7.3 Final analysis

Mice were sacrifice with CO_2 and opened to access the internal organs. Blood was drawn with a 23 G syringe from the vena cava and collected into a Microvette 500 LH-Gel tube and mixed by inverting. The liver was perfused with PBS through the portal vein until the complete liver was well-perfused indicated by a color change. Liver and spleen were excised and both organs stored in wash medium on ice until further processing no later than one hour after excision. Tissue for the extraction of DNA was cut into cubic pieces of approximately 5 mm edge length with a clean scalpel. Organs were weight before and after pieces were taken for other analyzes to determine which proportion of the organ was used for splenocyte and LAL isolation.

4.2.7.4 Blood and serum analyses

Peripheral blood in Microvette 500 LH-Gel tubes was centrifuged (10 000g, 5 min, RT) and the serum transferred into a new reaction tube. ALT activity was determined 1:4 diluted with PBS using the Reflotron ALT test. Serum HBsAg, HBeAg and anti-HBsAg antibody were quantified in different dilutions with PBS on an Architect™ platform using the quantitative HBsAg test

(Ref.: 6C36-44; Cutoff: 0.25 IU/ml), the HBeAg Reagent Kit (Ref.: 6C32-27) with HBeAg Quantitative Calibrators (Ref.: 7P24-01; Cutoff: 0.20 PEI U/ml) and the anti-HBs test (Ref.: 7C18-27; Cutoff: 12.5 mIU/ml).

4.2.8 Enzyme-linked immunosorbent assay

4.2.8.1 Cytokine-detection ELISA

Commercial ELISAs to determine concentrations of cytokines in supernatant were performed on MaxiSorb ELISA 96-well plates following manufacturer's instructions. TMB substrate conversion was determined by measurement of OD_{450} subtracted by OD_{560} on an ELISA-Reader infinite F200. Calculations were performed with GraphPad Prism. A standard curve for log_{10} transformed samples of known concentration using nonlinear regression with a sigmoidal dose-response equation was calculated. Concentrations of unknown samples were calculated accordingly. (for more details see: https://www.graphpad.com/support/faq/prism-3-analyzing-ria-and-elisa-data/)

4.2.8.2 Measurement of HBV parameters in cell culture experiments

Viral parameters of HBV infection in cell culture supernatant were determined by ELISA. For infection experiments with HepG2-NTCP cells, HBeAg was determined using the immunoassay Enzygnost measured on a BEP III, while HBeAg BioAssay ELISA Kit and HBsAg BioAssay ELISA Kit were used for HBeAg and HBsAg measurement in the case of PMH experiments. All assays were performed following manufacturer's instructions.

4.2.8.3 Detection of murine antibodies against the C8 scFv and human IgG1 by ELISA

The target proteins C8 scFv (0.1 µg/ml) and cetuximab as human IgG1 antibody (0.1 µg/ml) were coated in 100 µl PBS per well on MaxSorb 96-well ELISA plates (4°C, overnight). The following day, plates were washed four times with 300 µl PBS-T per well and subsequently blocked with 200 µl assay diluent (1 h, RT, 300 rpm). Serum was diluted as indicated (1:50 to 1:800) in assay diluent and 100 µl incubated per well (2 h, RT, 300 rpm). Next, wells were washed four times with 300 µl PBS-T and 100 µl HRP-labelled goat anti-mouse-IgG antibody (1:1000 in assay diluent) incubated per well (1 h, RT, 300 rpm). Wells were washed five times with 300 µl PBS-T interleaved by shaking (1 min, 300 rpm). 100 µl TMB was added per well and the substrate conversion stopped after 2 – 10 min with the addition of 100 µl 2N sulfuric acid. TMB substrate conversion was determined by measurement of absorbance (OD_{450} subtracted by OD_{560}) on an ELISA-Reader infinite F200.

4.2.9 Flow cytometry

4.2.9.1 General staining procedure

For a flow cytometry staining, up to 1 x 10^6 cells were transferred to a V-bottom 96-well plate and washed twice with FACS buffer before the first staining step. All centrifugation of non-permeabilized cells was performed at 450g for 2 minutes at 4°C. Stainings were performed with 50 µl/well antibodies or other reagents diluted in FACS buffer on ice and in the dark for 30 min if not indicated otherwise. Between serial staining steps, two washing steps with FACS buffer were performed. Dead cells were stained by three different means: Either cells were stained with fixable ethidium monoazide (EMA, 1 µg/ml) 10 min in the dark followed by 20 min in bright light before the addition of fluorochrome labelled antibodies. Secondly, dead cells were stained with other fixable live/dead stain without photoactivation. Thirdly, propidium iodide (1 mg/ml) was added to the cell suspension directly before measurement without subsequent washing. EMA or fixable live/dead stains were used if cells were permeabilized subsequently. If a CAR, EGFRt and other surface markers were analyzed, stainings were performed sequentially: At first the CAR was stained with an anti-human- or anti-murine-IgG antibody, followed by the primary stain of EGFRt with biotin-labelled cetuximab. In a last step, bound cetuximab was stained with fluorochrome-labelled streptavidin together with additional antibodies against surface markers. Alternatively, EGFRt was stained with fluorochrome-labelled cetuximab together with other surface markers after the preceding CAR staining step. Finally, cells were resuspended in 100 – 200 µl FACS buffer and analyzed on a FACS Canto II or CytoFLEX S flow cytometer. All obtained data was evaluated with FlowJo.

4.2.9.2 Intracellular cytokine staining

After surface staining including a fixable live/dead stain and subsequent washing, cells were permeabilized by resuspension in 100 µl Cytofix/Cytoperm and incubation for 20 min. Subsequent washing steps and stainings were performed with Perm/Wash buffer, and centrifugation intensity increased (650g, 3 min, 4°C). After permeabilization, intracellular cytokines could be stained. Finally, cells were resuspended in 100 – 200 µl Perm/Wash and analyzed on a FACS Canto II or CytoFLEX S flow cytometer.

4.2.9.3 Determination of absolute cell count by flow cytometry

To determine absolute count of a specific cell type by flow cytometry 10 µl CountBright™ Absolute Counting Beads were added to the cell suspension directly before measurement. The absolute input cell count was calculated with the following formula:

$$\text{input cells} = \text{measured cells} \times \frac{\text{input beads}}{\text{measured beads}}$$

Subsequently, the result was extrapolated to the concentration in blood or to the whole organ considering the proportion of the organ that was used to isolate splenocytes or LALs.

4.2.9.4 Detection of murine antibodies against the S-CAR and EGFRt by flow cytometry

PlatE were retrovirally transduced to express the S-CAR or EGFRt and 1 x 10^5 cells incubated with diluted serum (1:200 in FACS buffer). In a second step, bound murine IgG molecules were stained with PE-labeled anti-mouse-IgG antibody (eBioscience). Median fluorescence intensity of bound murine IgG antibodies was determined on a CytoFLEX S.

4.2.9.5 CFSE staining

To determine cell proliferation, cells were stained with CFSE. Therefore, cells were washed twice with PBS to remove all serum and 5 – 10 x 10^6 cells/ml stained with 1 μM CFSE in PBS (10 min, RT, in dark). Following, five-times the volume of hTCM was added and incubated (5 min, on ice, in dark). Cells were washed three times with hTCM and eventually seeded on pre-coated plates for stimulation.

4.2.10 Statistical analysis

Data are presented as mean values with standard deviation or as the latter in addition to individual values. Statistical significance was calculated as indicated in each figure using Prism 5.01 software.

5 Table of Figures

6 References

Almasbak, H., E. Walseng, A. Kristian, M.R. Myhre, E.M. Suso, L.A. Munthe, J.T. Andersen, M.Y. Wang, G. Kvalheim, G. Gaudernack, and J.A. Kyte. 2015. Inclusion of an IgG1-Fc spacer abrogates efficacy of CD19 CAR T cells in a xenograft mouse model. *Gene therapy* 22:391-403.

Arzumanyan, A., H.M. Reis, and M.A. Feitelson. 2013. Pathogenic mechanisms in HBV- and HCV-associated hepatocellular carcinoma. *Nat Rev Cancer* 13:123-135.

Attarwala, H. 2010. TGN1412: From Discovery to Disaster. *J Young Pharm* 2:332-336.

Bachmann, M.F., P. Wolint, K. Schwarz, P. Jager, and A. Oxenius. 2005. Functional properties and lineage relationship of CD8+ T cell subsets identified by expression of IL-7 receptor alpha and CD62L. *Journal of immunology (Baltimore, Md. : 1950)* 175:4686-4696.

Badieyan, Z.S., and S.S. Hoseini. 2018. Adverse Effects Associated with Clinical Applications of CAR Engineered T Cells. *Archivum immunologiae et therapiae experimentalis* 66:283-288.

Bengsch, B., B. Martin, and R. Thimme. 2014. Restoration of HBV-specific CD8+ T cell function by PD-1 blockade in inactive carrier patients is linked to T cell differentiation. *Journal of hepatology* 61:1212-1219.

Berger, C., D. Sommermeyer, M. Hudecek, M. Berger, A. Balakrishnan, P.J. Paszkiewicz, P.L. Kosasih, C. Rader, and S.R. Riddell. 2015. Safety of Targeting ROR1 in Primates with Chimeric Antigen Receptor–Modified T Cells. *Cancer immunology research* 3:206-216.

Berger, C., C.J. Turtle, M.C. Jensen, and S.R. Riddell. 2009. Adoptive transfer of virus-specific and tumor-specific T cell immunity. *Current opinion in immunology* 21:224-232.

Bertoletti, A., A. Costanzo, F.V. Chisari, M. Levrero, M. Artini, A. Sette, A. Penna, T. Giuberti, F. Fiaccadori, and C. Ferrari. 1994. Cytotoxic T lymphocyte response to a wild type hepatitis B virus epitope in patients chronically infected by variant viruses carrying substitutions within the epitope. *Journal of Experimental Medicine* 180:933-943.

Bility, M.T., L. Cheng, Z. Zhang, Y. Luan, F. Li, L. Chi, L. Zhang, Z. Tu, Y. Gao, Y. Fu, J. Niu, F. Wang, and L. Su. 2014. Hepatitis B virus infection and immunopathogenesis in a humanized mouse model: induction of human-specific liver fibrosis and M2-like macrophages. *PLoS pathogens* 10:e1004032.

Birkholz, K., A. Hombach, C. Krug, S. Reuter, M. Kershaw, E. Kampgen, G. Schuler, H. Abken, N. Schaft, and J. Dorrie. 2009. Transfer of mRNA encoding recombinant immunoreceptors reprograms CD4+ and CD8+ T cells for use in the adoptive immunotherapy of cancer. *Gene therapy* 16:596-604.

Bohne, F., M. Chmielewski, G. Ebert, K. Wiegmann, T. Kurschner, A. Schulze, S. Urban, M. Kronke, H. Abken, and U. Protzer. 2008. T cells redirected against hepatitis B virus surface proteins eliminate infected hepatocytes. *Gastroenterology* 134:239-247.

Boni, C., P. Fisicaro, C. Valdatta, B. Amadei, P. Di Vincenzo, T. Giuberti, D. Laccabue, A. Zerbini, A. Cavalli, G. Missale, A. Bertoletti, and C. Ferrari. 2007. Characterization of hepatitis B virus (HBV)-specific T-cell dysfunction in chronic HBV infection. *Journal of virology* 81:4215-4225.

Bonini, C., and A. Mondino. 2015. Adoptive T-cell therapy for cancer: The era of engineered T cells. *European journal of immunology* 45:2457-2469.

Böttinger, N. 2014. Adoptive immunotherapy for treatment of chronic hepatitis B. *Ph.D. Thesis*

Bouchard, M.J., and R.J. Schneider. 2004. The enigmatic X gene of hepatitis B virus. *Journal of virology* 78:12725-12734.

Bridgeman, J.S., R.E. Hawkins, S. Bagley, M. Blaylock, M. Holland, and D.E. Gilham. 2010. The optimal antigen response of chimeric antigen receptors harboring the CD3ζ transmembrane domain is dependent upon incorporation of the receptor into the endogenous TCR/CD3 complex. *The Journal of Immunology* 184:6938-6949.

Brower, V. 2017. First Chimeric Antigen Receptor T-Cell Therapy Approved. *Journal of the National Cancer Institute* 109:

Bruix, J., M. Reig, and M. Sherman. 2016. Evidence-Based Diagnosis, Staging, and Treatment of Patients With Hepatocellular Carcinoma. *Gastroenterology* 150:835-853.

Budde, L.E., C. Berger, Y. Lin, J. Wang, X. Lin, S.E. Frayo, S.A. Brouns, D.M. Spencer, B.G. Till, M.C. Jensen, S.R. Riddell, and O.W. Press. 2013. Combining a CD20 chimeric antigen receptor and an inducible caspase 9 suicide switch to improve the efficacy and safety of T cell adoptive immunotherapy for lymphoma. *PloS one* 8:e82742.

Bunse, M., G.M. Bendle, C. Linnemann, L. Bies, S. Schulz, T.N. Schumacher, and W. Uckert. 2014. RNAi-mediated TCR knockdown prevents autoimmunity in mice caused by mixed TCR dimers following TCR gene transfer. *Molecular therapy : the journal of the American Society of Gene Therapy* 22:1983-1991.

Burga, R.A., M. Thorn, G.R. Point, P. Guha, C.T. Nguyen, L.A. Licata, R.P. DeMatteo, A. Ayala, N. Joseph Espat, R.P. Junghans, and S.C. Katz. 2015. Liver myeloid-derived suppressor cells expand in response to liver metastases in mice and inhibit the anti-tumor efficacy of anti-CEA CAR-T. *Cancer immunology, immunotherapy : CII* 64:817-829.

Burwitz, B.J., J.M. Wettengel, M.A. Muck-Hausl, M. Ringelhan, C. Ko, M.M. Festag, K.B. Hammond, M. Northrup, B.N. Bimber, T. Jacob, J.S. Reed, R. Norris, B. Park, S. Moller-Tank, K. Esser, J.M. Greene, H.L. Wu, S. Abdulhaqq, G. Webb, W.F. Sutton, A. Klug, T. Swanson, A.W. Legasse, T.Q. Vu, A. Asokan, N.L. Haigwood, U. Protzer, and J.B. Sacha. 2017. Hepatocytic expression of human sodium-taurocholate cotransporting polypeptide enables hepatitis B virus infection of macaques. *Nature communications* 8:2146.

Buti, M., N. Tsai, J. Petersen, R. Flisiak, S. Gurel, Z. Krastev, R. Aguilar Schall, J.F. Flaherty, E.B. Martins, P. Charuworn, K.M. Kitrinos, G.M. Subramanian, E. Gane, and P. Marcellin. 2015. Seven-year efficacy and safety of treatment with tenofovir disoproxil fumarate for chronic hepatitis B virus infection. *Digestive diseases and sciences* 60:1457-1464.

Carpenito, C., M.C. Milone, R. Hassan, J.C. Simonet, M. Lakhal, M.M. Suhoski, A. Varela-Rohena, K.M. Haines, D.F. Heitjan, S.M. Albelda, R.G. Carroll, J.L. Riley, I. Pastan, and C.H. June. 2009. Control of large, established tumor xenografts with genetically retargeted human T cells containing CD28 and CD137 domains. *Proceedings of the National Academy of Sciences of the United States of America* 106:3360-3365.

Caruana, I., B. Savoldo, V. Hoyos, G. Weber, H. Liu, E.S. Kim, M.M. Ittmann, D. Marchetti, and G. Dotti. 2015. Heparanase promotes tumor infiltration and antitumor activity of CAR-redirected T lymphocytes. *Nature medicine* 21:524-529.

Chen, C., K. Li, H. Jiang, F. Song, H. Gao, X. Pan, B. Shi, Y. Bi, H. Wang, H. Wang, and Z. Li. 2017. Development of T cells carrying two complementary chimeric antigen receptors against glypican-3 and asialoglycoprotein receptor 1 for the treatment of hepatocellular carcinoma. *Cancer immunology, immunotherapy : CII* 66:475-489.

Chen, K.H., M. Wada, K.G. Pinz, H. Liu, X. Shuai, X. Chen, L.E. Yan, J.C. Petrov, H. Salman, L. Senzel, E.L.H. Leung, X. Jiang, and Y. Ma. 2018. A compound chimeric antigen receptor strategy for targeting multiple myeloma. *Leukemia* 32:402-412.

Chen, M.T., J.-N. Billaud, M. Sällberg, L.G. Guidotti, F.V. Chisari, J. Jones, J. Hughes, and D.R. Milich. 2004. A function of the hepatitis B virus precore protein is to regulate the immune response to the core antigen. *Proceedings of the National Academy of Sciences of the United States of America* 101:14913-14918.

Cheng, A.L., Y.K. Kang, Z. Chen, C.J. Tsao, S. Qin, J.S. Kim, R. Luo, J. Feng, S. Ye, T.S. Yang, J. Xu, Y. Sun, H. Liang, J. Liu, J. Wang, W.Y. Tak, H. Pan, K. Burock, J. Zou, D. Voliotis, and Z. Guan. 2009. Efficacy and safety of sorafenib in patients in the Asia-Pacific region with advanced hepatocellular carcinoma: a phase III randomised, double-blind, placebo-controlled trial. *Lancet Oncol* 10:25-34.

Cheng, J.C., M.C. Liu, S.Y. Tsai, W.T. Fang, J. Jer-Min Jian, and J.L. Sung. 2004. Unexpectedly frequent hepatitis B reactivation by chemoradiation in postgastrectomy patients. *Cancer* 101:2126-2133.

Cherkassky, L., A. Morello, J. Villena-Vargas, Y. Feng, D.S. Dimitrov, D.R. Jones, M. Sadelain, and P.S. Adusumilli. 2016. Human CAR T cells with cell-intrinsic PD-1 checkpoint blockade resist tumor-mediated inhibition. *The Journal of clinical investigation* 126:3130-3144.

Chmielewski, M., and H. Abken. 2017. CAR T Cells Releasing IL-18 Convert to T-Bet(high) FoxO1(low) Effectors that Exhibit Augmented Activity against Advanced Solid Tumors. *Cell reports* 21:3205-3219.

Chmielewski, M., C. Kopecky, A.A. Hombach, and H. Abken. 2011. IL-12 release by engineered T cells expressing chimeric antigen receptors can effectively Muster an antigen-independent macrophage response on tumor cells that have shut down tumor antigen expression. *Cancer research* 71:5697-5706.

Clauss, J., M. Obenaus, C. Miskey, Z. Ivics, Z. Izsvak, W. Uckert, and M. Bunse. 2018. Efficient Non-Viral T-Cell Engineering by Sleeping Beauty Minicircles Diminishing DNA Toxicity and miRNAs Silencing the Endogenous T-Cell Receptors. *Human gene therapy* 29:569-584.

Crump, M., S.S. Neelapu, U. Farooq, E. Van Den Neste, J. Kuruvilla, J. Westin, B.K. Link, A. Hay, J.R. Cerhan, L. Zhu, S. Boussetta, L. Feng, M.J. Maurer, L. Navale, J. Wiezorek, W.Y. Go, and C. Gisselbrecht. 2017. Outcomes in refractory diffuse large B-cell lymphoma: results from the international SCHOLAR-1 study. *Blood* 130:1800-1808.

Dane, D.S., C.H. Cameron, and M. Briggs. 1970. Virus-like particles in serum of patients with Australia-antigen-associated hepatitis. *Lancet* 1:695-698.

Davila, M.L., I. Riviere, X. Wang, S. Bartido, J. Park, K. Curran, S.S. Chung, J. Stefanski, O. Borquez-Ojeda, M. Olszewska, J. Qu, T. Wasielewska, Q. He, M. Fink, H. Shinglot, M. Youssif, M. Satter, Y. Wang, J. Hosey, H. Quintanilla, E. Halton, Y. Bernal, D.C. Bouhassira, M.E. Arcila, M. Gonen, G.J. Roboz, P. Maslak, D. Douer, M.G. Frattini, S. Giralt, M. Sadelain, and R. Brentjens. 2014. Efficacy and toxicity management of 19-28z CAR T cell therapy in B cell acute lymphoblastic leukemia. *Science translational medicine* 6:224ra225.

Dion, S., M. Bourgine, O. Godon, F. Levillayer, and M.L. Michel. 2013. Adeno-associated virus-mediated gene transfer leads to persistent hepatitis B virus replication in mice expressing HLA-A2 and HLA-DR1 molecules. *Journal of virology* 87:5554-5563.

Dunsford, H.A., S. Sell, and F.V. Chisari. 1990. Hepatocarcinogenesis due to chronic liver cell injury in hepatitis B virus transgenic mice. *Cancer research* 50:3400-3407.

Engels, B., H. Cam, T. Schuler, S. Indraccolo, M. Gladow, C. Baum, T. Blankenstein, and W. Uckert. 2003. Retroviral vectors for high-level transgene expression in T lymphocytes. *Human gene therapy* 14:1155-1168.

Eyquem, J., J. Mansilla-Soto, T. Giavridis, S.J. van der Stegen, M. Hamieh, K.M. Cunanan, A. Odak, M. Gonen, and M. Sadelain. 2017. Targeting a CAR to the TRAC locus with CRISPR/Cas9 enhances tumour rejection. *Nature* 543:113-117.

Fioravanti, J., P. Di Lucia, D. Magini, F. Moalli, C. Boni, A.P. Benechet, V. Fumagalli, D. Inverso, A. Vecchi, A. Fiocchi, S. Wieland, R. Purcell, C. Ferrari, F.V. Chisari, L.G. Guidotti, and M. Iannacone. 2017. Effector CD8(+) T cell-derived interleukin-10 enhances acute liver immunopathology. *Journal of hepatology* 67:543-548.

Fisicaro, P., C. Valdatta, M. Massari, E. Loggi, E. Biasini, L. Sacchelli, M.C. Cavallo, E.M. Silini, P. Andreone, and G. Missale. 2010. Antiviral intrahepatic T-cell responses can be restored by blocking programmed death-1 pathway in chronic hepatitis B. *Gastroenterology* 138:682-693. e684.

Fisicaro, P., C. Valdatta, M. Massari, E. Loggi, L. Ravanetti, S. Urbani, T. Giuberti, A. Cavalli, C. Vandelli, and P. Andreone. 2012. Combined blockade of programmed death-1 and activation of CD137 increase responses of human liver T cells against HBV, but not HCV. *Gastroenterology* 143:1576-1585. e1574.

Furuichi, Y., H. Tokuyama, S. Ueha, M. Kurachi, F. Moriyasu, and K. Kakimi. 2005. Depletion of CD25+CD4+T cells (Tregs) enhances the HBV-specific CD8+ T cell response primed by DNA immunization. *World journal of gastroenterology : WJG* 11:3772-3777.

Ganem, D. 1991. Assembly of hepadnaviral virions and subviral particles. In Hepadnaviruses. Springer, 61-83.

Gao, H., K. Li, H. Tu, X. Pan, H. Jiang, B. Shi, J. Kong, H. Wang, S. Yang, J. Gu, and Z. Li. 2014. Development of T cells redirected to glypican-3 for the treatment of hepatocellular carcinoma. *Clinical cancer research : an official journal of the American Association for Cancer Research* 20:6418-6428.

Gehring, A.J., S.-A. Xue, Z.Z. Ho, D. Teoh, C. Ruedl, A. Chia, S. Koh, S.G. Lim, M.K. Maini, and H. Stauss. 2011. Engineering virus-specific T cells that target HBV infected hepatocytes and hepatocellular carcinoma cell lines. *Journal of hepatology* 55:103-110.

Giavridis, T., S.J.C. van der Stegen, J. Eyquem, M. Hamieh, A. Piersigilli, and M. Sadelain. 2018. CAR T cell-induced cytokine release syndrome is mediated by macrophages and abated by IL-1 blockade. *Nature medicine* 24:731-738.

Gish, R.G., B.D. Given, C.-L. Lai, S.A. Locarnini, J.Y. Lau, D.L. Lewis, and T. Schluep. 2015. Chronic hepatitis B: virology, natural history, current management and a glimpse at future opportunities. *Antiviral research* 121:47-58.

Gomes-Silva, D., M. Mukherjee, M. Srinivasan, G. Krenciute, O. Dakhova, Y. Zheng, J.M.S. Cabral, C.M. Rooney, J.S. Orange, M.K. Brenner, and M. Mamonkin. 2017. Tonic 4-1BB Costimulation in Chimeric Antigen Receptors Impedes T Cell Survival and Is Vector-Dependent. *Cell reports* 21:17-26.

Gross, G., T. Waks, and Z. Eshhar. 1989. Expression of immunoglobulin-T-cell receptor chimeric molecules as functional receptors with antibody-type specificity. *Proceedings of the National Academy of Sciences of the United States of America* 86:10024-10028.

Guedan, S., A.D. Posey, Jr., C. Shaw, A. Wing, T. Da, P.R. Patel, S.E. McGettigan, V. Casado-Medrano, O.U. Kawalekar, M. Uribe-Herranz, D. Song, J.J. Melenhorst, S.F. Lacey, J. Scholler, B. Keith, R.M. Young, and C.H. June. 2018. Enhancing CAR T cell persistence through ICOS and 4-1BB costimulation. *JCI insight* 3:

Guidotti, L.G., T. Ishikawa, M.V. Hobbs, B. Matzke, R. Schreiber, and F.V. Chisari. 1996. Intracellular inactivation of the hepatitis B virus by cytotoxic T lymphocytes. *Immunity* 4:25-36.

Guidotti, L.G., R. Rochford, J. Chung, M. Shapiro, R. Purcell, and F.V. Chisari. 1999. Viral clearance without destruction of infected cells during acute HBV infection. *Science* 284:825-829.

Gust, J., K.A. Hay, L.A. Hanafi, D. Li, D. Myerson, L.F. Gonzalez-Cuyar, C. Yeung, W.C. Liles, M. Wurfel, J.A. Lopez, J. Chen, D. Chung, S. Harju-Baker, T. Ozpolat, K.R. Fink, S.R. Riddell, D.G. Maloney, and C.J. Turtle. 2017. Endothelial Activation and Blood-Brain Barrier Disruption in Neurotoxicity after Adoptive Immunotherapy with CD19 CAR-T Cells. *Cancer discovery* 7:1404-1419.

Hale, M., T. Mesojednik, G.S. Romano Ibarra, J. Sahni, A. Bernard, K. Sommer, A.M. Scharenberg, D.J. Rawlings, and T.A. Wagner. 2017. Engineering HIV-Resistant, Anti-HIV Chimeric Antigen Receptor T Cells. *Molecular therapy : the journal of the American Society of Gene Therapy* 25:570-579.

Harris, D.T., M.V. Hager, S.N. Smith, Q. Cai, J.D. Stone, P. Kruger, M. Lever, O. Dushek, T.M. Schmitt, P.D. Greenberg, and D.M. Kranz. 2018. Comparison of T Cell Activities Mediated by Human TCRs and CARs That Use the Same Recognition Domains. *Journal of immunology (Baltimore, Md. : 1950)* 200:1088-1100.

Harris, D.T., and D.M. Kranz. 2016. Adoptive T Cell Therapies: A Comparison of T Cell Receptors and Chimeric Antigen Receptors. *Trends in pharmacological sciences* 37:220-230.

Hartmann, J., M. Schüßler-Lenz, A. Bondanza, and C.J. Buchholz. 2017. Clinical development of CAR T cells—challenges and opportunities in translating innovative treatment concepts. *EMBO molecular medicine* e201607485.

Hasreiter, J. 2018. Immunotherapeutic Approaches for the Treatment of Chronic HBV Infection and Hepatocellular Carcinoma. *Ph.D. Thesis*

Holzapfel, B.M., F. Wagner, L. Thibaudeau, J.P. Levesque, and D.W. Hutmacher. 2015. Concise review: humanized models of tumor immunology in the 21st century: convergence of cancer research and tissue engineering. *Stem Cells* 33:1696-1704.

Hombach, A.A., and H. Abken. 2011. Costimulation by chimeric antigen receptors revisited the T cell antitumor response benefits from combined CD28-OX40 signalling. *International journal of cancer. Journal international du cancer* 129:2935-2944.

Hombach, A.A., M. Chmielewski, G. Rappl, and H. Abken. 2013. Adoptive immunotherapy with redirected T cells produces CCR7- cells that are trapped in the periphery and benefit from combined CD28-OX40 costimulation. *Human gene therapy* 24:259-269.

Hombach, A.A., J. Heiders, M. Foppe, M. Chmielewski, and H. Abken. 2012. OX40 costimulation by a chimeric antigen receptor abrogates CD28 and IL-2 induced IL-10 secretion by redirected CD4(+) T cells. *Oncoimmunology* 1:458-466.

Hu, B., J. Ren, Y. Luo, B. Keith, R.M. Young, J. Scholler, Y. Zhao, and C.H. June. 2017. Augmentation of Antitumor Immunity by Human and Mouse CAR T Cells Secreting IL-18. *Cell reports* 20:3025-3033.

Huang, J., M. Brameshuber, X. Zeng, J. Xie, Q.J. Li, Y.H. Chien, S. Valitutti, and M.M. Davis. 2013a. A single peptide-major histocompatibility complex ligand triggers digital cytokine secretion in CD4(+) T cells. *Immunity* 39:846-857.

Huang, L.R., D. Wohlleber, F. Reisinger, C.N. Jenne, R.L. Cheng, Z. Abdullah, F.A. Schildberg, M. Odenthal, H.P. Dienes, N. van Rooijen, E. Schmitt, N. Garbi, M. Croft, C. Kurts, P. Kubes, U. Protzer, M. Heikenwalder, and P.A. Knolle. 2013b. Intrahepatic myeloid-cell aggregates enable local proliferation of CD8(+) T cells and successful immunotherapy against chronic viral liver infection. *Nature immunology* 14:574-583.

Hudecek, M., D. Sommermeyer, P.L. Kosasih, A. Silva-Benedict, L. Liu, C. Rader, M.C. Jensen, and S.R. Riddell. 2015. The nonsignaling extracellular spacer domain of chimeric antigen receptors is decisive for in vivo antitumor activity. *Cancer immunology research* 3:125-135.

Humphreys, I.R., A. Loewendorf, C. de Trez, K. Schneider, C.A. Benedict, M.W. Munks, C.F. Ware, and M. Croft. 2007. OX40 costimulation promotes persistence of cytomegalovirus-specific CD8 T Cells: A CD4-dependent mechanism. *Journal of immunology (Baltimore, Md. : 1950)* 179:2195-2202.

Ilan, Y., A. Nagler, R. Adler, E. Naparstek, R. Or, S. Slavin, C. Brautba, and D. Shouva. 1993. Adoptive transfer of immunity to hepatitis B virus after T cell–depleted allogeneic bone marrow transplantation. *Hepatology* 18:246-252.

Imai, C., K. Mihara, M. Andreansky, I.C. Nicholson, C.H. Pui, T.L. Geiger, and D. Campana. 2004. Chimeric receptors with 4-1BB signaling capacity provoke potent cytotoxicity against acute lymphoblastic leukemia. *Leukemia* 18:676-684.

Jensen, M.C., and S.R. Riddell. 2014. Design and implementation of adoptive therapy with chimeric antigen receptor-modified T cells. *Immunological reviews* 257:127-144.

Jiang, B., K. Himmelsbach, H. Ren, K. Boller, and E. Hildt. 2015. Subviral Hepatitis B Virus Filaments, like Infectious Viral Particles, Are Released via Multivesicular Bodies. *Journal of virology* 90:3330-3341.

John, L.B., C. Devaud, C.P. Duong, C.S. Yong, P.A. Beavis, N.M. Haynes, M.T. Chow, M.J. Smyth, M.H. Kershaw, and P.K. Darcy. 2013a. Anti-PD-1 antibody therapy potently enhances the eradication of established tumors by gene-modified T cells. *Clinical cancer research : an official journal of the American Association for Cancer Research* 19:5636-5646.

John, L.B., M.H. Kershaw, and P.K. Darcy. 2013b. Blockade of PD-1 immunosuppression boosts CAR T-cell therapy. *Oncoimmunology* 2:e26286.

Jonnalagadda, M., A. Mardiros, R. Urak, X. Wang, L.J. Hoffman, A. Bernanke, W.C. Chang, W. Bretzlaff, R. Starr, S. Priceman, J.R. Ostberg, S.J. Forman, and C.E. Brown. 2015. Chimeric antigen receptors with mutated IgG4 Fc spacer avoid fc receptor binding and improve T cell persistence and antitumor efficacy. *Molecular therapy : the journal of the American Society of Gene Therapy* 23:757-768.

Jung, J.K., P. Arora, J.S. Pagano, and K.L. Jang. 2007. Expression of DNA methyltransferase 1 is activated by hepatitis B virus X protein via a regulatory circuit involving the p16INK4a-cyclin D1-CDK 4/6-pRb-E2F1 pathway. *Cancer research* 67:5771-5778.

Kagoya, Y., S. Tanaka, T. Guo, M. Anczurowski, C.H. Wang, K. Saso, M.O. Butler, M.D. Minden, and N. Hirano. 2018. A novel chimeric antigen receptor containing a JAK-STAT signaling domain mediates superior antitumor effects. *Nature medicine* 24:352-359.

Kah, J., S. Koh, T. Volz, E. Ceccarello, L. Allweiss, M. Lutgehetmann, A. Bertoletti, and M. Dandri. 2017. Lymphocytes transiently expressing virus-specific T cell receptors reduce hepatitis B virus infection. *The Journal of clinical investigation* 127:3177-3188.

Kamiya, T., D. Wong, Y.T. Png, and D. Campana. 2018. A novel method to generate T-cell receptor-deficient chimeric antigen receptor T cells. *Blood advances* 2:517-528.

Karlsson, H., E. Svensson, C. Gigg, M. Jarvius, U. Olsson-Stromberg, B. Savoldo, G. Dotti, and A. Loskog. 2015. Evaluation of Intracellular Signaling Downstream Chimeric Antigen Receptors. *PloS one* 10:e0144787.

Kawalekar, O.U., R.S. O'Connor, J.A. Fraietta, L. Guo, S.E. McGettigan, A.D. Posey, Jr., P.R. Patel, S. Guedan, J. Scholler, B. Keith, N.W. Snyder, I.A. Blair, M.C. Milone, and C.H. June. 2016. Distinct Signaling of Coreceptors Regulates Specific Metabolism Pathways and Impacts Memory Development in CAR T Cells. *Immunity* 44:380-390.

Kershaw, M.H., J.A. Westwood, L.L. Parker, G. Wang, Z. Eshhar, S.A. Mavroukakis, D.E. White, J.R. Wunderlich, S. Canevari, and L. Rogers-Freezer. 2006. A phase I study on adoptive immunotherapy using gene-modified T cells for ovarian cancer. *Clinical Cancer Research* 12:6106-6115.

Khalil, D.N., E.L. Smith, R.J. Brentjens, and J.D. Wolchok. 2016. The future of cancer treatment: immunomodulation, CARs and combination immunotherapy. *Nature reviews Clinical oncology* 13:273.

Knolle, P.A., and R. Thimme. 2014. Hepatic immune regulation and its involvement in viral hepatitis infection. *Gastroenterology* 146:1193-1207.

Ko, C., T. Michler, and U. Protzer. 2017. Novel viral and host targets to cure hepatitis B. *Curr Opin Virol* 24:38-45.

Kochenderfer, J.N., S.A. Feldman, Y. Zhao, H. Xu, M.A. Black, R.A. Morgan, W.H. Wilson, and S.A. Rosenberg. 2009. Construction and pre-clinical evaluation of an anti-CD19 chimeric antigen receptor. *Journal of immunotherapy (Hagerstown, Md.: 1997)* 32:689.

Kowolik, C.M., M.S. Topp, S. Gonzalez, T. Pfeiffer, S. Olivares, N. Gonzalez, D.D. Smith, S.J. Forman, M.C. Jensen, and L.J. Cooper. 2006. CD28 costimulation provided through a CD19-specific chimeric antigen receptor enhances in vivo persistence and antitumor efficacy of adoptively transferred T cells. *Cancer research* 66:10995-11004.

Kramvis, A. 2014. Genotypes and genetic variability of hepatitis B virus. *Intervirology* 57:141-150.

Krebs, K., N. Bottinger, L.R. Huang, M. Chmielewski, S. Arzberger, G. Gasteiger, C. Jager, E. Schmitt, F. Bohne, M. Aichler, W. Uckert, H. Abken, M. Heikenwalder, P. Knolle, and U. Protzer. 2013. T cells expressing a chimeric antigen receptor that binds hepatitis B virus envelope proteins control virus replication in mice. *Gastroenterology* 145:456-465.

Kudo, M., R.S. Finn, S. Qin, K.H. Han, K. Ikeda, F. Piscaglia, A. Baron, J.W. Park, G. Han, J. Jassem, J.F. Blanc, A. Vogel, D. Komov, T.R.J. Evans, C. Lopez, C. Dutcus, M. Guo, K. Saito, S. Kraljevic, T. Tamai, M. Ren, and A.L. Cheng. 2018. Lenvatinib versus sorafenib in first-line treatment of patients with unresectable hepatocellular carcinoma: a randomised phase 3 non-inferiority trial. *Lancet* 391:1163-1173.

Kumar, M., T. Singh, and S. Sinha. 2012. Chronic hepatitis B virus infection and pregnancy. *Journal of clinical and experimental hepatology* 2:366-381.

Kunkele, A., A.J. Johnson, L.S. Rolczynski, C.A. Chang, V. Hoglund, K.S. Kelly-Spratt, and M.C. Jensen. 2015. Functional Tuning of CARs Reveals Signaling Threshold above Which CD8+ CTL Antitumor Potency Is Attenuated due to Cell Fas-FasL-Dependent AICD. *Cancer immunology research* 3:368-379.

Kunkele, A., A. Taraseviciute, L.S. Finn, A.J. Johnson, C. Berger, O. Finney, C.A. Chang, L.S. Rolczynski, C. Brown, S. Mgebroff, M. Berger, J.R. Park, and M.C. Jensen. 2017. Preclinical Assessment of CD171-Directed CAR T-cell Adoptive Therapy for Childhood Neuroblastoma: CE7 Epitope Target Safety and Product Manufacturing Feasibility. *Clinical cancer research : an official journal of the American Association for Cancer Research* 23:466-477.

Kürschner, T. 2000. Konstruktion und Screening von Antikörperbibliotheken gegen Oberflächenantigene. *Ph.D. Thesis*

Lamers, C.H., S. Sleijfer, A.G. Vulto, W.H. Kruit, M. Kliffen, R. Debets, J.W. Gratama, G. Stoter, and E. Oosterwijk. 2006. Treatment of metastatic renal cell carcinoma with autologous T-lymphocytes genetically retargeted against carbonic anhydrase IX: first clinical

experience. *Journal of clinical oncology : official journal of the American Society of Clinical Oncology* 24:e20-22.

Lamers, C.H., R. Willemsen, P. van Elzakker, S. van Steenbergen-Langeveld, M. Broertjes, J. Oosterwijk-Wakka, E. Oosterwijk, S. Sleijfer, R. Debets, and J.W. Gratama. 2011. Immune responses to transgene and retroviral vector in patients treated with ex vivo–engineered T cells. *Blood* 117:72-82.

Lamichhane, P., L. Karyampudi, B. Shreeder, J. Krempski, D. Bahr, J. Daum, K.R. Kalli, E.L. Goode, M.S. Block, M.J. Cannon, and K.L. Knutson. 2017. IL10 Release upon PD-1 Blockade Sustains Immunosuppression in Ovarian Cancer. *Cancer research* 77:6667-6678.

Lau, G.K., A.S. Lok, R.H. Liang, C.L. Lai, E.K. Chiu, Y.L. Lau, and S.K. Lam. 1997. Clearance of hepatitis B surface antigen after bone marrow transplantation: role of adoptive immunity transfer. *Hepatology* 25:1497-1501.

Le, R.Q., L. Li, W. Yuan, S.S. Shord, L. Nie, B.A. Habtemariam, D. Przepiorka, A.T. Farrell, and R. Pazdur. 2018. FDA Approval Summary: Tocilizumab for Treatment of Chimeric Antigen Receptor T Cell-Induced Severe or Life-Threatening Cytokine Release Syndrome. *The oncologist* 23:943-947.

Lee, H.W., S.J. Park, B.K. Choi, H.H. Kim, K.O. Nam, and B.S. Kwon. 2002. 4-1BB promotes the survival of CD8+ T lymphocytes by increasing expression of Bcl-xL and Bfl-1. *Journal of immunology (Baltimore, Md. : 1950)* 169:4882-4888.

Leibman, R.S., M.W. Richardson, C.T. Ellebrecht, C.R. Maldini, J.A. Glover, A.J. Secreto, I. Kulikovskaya, S.F. Lacey, S.R. Akkina, Y. Yi, F. Shaheen, J. Wang, K.A. Dufendach, M.C. Holmes, R.G. Collman, A.S. Payne, and J.L. Riley. 2017. Supraphysiologic control over HIV-1 replication mediated by CD8 T cells expressing a re-engineered CD4-based chimeric antigen receptor. *PLoS pathogens* 13:e1006613.

Levine, B.L., J. Miskin, K. Wonnacott, and C. Keir. 2017. Global Manufacturing of CAR T Cell Therapy. *Molecular therapy. Methods & clinical development* 4:92-101.

Li, S., N. Siriwon, X. Zhang, S. Yang, T. Jin, F. He, Y.J. Kim, J. Mac, Z. Lu, S. Wang, X. Han, and P. Wang. 2017. Enhanced Cancer Immunotherapy by Chimeric Antigen Receptor-Modified T Cells Engineered to Secrete Checkpoint Inhibitors. *Clinical cancer research : an official journal of the American Association for Cancer Research* 23:6982-6992.

Li, S., J. Zhang, M. Wang, G. Fu, Y. Li, L. Pei, Z. Xiong, D. Qin, R. Zhang, X. Tian, Z. Wei, R. Chen, X. Chen, J. Wan, J. Chen, X. Wei, Y. Xu, P. Zhang, P. Wang, X. Peng, S. Yang, J. Shen, Z. Yang, J. Chen, and C. Qian. 2018. Treatment of acute lymphoblastic leukaemia with the second generation of CD19 CAR-T containing either CD28 or 4-1BB. *British journal of haematology* 181:360-371.

Lin, C.L., H.C. Yang, and J.H. Kao. 2016. Hepatitis B virus: new therapeutic perspectives. *Liver international : official journal of the International Association for the Study of the Liver* 36 Suppl 1:85-92.

Linnemann, C., R. Mezzadra, and T.N. Schumacher. 2014. TCR repertoires of intratumoral T-cell subsets. *Immunological reviews* 257:72-82.

Liu, J., E. Zhang, Z. Ma, W. Wu, A. Kosinska, X. Zhang, I. Moller, P. Seiz, D. Glebe, B. Wang, D. Yang, M. Lu, and M. Roggendorf. 2014. Enhancing virus-specific immunity in vivo by combining therapeutic vaccination and PD-L1 blockade in chronic hepadnaviral infection. *PLoS pathogens* 10:e1003856.

Llovet, J.M., S. Ricci, V. Mazzaferro, P. Hilgard, E. Gane, J.F. Blanc, A.C. de Oliveira, A. Santoro, J.L. Raoul, A. Forner, M. Schwartz, C. Porta, S. Zeuzem, L. Bolondi, T.F. Greten, P.R. Galle, J.F. Seitz, I. Borbath, D. Haussinger, T. Giannaris, M. Shan, M. Moscovici, D. Voliotis, J. Bruix, and S.I.S. Group. 2008. Sorafenib in advanced hepatocellular carcinoma. *The New England journal of medicine* 359:378-390.

Lok, A.S., R.H. Liang, E.K. Chiu, K.L. Wong, T.K. Chan, and D. Todd. 1991. Reactivation of hepatitis B virus replication in patients receiving cytotoxic therapy. Report of a prospective study. *Gastroenterology* 100:182-188.

Long, A.H., W.M. Haso, J.F. Shern, K.M. Wanhainen, M. Murgai, M. Ingaramo, J.P. Smith, A.J. Walker, M.E. Kohler, V.R. Venkateshwara, R.N. Kaplan, G.H. Patterson, T.J. Fry, R.J.

Orentas, and C.L. Mackall. 2015. 4-1BB costimulation ameliorates T cell exhaustion induced by tonic signaling of chimeric antigen receptors. *Nature medicine* 21:581-590.

Lopes, A.R., P. Kellam, A. Das, C. Dunn, A. Kwan, J. Turner, D. Peppa, R.J. Gilson, A. Gehring, A. Bertoletti, and M.K. Maini. 2008. Bim-mediated deletion of antigen-specific CD8 T cells in patients unable to control HBV infection. *The Journal of clinical investigation* 118:1835-1845.

Louis, C.U., B. Savoldo, G. Dotti, M. Pule, E. Yvon, G.D. Myers, C. Rossig, H.V. Russell, O. Diouf, and E. Liu. 2011. Antitumor activity and long-term fate of chimeric antigen receptor–positive T cells in patients with neuroblastoma. *Blood* 118:6050-6056.

Lucifora, J., Y. Xia, F. Reisinger, K. Zhang, D. Stadler, X. Cheng, M.F. Sprinzl, H. Koppensteiner, Z. Makowska, T. Volz, C. Remouchamps, W.M. Chou, W.E. Thasler, N. Huser, D. Durantel, T.J. Liang, C. Munk, M.H. Heim, J.L. Browning, E. Dejardin, M. Dandri, M. Schindler, M. Heikenwalder, and U. Protzer. 2014. Specific and nonhepatotoxic degradation of nuclear hepatitis B virus cccDNA. *Science* 343:1221-1228.

Mackall, C.L., and D.B. Miklos. 2017. CNS Endothelial Cell Activation Emerges as a Driver of CAR T Cell-Associated Neurotoxicity. *Cancer discovery* 7:1371-1373.

MacLeod, D.T., J. Antony, A.J. Martin, R.J. Moser, A. Hekele, K.J. Wetzel, A.E. Brown, M.A. Triggiano, J.A. Hux, C.D. Pham, V.V. Bartsevich, C.A. Turner, J. Lape, S. Kirkland, C.W. Beard, J. Smith, M.L. Hirsch, M.G. Nicholson, D. Jantz, and B. McCreedy. 2017. Integration of a CD19 CAR into the TCR Alpha Chain Locus Streamlines Production of Allogeneic Gene-Edited CAR T Cells. *Molecular therapy : the journal of the American Society of Gene Therapy* 25:949-961.

Maini, M.K., C. Boni, C.K. Lee, J.R. Larrubia, S. Reignat, G.S. Ogg, A.S. King, J. Herberg, R. Gilson, A. Alisa, R. Williams, D. Vergani, N.V. Naoumov, C. Ferrari, and A. Bertoletti. 2000. The role of virus-specific CD8(+) cells in liver damage and viral control during persistent hepatitis B virus infection. *The Journal of experimental medicine* 191:1269-1280.

Maini, M.K., C. Boni, G.S. Ogg, A.S. King, S. Reignat, C.K. Lee, J.R. Larrubia, G.J. Webster, A.J. McMichael, C. Ferrari, R. Williams, D. Vergani, and A. Bertoletti. 1999. Direct ex vivo analysis of hepatitis B virus-specific CD8(+) T cells associated with the control of infection. *Gastroenterology* 117:1386-1396.

Markley, J.C., and M. Sadelain. 2010. IL-7 and IL-21 are superior to IL-2 and IL-15 in promoting human T cell–mediated rejection of systemic lymphoma in immunodeficient mice. *Blood* 115:3508-3519.

Martyniszyn, A., A.C. Krahl, M.C. Andre, A.A. Hombach, and H. Abken. 2017. CD20-CD19 Bispecific CAR T Cells for the Treatment of B-Cell Malignancies. *Human gene therapy* 28:1147-1157.

Maude, S.L., N. Frey, P.A. Shaw, R. Aplenc, D.M. Barrett, N.J. Bunin, A. Chew, V.E. Gonzalez, Z. Zheng, S.F. Lacey, Y.D. Mahnke, J.J. Melenhorst, S.R. Rheingold, A. Shen, D.T. Teachey, B.L. Levine, C.H. June, D.L. Porter, and S.A. Grupp. 2014. Chimeric antigen receptor T cells for sustained remissions in leukemia. *The New England journal of medicine* 371:1507-1517.

Melero, I., W.W. Shuford, S.A. Newby, A. Aruffo, J.A. Ledbetter, K.E. Hellstrom, R.S. Mittler, and L. Chen. 1997. Monoclonal antibodies against the 4-1BB T-cell activation molecule eradicate established tumors. *Nature medicine* 3:682-685.

Meng, F., S. Zhen, and B. Song. 2017. HBV-specific CD4+ cytotoxic T cells in hepatocellular carcinoma are less cytolytic toward tumor cells and suppress CD8+ T cell-mediated antitumor immunity. *APMIS* 125:743-751.

Mestas, J., and C.C. Hughes. 2004. Of mice and not men: differences between mouse and human immunology. *The Journal of Immunology* 172:2731-2738.

Meyer-Berg, H. 2016. Inducible Interleukin-12 Expression and its Influence on the Activity of S-CAR Redirected T Cells. *Master's Thesis*

Miller, A.D., J.V. Garcia, N. von Suhr, C.M. Lynch, C. Wilson, and M.V. Eiden. 1991. Construction and properties of retrovirus packaging cells based on gibbon ape leukemia virus. *Journal of virology* 65:2220-2224.

Milone, M.C., J.D. Fish, C. Carpenito, R.G. Carroll, G.K. Binder, D. Teachey, M. Samanta, M. Lakhal, B. Gloss, G. Danet-Desnoyers, D. Campana, J.L. Riley, S.A. Grupp, and C.H. June. 2009. Chimeric receptors containing CD137 signal transduction domains mediate enhanced survival of T cells and increased antileukemic efficacy in vivo. *Molecular therapy : the journal of the American Society of Gene Therapy* 17:1453-1464.

Miyazoe, S., K. Hamasaki, K. Nakata, Y. Kajiya, K. Kitajima, K. Nakao, M. Daikoku, H. Yatsuhashi, M. Koga, M. Yano, and K. Eguchi. 2002. Influence of interleukin-10 gene promoter polymorphisms on disease progression in patients chronically infected with hepatitis B virus. *The American journal of gastroenterology* 97:2086-2092.

Monjezi, R., C. Miskey, T. Gogishvili, M. Schleef, M. Schmeer, H. Einsele, Z. Ivics, and M. Hudecek. 2017. Enhanced CAR T-cell engineering using non-viral Sleeping Beauty transposition from minicircle vectors. *Leukemia* 31:186-194.

Morgan, R.A., J.C. Yang, M. Kitano, M.E. Dudley, C.M. Laurencot, and S.A. Rosenberg. 2010. Case report of a serious adverse event following the administration of T cells transduced with a chimeric antigen receptor recognizing ERBB2. *Molecular therapy : the journal of the American Society of Gene Therapy* 18:843-851.

Moudi, B., Z. Heidari, H. Mahmoudzadeh-Sagheb, M. Hashemi, M. Metanat, S. Khosravi, and P. Farrokh. 2016. Association Between IL-10 Gene Promoter Polymorphisms (-592 A/C, -819 T/C, -1082 A/G) and Susceptibility to HBV Infection in an Iranian Population. *Hepatitis monthly* 16:e32427.

Mueller, D.L. 2010. Mechanisms maintaining peripheral tolerance. *Nature immunology* 11:21-27.

Mullard, A. 2017. Second anticancer CAR T therapy receives FDA approval. *Nature reviews. Drug discovery* 16:818.

Murphy, K., and C. Weaver. 2016. Janeway's immunobiology. Garland Science,

Nakabayashi, H., K. Taketa, K. Miyano, T. Yamane, and J. Sato. 1982. Growth of human hepatoma cell lines with differentiated functions in chemically defined medium. *Cancer research* 42:3858-3863.

Nakamura, Y., T. Motokura, A. Fujita, T. Yamashita, and E. Ogata. 1996. Severe hepatitis related to chemotherapy in hepatitis B virus carriers with hematologic malignancies. Survey in Japan, 1987-1991. *Cancer* 78:2210-2215.

Neelapu, S.S., F.L. Locke, N.L. Bartlett, L.J. Lekakis, D.B. Miklos, C.A. Jacobson, I. Braunschweig, O.O. Oluwole, T. Siddiqi, Y. Lin, J.M. Timmerman, P.J. Stiff, J.W. Friedberg, I.W. Flinn, A. Goy, B.T. Hill, M.R. Smith, A. Deol, U. Farooq, P. McSweeney, J. Munoz, I. Avivi, J.E. Castro, J.R. Westin, J.C. Chavez, A. Ghobadi, K.V. Komanduri, R. Levy, E.D. Jacobsen, T.E. Witzig, P. Reagan, A. Bot, J. Rossi, L. Navale, Y. Jiang, J. Aycock, M. Elias, D. Chang, J. Wiezorek, and W.Y. Go. 2017. Axicabtagene Ciloleucel CAR T-Cell Therapy in Refractory Large B-Cell Lymphoma. *The New England journal of medicine* 377:2531-2544.

Nellan, A., C. Rota, R. Majzner, C.M. Lester-McCully, A.M. Griesinger, J.M. Mulcahy Levy, N.K. Foreman, K.E. Warren, and D.W. Lee. 2018. Durable regression of Medulloblastoma after regional and intravenous delivery of anti-HER2 chimeric antigen receptor T cells. *Journal for immunotherapy of cancer* 6:30.

Nemazee, D. 2017. Mechanisms of central tolerance for B cells. *Nature reviews. Immunology* 17:281-294.

Nishimura, H., N. Minato, T. Nakano, and T. Honjo. 1998. Immunological studies on PD-1 deficient mice: implication of PD-1 as a negative regulator for B cell responses. *International immunology* 10:1563-1572.

Norelli, M., B. Camisa, G. Barbiera, L. Falcone, A. Purevdorj, M. Genua, F. Sanvito, M. Ponzoni, C. Doglioni, P. Cristofori, C. Traversari, C. Bordignon, F. Ciceri, R. Ostuni, C. Bonini, M. Casucci, and A. Bondanza. 2018. Monocyte-derived IL-1 and IL-6 are differentially required for cytokine-release syndrome and neurotoxicity due to CAR T cells. *Nature medicine* 24:739-748.

Odorizzi, P.M., K.E. Pauken, M.A. Paley, A. Sharpe, and E.J. Wherry. 2015. Genetic absence of PD-1 promotes accumulation of terminally differentiated exhausted CD8+ T cells. *The Journal of experimental medicine* 212:1125-1137.

Ono, A., F. Suzuki, Y. Kawamura, H. Sezaki, T. Hosaka, N. Akuta, M. Kobayashi, Y. Suzuki, S. Saitou, Y. Arase, K. Ikeda, M. Kobayashi, S. Watahiki, R. Mineta, and H. Kumada. 2012. Long-term continuous entecavir therapy in nucleos(t)ide-naive chronic hepatitis B patients. *Journal of hepatology* 57:508-514.

Paszkiewicz, P.J., S.P. Frassle, S. Srivastava, D. Sommermeyer, M. Hudecek, I. Drexler, M. Sadelain, L. Liu, M.C. Jensen, S.R. Riddell, and D.H. Busch. 2016. Targeted antibody-mediated depletion of murine CD19 CAR T cells permanently reverses B cell aplasia. *The Journal of clinical investigation* 126:4262-4272.

Peeridogaheh, H., Z. Meshkat, S. Habibzadeh, M. Arzanlou, J.M. Shahi, S. Rostami, S. Gerayli, and R. Teimourpour. 2018. Current concepts on immunopathogenesis of hepatitis B virus infection. *Virus research* 245:29-43.

Perceau, G., N. Diris, O. Estines, C. Derancourt, S. Levy, and P. Bernard. 2006. Late lethal hepatitis B virus reactivation after rituximab treatment of low-grade cutaneous B-cell lymphoma. *Br J Dermatol* 155:1053-1056.

Perrillo, R.P., R. Gish, and Y.T. Falck-Ytter. 2015. American Gastroenterological Association Institute technical review on prevention and treatment of hepatitis B virus reactivation during immunosuppressive drug therapy. *Gastroenterology* 148:221-244 e223.

Pollok, K.E., Y.J. Kim, Z. Zhou, J. Hurtado, K.K. Kim, R.T. Pickard, and B.S. Kwon. 1993. Inducible T cell antigen 4-1BB. Analysis of expression and function. *Journal of immunology (Baltimore, Md. : 1950)* 150:771-781.

Posselt, A.M., C.F. Barker, J.E. Tomaszewski, J.F. Markmann, M.A. Choti, and A. Naji. 1990. Induction of donor-specific unresponsiveness by intrathymic islet transplantation. *Science* 249:1293-1295.

Proietto, A.I., M.H. Lahoud, and L. Wu. 2008. Distinct functional capacities of mouse thymic and splenic dendritic cell populations. *Immunology and cell biology* 86:700-708.

Qasim, W., M. Brunetto, A.J. Gehring, S.A. Xue, A. Schurich, A. Khakpoor, H. Zhan, P. Ciccorossi, K. Gilmour, D. Cavallone, F. Moriconi, F. Farzhenah, A. Mazzoni, L. Chan, E. Morris, A. Thrasher, M.K. Maini, F. Bonino, H. Stauss, and A. Bertoletti. 2015. Immunotherapy of HCC metastases with autologous T cell receptor redirected T cells, targeting HBsAg in a liver transplant patient. *Journal of hepatology* 62:486-491.

Richman, S.A., S. Nunez-Cruz, B. Moghimi, L.Z. Li, Z.T. Gershenson, Z. Mourelatos, D.M. Barrett, S.A. Grupp, and M.C. Milone. 2018. High-Affinity GD2-Specific CAR T Cells Induce Fatal Encephalitis in a Preclinical Neuroblastoma Model. *Cancer immunology research* 6:36-46.

Ringehan, M., J.A. McKeating, and U. Protzer. 2017. Viral hepatitis and liver cancer. *Phil. Trans. R. Soc. B* 372:20160274.

Rivino, L., N. Le Bert, U.S. Gill, K. Kunasegaran, Y. Cheng, D.Z. Tan, E. Becht, N.K. Hansi, G.R. Foster, T.H. Su, T.C. Tseng, S.G. Lim, J.H. Kao, E.W. Newell, P.T. Kennedy, and A. Bertoletti. 2018. Hepatitis B virus-specific T cells associate with viral control upon nucleos(t)ide-analogue therapy discontinuation. *The Journal of clinical investigation* 128:668-681.

Roybal, K.T., L.J. Rupp, L. Morsut, W.J. Walker, K.A. McNally, J.S. Park, and W.A. Lim. 2016. Precision Tumor Recognition by T Cells With Combinatorial Antigen-Sensing Circuits. *Cell* 164:770-779.

Ruby, C.E., W.L. Redmond, D. Haley, and A.D. Weinberg. 2007. Anti-OX40 stimulation in vivo enhances CD8+ memory T cell survival and significantly increases recall responses. *European journal of immunology* 37:157-166.

Safaie, P., M. Poongkunran, P.P. Kuang, A. Javaid, C. Jacobs, R. Pohlmann, I. Nasser, and D.T. Lau. 2016. Intrahepatic distribution of hepatitis B virus antigens in patients with and without hepatocellular carcinoma. *World journal of gastroenterology : WJG* 22:3404-3411.

San Jose, E., A. Borroto, F. Niedergang, A. Alcover, and B. Alarcon. 2000. Triggering the TCR complex causes the downregulation of nonengaged receptors by a signal transduction-dependent mechanism. *Immunity* 12:161-170.

Sartorius, K., B. Sartorius, C. Aldous, P.S. Govender, and T.E. Madiba. 2015. Global and country underestimation of hepatocellular carcinoma (HCC) in 2012 and its implications. *Cancer Epidemiol* 39:284-290.

Sautto, G.A., K. Wisskirchen, N. Clementi, M. Castelli, R.A. Diotti, J. Graf, M. Clementi, R. Burioni, U. Protzer, and N. Mancini. 2016. Chimeric antigen receptor (CAR)-engineered T cells redirected against hepatitis C virus (HCV) E2 glycoprotein. *Gut* 65:512-523.

Schurich, A., P. Khanna, A.R. Lopes, K.J. Han, D. Peppa, L. Micco, G. Nebbia, P.T. Kennedy, A.M. Geretti, G. Dusheiko, and M.K. Maini. 2011. Role of the coinhibitory receptor cytotoxic T lymphocyte antigen-4 on apoptosis-Prone CD8 T cells in persistent hepatitis B virus infection. *Hepatology* 53:1494-1503.

Schuster, S.J., J. Svoboda, E.A. Chong, S.D. Nasta, A.R. Mato, O. Anak, J.L. Brogdon, I. Pruteanu-Malinici, V. Bhoj, D. Landsburg, M. Wasik, B.L. Levine, S.F. Lacey, J.J. Melenhorst, D.L. Porter, and C.H. June. 2017. Chimeric Antigen Receptor T Cells in Refractory B-Cell Lymphomas. *The New England journal of medicine* 377:2545-2554.

Seeger, C., and W.S. Mason. 2015. Molecular biology of hepatitis B virus infection. *Virology* 479-480:672-686.

Seok, J., H.S. Warren, A.G. Cuenca, M.N. Mindrinos, H.V. Baker, W. Xu, D.R. Richards, G.P. McDonald-Smith, H. Gao, L. Hennessy, C.C. Finnerty, C.M. Lopez, S. Honari, E.E. Moore, J.P. Minei, J. Cuschieri, P.E. Bankey, J.L. Johnson, J. Sperry, A.B. Nathens, T.R. Billiar, M.A. West, M.G. Jeschke, M.B. Klein, R.L. Gamelli, N.S. Gibran, B.H. Brownstein, C. Miller-Graziano, S.E. Calvano, P.H. Mason, J.P. Cobb, L.G. Rahme, S.F. Lowry, R.V. Maier, L.L. Moldawer, D.N. Herndon, R.W. Davis, W. Xiao, R.G. Tompkins, Inflammation, and L.S.C.R.P. Host Response to Injury. 2013. Genomic responses in mouse models poorly mimic human inflammatory diseases. *Proceedings of the National Academy of Sciences of the United States of America* 110:3507-3512.

Serganova, I., E. Moroz, I. Cohen, M. Moroz, M. Mane, J. Zurita, L. Shenker, V. Ponomarev, and R. Blasberg. 2017. Enhancement of PSMA-Directed CAR Adoptive Immunotherapy by PD-1/PD-L1 Blockade. *Molecular therapy oncolytics* 4:41-54.

Sharma, S., R. Khosla, P. David, A. Rastogi, A. Vyas, D. Singh, A. Bhardwaj, A. Sahney, R. Maiwall, S.K. Sarin, and N. Trehanpati. 2015. CD4+CD25+CD127(low) Regulatory T Cells Play Predominant Anti-Tumor Suppressive Role in Hepatitis B Virus-Associated Hepatocellular Carcinoma. *Frontiers in immunology* 6:49.

Shen, C.J., Y.X. Yang, E.Q. Han, N. Cao, Y.F. Wang, Y. Wang, Y.Y. Zhao, L.M. Zhao, J. Cui, P. Gupta, A.J. Wong, and S.Y. Han. 2013. Chimeric antigen receptor containing ICOS signaling domain mediates specific and efficient antitumor effect of T cells against EGFRvIII expressing glioma. *Journal of hematology & oncology* 6:33.

Shi, Y., Q. Song, D. Hu, X. Zhuang, and S. Yu. 2015. Tumor-infiltrating lymphocyte activity is enhanced in tumors with low IL-10 production in HBV-induced hepatocellular carcinoma. *Biochemical and biophysical research communications* 461:109-114.

Shultz, L.D., M.A. Brehm, J.V. Garcia-Martinez, and D.L. Greiner. 2012. Humanized mice for immune system investigation: progress, promise and challenges. *Nature reviews. Immunology* 12:786-798.

Siegler, E.L., and P. Wang. 2018. Preclinical Models in Chimeric Antigen Receptor-Engineered T-Cell Therapy. *Human gene therapy* 29:534-546.

Sommermeyer, D., T. Hill, S.M. Shamah, A.I. Salter, Y. Chen, K.M. Mohler, and S.R. Riddell. 2017. Fully human CD19-specific chimeric antigen receptors for T-cell therapy. *Leukemia* 31:2191-2199.

Song, D.G., Q. Ye, C. Carpenito, M. Poussin, L.P. Wang, C. Ji, M. Figini, C.H. June, G. Coukos, and D.J. Powell, Jr. 2011. In vivo persistence, tumor localization, and antitumor activity of CAR-engineered T cells is enhanced by costimulatory signaling through CD137 (4-1BB). *Cancer research* 71:4617-4627.

Song, D.G., Q. Ye, M. Poussin, G.M. Harms, M. Figini, and D.J. Powell, Jr. 2012. CD27 costimulation augments the survival and antitumor activity of redirected human T cells in vivo. *Blood* 119:696-706.

Spear, P., A. Barber, A. Rynda-Apple, and C.L. Sentman. 2012. Chimeric antigen receptor T cells shape myeloid cell function within the tumor microenvironment through IFN-γ and GM-CSF. *The Journal of Immunology* 188:6389-6398.

Staples, P.J., I. Gery, and B.H. Waksman. 1966. Role of the thymus in tolerance: III. Tolerance to bovine gamma globulin after direct injection of antigen into the shielded thymus of irradiated rats. *Journal of Experimental Medicine* 124:127-139.

Stone, J.D., D.H. Aggen, A. Schietinger, H. Schreiber, and D.M. Kranz. 2012. A sensitivity scale for targeting T cells with chimeric antigen receptors (CARs) and bispecific T-cell Engagers (BiTEs). *Oncoimmunology* 1:863-873.

Stoop, J.N., R.G. van der Molen, C.C. Baan, L.J. van der Laan, E.J. Kuipers, J.G. Kusters, and H.L. Janssen. 2005. Regulatory T cells contribute to the impaired immune response in patients with chronic hepatitis B virus infection. *Hepatology* 41:771-778.

Strick-Marchand, H., M. Dusseaux, S. Darche, N.D. Huntington, N. Legrand, G. Masse-Ranson, E. Corcuff, J. Ahodantin, K. Weijer, H. Spits, D. Kremsdorf, and J.P. Di Santo. 2015. A novel mouse model for stable engraftment of a human immune system and human hepatocytes. *PloS one* 10:e0119820.

Su, T.H., T.H. Hu, C.Y. Chen, Y.H. Huang, W.L. Chuang, C.C. Lin, C.C. Wang, W.W. Su, M.Y. Chen, C.Y. Peng, R.N. Chien, Y.W. Huang, H.Y. Wang, C.L. Lin, S.S. Yang, T.M. Chen, L.R. Mo, S.J. Hsu, K.C. Tseng, T.Y. Hsieh, F.M. Suk, C.T. Hu, M.J. Bair, C.C. Liang, Y.C. Lei, T.C. Tseng, C.L. Chen, J.H. Kao, C.T.s. group, and C. the Taiwan Liver Diseases. 2016. Four-year entecavir therapy reduces hepatocellular carcinoma, cirrhotic events and mortality in chronic hepatitis B patients. *Liver international : official journal of the International Association for the Study of the Liver* 36:1755-1764.

Sung, W.K., H. Zheng, S. Li, R. Chen, X. Liu, Y. Li, N.P. Lee, W.H. Lee, P.N. Ariyaratne, C. Tennakoon, F.H. Mulawadi, K.F. Wong, A.M. Liu, R.T. Poon, S.T. Fan, K.L. Chan, Z. Gong, Y. Hu, Z. Lin, G. Wang, Q. Zhang, T.D. Barber, W.C. Chou, A. Aggarwal, K. Hao, W. Zhou, C. Zhang, J. Hardwick, C. Buser, J. Xu, Z. Kan, H. Dai, M. Mao, C. Reinhard, J. Wang, and J.M. Luk. 2012. Genome-wide survey of recurrent HBV integration in hepatocellular carcinoma. *Nat Genet* 44:765-769.

Sykulev, Y., M. Joo, I. Vturina, T.J. Tsomides, and H.N. Eisen. 1996. Evidence that a single peptide–MHC complex on a target cell can elicit a cytolytic T cell response. *Immunity* 4:565-571.

Szyska, M., S. Herda, S. Althoff, A. Heimann, J. Russ, D. D'Abundo, T.M. Dang, I. Durieux, B. Dorken, T. Blankenstein, and I.K. Na. 2018. A Transgenic Dual-Luciferase Reporter Mouse for Longitudinal and Functional Monitoring of T Cells In Vivo. *Cancer immunology research* 6:110-120.

Taraseviciute, A., V. Tkachev, R. Ponce, C.J. Turtle, J.M. Snyder, H.D. Liggitt, D. Myerson, L. Gonzalez-Cuyar, A. Baldessari, C. English, A. Yu, H. Zheng, S.N. Furlan, D.J. Hunt, V. Hoglund, O. Finney, H. Brakke, B.R. Blazar, C. Berger, S.R. Riddell, R. Gardner, L.S. Kean, and M.C. Jensen. 2018. Chimeric Antigen Receptor T Cell-Mediated Neurotoxicity in Nonhuman Primates. *Cancer discovery* 8:750-763.

Tenney, D.J., R.E. Rose, C.J. Baldick, K.A. Pokornowski, B.J. Eggers, J. Fang, M.J. Wichroski, D. Xu, J. Yang, and R.B. Wilber. 2009. Long-term monitoring shows hepatitis B virus resistance to entecavir in nucleoside-naïve patients is rare through 5 years of therapy. *Hepatology* 49:1503-1514.

Terrault, N.A., N.H. Bzowej, K.M. Chang, J.P. Hwang, M.M. Jonas, M.H. Murad, and D. American Association for the Study of Liver. 2016. AASLD guidelines for treatment of chronic hepatitis B. *Hepatology* 63:261-283.

Torres, H.A., J. Hosry, P. Mahale, M.P. Economides, Y. Jiang, and A.S. Lok. 2018. Hepatitis C virus reactivation in patients receiving cancer treatment: A prospective observational study. *Hepatology* 67:36-47.

Turtle, C.J., C. Berger, D. Sommermeyer, L.-A. Hanafi, B. Pender, E.M. Robinson, K. Melville, T.M. Budiarto, N.N. Steevens, and C. Chaney. 2015. Anti-CD19 chimeric antigen

receptor-modified T cell therapy for B cell non-Hodgkin lymphoma and chronic lymphocytic leukemia: fludarabine and cyclophosphamide lymphodepletion improves in vivo expansion and persistence of CAR-T cells and clinical outcomes. In Am Soc Hematology.

Turtle, C.J., L.A. Hanafi, C. Berger, T.A. Gooley, S. Cherian, M. Hudecek, D. Sommermeyer, K. Melville, B. Pender, T.M. Budiarto, E. Robinson, N.N. Steevens, C. Chaney, L. Soma, X. Chen, C. Yeung, B. Wood, D. Li, J. Cao, S. Heimfeld, M.C. Jensen, S.R. Riddell, and D.G. Maloney. 2016. CD19 CAR-T cells of defined CD4+:CD8+ composition in adult B cell ALL patients. *The Journal of clinical investigation* 126:2123-2138.

Turvey, S.E., M. Hara, P.J. Morris, and K.J. Wood. 1999. Mechanisms of tolerance induction after intrathymic islet injection: determination of the fate of alloreactive thymocytes. *Transplantation* 68:30-39.

Valitutti, S., S. Müller, M. Cella, E. Padovan, and A. Lanzavecchia. 1995. Serial triggering of many T-cell receptors by a few peptide–MHC complexes. *Nature* 375:148.

Van Caeneghem, Y., S. De Munter, P. Tieppo, G. Goetgeluk, K. Weening, G. Verstichel, S. Bonte, T. Taghon, G. Leclercq, T. Kerre, R. Debets, D. Vermijlen, H. Abken, and B. Vandekerckhove. 2017. Antigen receptor-redirected T cells derived from hematopoietic precursor cells lack expression of the endogenous TCR/CD3 receptor and exhibit specific antitumor capacities. *Oncoimmunology* 6:e1283460.

VanSeggelen, H., J.A. Hammill, A. Dvorkin-Gheva, D.G. Tantalo, J.M. Kwiecien, G.F. Denisova, B. Rabinovich, Y. Wan, and J.L. Bramson. 2015. T Cells Engineered With Chimeric Antigen Receptors Targeting NKG2D Ligands Display Lethal Toxicity in Mice. *Molecular therapy : the journal of the American Society of Gene Therapy* 23:1600-1610.

Wang, X., W.C. Chang, C.W. Wong, D. Colcher, M. Sherman, J.R. Ostberg, S.J. Forman, S.R. Riddell, and M.C. Jensen. 2011. A transgene-encoded cell surface polypeptide for selection, in vivo tracking, and ablation of engineered cells. *Blood* 118:1255-1263.

Ward, M., R. Sattler, I.R. Grossman, A.J. Bell, Jr., D. Skerrett, L. Baxi, and A. Bank. 2003. A stable murine-based RD114 retroviral packaging line efficiently transduces human hematopoietic cells. *Molecular therapy : the journal of the American Society of Gene Therapy* 8:804-812.

Watanabe, K., S. Terakura, A.C. Martens, T. van Meerten, S. Uchiyama, M. Imai, R. Sakemura, T. Goto, R. Hanajiri, N. Imahashi, K. Shimada, A. Tomita, H. Kiyoi, T. Nishida, T. Naoe, and M. Murata. 2015. Target antigen density governs the efficacy of anti-CD20-CD28-CD3 zeta chimeric antigen receptor-modified effector CD8+ T cells. *Journal of immunology (Baltimore, Md. : 1950)* 194:911-920.

Watanabe, T., E.M. Sorensen, A. Naito, M. Schott, S. Kim, and P. Ahlquist. 2007. Involvement of host cellular multivesicular body functions in hepatitis B virus budding. *Proceedings of the National Academy of Sciences of the United States of America* 104:10205-10210.

Wege, A.K. 2018. Humanized Mouse Models for the Preclinical Assessment of Cancer Immunotherapy. *BioDrugs : clinical immunotherapeutics, biopharmaceuticals and gene therapy* 32:245-266.

Wei, G., Y. Hu, C. Pu, J. Yu, Y. Luo, J. Shi, Q. Cui, W. Wu, J. Wang, L. Xiao, Z. Wu, and H. Huang. 2018. CD19 targeted CAR-T therapy versus chemotherapy in re-induction treatment of refractory/relapsed acute lymphoblastic leukemia: results of a case-controlled study. *Annals of hematology* 97:781-789.

Weinberg, A.D., M.M. Rivera, R. Prell, A. Morris, T. Ramstad, J.T. Vetto, W.J. Urba, G. Alvord, C. Bunce, and J. Shields. 2000. Engagement of the OX-40 receptor in vivo enhances antitumor immunity. *Journal of immunology (Baltimore, Md. : 1950)* 164:2160-2169.

Weissmuller, S., S. Kronhart, D. Kreuz, B. Schnierle, U. Kalinke, J. Kirberg, K.M. Hanschmann, and Z. Waibler. 2016. TGN1412 Induces Lymphopenia and Human Cytokine Release in a Humanized Mouse Model. *PloS one* 11:e0149093.

Wherry, E.J., S.J. Ha, S.M. Kaech, W.N. Haining, S. Sarkar, V. Kalia, S. Subramaniam, J.N. Blattman, D.L. Barber, and R. Ahmed. 2007. Molecular signature of CD8+ T cell exhaustion during chronic viral infection. *Immunity* 27:670-684.

WHO. 2009. Hepatitis B vaccines WHO position paper. *Weekly Epidemiological Record* 84:405-419.

WHO. 2017. Hepatitis B, Fact sheet, Updated July 2017. In http://www.who.int/en/news-room/fact-sheets/detail/hepatitis-b [Accessed 10.06.2018].

Wieland, S.F. 2015. The chimpanzee model for hepatitis B virus infection. *Cold Spring Harb Perspect Med* 5:a021469.

Wisskirchen, K., K. Metzger, S. Schreiber, T. Asen, L. Weigand, C. Dargel, K. Witter, E. Kieback, M.F. Sprinzl, W. Uckert, M. Schiemann, D.H. Busch, A.M. Krackhardt, and U. Protzer. 2017. Isolation and functional characterization of hepatitis B virus-specific T-cell receptors as new tools for experimental and clinical use. *PloS one* 12:e0182936.

Wursthorn, K., M. Lutgehetmann, M. Dandri, T. Volz, P. Buggisch, B. Zollner, T. Longerich, P. Schirmacher, F. Metzler, M. Zankel, C. Fischer, G. Currie, C. Brosgart, and J. Petersen. 2006. Peginterferon alpha-2b plus adefovir induce strong cccDNA decline and HBsAg reduction in patients with chronic hepatitis B. *Hepatology* 44:675-684.

Xia, Y., D. Stadler, J. Lucifora, F. Reisinger, D. Webb, M. Hosel, T. Michler, K. Wisskirchen, X. Cheng, K. Zhang, W.M. Chou, J.M. Wettengel, A. Malo, F. Bohne, D. Hoffmann, F. Eyer, R. Thimme, C.S. Falk, W.E. Thasler, M. Heikenwalder, and U. Protzer. 2016. Interferon-gamma and Tumor Necrosis Factor-alpha Produced by T Cells Reduce the HBV Persistence Form, cccDNA, Without Cytolysis. *Gastroenterology* 150:194-205.

Yan, H., G. Zhong, G. Xu, W. He, Z. Jing, Z. Gao, Y. Huang, Y. Qi, B. Peng, and H. Wang. 2012. Sodium taurocholate cotransporting polypeptide is a functional receptor for human hepatitis B and D virus. *elife* 1:

Zhao, Y., E. Moon, C. Carpenito, C.M. Paulos, X. Liu, A.L. Brennan, A. Chew, R.G. Carroll, J. Scholler, B.L. Levine, S.M. Albelda, and C.H. June. 2010. Multiple injections of electroporated autologous T cells expressing a chimeric antigen receptor mediate regression of human disseminated tumor. *Cancer research* 70:9053-9061.

Zhao, Z., M. Condomines, S.J.C. van der Stegen, F. Perna, C.C. Kloss, G. Gunset, J. Plotkin, and M. Sadelain. 2015. Structural Design of Engineered Costimulation Determines Tumor Rejection Kinetics and Persistence of CAR T Cells. *Cancer cell* 28:415-428.

Zhen, A., M. Kamata, V. Rezek, J. Rick, B. Levin, S. Kasparian, I.S. Chen, O.O. Yang, J.A. Zack, and S.G. Kitchen. 2015. HIV-specific Immunity Derived From Chimeric Antigen Receptor-engineered Stem Cells. *Molecular therapy : the journal of the American Society of Gene Therapy* 23:1358-1367.

Zhen, A., C.W. Peterson, M.A. Carrillo, S.S. Reddy, C.S. Youn, B.B. Lam, N.Y. Chang, H.A. Martin, J.W. Rick, J. Kim, N.C. Neel, V.K. Rezek, M. Kamata, I.S.Y. Chen, J.A. Zack, H.P. Kiem, and S.G. Kitchen. 2017. Long-term persistence and function of hematopoietic stem cell-derived chimeric antigen receptor T cells in a nonhuman primate model of HIV/AIDS. *PLoS pathogens* 13:e1006753.

Zhong, X.S., M. Matsushita, J. Plotkin, I. Riviere, and M. Sadelain. 2010. Chimeric antigen receptors combining 4-1BB and CD28 signaling domains augment PI3kinase/AKT/Bcl-XL activation and CD8+ T cell-mediated tumor eradication. *Molecular therapy : the journal of the American Society of Gene Therapy* 18:413-420.

Publications and meetings

a) Publications in peer-reviewed journals

Burwitz, B.J., J.M. Wettengel, M.A. Muck-Hausl, M. Ringelhan, C. Ko, **M.M. Festag**, K.B. Hammond, M. Northrup, B.N. Bimber, T. Jacob, J.S. Reed, R. Norris, B. Park, S. Moller-Tank, K. Esser, J.M. Greene, H.L. Wu, S. Abdulhaqq, G. Webb, W.F. Sutton, A. Klug, T. Swanson, A.W. Legasse, T.Q. Vu, A. Asokan, N.L. Haigwood, U. Protzer, and J.B. Sacha. 2017. Hepatocytic expression of human sodium-taurocholate cotransporting polypeptide enables hepatitis B virus infection of macaques. *Nature communications* 8:2146.

Festag, M.M. et al. Evaluation of a fully human, hepatitis B virus-specific chimeric antigen receptor (CAR) in an immunocompetent mouse model *Manuscript in preparation.*

b) Scientific contributions at conferences and symposia

2018 Final symposium of the SFB TR36

“Principles and Applications of Adoptive T-cell Therapy”

Oral presentation: Evaluation of a fully human hepatitis B virus-specific chimeric antigen receptor for adoptive T-cell therapy in an immunocompetent mouse model

2016 International symposium of the SFB TR36

“Principles and Applications of Adoptive T-cell Therapy”

Poster presentation: Dissecting the influence of interleukin-10 on the treatment of chronic hepatitis B virus infection by adoptive T-cell therapy

2015 XXI. Annual Meeting German Society for Gene Therapy

Poster presentation: Redirection of T cells against cells expressing HBsAg

Acknowledgments

First of all, I would like to thank Ulrike Protzer for giving me the opportunity to work on my desired project with CAR T cells. You always provided support when it was needed while leaving me freedom to develop into an independent scientist. I am glad that your door was always open for urgent matters as needed.

Thank you, Angela Krackhardt and Sebastian Kobold, as members of my thesis committee, and Percy Knolle as additional advisor, you gave great input during our meetings and supported thereby my progress substantially.

Very special thanks go to Karin Wisskirchen, my unofficial supervisor. In our weekly meetings, discussing recent results and planning future experiments, you challenged my scientific thinking and supported me to become more and more independent. Even when you were on maternity leave, you were available for me and helped me to stay on track for a successful completion of my projects. Last but not least, also during maternity leave, you did proof reading of this thesis. Thank you!

Sophia Schreiber, Antje Malo and Alexandre Klopp, you always contributed in lively discussions during our weekly T-cell therapy subgroup meetings. Furthermore, you contributed substantially to the great work atmosphere in the „small lab".

Natalie Röder, Stefanie Prosser and Nina Kallin, I would like to thank for teaching me the skills to perform *in vivo* mouse experiments independently.

However, since big mouse experiments are tough to be handled alone, Theresa Asen, Philipp Hagen, Romina Bester and Anna Kosinska, you helped when I was not available and on sacrifice days. It is amazing how we worked smoothly in a team and rendered days with huge workload almost relaxed eventually.

I also would like to thank all other laboratory members, including former members, naming especially Oliver Quitt, Lisa Wolff, Wen-Min Chou, Chunkyu Ko, Martin Mück-Häusl, Daniela Stadler, Anindita Chakraborty, Andreas Oswald, Stoyan Velkov, Samuel Jeske, Jochen Wettengel, Jinpeng Su, Florian Wilsch, Sebastian Altstetter, Christoph Blossey, Martin Kächele, Julia Sacherl, Katrin Singethan, Suliman Afridi, Kathrin Kappes, Felix Bohne, Thomas Michler, Lili Zhao and Maarten van de Klundert. I feel like we became more than colleagues. Although the laboratory tends to be crowded, you kept the atmosphere friendly, supportive, humorous, and at the same time productive.

My interns and master students Michael Lauber, Helena Meyer-Berg, Katharina Bösing and Anna Näger, thank you for contribution during the last four years, for your intelligent scientific questions and for helping me to grow into the role to supervise people.

Furthermore, I would like to thank all members of the virology diagnostics department. You were even very supportive, if there were urgent spontaneous measurements needed.

Thank you to Frank Thiele, Cauleen Noel, Doris Pelz and Daniela Rizzi for your support regarding mouse experiment approvals and other office work.

I would also like to thank my cooperation partners Michael Hudecek, Hinrich Abken, Stan Riddell and Annette Oxenius for providing material and mice for my research studies. Simon Fräßle, thank you for scientific discussions and for helping with irradiating mice. And, importantly, Benjamin Burwitz and Jonah Sasha, thank you for inviting me to work in your laboratories for two months and supporting my projects thereby.

As member of the SFB TR36 for „Principles and Applications of Adoptive T Cell Therapy", I would also like to thank all the members in Munich and Berlin and all invited guests for scientific discussions in seminars, conferences, symposia and retreats.

An important thank you goes to my family, my brother, my former host-parents in the U.S, and my friends all over Germany in Wuppertal, Freiburg and Munich. Thank you for all the support throughout my life, for all thoughts and laughter, serious and silly moments as well as your patients.

Last but not least, I would like to thank Julia Hasreiter, my fiancé, soulmate and coworker. I could have named you in almost all paragraphs in this section, including scientific input, practical help in the laboratory, as well as of course mental support to master the deepest valleys during my Ph.D. work. THANK YOU!